HUMAN SCAVENGER RECEPTOR CLASS B, TYPE II (SR-BII) AND CELLULAR CHOLESTEROL EFFLUX

by

Jane Victoria Mulcahy

A thesis submitted in partial fulfilment of the requirements for the degree of:

Doctor of Philosophy

Royal Free & University College Medical School,
University of London

2002

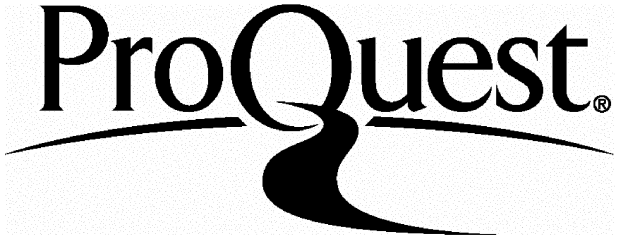

HUMAN SCAVENGER RECEPTOR CLASS B, TYPE II (SR-BII) AND CELLULAR CHOLESTEROL EFFLUX

Abstract

A key feature of atherosclerotic lesions is the presence of cholesteryl ester (CE)-engorged macrophages within the arterial intima. Cholesterol mobilisation from intracellular stores involves high-density lipoprotein (HDL) binding to an unknown cell surface receptor, activation of signalling pathways, and translocation of free cholesterol to the plasma membrane for efflux. The scavenger receptor, class B *(SR-B)* gene encodes for two different splice variants (types I and II), which have identical extracellular regions that bind HDL but C-terminal cytoplasmic tails that differ. I identified a number of putative signalling motifs in the C-terminus of SR-BII, which are absent from SR-BI, and hypothesised that: ***'upon HDL stimulation of SR-BII, its C-terminal cytoplasmic tail interacts with a signalling molecule to activate the CE mobilisation pathway.'***

'Pull-down' assays to screen potential binding proteins revealed that biotin-tagged cytoplasmic SR-BII interacts with the Src Homology 3 domain of phospholipase C-γ1, in an isoform-specific manner. However, I failed to detect this interaction within more physiological, cellular environments. Full-length SR-BI or SR-BII sequences were over-expressed in Chinese hamster ovary cells (CHO-SR-BI/II), and caveolae (cholesterol-rich microdomains of the plasma membrane) were isolated from cell lysates using sucrose density gradient ultracentrifugation. Human SR-BII was detected in this membrane fraction, while co-immunoprecipitation with caveolin-1 confirmed its true caveolar localisation. This finding implicates SR-BII in both signalling and cholesterol flux; two functions associated with caveolae.

Following the generation of an isoform-specific human SR-BII antiserum, cell surface expression of SR-BII protein in THP-1 monocytes and macrophages was revealed. To investigate the role of this isoform in CE mobilisation, recombinant CHO-SR-BII cells were labelled with [^{3}H]-oleic acid and reductions of cellular cholesteryl oleate were monitored during HDL incubation. Over-expression of SR-BII, however, failed to promote the release of stored CE pools. In contrast, studies comparing HDL-stimulated efflux of free [^{3}H]-cholesterol from CHO-SR-BI/II cells showed that SR-BII is significantly better than SR-BI at cellular cholesterol efflux. I conclude that SR-BII has an important role in cellular cholesterol homeostasis and reverse cholesterol transport.

TABLE OF CONTENTS

LIST OF FIGURES

CHAPTER 4

LIST OF TABLES

DEDICATION

I wish to dedicate this thesis to my loving husband, James, and to my parents, Roger and Joanna Southgate, for their love, support and encouragement through the years.

ACKNOWLEDGEMENTS

I would like to start by thanking my PhD supervisor Dr. Jim Owen for his guidance, encouragement and support over the last four years. I am also extremely grateful to him and my colleagues, Dr. A. Stannard and Dr. S. Schepelmann, for their critical reviewing of this manuscript.

I wish to express my gratitude to Dr. D. Riddell who gave me constant guidance, as well as friendship, during the first two years of my project. Thanks must also go to Dr. A. Stannard for assisting me with flow cytometry analysis. In addition, I thank Mr. A. Tagalakis, Mrs. Z. Mohri, Dr. A. Manzano and Dr. G. Sperber for all the fun times that we have shared together in the laboratory. I would also like to acknowledge the financial support of the British Heart Foundation.

Finally, I wish to thank my husband Dr. James Mulcahy for supporting me both emotionally and financially through my PhD. I would not have made it this far without you.

Jane Mulcahy, July 2002

ABBREVIATIONS

α..... anti-
ABCA1..... ATP-binding cassette transporter, class A1
ACAT..... acyl-CoA:cholesterol acyltransferase
Ac-LDL..... acetylated low-density lipoprotein
AD..... activation domain
ALCAM..... activated-leukocyte cell adhesion molecule
apo..... apolipoprotein
apoER2..... apoE receptor 2
APS.....ammonium persulphate
BCA..... bicinchoninic acid
bisacrylamide..... N,N'-methylenebisacrylamide
BSA.....bovine serum albumin
CE.....cholesteryl ester
CEH.....cholesteryl ester hydrolase
CETP.....cholesteryl ester transfer protein
CHO.....Chinese hamster ovary
CIP.....calf intestinal alkaline phosphatase
CLA-1.....CD36 and LIMPII analogous-1
CLM..... caveolin-rich light membranes
Dab1..... disabled-1
DAG..... diacylglycerol
DBD.....DNA binding domain
DEPC.....diethylpyrocarbonate
DMSO.....dimethylsulphoxide
dNTPs..... deoxynucleotide triphosphates
dpm..... disintegrations per minute
DTT..... dithiothreitol
ECL.....enhanced chemiluminescence
EDTA.....ethylenediaminetetra-acetate
EGF.....epidermal growth factor
eNOS..... endothelial nitric oxide synthase
ER.....endoplasmic reticulum
FACS..... fluorescent activated cell sorter
FBS..... fetal bovine serum
FC..... free cholesterol
FH.....familial hypercholesterolaemia

FITC..... fluorescein isothiocyanate

GFP..... green fluorescent protein

GST..... glutathione *S*-transferase

h..... human

ha..... hamster

HB_1..... high-density lipoprotein binding protein 1

HB_2..... high-density lipoprotein binding protein 2

HBP..... high-density lipoprotein binding protein

HDL..... high-density lipoprotein

HL..... hepatic lipase

HMG-CoA..... 3-hydroxy-3-methylglutaryl-CoA

HRP..... horseradish peroxidase

ICAM-1..... intercellular adhesion molecule-1

IDL..... intermediate-density lipoprotein

IF-B_{12}..... intrinsic factor vitamin B_{12} complex

Ig..... immunoglobulin

IPTG..... isopropyl β-D-thiogalactopyranoside

LCAT..... lecithin-cholesterol acyltransferase

LDL..... low-density lipoprotein

LIMP..... lysosomal integral membrane protein

Lp(a)..... lipoprotein (a)

LPL..... lipoprotein lipase

LRP..... low-density lipoprotein receptor-related protein

LSC..... liquid scintillation counting

m..... murine

mAb..... monoclonal antibody

MCS..... multiple cloning site

MWCO..... molecular weight cut-off

nCEH..... neutral cholesteryl ester hydrolase

nLDL..... native low-density lipoprotein

NO..... nitric oxide

Ox-LDL..... oxidised low-density lipoprotein

pAb..... polyclonal antibody

PBS..... phosphate buffered saline

PBS-T..... phosphate buffered saline-tween

PCR..... polymerase chain reaction

PIP_2 ..... phosphatidylinositol 4,5-bisphosphate

PKA..... protein kinase A

PKC.....protein kinase C

plc-γ1..... phospholipase C-γ1

PLTP.....phospholipid transfer protein

PMA..... phorbol 12-myristate 13-acetate

PMSF.....phenylmethyl-sulphonyl fluoride

pS.....phosphoserine

pT.....phosphothreonine

pY.....phosphotyrosine

RCT.....reverse cholesterol transport

RT-PCR..... reverse transcription-polymerase chain reaction

SD..... synthetic dropout

SDS-PAGE..... sodium dodecyl sulphate-polyacrylamide gel electrophoresis

SH2..... src homology 2

SH3..... src homology 3

SMC..... smooth muscle cell

SR-BI.....scavenger receptor class B, type I

SR-BII.....scavenger receptor class B, type II

TBE.....tris-borate ethylenediaminetetra-acetate

TBS.....tris buffered saline

TBS-T.....tris buffered saline-tween

TCA ..... trichloracetic acid

TEMED..... N, N, N, N'-tetramethylethylenediamine

TGN..... trans-Golgi network

TLC..... thin layer chromatography

TNF..... tumor necrosis factor

TRL..... triglyceride-rich lipoproteins

VCAM-1.....vascular cell adhesion molecule-1

VLDL..... very low-density lipoprotein

VLDLR..... very low-density lipoprotein receptor

X-gal..... 5-bromo-4-chloro-3-indolyl-β-D-galactopyranoside

Chapter 1

1. INTRODUCTION

1.1 Atherosclerosis

Cardiovascular disease is the leading cause of death in the United States and Western Europe [1]. Myocardial and cerebral infarctions, secondary to atherosclerotic disease, account for the majority of these deaths [2]. Atherogenesis is a molecularly complex phenomenon involving interactions between cell types endogenous to the arterial wall with both circulating lipoprotein particles, and a variety of inflammatory cells, such as monocyte-macrophages. The disease begins in childhood and develops progressively over decades of life [3]. As increasingly complex vascular lesions form, the arterial wall thickens and blood flow becomes impeded. At later stages of the disease, plaque rupture and occlusive thrombosis lead to the clinical events associated with complex atherosclerotic lesions [1].

The endothelial cell is constantly exposed to various potential stimuli that can trigger atherogenesis: hyperlipoproteinaemia, oxidised lipids, shear stress, inflammatory agents and cytokines [4]. Repetitive stimulation of the vascular endothelium can cause endothelial dysfunction, allowing lipoproteins to penetrate and lipids to accumulate in the sub-endothelial space. The activated endothelium becomes hyperadhesive to promote leukocyte adhesion. This involves upregulating the expression of several adhesion molecules, such as the intercellular adhesion molecule-1 (ICAM-1) and the vascular cell adhesion molecule-1 (VCAM-1), by cytokines [2]. Having tethered monocytes to the endothelial surface using E- and P-selectin, the monocytes subsequently firmly adhere to endothelial adhesion molecules via their complementary receptors. Following monocyte migration across the endothelium and recruitment into the artery wall, differentiation of the monocytes into macrophages occurs [4].

Early atherosclerotic lesions are characterised by cholesteryl ester (CE)-engorged macrophages, known as foam cells, in the arterial intima [5]. These cholesterol-loaded foam cells are the hallmark of fatty streaks and atherosclerotic plaques that form when macrophage cholesterol uptake from circulating lipoproteins exceeds cholesterol efflux. Macrophages limit the uptake of lipids poorly and since no cellular cholesterol catabolism occurs, cholesterol homeostasis can easily be disturbed. Macrophage scavenger receptors bind a diverse array of endogenous and foreign molecules, and play

important roles in host defence [6]. However, these receptors also contribute to the progression of atherogenesis, as they rapidly engulf modified low-density lipoproteins (LDL), such as oxidised LDL (Ox-LDL) [7]. This occurs in an uncontrolled manner because, unlike native LDL receptors, cellular cholesterol levels do not control the levels of scavenger receptor expression [8]. Scavenger receptors provide the major mechanism for the uptake of lipids by macrophages, although the LDL receptor-related protein (LRP) [9] and the VLDL receptor (VLDLR) [10] also contribute to the progression of atherogenesis, by mediating the uptake of triglyceride-depleted remnant particles [11]. Furthermore, uptake of LDL takes place using a receptor-independent pathway, via the internalisation of cell surface proteoglycan-bound lipoprotein lipase-LDL (LPL-LDL) complexes [12]. It is believed that LPL utilises both its heparan- and lipid-binding domains to act as a bridge between the matrix proteoglycans and the lipoprotein particle. In addition to lipid accumulation within macrophages, lipid also accumulates in large quantities in the extracellular space. This acellular lipid-rich core of atherosclerotic lesions results from the deposition of plasma lipoproteins and the death of cholesterol-loaded macrophages [13].

Endothelial injury is also associated with platelet adhesion and aggregation of platelets to the damaged endothelium [14], and smooth muscle cell (SMC) infiltration into the intima [15]. The subsequent proliferation of SMCs within the intima contributes to the advancement of lesion development. Advanced atherosclerotic plaques comprise a necrotic core surrounded by a fibrous cap consisting of SMCs and extracellular matrix under a single endothelial layer. Eventually, as the cap calcifies and becomes more unstable, the plaque can rupture and release the highly thrombogenic debris from its necrotic core into the bloodstream [16]. The thrombus that forms may occlude the artery, prevent blood flow and cause a myocardial infarction.

For decades, scientists have sought to identify the important regulatory processes of atherogenesis, in order to develop new therapeutic strategies to slow disease progression. Epidemiological studies have revealed a number of risk factors for atherosclerosis, including hypertension, cigarette smoking, hereditary factors, diabetes, obesity, age and gender [17]. Not surprisingly, one of the most significant risk factors is the level of cholesterol, and its major carrier LDL, in the bloodstream [18]. Considerable interest has focused on controlling plasma LDL levels as a means of slowing atherogenesis. This interest resulted in the pharmaceutical generation of statins: effective

lipid lowering drugs that upregulate LDL receptor expression and increase LDL clearance from the bloodstream [19]. However, these drugs do not significantly increase low levels of plasma high-density lipoprotein (HDL), which is an equally important risk factor for atherogenesis [20]. Despite the discovery that HDL functions in an atheroprotective manner to promote clearance of cholesterol from peripheral cells, the underlying mechanisms involved in cellular cholesterol efflux remained elusive for over twenty years. During this time, our understanding of HDL-cell interactions failed to develop at the same rate as that of LDL, since no physiological HDL receptors had been identified. Recently, however, two important proteins involved in HDL metabolism were discovered: the scavenger receptor class B, type I (SR-BI), and the ATP-binding cassette transporter, class A1 (ABCA1) [reviewed in 21,22]. Thus, the situation has now changed, as scientists seek to understand the mechanisms by which HDL enhances cellular cholesterol efflux, and thereby promotes the regression of pre-existing atherosclerotic lesions. It is likely that these mechanisms will provide new therapeutic targets in the future. In this thesis, I studied the alternative splice variant of SR-BI (SR-BII) and sought to establish an atheroprotective role for this HDL receptor.

1.2 Cellular Cholesterol Homeostasis

Cholesterol is an essential component of cellular membranes, where it functions to modulate fluidity and maintain the barrier between the cell and its environment. In hepatocytes and steroidogenic tissues, it also provides the raw material for the manufacture of bile acids and steroid hormones, respectively (Figure 1.1). Nevertheless, there is a darker side to cholesterol, as it contributes to the pathology of disease, such as coronary heart disease. In this case, cholesterol accumulates in the arterial wall where it cannot be readily mobilised, and its presence promotes the development of an atherosclerotic plaque [22,23]. Therefore, in order to prevent cholesterol accumulation and maintain cellular cholesterol homeostasis, it is critical that cells tightly control both cholesterol synthesis and uptake, as well as cholesterol deposition, mobilisation and efflux.

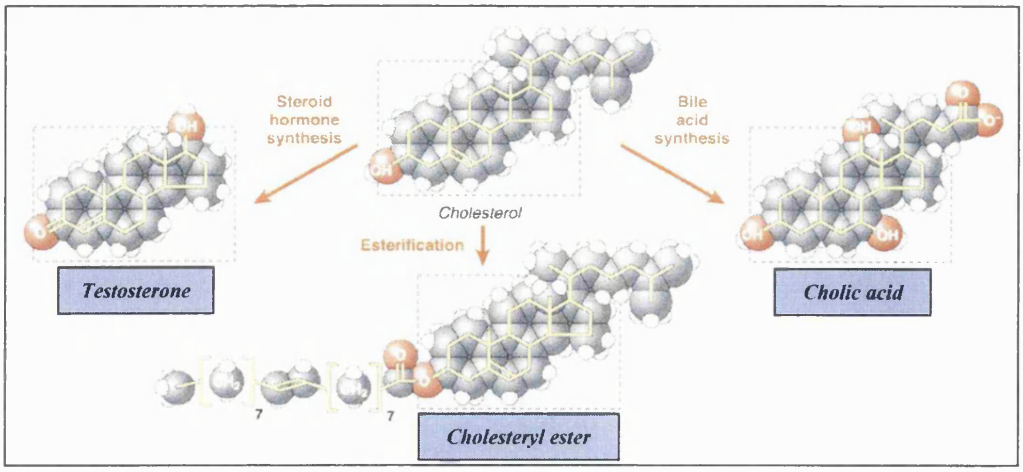

Figure 1.1 Cholesterol metabolism

Cholesterol is an essential constituent of cell membranes and is the building block for steroid hormones (e.g. testosterone) and bile acids (e.g. cholic acid). It is esterified with fatty acids for storage as CE, either in the core of lipoproteins or as intracellular lipid droplets.

1.2.1 CHOLESTEROL SYNTHESIS AND UPTAKE

Cells obtain cholesterol from lipoprotein endocytosis, as well as endogenous synthesis. Cholesterol synthesis *de novo* transforms a simple two-carbon substrate (acetate) into a complex four-ring structure, containing twenty-seven carbons, through the action of at least thirty enzymes. The pathway can be broken down into three stages, beginning with the generation of mevalonate in the endoplasmic reticulum (ER). Three molecules of acetyl-CoA condense to generate 3-hydroxy-3-methylglutaryl-CoA (HMG-CoA). The HMG-CoA reductase enzyme is then responsible for catalysing the reduction of HMG-CoA to mevalonate. This reaction represents the first committed step in cholesterol synthesis. The second stage involves several cytosolic reactions, which convert mevalonate into squalene. Lastly, squalene undergoes cyclisation to lanesterol in the ER, before a further twenty reactions finally generate cholesterol [24].

Another important source of cholesterol for peripheral tissues is the uptake of esterified cholesterol from circulating LDL particles by endocytosis. Circulating LDL particles contain two-thirds of total plasma cholesterol, with CE contributing to 40 % of their weight. LDL therefore plays a crucial role in the delivery of cholesterol to peripheral tissues [24]. In addition, hepatocytes and steroidogenic tissues are able to selectively remove CE from HDL *(Section 1.6.3.1)*. The importance of successful LDL CE delivery to extrahepatic cells is highlighted in patients with the hereditary condition

known as familial hypercholesterolaemia (FH). Patients suffering with the rare homozygous form of this disease exhibit grossly elevated plasma cholesterol levels and develop advanced atherosclerotic lesions early on in life, usually resulting in heart disease and death by the age of twenty. Patients with the more common heterozygous form exhibit less severely elevated levels of cholesterol, but still are at a higher risk of heart disease before the age of fifty.

In 1972, Goldstein and Brown began to study this disease using cultured fibroblasts from patients with FH and from healthy individuals. Normal fibroblasts were incubated in the presence of serum and the activity of HMG-CoA reductase was found to be low, indicating that endogenous cholesterol synthesis was also low. When lipoproteins were removed from the culture medium, HMG-CoA reductase activity in normal fibroblasts rose by at least 50-fold over 24 h. This enzyme activation was subsequently rapidly suppressed by the addition of lipoproteins back to the medium. In fact, of the two major cholesterol-carrying lipoproteins in human plasma, LDL and HDL, only LDL was effective. In contrast, fibroblasts from FH patients exhibited HMG-CoA reductase activities that were 50- to 100-fold above normal whether cultured in the presence or absence of serum [25,26]. Their findings suggested that normal fibroblasts were transporting cholesterol into the cell, where it regulates its own synthesis by suppressing the activity of the rate-limiting enzyme, HMG-CoA reductase. In FH patients, it appeared as though this cellular cholesterol uptake was defective. Brown and Goldstein went on to demonstrate the presence of high-affinity LDL-binding sites (i.e. LDL receptors) on the surface of normal cells, which were absent on FH-homozygous cells [27]. Mutations in the *LDL receptor* gene subsequently explained the inability of FH patients to take up LDL cholesterol. These mutations interrupt either receptor synthesis, binding, processing or subcellular localisation [19].

The LDL receptor was found to cluster in clathrin-coated pits and mediate LDL uptake by endocytosis [28]. Receptor-mediated endocytosis is a process by which cells internalise and degrade many extracellular molecules, including LDL (Figure 1.2). Following LDL receptor synthesis, the receptors concentrate in coated pits and bind any available LDL. Within 3-5 min the coated pits invaginate to produce endocytic vesicles, which subsequently fuse and generate endosomes. Once the pH of the endosomes falls below 6.5, LDL particles dissociate from their receptors, which recycle back to the surface. A receptor undergoes a cycle of endocytosis every 10 minutes, irrespective of

LDL binding interactions. Finally, the endosome containing LDL fuses with a lysosome, where the protein component of LDL is hydrolysed to amino acids, and the CE is hydrolysed by lysosomal acid lipase to free cholesterol (FC) [19]. Lipoprotein-derived cholesterol subsequently joins the intracellular FC pool, to be used by the cell during the synthesis of plasma membranes, bile acids and steroid hormones, or stored as cytosolic CE lipid droplets.

Intracellular FC acts on three different pathways in order to regulate cellular synthesis and uptake of cholesterol. Firstly, it suppresses *HMG-CoA reductase* gene transcription [29] and accelerates degradation of the enzyme [30]. In addition, cholesterol is responsible for suppressing LDL receptor synthesis [31], as well as activating a cholesterol-esterifying enzyme called acyl-CoA:cholesterol acyltransferase (ACAT) [32]. ACAT acts to promote the storage of excess cholesterol as cytosolic CE droplets [33]. Together these regulatory mechanisms serve to maintain a constant level of unesterified cholesterol, despite fluctuations in cellular requirements and exogenous supplies.

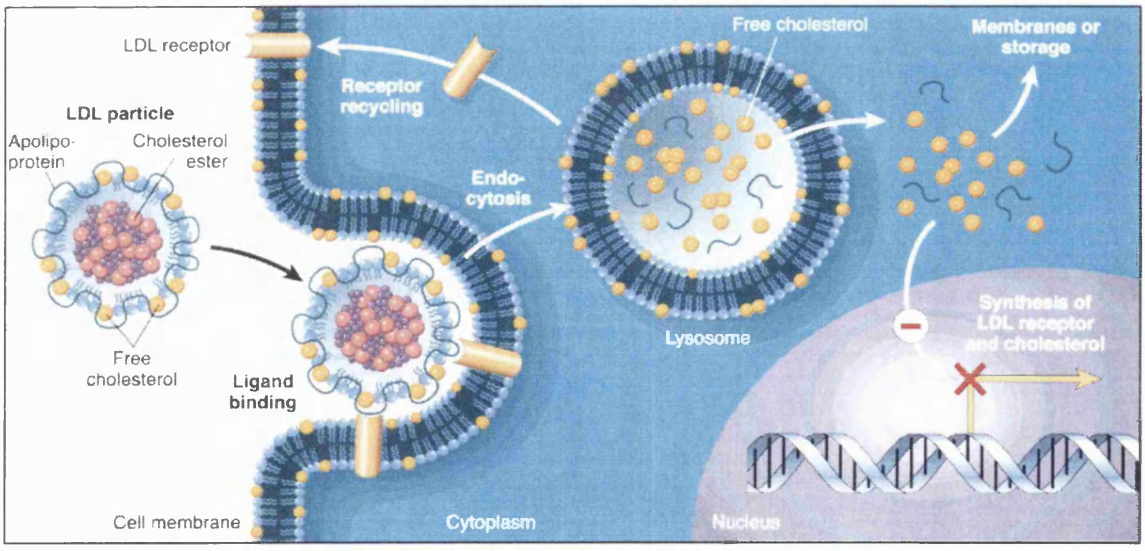

Figure 1.2 Internalisation of LDL by receptor-mediated endocytosis

LDL receptors cluster in clathrin-coated pits, bind LDL particles, and mediate endocytosis. The LDL is degraded in lysosomes to release FC, while the receptor recycles back to the surface. As cellular cholesterol accumulates, synthesis of LDL receptors and endogenous cholesterol synthesis is suppressed.

1.2.2 CHOLESTEROL DEPOSITION AND MOBILISATION

Interconversion of cellular FC and CE, by re-esterification-hydrolysis cycling, is controlled by the action of two enzymes, ACAT and CE hydrolase (CEH). These enzymes help to maintain cellular FC within narrow limits, since the sterol can be toxic when present in excess [34]. As intracellular FC accumulates in the ER, ACAT is activated to promote esterification in order to maintain membrane integrity [33]. The addition of long chain fatty acids reduces the solubility of FC in the membrane thereby causing the CE to form lipid droplets within the cytoplasm [35]. Cytosolic CE is converted back to FC by the action of neutral (n) CEH, activated by a cAMP-dependent protein kinase A (PKA) [36]. The released cholesterol is transferred to the plasma membrane, where it can be transported to the ER for another cycle of re-esterification-hydrolysis [33]. This cycling is interrupted by the presence of extracellular cholesterol acceptors, such as HDL, that promote FC efflux [37,38].

Specialised cells employ additional mechanisms to maintain cellular FC levels. For example, hepatocytes and enterocytes are able to secrete FC and CE in VLDL and chylomicrons, respectively. In both of these cells, a second ACAT gene product is active, named ACAT2 [35]. Following absorption of dietary and endogenous FC from the intestinal lumen by mucosal cells, intestinal ACAT2 esterifies 75-80 % of the cholesterol. Generated CEs are then secreted into the circulation contained within chylomicron particles. Not surprisingly, transgenic mice deficient in ACAT2 exhibit reduced intestinal cholesterol absorption [39]. Chylomicron CEs are subsequently removed from the circulation by the liver and hydrolysed. Hepatic ACAT2 then re-esterifies the FC to produce CE, which in turn gets incorporated with triglycerides to form secreted VLDL particles, or is recycled back to FC by nCEH. Hepatocytes also convert FC to bile acids, which are secreted along with FC into bile. Finally, steroidogenic tissues use FC as a substrate for the generation of steroid hormones [38].

The regulation of cholesterol mobilisation and efflux from macrophages is of great interest, since these cells cannot self-limit cholesterol uptake and therefore accumulate a large proportion of intracellular cholesterol. Following lipoprotein uptake and lysosomal hydrolysis of the CE, the unesterified cholesterol is transferred to the ER either directly or indirectly via the plasma membrane. In the ER, ACAT re-esterifies FC to CE, which appears as cytosolic lipid droplets, and gives cholesterol-engorged macrophages their foamy appearance [8]. In order to increase cholesterol efflux and

prevent foam cell development, macrophages must divert FC from esterification by ACAT, promote net CE hydrolysis by nCEH, and transfer FC to the plasma membrane. It appears as though HDL interactions with the macrophage cell surface might promote each of these steps [11]: firstly, when cholesterol-loaded mouse peritoneal macrophages were incubated in the presence of HDL, CE levels were significantly reduced [40,41]; and secondly, apolipoprotein (apo) A-I-mediated cholesterol efflux from macrophages has been linked to the mobilisation of cholesterol from an intracellular pool used by ACAT to a specific pool for FC efflux [42].

HDL not only acts as an extracellular acceptor of cholesterol, but also promotes the trafficking of cholesterol from intracellular pools to the plasma membrane using cellular signalling pathways [43]. Slotte *et al.* [44] used cultured human fibroblasts to show that binding of HDL apolipoproteins to a high affinity cell surface receptor induced cholesterol movement from intracellular stores to the plasma membrane. Identical conclusions were also obtained using cholesterol-loaded human monocyte-derived macrophages [45]. Subsequently, Théret *et al.* [46] provided the first evidence that a signalling pathway controlled this HDL-stimulated efflux. This group showed a rapid and transient formation of diacylglycerol (DAG) by adipose cells in response to HDL_3. Consistent with these findings, cholesterol-loaded fibroblasts treated with HDL_3 promoted a transient increase in membrane-associated protein kinase C (PKC) activity [47]. This activation only occurred in response to HDL_3 binding to the cell surface, as tetranitromethane-modified HDL_3 was without effect. In addition, translocation of intracellular cholesterol to the plasma membrane was stimulated with PKC activators and reduced with PKC inhibitors [47]. Finally, in the presence of HDL, cAMP was found to stimulate CE clearance from macrophages [36], possibly via PKA activation [48]. PKA is believed to phosphorylate nCEH and promote the hydrolysis of cytosolic CE, thereby increasing CE mobilisation and FC efflux [8,49]. The receptor(s) involved in binding HDL and activating the mobilisation and efflux of stored cholesterol via signal transduction is central to this process but, to date, the nature of this receptor remains elusive.

1.2.3 CAVEOLAE AND INTRACELLULAR CHOLESTEROL TRAFFICKING

Caveolae are small clathrin-free invaginations of the plasma membrane containing cholesterol-binding proteins, called caveolins, which are essential for caveolae formation. [reviewed in 50,51]. Relative to other domains of the plasma

membrane, caveolae are rich in FC and sphingomyelin and play an important role in cellular cholesterol flux. Caveolae serve as a terminus for the intracellular trafficking of recycled and newly synthesised cellular FC, and as a site for cellular FC efflux. In addition, caveolae are rich in several other intermediates of lipid signalling pathways, including ceramide and phosphoinosides [52,53]. These microdomains have been implicated, therefore, as scaffolds where signalling complexes are assembled and second messenger pathways are activated [54]. Finally, caveolae also serve to internalise selected ligands by endocytosis [50].

FC, derived from *de novo* synthesis, translocates in complexes containing caveolin from the ER to caveolae [55-57], possibly via an intermediate compartment, such as the trans-Golgi network (TGN) [50]. If an extracellular acceptor is present, the majority of FC is transferred out of the cell. However, in the absence of acceptors, newly synthesised FC distributes to other domains of the plasma membrane. Subsequently, FC-depleted caveolin is thought to recycle from the cell surface back to the ER, although this mechanism is poorly understood [50]. The majority of intracellular FC trafficking, however, does not result from FC synthesised *de novo*, but instead involves the recycling of lipoprotein-derived cholesterol. Two alternative models have been proposed, and each model involves the initial fusion of FC-depleted caveolin with endosomes containing LDL-derived FC. These vesicles would then either return to the cell surface directly, or via the TGN, where this pathway might integrate with the trafficking of FC synthesised *de novo*, as described above [50].

The majority of FC efflux from plasma membranes occurs by diffusion: cholesterol desorbs from the plasma membrane pool to the surface of extracellular phospholipid-containing acceptor particles, such as bulk HDL, due to a cholesterol concentration gradient between the membrane and acceptor [58]. Since the caveolar FC pool is the only plasma membrane pool of FC found to be reactive with cholesterol oxidase [59], caveolae are thought to contribute to cholesterol efflux by increasing the accessibility of FC in this microdomain to its extracellular acceptor. The structural protein caveolin is believed to displace FC to the extracellular leaflet of the plasma membrane and thereby promote its efflux [51]. A number of sterol–response elements have been identified in the promoter region of the *caveolin-1* gene, indicating that cellular levels of FC control the expression of this cholesterol-binding protein [60]. Indeed, LDL-derived FC has been found to upregulate the expression of caveolin and

caveolae in many different cell types [61,62]. These findings are consistent with the postulated role of caveolae in FC efflux.

1.3 High-Density Lipoproteins (HDL)

The primary function of lipoproteins is to transport water-insoluble lipids around the bloodstream. It is not surprising, therefore, that each member of the lipoprotein family shares a common macromolecular structure: a lipid-rich core of triglycerides and CE, contained within an amphipathic layer comprising phospholipid and FC molecules, as well as a variety of polypeptides, named apolipoproteins (Figure 1.3). The principal apolipoproteins of HDL are apoA-I and apoA-II, although smaller amounts of apoE and apoC apolipoproteins are also present.

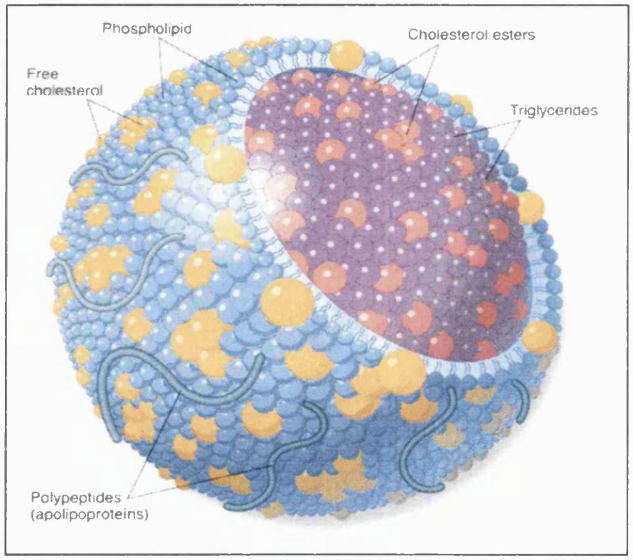

Figure 1.3 Structure of lipoprotein particles

All lipoprotein classes share a common structure: a lipid core of CE and triglycerides contained within a surface coat of various apolipoprotein, phospholipid and FC molecules.

1.3.1 HDL SUBCLASSES

HDL particles are smaller (5 to 17 nm) and have a higher density (>1.063 g/ml) than LDL and VLDL particles. In addition, they are also present in human plasma at higher molar concentrations (10-20-fold) [8]. However, within this class of lipoproteins the HDL particles exhibit a large degree of heterogeneity, varying in size, density, charge, and shape [63]. These characteristics result from differences in lipid concentration, as well as apolipoprotein, enzyme, and lipid transfer protein content. Various subclasses of HDL exist, therefore, which can be isolated using different methods of separation.

Following plasma separation with agarose gel electrophoresis, and immunoblotting with anti-apoA-I, the majority of apoA-I (>85 %) is found to be associated with a fraction that migrates with α-electrophoretic mobility. This α-LpA-I fraction constitutes spherical HDL particles that contain large quantities of stored cholesterol in their lipid-rich cores [8]. The rest of apoA-I (5-15 %) is associated with particles that have pre-β-electrophoretic mobility. This pre-β-LpA-I fraction contains small lipid-poor complexes and flattened HDL particles that are discoidal in shape ('ice hockey puck-like particles'). These particles are separated according to size using polyacrylamide gradient gel electrophoresis: pre-β_1-LpA-I, pre-β_2-LpA-I, and pre-β_3-LpA-I. Lipid-poor pre-β_1-LpA-I particles are the smallest, since they are made up of apoA-I alone, or apoA-I with a few molecules of phosphatidylcholine and sphingomyelin. The larger pre-β_2-LpA-I and pre-β_3-LpA-I discoidal particles are rich in phosphatidylcholine and contain smaller proportions of sphingomyelin and cholesterol compared to the lipid-poor complexes [64,65]. Synthetic discoidal HDL particles were found to vary in lipid content as well as the number of apoA-I polypeptides per particle, which caused particles to differ in diameter, but the thickness of each disc remained constant. Sectional electron microscopy revealed that constant disc thickness resulted from all discs comprising a single bilayer [66]. In addition to pre-β-LpA-I particles, electrophoretic separation also reveals lipid-poor pre-β-LpA-IV and γ-LpE particles, which contain apoA-IV and apoE, respectively, as their only apolipoproteins. Together with the pre-β-LpA-I fraction, these lipid-poor particles avidly sequester excess cellular cholesterol [67,68].

Spherical α-HDL particles can be further differentiated using ultracentrifugation and immunoaffinity chromatography techniques. Firstly, standard ultracentrifugation distinguishes HDL_2 and HDL_3 particles, which are isolated according to density (HDL_2: 1.063-1.125 g/ml; HDL_3: 1.125-1.21 g/ml). Secondly, immunoaffinity chromatography subdivides α-HDL particles according to apolipoprotein content: α-LpA-I/A-II contains both apoA-I and apoA-II, whereas α-LpA-I contains apoA-I as the sole apolipoprotein [69].

1.3.2 APOLIPOPROTEIN A-I STRUCTURE

ApoA-I is synthesised both in the liver [70] and the intestine [71] as pre-pro-apoA-I. Following co-translational cleavage of the 18-residue signal peptide, apoA-I appears in the circulation as the 249 amino acid pro-protein [72]. Finally, this is processed to the 243 residue mature form of apoA-I comprising a globular amino-terminal domain (residues 1-43) and a lipid-binding carboxyl-terminal domain (residues 44-243), containing a number of amphipathic α-helices [73]. The amphipathic α-helix was originally defined as an α-helix with opposing polar and non-polar faces oriented along the long axis of the helix [74]. It is a common structural motif shared by all exchangeable apolipoproteins (A-I, A-II, A-IV, CI, CII, CIII and E) that serves to associate with lipid and stabilise the lipoprotein structure [73]. Protein sequence analysis of apoA-I lipid-binding domain revealed ten repeated amino acid sequences (eight 22-mer and two 11-mer repeats) in tandem, with each repeat having the periodicity of an amphipathic α-helix [75]. Nolte and Atkinson subsequently used circular dichroism to determine its secondary structure, and proposed an α-helical structure for this lipid-binding domain [76]. When this C-terminal domain was studied using 4-Å resolution X-ray crystallography, an almost continuous amphipathic α-helical horseshoe-shaped structure with proline-induced kinks was determined [77]. In addition, four apoA-I lipid-binding domains were found to associate via their hydrophobic faces to produce two antiparellel dimers. Unfortunately, it was not possible to conclude that the structure determined using X-ray crystallography was identical to that of lipid-associated apoA-I, since the data had been generated from aqueous phase crystals.

Two different models have been proposed for the correct orientation and conformation of apoA-I on the rim of discoidal nascent HDL particles: firstly the 'picket-fence' model, where the amphipathic helical repeats form tandem anti-parallel helices, perpendicular to the disc plane [78]; and secondly the 'double-belt' model, where two apoA-I molecules form essentially continuous amphipathic helices around, and parallel to the plane of, the disc [79] (Figure 1.4). More recently, a detailed molecular belt model was proposed for the structure of the lipid-binding domain of apoA-I on the smallest discoidal HDL particles [80]. These particles comprise two apoA-I molecules wrapped around a bilayer containing 160 lipid molecules. The predicted structure uses the assumption that lipids force constraints on the orientation and conformation of their associated proteins, as well as the hypothesis that apoA-I conformation results from the maximisation of interhelical salt bridge interactions. Having explored all possible

geometries for generating apoA-I dimers, the apoA-I structure resulting in the best alignment of salt bridges was found to be identical to that of lipid-free apoA-I, determined by X-ray crystallography [77]. It therefore appears that the structure of apoA-I dimers in nascent discoidal HDL conforms to this double-belt model.

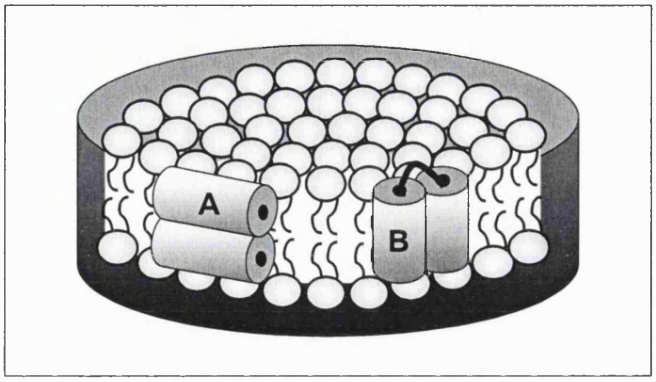

Figure 1.4 Possible orientations of apoA-I amphipathic helices in discoidal HDL

This figure is adapted from Segrest et al. [81]. ***A,*** *'Double-belt' model: two apoA-I molecules form essentially continuous amphipathic helices around, and parallel to the plane of, the disc.* ***B,*** *'Picket-fence' model: the amphipathic helical repeats form tandem anti-parallel helices, perpendicular to the disc plane.*

1.4 HDL Metabolism

Unlike triglyceride-rich lipoproteins that are generated and secreted from the liver, HDL formation occurs in the circulation. HDL biogenesis begins with the association of circulating lipid-poor apoA-I particles with cholesterol and phospholipid, to generate discoidal pre-β-HDL particles. The HDL-associated enzyme lecithin-cholesterol acyl transferase (LCAT) is then responsible for esterifying FC and generating mature, spherical HDL particles, which can be further remodelled by the action of plasma enzymes and transfer proteins [reviewed in 65].

1.4.1 GENERATION OF DISCOIDAL PRE-β-HDL PARTICLES

Circulating lipid-free apoA-I or lipid-poor apoA-I particles are generated and secreted from hepatocytes [70] and intestinal mucosal cells [71]. These lipid-poor precursors avidly sequester FC and phospholipids from plasma membranes as well as triglyceride-rich lipoproteins (e.g. VLDL), to generate discoidal pre-β-HDL.

The 'gatekeeper' for phospholipid and FC efflux from peripheral cell membranes has recently been defined as the ABCA1 transporter [reviewed in 82]. Its critical role in HDL biogenesis was determined following the discovery of *ABCA1* gene mutations in patients with Tangier disease: a rare recessive disorder resulting in the defective removal of cellular cholesterol and phospholipids by lipid-poor apoA-I (Figure 1.5) [83-86]. Since apoA-I is unable to sequester cholesterol and phospholipid to generate discoidal pre-β-HDL, the apoA-I protein is rapidly catabolised by the kidney *(Section 1.6.4)*, and the disease is therefore characterised by extremely low levels of apoA-I and HDL, with CE accumulation in cells [87].

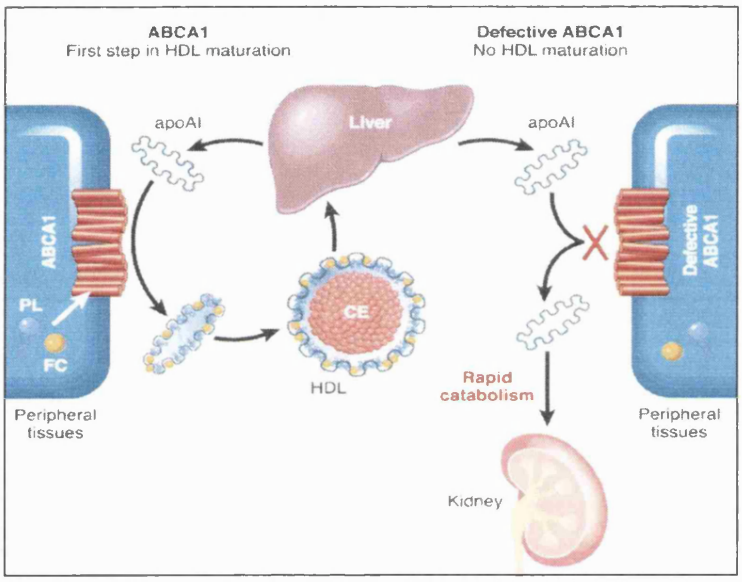

Figure 1.5 ABCA1 controls the first step in HDL maturation

In the first stage of HDL maturation, ABCA1 mediates the efflux of cellular phospholipid and cholesterol to lipid-poor apoA-I. In Tangier disease, defective ABCA1 fails to promote enough lipid efflux to apoA-I, which is then rapidly cleared by the kidney rather than entering the HDL maturation cascade.

ABCA1 belongs to the ATP-binding cassette family of genes encoding transmembrane proteins that use ATP as a source of energy for the transportation of a wide range of substrates (e.g. ions, amino acids and proteins, sugars, phospholipids and a range of drugs) across the plasma membrane, as well as intracellular membranes of the ER and mitochondria [88]. Each member of the family contains six membrane-spanning domains and a cytosolic ATP-binding cassette, comprising two conserved peptide motifs (Walker A and Walker B motifs) and a unique amino acid signature sequence between each Walker motif [89]. ABC transporters with only one cassette and transmembrane

region are known as 'half-transporters', that assemble their units as homo- or hetero-dimers to make a functional transporter [90]. ABCA1, however, contains two of these units, linked by a highly hydrophobic segment, which is presumably an essential component for the translocation of lipids.

Since both HDL cholesterol and phospholipids are almost completely absent in plasma from patients with Tangier disease, it was initially concluded that ABCA1 functions to transport both of these lipids across the plasma membrane: upon ATP binding and hydrolysis, cholesterol and phospholipids are rapidly flipped from the inner to the outer leaflet of the membrane bilayer, where lipid-poor apoA-I avidly sequesters them. However, a direct role for ABCA1 in the translocation of either lipid had not been demonstrated. Cholesterol and phospholipid efflux studies on SMCs and endothelial cells by Fielding *et al.* [91] revealed that translocation of these two lipids is not concurrent but takes place in two stages. When FC efflux from SMCs expressing high levels of ABCA1 was inhibited, phospholipid efflux was still found to occur. In addition, when conditioned media (containing apoA-I previously incubated with SMCs) was transferred to ABCA1-deficient endothelial cells, it stimulated the efflux of FC from endothelial cells, but not phospholipid. They also found phospholipid-apoA-I complexes to be much better acceptors of FC than apoA-I itself. Similar studies have also revealed that apoA-I binding to ABCA1 is closely associated with phospholipid translocation, and that this activity can be completely dissociated from FC efflux [92]. Taken together these experiments point towards a two-step mechanism of phospholipid and FC efflux: initially ABCA1 actively translocates phospholipids across the membrane to circulating lipid-poor apoA-I particles to generate discoidal phospholipid-apoA-I complexes, which then avidly sequester FC that traverses the plasma membrane by diffusion (Figure 1.6). ABCA1 therefore functions indirectly as a cholesterol efflux regulatory protein to promote pre-β-HDL formation.

A second source of FC and phospholipids for pre-β-HDL generation is provided by triglyceride-rich lipoproteins (TRL), such as VLDL. Following hydrolysis of core triglycerides by LPL, much of the phospholipid monolayer becomes redundant relative to the depleted lipid core. The phospholipid transfer protein (PLTP) transfers phospholipid and FC from the surface of TRL to lipid-poor apoA-I particles. The important role of PLTP in HDL metabolism was established using PLTP-knockout mice: firstly, the *in vivo* transfer of radiolabelled phospholipid from VLDL to HDL was

completely abolished and secondly, the mice showed marked decreases in HDL phospholipid (60 %) and cholesterol (65 %), but no significant changes in apoB levels or non-HDL lipid compared to wild-type mice [93]. Furthermore, LPL knockout mice, which only survived up to 18 h after birth, were found to have massive hypertriglyceridaemia and very low plasma HDL levels [94], whereas over-expression of human LPL increased plasma HDL and lowered levels of triglyceride-rich lipoproteins [95]. These experiments show an inverse relationship between hypertriglyceridaemia and plasma HDL levels, and demonstrate the importance of successful transfer of surface components from triglyceride-rich lipoproteins for HDL biogenesis and maintenance of plasma HDL levels.

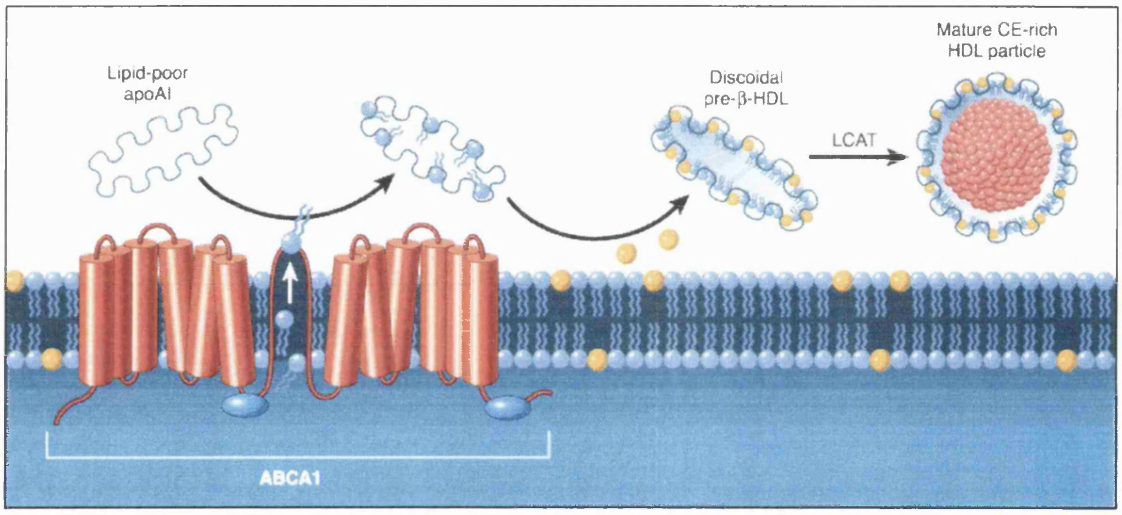

Figure 1.6 ABCA1 effluxes cholesterol by a two-step mechanism

The true ABCA1 substrates are now identified as phospholipids, which are flipped across the membrane to bind apoA-I and form discoidal phospholipid-apoA-I complexes. These complexes then avidly sequester excess cholesterol, which unlike phospholipids rapidly traverses the membrane by diffusion.

1.4.2 GENERATION OF SPHERICAL α-HDL PARTICLES

Maturation of discoidal pre-β-HDL particles into lipid-rich, spherical α-LpA-I particles results from three processes. Firstly, the lipid-poor apoA-I particles acquire FC and phospholipids derived from cell membranes or circulating apoB-containing lipoproteins. Secondly, the FC becomes esterified at its hydroxyl position with a long-chain fatty acid. Thirdly, the apoA-I containing particles associate with additional apolipoproteins, such as apoE and apoC. Cholesterol esterification involves the transfer of an acyl chain from phosphatidylcholine (lecithin) to cholesterol, and is mediated by the action of LCAT [96-98]. LCAT is a soluble enzyme that is secreted by the liver and

binds to the surface of HDL. It is activated by the major apolipoprotein of HDL, apoA-I, to catalyse the following reaction:

cholesterol + lecithin → cholesteryl ester + 2-lysolecithin

HDL lipid composition is thought to contribute significantly to the ability of apoA-I to activate LCAT, either by determining apoA-I conformation or the availability of the enzyme to its substrate [99]. Indeed, small complexes with a low phospholipid/A-I molar ratio are found to be more efficient at LCAT activation than larger complexes with a higher ratio [100]. The mechanism by which apoA-I activates LCAT is not clear, although natural and synthetic apoA-I mutants have identified the central helixes 5-7 of apoA-I to be involved [99]. In small, discoidal pre-β-HDL, the central helices of apoA-I may not interact completely with lipids, allowing greater accessibility of LCAT to the lipid interface and the central domain of apoA-I, thereby promoting its activity in these particles.

The importance of LCAT for the generation of mature spherical HDL is seen in transgenic mice deficient in LCAT, which exhibit greater than 90 % reduction in HDL levels [101]. LCAT esterification of amphipathic cholesterol generates hydrophobic CE, which partitions into the lipid-rich core of the lipoprotein particle, thereby causing the discoidal particle to become spherical in shape. The increasing core CE content contributes to the progressive enlargement of HDL_3 particles to HDL_2 and HDL_1 particles. These mature HDL particles are found to induce cholesterol efflux, in a non-specific, slow, saturable and bi-directional manner, which appears to take place by aqueous diffusion [8]. LCAT contributes to this process by removing diffusible FC from the surface of HDL and maintaining the cholesterol gradient from the cellular plasma membrane to HDL [102]. Lipid-rich HDL particles also induce specific cholesterol efflux: HDL-mediated cholesterol efflux correlates with expression of SR-BI *(Section 1.6.3)*.

The majority of HDL CE is subsequently returned to the liver for bile synthesis and excretion, although HDL CE is also delivered to steroidogenic tissues for steroid hormone production. Selective uptake of HDL CE by steroidogenic tissues and the liver takes place directly via SR-BI [103], or indirectly in a process involving the cholesteryl ester transfer protein (CETP). This protein mediates the transferral of HDL CE to TRL,

by stimulating the exchange of CE and triglycerides [8], followed by the uptake of TRL remnants by the liver.

1.4.3 REMODELLING OF HDL PARTICLES

In humans, circulating HDL particles are continuously remodelled by lipid transfer proteins, such as CETP and PLTP, and the enzyme, hepatic lipase (HL). A schematic diagram representing the key players in HDL metabolism is shown in Figure 1.7. The CETP-mediated transfer of CE from HDL to TRL not only promotes the reduction in HDL particle size, but it is also accompanied by the progressive dissociation of lipid-free apoA-I from the HDL particles [104]. HL functions in a similar manner to CETP: HL is associated with reduced α-HDL particle size, as well as pre-β_1-HDL formation [105]. HL is a cell surface-bound enzyme capable of hydrolysing phospholipids and triglycerides in plasma lipoproteins. In HDL metabolism, phospholipid hydrolysis is likely to be the most physiologically relevant action of HL since HDL particles contain larger quantities of phospholipid than triglyceride. HL acts to deplete HDL phospholipid and thereby facilitates the removal of CE from HDL by CETP [106] and SR-BI uptake [107]. Both HL and CETP have important roles to play in HDL catabolism: patients with genetic deficiencies of CETP or HL show markedly increased levels of plasma HDL [108,109]. These two HDL remodelling enzymes therefore serve to shrink HDL size and regenerate lipid-poor pre-β_1-HDL particles, which then begin another round of HDL biogenesis.

In addition to its role as a remodelling enzyme, HL has been found to enhance both the binding and uptake of apoB-containing lipoproteins and/or their lipids, by different cells *in vitro* [110]. More recently, HL was shown to enhance SR-BI-mediated CE uptake from HDL 3-fold; this process involved both the lipolytic and the non-lipolytic functions of the enzyme. SR-BI and HL therefore act synergistically to promote the uptake of lipids from mature HDL particles [107].

The final HDL remodelling enzyme to be discussed is PLTP, which is able to fuse together two HDL_3 particles, leading to the concomitant formation of a large, CE-rich HDL_2 particle and a small pre-β_1-HDL particle [111]. It appears, therefore, as though PLTP functions to enhance both pre-β_1-HDL-mediated cholesterol efflux from cells, as well as the efficient delivery of CE to the liver via large, CE-rich HDL_2 particles [112].

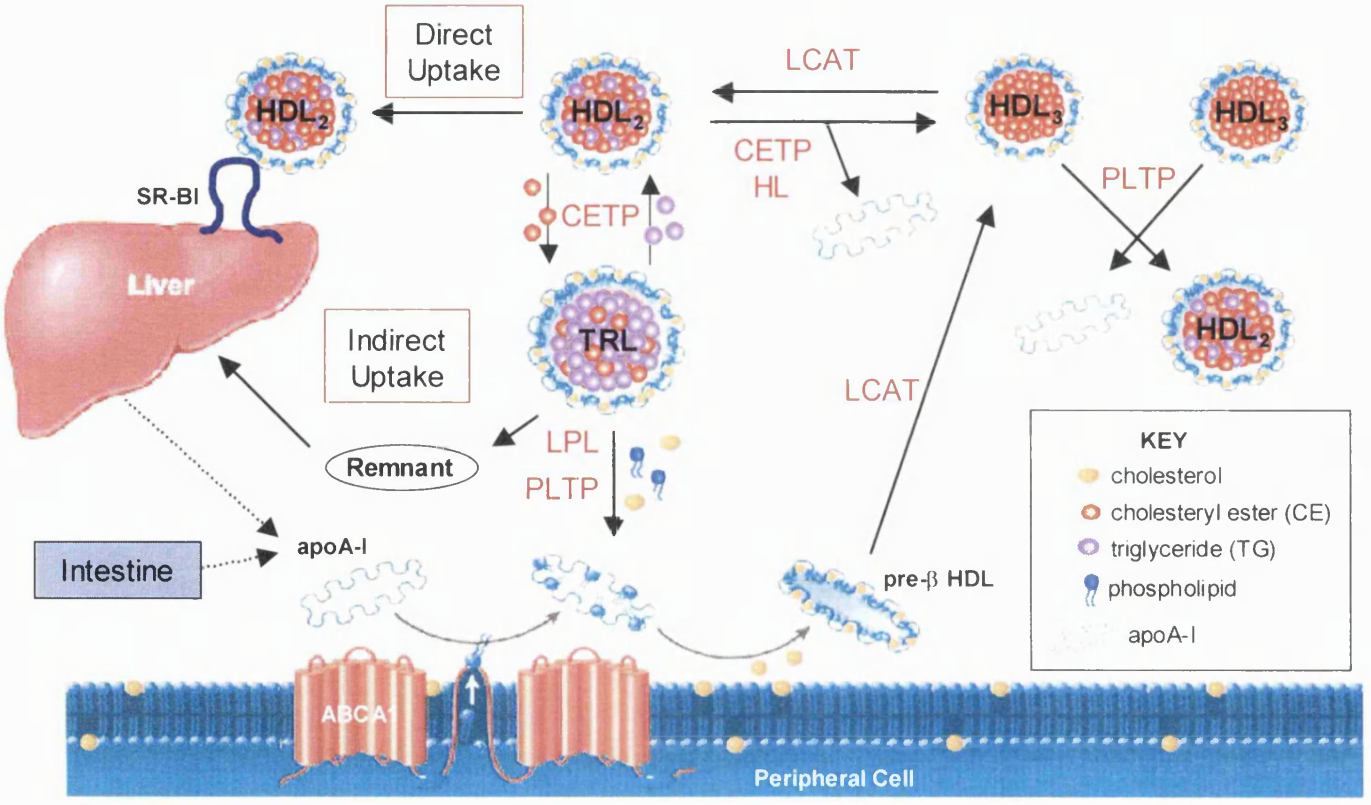

Figure 1.7 Schematic diagram representing the key enzymes involved in HDL metabolism

The liver and intestine secrete lipid-poor apoA-I. ABCA1 actively transports phospholipids and cholesterol (indirectly) from peripheral cells to apoA-I to generate discoidal pre-β-HDL particles (as described in Figure 1.5). Cholesterol is esterified by lecithin-cholesterol acyl transferase (LCAT) to produce CE, which partitions to the hydrophobic core of mature, spherical HDL_3 and then HDL_2 particles. HDL CE is taken up directly by the liver via SR-BI, or it is exchanged for TG from triglyceride-rich lipoproteins (TRL) by the cholesteryl ester transfer protein (CETP). TRL are subsequently hydrolysed by lipoprotein lipase (LPL) to generate remnants that are cleared by the liver (indirect uptake), and lipids that are transferred to apoA-I via the phospholipid transfer protein (PLTP) to generate pre-β-HDL. The actions of CETP and hepatic lipase (HL) promote the reduction of HDL particle size (HDL_2 to HDL_3) and the dissociation of lipid-poor apoA-I particles, whereas PLTP is able to fuse two HDL_3 particles and generate HDL_2 and lipid-poor apoA-I. These apoA-I particles enter another cycle of HDL biogenesis.

1.5 Biological Functions of HDL

It is well established that an inverse correlation exists between plasma levels of HDL cholesterol and coronary heart disease [113]. This relationship can be explained by the ability of HDL to maintain cholesterol homeostasis in the body by collecting excess peripheral cholesterol and delivering it to the liver for excretion into bile; the process known as reverse cholesterol transport (RCT) [8]. In addition to RCT, HDL also exerts several other atheroprotective activities, including the inhibition of LDL oxidation, platelet aggregation, and leukocyte adhesion to the endothelium [reviewed in 114].

1.5.1 REVERSE CHOLESTEROL TRANSPORT

All cells require cholesterol, a key structural component of membranes, which they either obtain from the internalisation of LDL, via specific cell surface receptors, or synthesise *de novo (Section 1.2.1)*. However, apart from hepatocytes, cells are unable to catabolise excess cholesterol that accumulates. Therefore, in order for cellular cholesterol homeostasis to be maintained, it is critical that excess cholesterol is transported from the periphery for catabolism by the liver. Distortion of this process may promote the deposition of cholesterol in the arterial wall and progression of atherosclerosis [114].

Since HDL biogenesis necessitates the removal of membrane FC to generate discoidal pre-β-HDL particles, HDL therefore promotes RCT during its generation. Mature, spherical α-LpA-I particles also contribute significantly to RCT by promoting aqueous diffusion of excess cholesterol, as well as receptor-mediated cholesterol efflux [115,116]. Furthermore, the HDL-associated enzyme LCAT plays a vital role in driving RCT: LCAT esterification of FC prevents re-diffusion of FC from HDL back to the membrane, and therefore enhances net cholesterol efflux [102]. LCAT esterification also promotes the generation of mature, spherical α-LpA-I particles, which can then be cleared from the circulation by the liver, during the final step of RCT *(Section 1.4.2)*. Finally, in addition to HDL cholesterol clearance by the liver, HDL cholesterol is also delivered to steroidogenic tissues for steroid hormone production. This represents another important function of HDL [117].

1.5.2 ADDITIONAL ATHEROPROTECTIVE FUNCTIONS OF HDL

1.5.2.1 Inhibition of LDL oxidation

Ox-LDL is central to the pathogenesis of atherosclerosis. For example, Ox-LDL induces endothelial cells to express monocyte-specific chemoattractants [118] and adhesion molecules [119]; it is rapidly engulfed by macrophages to generate foam cells; and it stimulates SMC migration and proliferation [120]. During oxidation of LDL, polyunsaturated fatty acyl chains are attacked by reactive oxygen species to yield highly reactive lipid peroxidation products, which promote atherogenesis. HDL has a vital anti-atherogenic function to protect LDL against oxidative damage [121]. This protection involves HDL-associated enzymes that metabolise oxidised lipids [122-125], including paraoxonase, platelet-activating factor-acetyl hydrolase and LCAT. In addition, the HDL apolipoproteins, apoA-I and apoE, have intrinsic antioxidant activity; for example, lipid-free apoE is thought to inhibit copper-mediated lipoprotein oxidation by binding metal ions [126].

1.5.2.2 Protection of endothelial cells

HDL plays an important anti-atherogenic role in the prevention of Ox-LDL-mediated endothelial dysfunction. Firstly, HDL is proposed to antagonise Ox-LDL inhibition of endothelial nitric oxide (NO) production [127]. NO functions in a variety of atheroprotective ways: it increases vessel relaxation, inhibits SMC proliferation and platelet activation, and reduces monocyte recruitment to the vessel wall [114]. Secondly, HDL functions to promote endothelial cell proliferation, thereby maintaining integrity of the endothelial cell layer and decreasing exposure of the thrombogenic vessel wall [128]. Finally, HDL is found to increase prostacyclin and natriuretic peptide C synthesis by endothelial cells [129,130], which act to promote vasodilation and inhibit SMC proliferation. In addition, prostacyclin also inhibits platelet activation [114].

1.5.2.3 Inhibition of leukocyte adhesion to the endothelium

Leukocyte adhesion to activated endothelial cells signifies a crucial development in atherogenesis, as it precedes the transmigration of monocytes into the arterial wall and subsequent foam cell generation. E-selectin is responsible for tethering and rolling monocytes on the endothelial surface, before they become firmly adhered to VCAM-1 or ICAM-1. HDL was reported to strongly inhibit the expression of each of these adhesion molecules in human umbilical vein endothelial cells, activated by tumor necrosis factor

(TNF) or interleukin-1 [131]. Further studies revealed a potential mechanism by which HDL might inhibit E-selectin expression: HDL inhibited TNF-α stimulated activation of sphingosine kinase, and thereby prevented the generation of sphingosine-1-phosphate, which induces E-selectin expression in endothelial cells [132]. However, this atheroprotective function of HDL is controversial, as more recent findings using human coronary artery endothelial cells, a model directly relevant to blood vessels susceptible to atherosclerosis, revealed an inability of HDL to inhibit cell adhesion molecule expression [133].

1.5.2.4 Inhibition of platelet aggregation

HDL exerts an inhibitory effect on another process associated with endothelial injury in atherogenesis: platelet activation. Initially, *in vitro* studies revealed a role for HDL in the inhibition of induced platelet aggregation [134]. More recently, low HDL cholesterol was found to be an independent predictor of platelet-dependent thrombus formation *in vivo* [135], revealing another important anti-atherogenic role for HDL. HDL exerts inhibition of platelet activity using two different pathways. The first mechanism is dependent upon the presence of apoE within the lipoprotein particles [136]. ApoE is believed to bind to the apoE receptor 2 (apoER2) on platelets [137], which in turn activates NO synthase to generate NO [138]. The second mechanism is apoE-independent, as HDL particles lacking apoE are still able to exert inhibitory effects on thrombin-induced platelet activation [139]. This pathway involves HDL activation of PKC, which inhibits the release of intracellular calcium by promoting alkalinisation of the cytoplasmic compartment [140], and by inhibiting thrombin-induced phosphatidylinositol-specific phospholipase C [141].

1.6 HDL Receptors

1.6.1 LIPOPROTEIN RECEPTORS

The majority of lipoprotein receptors belong to the LDL-receptor gene family. Currently, there are seven type I membrane proteins that make up this family, including the LDL receptor, VLDLR, LRP, megalin and apoER2 [reviewed in 142,143]. Family members are modular in structure, with large extracellular domains containing a variable number of LDL receptor ligand binding repeats. The varying number and arrangement of these repeats contribute to the diverse ligand-binding potential of the receptors. These

receptors also contain epidermal growth factor (EGF) precursor repeats, which are necessary for acid-dependent ligand release in endosomal compartments [144], as well as a single membrane-spanning segment. Their intracellular domains also contain protein docking sites, and the NPXY internalisation motif to direct receptors to clathrin-coated pits. Ligand endocytosis is yet another common feature exhibited by all members of the LDL receptor gene family and is essential for their physiological function. Furthermore, in addition to receptor-mediated endocytosis, recent data also implicates certain members of this family to have a pivotal role in transmembrane signalling and neuronal development *(Section 1.6.5.3).*

In contrast to the well-characterised process of LDL uptake by receptor-mediated endocytosis *(Section 1.2.1)*, little was known regarding the mechanism of HDL lipid uptake, as no physiological HDL receptor had been identified. The mechanism, however, appeared to be distinct from the LDL receptor paradigm since pharmacological inhibitors of endocytosis failed to inhibit HDL lipid uptake [145]. Over the last five years, our understanding of HDL-cell interactions has vastly increased with the identification of SR-BI as a physiologically relevant HDL-binding protein that mediates HDL lipid uptake *(Section 1.6.3).*

1.6.2 HDL-BINDING PROTEINS

Twenty years ago, a variety of cultured cells, including hepatocytes, fibroblasts, and steroidogenic tissues, were reported to contain specific HDL binding sites [146-148]. This discovery prompted the search for the identity of cell surface receptors that can recognise HDL. Unfortunately, the search was hampered due to the large number of non-specific, cell surface HDL binding sites that introduced many false positives into the purification and cloning procedures [reviewed in 149]. In the last decade, a few HDL binding proteins have been identified and these will be discussed below.

1.6.2.1 HDL binding protein (HBP)

Initially, ligand-blotting studies revealed a membrane protein of 110 kDa, which bound HDL as well as apoA-I and apoA-II proteoliposomes, and exhibited enhanced binding activity upon cholesterol loading [150]. Following isolation of a cDNA clone encoding this novel protein, named HDL binding protein (HBP), McKnight *et al.* [151] subsequently demonstrated that mRNA expression of HBP was indeed upregulated upon cholesterol loading. Unfortunately, this 'novel' HDL binding protein was later found to

be identical to vigilin. The predicted structure of HBP/vigilin revealed that it neither contained a transmembrane domain nor any clearly defined cytoplasmic/extracellular domains and therefore lacked the properties of a typical cell surface receptor. Although cytoplasmic HBP/vigilin may become attached to the cell surface where it can then bind HDL, it appeared unlikely that HBP/vigilin functions as a physiological HDL receptor. Since vigilin binds RNA, it is more likely that this cytoplasmic protein influences RNA metabolism by stabilising mRNA [152].

1.6.2.2 HDL-binding proteins 1 and 2 (HB_1 and HB_2)

More recently, two candidate liver HDL receptors, named HB_1 and HB_2, with molecular weights of 120 and 100 kDa, respectively, have also been isolated and purified [153]. Since HB_1 is present in such low amounts, its sequence has yet to be determined. However, the more abundant candidate HDL receptor, HB_2, was purified in sufficient quantities to generate sequence data and was subsequently cloned and characterised [154]. The cDNA of HB_2 encoded a 65 kDa protein, which was considerably smaller than the apparent size of the 100 kDa protein identified by ligand blotting, indicating that this receptor is heavily glycosylated. HB_2 was not found to be structurally related to any of the other lipoprotein receptors, yet over the entire coding region, rat HB_2 showed a high degree of homology with two adhesion proteins from the immunoglobulin (Ig) superfamily: 93 % homology with human activated-leukocyte cell adhesion molecule (ALCAM) and 70 % homology with the avian bursal epithelium and neuron protein. This group of membrane proteins are characterised by the presence of a 32-amino acid C-terminal cytoplasmic tail, a 24-amino acid hydrophobic transmembrane domain and a large extracellular and N-terminal domain comprising approximately 500 residues with eight potential glycosylation sites [149].

When HB_2 cDNA was transfected into COS, HepG2 and CHO cells, HDL_3 binding was increased by 80-100 %. More interestingly, upon differentiation of THP-1 monocytes into macrophages, there was a remarkable increase in HB_2 mRNA expression, from almost undetectable levels in undifferentiated monocytes. And upon cholesterol loading of the macrophages, a dose-dependent decrease in HB_2 was observed [154]. Since HB_2/ALCAM is an adhesion molecule, this surface protein may contribute to the initial stages of atherogenesis by increasing macrophage migration into the vessel wall. HB_2/ALCAM binding of HDL would therefore reduce migration by competing for binding sites. It is in this way that HDL might exert another anti-atherogenic effect on

adhesion molecules *(Section 1.5.2.3).* Furthermore, due to evidence that HDL promotes signalling pathways [43] and that some members of the adhesion molecule family act as signalling receptors, HB_2/ALCAM may also function to activate signal transduction [149]. Therefore, due to its typical surface receptor properties, and to the association between its expression and cholesterol metabolism, HB_2/ALCAM is much more likely than HBP to function as a physiological HDL receptor, although further work is necessary to fully elucidate its role as such.

1.6.3 SCAVENGER RECEPTOR CLASS B, TYPE I (SR-BI)

In 1994, Acton *et al.* [155] used expression cloning to identify the cDNA for a new scavenger receptor, named scavenger receptor class B, type I (SR-BI). Hamster (ha) SR-BI was cloned on the basis of its ability to bind chemically modified LDL, such as Ox-LDL and acetylated LDL (Ac-LDL). Subsequent ligand binding studies revealed that the ligand specificity of haSR-BI was similar to that of the CD36 scavenger receptor; for example, only these two scavenger receptors are able to bind HDL. SR-BI and CD36 were therefore placed together as members of a new family of scavenger receptors, designated class B. Surprisingly, unlike all other scavenger receptors, haSR-BI was also found to bind native LDL with high affinity [155]. A year previously, the human homologue of haSR-BI had been cloned by PCR methodology and termed CLA-1 (CD36 and LIMPII Analogous-1) due to its homology with the scavenger receptor CD36 and the lysosomal integral membrane protein (LIMP) II [156], but its function had never been reported [157]. Following identification of haSR-BI as a novel scavenger receptor, human CLA-1 was characterised and found to share identical properties [158] and has since been renamed SR-BI.

1.6.3.1 SR-BI: the first physiological HDL receptor

A major breakthrough in our understanding of HDL metabolism came in 1996, when Acton *et al.* [103] identified murine (m) SR-BI as a physiologically relevant HDL receptor: SR-BI binds HDL with high affinity; SR-BI is abundantly expressed in tissues involved in HDL CE selective uptake, such as the liver and steroidogenic tissues; and SR-BI mediates the selective uptake of cholesterol from HDL. Firstly, LDL receptor-negative CHO cells transfected with mSR-BI cDNA were found to specifically associate with ^{125}I-labelled HDL with high affinity and saturability, whereas significantly fewer HDL particles associated with untransfected cells. Following HDL binding to SR-BI, the fates of HDL protein (apoA-I) and lipid were compared: unlike the apolipoprotein B

protein component of LDL, which gets broken down in the lysosome following LDL receptor endocytosis, apoA-I was not degraded, yet radiolabelled lipid still accumulated within the cells. This data was consistent with the findings of Pittman *et al.* [145], who showed that pharmacological inhibitors of endocytosis mediated by clathrin-coated pits failed to inhibit HDL selective uptake. This indicated that SR-BI uses an alternative mechanism of lipid uptake to that used by the LDL receptor.

1.6.3.2 *In vivo* role for SR-BI in cholesterol uptake

Since the identification of SR-BI as an HDL receptor involved in lipid uptake, transgenic and gene-targeting experiments in mice have confirmed the crucial role that hepatic SR-BI plays in murine HDL metabolism *in vivo*. Hepatic over-expression of the *SR-BI* gene in mice, using adenovirus-mediated gene transfer, resulted in lower plasma HDL cholesterol concentrations [159-161] and increased biliary cholesterol concentrations [159]. In contrast, SR-BI knockout mice exhibit elevated plasma HDL cholesterol concentrations, decreased biliary cholesterol content and adrenal cholesterol insufficiency [117,162,163]. Furthermore, anti-SR-BI blocking antibodies that prevent HDL particles from binding the extracellular domain of SR-BI, blocked HDL CE uptake by cultured mouse adrenocortical cells, resulting in a decreased production of steroid hormones [164]. Finally, transgenic mice with moderate SR-BI over-expression exhibited a two-fold decrease in the development of diet-induced atherosclerotic lesions [165]. This prominent anti-atherogenic effect of moderate SR-BI expression provides *in vivo* support for the role of SR-BI in facilitating RCT. Taken together, these findings show the importance of SR-BI in controlling the uptake of HDL cholesterol from the circulation by hepatocytes (for its secretion into bile) and steroidogenic tissues (for hormone production).

1.6.3.3 Regulation of SR-BI expression

In agreement with its role as a physiological HDL receptor, SR-BI expression is under feedback control. When high-dose estrogen treatment was administered to rats, SR-BI expression was dramatically reduced in the liver, yet increased in the adrenal gland and corpus luteal cells of the ovary [166]. The cholesterol content of adrenal cells was also found to independently control SR-BI expression *in vivo* [167], although this was overridden by adrenocorticotrophic hormone regulation [168]. These studies are consistent with the idea that key steroid hormones upregulate SR-BI expression in order to supply greater quantities of precursor cholesterol to tissues for the synthesis of

additional steroid hormones. Furthermore, SR-BI expression can be regulated by dietary manipulations: hamsters fed a high polyunsaturated fat diet exhibited upregulation of hepatic SR-BI expression by ~50 %, compared to hamsters fed saturated fatty acids [169]. This finding provided a mechanistic basis to explain how high levels of polyunsaturated fatty acids might lower plasma HDL concentrations [170]. The promoter region of the human SR-BI gene contains consensus-DNA binding sequences for the following transcription factors: steroidogenic factor-1, sterol regulatory element binding proteins, and Sp1 family members [171-173]. It is likely that these transcription factors regulate SR-BI expression in response to hormones, cholesterol and polyunsaturated fatty acids.

Finally, since SR-BI also facilitates the cellular uptake of non-lipoprotein cholesterol [174] and is expressed in the intestine of rodents [166], scientists investigated the regulation of intestinal SR-BI expression. Voshol *et al.* [175] discovered that intestinal SR-BI levels were reduced in rodents with deficient bile delivery to the intestine, although mRNA levels were unaffected. This indicates that bile components may play a role in post-transcriptional regulation of SR-BI expression. However as yet, the exact role of SR-BI in dietary cholesterol absorption has not been defined.

1.6.3.4 Structure and localisation of SR-BI

The 509-amino acid sequence of SR-BI is very similar in structure to the other class B scavenger receptor, CD36: they both contain short N-terminal and C-terminal cytoplasmic tail sequences, which sit adjacent to hydrophobic transmembrane domains, and the majority of each polypeptide chain is located in between the membrane-spanning domains in a large extracellular loop (SR-BI is represented in Figure 1.8). Both extracellular regions contain many potential glycosylation sites. Indeed, SR-BI is found to be substantially glycosylated with N-linked oligosaccharide chains, to the extent that deglycosylation results in a reduction of molecular mass from 82 kDa to 54 kDa [176]. These two class B scavenger receptors are also found to be palmitoylated [176,177]; palmitoylation of SR-BI is believed to occur on two cysteine residues located at the junction between the C-terminal cytoplasmic tail and the transmembrane domain (Cys^{462} and Cys^{470}). Further metabolic labelling studies revealed that mSR-BI is also myristoylated [176]. This fatty acylation is thought to take place within the first eight residues of mSR-BI, which are compatible with consensus myristoylation sequences, based on Src family sequences [178] and the activity of *N*-myristoyltransferase [179].

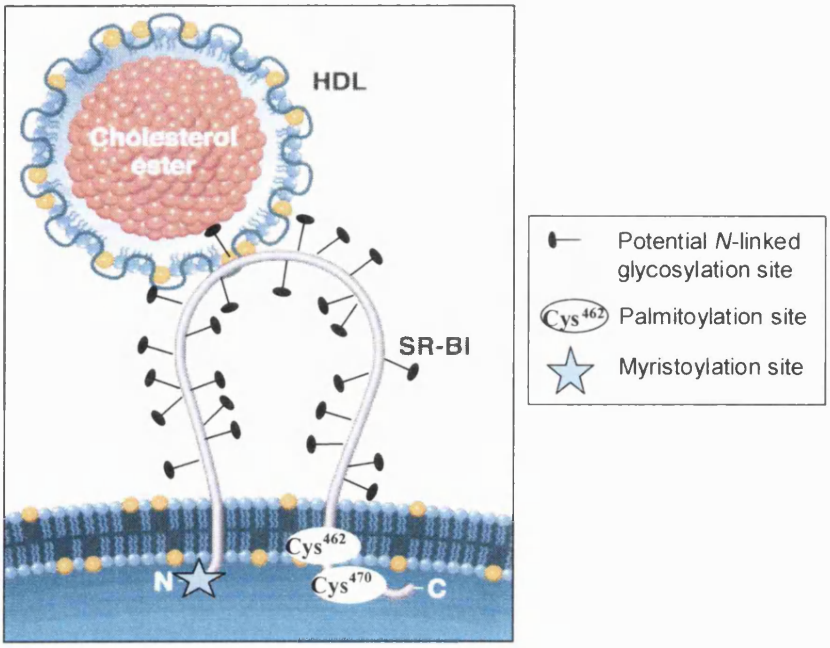

Figure 1.8 Structure and post-translational modification of SR-BI

SR-BI contains short N-terminal and C-terminal cytoplasmic tail sequences, which sit adjacent to hydrophobic transmembrane domains. The majority of each polypeptide chain is located in between the membrane-spanning domains in a large extracellular loop, containing many potential N-linked glycosylation sites. Palmitoylation of SR-BI is thought to occur on two conserved cysteine residues located at the junction between the C-terminal cytoplasmic tail and the transmembrane domain (Cys^{462} and Cys^{470}), whereas myristoylation takes place at the N-terminus.

Modification of proteins by fatty acylation increases the hydrophobicity of the amino acid side chains, which may assist in targeting proteins to membranes [180,181]. Indeed, dual myristoylation and palmitoylation of membrane proteins, such as endothelial NO synthase (eNOS), was found to be both necessary and sufficient for protein targeting to specialised microdomains of the plasma membrane called caveolae [182-184]. Caveolae are invaginations of the plasma membrane involved in cellular cholesterol flux and signal transduction *(Section 1.2.3)*. These microdomains are enriched in cholesterol and sphingomyelin, and contain the cholesterol binding protein caveolin, which is necessary for caveolae formation [185,186]. Like CD36, fatty acylated SR-BI is found to co-localise with caveolae in recombinant cells, and co-purifies with caveolin-1, the major structural protein of caveolae [176,187,188]. SR-BI therefore concentrates in microdomains of the plasma membrane distinct to the LDL receptor, which localises to clathrin-coated pits [189]. Not surprisingly, caveolae were

found to be the initial acceptors of SR-BI-mediated selective lipid uptake [190]. In addition, THP-1 differentiation into macrophages caused caveolin-1 expression to be dramatically upregulated and selective lipid uptake from HDL to be increased, although SR-BI expression remained constant [191]. This finding indicates that co-expression of SR-BI and caveolin-1 is associated with enhanced lipid uptake in THP-1 macrophages, and highlights the important role of caveolae in cholesterol flux. Finally, localisation of SR-BI to caveolae may also promote HDL signal transduction: HDL binding to SR-BI was recently found to activate the caveolar protein eNOS [192].

1.6.3.5 SR-BI promotes cholesterol uptake and efflux to HDL and LDL

SR-BI not only mediates selective lipid uptake from HDL, but also promotes lipid uptake from native LDL [193,194]. The HDL and LDL binding sites on SR-BI appear to be distinct since specific mutations near the C-terminal transmembrane domain of mSR-BI blocked the majority of HDL binding and lipid uptake, without interfering with LDL binding or the uptake of LDL cholesterol [195]. In addition to its role in cholesterol uptake, SR-BI also promotes cellular cholesterol efflux to high- and low-density lipoproteins, where there is a favourable cholesterol gradient [116,196]. In contrast to HDL cholesterol uptake, the mechanism of SR-BI-mediated efflux is poorly understood and there is much controversy as to whether HDL must physically bind to SR-BI in order to remove cholesterol. Initially, HDL-mediated cholesterol efflux from recombinant COS-7 cells expressing CD36 and SR-BI was compared. Even though both receptors bound HDL efficiently, CD36 was not able to significantly increase radiolabelled cholesterol efflux to HDL [197]. In addition, phospholipid acceptor vesicles that do not bind surface receptors promoted more cholesterol efflux from SR-BI-expressing cells than from CD36-expresing cells [197]. These results indicated that SR-BI does not mediate efficient cholesterol efflux to HDL by merely tethering HDL particles to the cell surface. Rothblat and co-workers later found that over-expression of SR-BI in recombinant COS cells altered the lipid organisation of the plasma membrane [198], and suggested that SR-BI might promote efflux in a binding-independent manner by redistributing cholesterol to membrane domains that facilitate FC flux between cells and lipoproteins, such as caveolae. However, more recent studies, using blocking antibodies and SR-BI mutations to prevent lipoprotein binding, have shown that binding of HDL and LDL to SR-BI is a prerequisite for SR-BI-mediated cholesterol efflux to these lipoproteins [196].

Recently, Chen *et al.* [199] performed experiments on macrophages to determine whether the SR-BI- and ABCA1-mediated cholesterol efflux pathways interact. They hypothesised that these two membrane receptors might act synergistically to promote cholesterol efflux. For example, the nascent HDL particles generated as a result of ABCA1 lipid efflux might serve as acceptors for SR-BI-mediated cholesterol efflux. However the results were surprising, as SR-BI expression was found to inhibit ABCA1-mediated cholesterol efflux. Since ABCA1 mRNA levels and ABCA1-mediated phospholipid efflux were not affected, and SR-BI neutralising antibodies reversed the inhibition, SR-BI is thought to exert inhibition by promoting the re-uptake of cholesterol that has already undergone ABCA1-mediated efflux [92]. Therefore, this generates a futile cycle of cholesterol flux in non-polarised cells. However, in polarised cells, such as hepatocytes, it is possible that expression of ABCA1 and SR-BI on different sides of the cell might promote the movement of cholesterol across the cell [199]. Finally, although SR-BI promotes the bi-directional flux of cholesterol across plasma cellular membranes, these findings emphasise the physiological role of SR-BI in cellular cholesterol uptake.

1.6.3.6 SR-BI binds HDL via apoA-I

Since SR-BI is a multi-ligand receptor, it was postulated that HDL apolipoproteins might not be directly involved in HDL binding to this receptor. However, when Xu *et al.* [200] generated phospholipid/cholesterol complexes containing individual human HDL apolipoproteins (apoA-I, apoA-II and apoC-III) and studied the ability of each apolipoprotein to bind mSR-BI expressed in recombinant cells, the results showed that all three apolipoproteins are able to directly mediate binding to mSR-BI. Further studies using direct binding analysis and chemical cross-linking were subsequently performed to examine the interaction between apoA-I and mSR-BI: apoA-I was found to bind mSR-BI whether in HDL_3, discoidal particles, or a lipid-free state [201]. Furthermore, a model class A amphipathic α-helix also exhibited high-affinity binding and cross-linking to mSR-BI; this promotes the hypothesis that SR-BI interacts with a wide variety of apolipoproteins via α-helical secondary structures common to the apolipoproteins of HDL and LDL [201]. Indeed, a recent report revealed that discoidal apoE-phospholipid particles are also ligands for SR-BI [202]. Finally, the conformation of apoA-I within different-sized particles was found to influence apoA-I recognition by SR-BI: larger particles, such as HDL_2, have a greater affinity for SR-BI than smaller particles [203,204]. This finding is consistent with the involvement of SR-BI in HDL

cholesterol uptake, as preferential binding of SR-BI to larger CE-rich HDL particles would promote greater uptake of cholesterol than from smaller, lipid-poor HDL particles.

1.6.3.7 Mechanism of cholesterol uptake by SR-BI

Until last year, the mechanism by which SR-BI mediates the selective uptake of cholesterol from HDL was poorly understood. Initially, SR-BI was thought to simply tether HDL to the cell surface and thereby promote the transfer of CE down a concentration gradient into the plasma membrane, whereupon the hydrophobic lipid was rapidly internalised [205]. However, further studies revealed that the efficient transfer of cholesterol between HDL and the cell surface involved more than simply HDL 'docking' to the recipient plasma membrane: like SR-BI, CD36 is located in caveolae and binds HDL with high affinity, yet CD36 cannot mediate the efficient uptake of cholesterol into cells [206]. Further studies using CD36/SR-BI chimaeras revealed that the extracellular domain of SR-BI is responsible for facilitating HDL lipid transfer [207,208]. It was postulated that SR-BI might associate with other surface proteins, which in turn mediate the selective uptake of CE; alternatively, CE may be transferred down a concentration gradient, through a hydrophobic channel formed by the receptor [205]. However, one major problem with the model that CE enters the plasma membrane directly is that CE, unlike unesterified cholesterol, has a very low solubility in phospholipid bilayers [209].

This problem led Alan Tall and his colleagues to examine more closely the fate of SR-BI at the plasma membrane. This group used fluorescence confocal microscopy and pulse-chase biotinylation techniques on transfected CHO cells and hepatocytes, to show that SR-BI is in fact an endocytic receptor that mediates both the uptake and recycling of HDL particles [210]. The first stage of selective lipid uptake involves HDL binding to SR-BI and endocytosis of intact HDL particles into the early endosome system. Subsequent hydrolysis of CE by nCEH [211] allows cholesterol to diffuse into endosomal membranes while SR-BI and its lipid-depleted HDL are recycled to the cell surface (Figure 1.9). A further sorting event results in the polarised secretion of HDL cholesterol from the canalicular membrane into bile. It is postulated that SR-BI may also be involved in this process by perhaps mediating cholesterol efflux from this membrane directly onto micelles [212]. This new model of selective uptake not only obviates the need for CE transfer across the phospholipid bilayer and solves the aforementioned dilemma, but also is consistent with earlier findings. For example, SR-BI was shown to function as an endocytic receptor when it bound and endocytosed radiolabelled

complexes containing advanced glycation end products and bovine serum albumin [213]. Therefore, even though SR-BI was widely considered for many years to function as a non-endocytic receptor, it now appears as though SR-BI shares an additional property with CD36 and functions as an endocytic receptor [214].

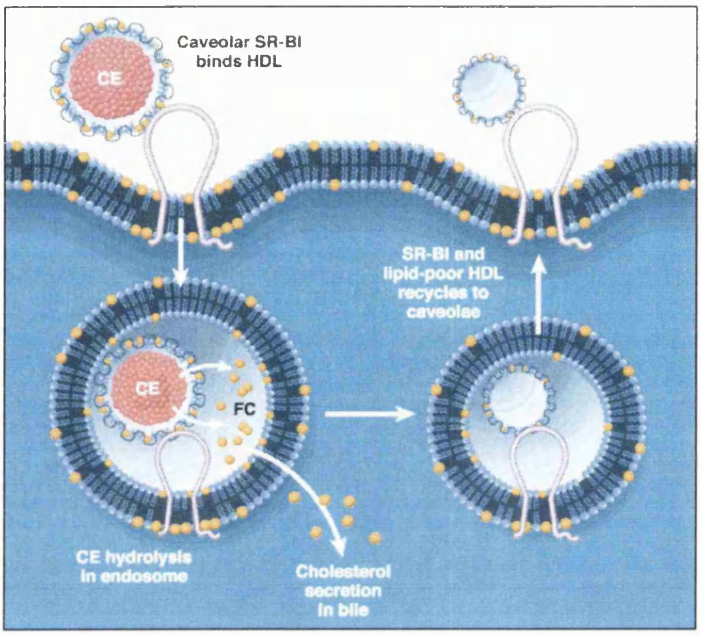

Figure 1.9 SR-BI uptake of HDL CE by lipoprotein endocytosis

When SR-BI, localised in membrane caveolae, binds HDL, the intact lipoprotein particles are taken up into endosomes by endocytosis. The CE is hydrolysed to FC, and the receptor and its lipid-depleted HDL are recycled back to the cell surface.

Alan Tall and colleagues also investigated the mechanism of HDL endocytosis, which was found to occur via a non-clathrin pathway. In clathrin-coated pits, dynamin mediates internalisation of the vesicle from the plasma membrane [215], yet cells deficient in dynamin-1 were still able to mediate HDL internalisation [210]. This finding is consistent with earlier results [145] as well as SR-BI sequence data, which show that SR-BI does not contain obvious signals for selective inclusion into clathrin-coated vesicles (e.g. NPXY) [216]. Therefore, in contrast with the well-defined process of LDL uptake, resulting in the degradation of LDL CE and protein in lysosomes, HDL uptake and trafficking appears to use a distinct endocytic pathway. Furthermore, it appears as though internalisation of HDL by endocytosis is not the only mechanism for uptake of HDL-derived CE. A recent report demonstrates that caveolin associates with HDL CE and annexin II in a lipid-protein complex that is involved in the internalisation of CE

from caveolae to internal membranes [217]. Additional studies will be needed to determine the extent to which these lipid-protein complexes contribute to cellular sterol internalisation.

Finally, since SR-BI was recently found to bind cholesterol directly, it has been postulated that selective lipid uptake may begin at the plasma membrane and then continue with CE hydrolysis during endocytic recycling [212]. Indeed, over-expression of SR-BI in mice enhanced hepatic secretion of HDL cholesterol radioactivity into bile, including both the initial secretion of HDL FC, as well as the slower secretion of FC, derived from the hydrolysis of HDL CE [218]. However, the relative contribution of each of these processes to cellular lipid uptake has yet to be defined.

1.6.3.8 C-terminal cytoplasmic SR-BI interactions

Ikemoto *et al.* [219] provided the first evidence that SR-BI may interact with other membrane proteins. This group used a glutathione *S*-transferase (GST) fusion of SR-BI C-terminal cytoplasmic tail and rat liver membrane extracts to detect interactions between SR-BI and a PDZ-domain-containing protein called CLAMP. PDZ domains are typically involved in the formation of protein complexes at the plasma membrane, and the polar expression of proteins, as well as endocytosis and signalling of receptors [220]. CLAMP has been independently identified four times and its generic name is PDZK1 [221]. Despite containing four PDZ domains, only the first N-terminal domain interacts with the C-terminus of SR-BI. Co-expression of SR-BI with PDZK1 in CHO cells caused an increase in SR-BI levels, suggesting that PDZK1 may increase the stability of SR-BI in the plasma membrane. Furthermore, a 50 % reduction in the conversion of HDL CE to FC was also detected [219]. Taken together these findings suggest that PDZK1 may inhibit the delivery of CE into the cell. However, since these experiments were over-expression experiments, it is unclear whether PDZK1 functions in a similar manner in polarised hepatocytes *in vivo*.

1.6.4 CUBILIN

In contrast to our understanding of SR-BI and its crucial role in HDL cholesterol metabolism, much less is known about receptors involved in the catabolism of HDL apolipoproteins, including apoA-I, apoA-II, apoC and apoE. Twenty years ago, Glass *et al.* [222] found that the kidney cortex was the principal tissue for apoA-I uptake, yet it took until 1999 for the receptor involved in apoA-I and HDL endocytosis to be identified

as cubilin [223,224]. Cubilin was previously known as the receptor involved in intestinal vitamin B_{12} uptake [225].

Cubilin is expressed in various absorptive epithelia, such as the intestine, where it localises to coated pits and mediates the uptake of intrinsic factor-vitamin B_{12} complex (IF-B_{12}) by endocytosis [226]. Since cubilin is highly expressed in non-intestinal tissues, where no IF-B_{12} uptake takes place, this receptor was thought to have diverse biological functions. When cubilin-affinity chromatography of serum was performed, apoA-I was identified as a ligand for cubilin [223]. Cellular HDL uptake studies using radiolabelled apoA-I revealed that cubilin mediates efficient HDL endocytosis and delivery of the ligand to lysosomes, in a similar manner to LDL endocytosis [223,224]. Binding of apoA-I to cubilin was subsequently found to be essential for HDL uptake, as antibodies against either protein strongly inhibited this process [223]. Like SR-BI, cubilin is described as a multiligand receptor, since it binds IgG light chains [227], in addition to IF-B_{12} and apoA-I/HDL.

In addition to the finding that cubilin is co-expressed with megalin (a member of the LDL receptor family), it also binds strongly to megalin *in vitro*, which supports the idea that megalin may function as a co-receptor for cubilin-ligand complex endocytosis [228,229]. Consistent with this proposal, anti-megalin antibodies inhibited the uptake of apoE-depleted HDL by 50 % [223]. Since these two receptors are highly expressed in the proximal tubule of the renal cortex they are thought to co-function to promote lipid-poor apoA-I uptake (from the glomerular ultrafiltrate), and delivery to lysosomes for degradation [226]. Therefore, by removing excess apoA-I, cubilin and megalin help to maintain the equilibrium between hepatic and intestinal generation of apoA-I and its catabolism by the kidney. In contrast to lipid-poor apoA-I uptake in the kidney, cubilin is also thought to have an important role in maternal-fetal cholesterol transport by mediating HDL holoparticle uptake in the yolk sac of rodents [230] and the early placenta of humans [231]. Cubilin therefore functions as another physiologically relevant HDL receptor.

1.6.5 SCAVENGER RECEPTOR CLASS B, TYPE II (SR-BII)

In 1997, Webb *et al.* [232] isolated a murine cDNA clone encoding an alternative form of SR-BI, named scavenger receptor class B, type II (SR-BII). It arises from the alternative splicing of SR-BI precursor transcripts, which generates a type II receptor

with an almost entirely different C-terminal cytoplasmic tail (Figure 1.10). An exon skipping mechanism is employed to generate SR-BII mRNA in which the 129 bp sequence comprising exon 12 of SR-BI is spliced out [233]. Since this exon contains the translation stop codon of SR-BI (TAG), alternative splicing serves to shift the open reading frame so that the 3' untranslated region of SR-BI transcript becomes the coding sequence in the SR-BII transcript. This region also contains the conserved translation stop codon for SR-BII (TGA) 120 bp downstream of the splice junction.

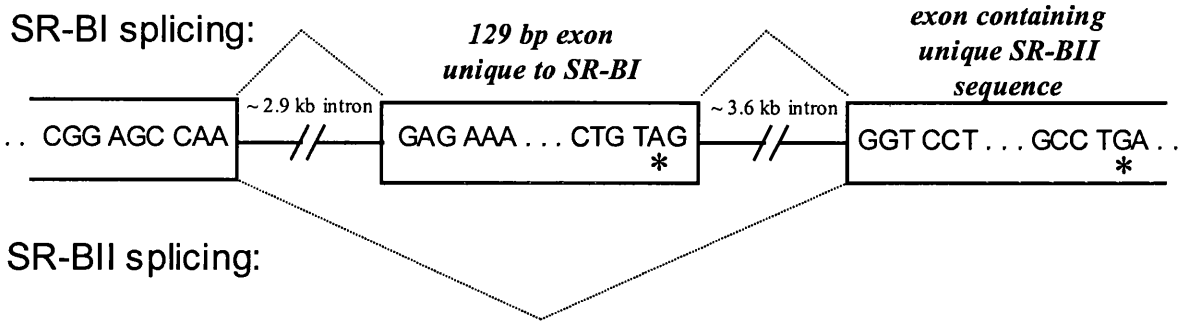

Figure 1.10 Alternative splicing of C-terminal hSR-BI/II primary mRNA transcript

This figure is adapted from Webb et al. [233]. Generation of SR-BI mRNA requires only the removal of introns from the primary transcript. However, in order to generate SR-BII mRNA, the 129 bp exon unique to SR-BI is also spliced out using an exon skipping mechanism (represented in this schematic diagram). An asterisk denotes the SR-BI/II translation stop codons.

Murine SR-BI and SR-BII share identical extracellular and transmembrane domain sequences, as well as N-terminal cytoplasmic tails. The extracellular domain ligand-binding specificities of the two isoforms are therefore identical, and SR-BII is classified as an HDL receptor. In addition, the first five residues of the C-terminal cytoplasmic tail sequences are also the same. However, beyond the splice junction the 3' C-terminal cytoplasmic tail sequences of each isoform are distinct: the unique SR-BI tail sequence comprises 42 residues, whereas the unique SR-BII tail sequence is only 39 residues long. Upon examination of the 3'-untranslated regions of bovine, mouse and hamster SR-BI cDNAs, the predicted translation products for cytoplasmic SR-BII were found to have the same length and showed a high degree of sequence similarity ranging from 62-67 % identity when compared to the human sequence. These results suggested that SR-BII homologues exist in each of these species [233].

1.6.5.1 SR-BII expression

SR-BII expression in human cells was confirmed by reverse transcription-polymerase chain reaction (RT-PCR) on RNA isolated from HeLa, THP-1 and HepG2 cells, using specific human primers [232]. Subsequently, S1 nuclease protection assays were employed to establish relative amounts of SR-BI and SR-BII mRNA in human cells and selected mouse tissues. In HepG2, HeLa, and THP-1 cells, SR-BII mRNA represents 21 %, 22 %, and 31 % of total SR-BI/II mRNA, respectively [233]. Both transcripts were also detected in mouse tissues, but their expression levels differed substantially: SR-BII mRNA represented 79 %, 61 %, 43 %, and 32 % of total SR-BI/II mRNA in testes, adipose tissue, liver, and adrenal glands, respectively [232].

In order to determine relative levels of SR-BI and SR-BII protein in each of the mouse tissues, rabbit anti-peptide antisera directed against the unique C-terminal cytoplasmic tail sequences of murine SR-BI and SR-BII were generated. SR-BII was found to represent ~12 % of the total immunodetectable SR-BI/II in mouse liver, and lesser amounts (~5 %) in mouse testes and adrenal glands [233]. The levels of SR-BII were surprisingly low relative to the abundance of SR-BII transcripts in these tissues. This discrepancy might result from instability of the translation product or inefficient translation of the transcript. The former explanation is not likely, since pulse-chase experiments revealed the apparent half-lives of SR-BI and SR-BII in transfected CHO cells to be similar [233]. Inefficient translation of SR-BII mRNA is a more likely explanation, but this would have to result from differences in mRNA structure at the 3' end of the transcript, as the SR-BI and SR-BII transcripts are presumably otherwise identical. Finally, the mouse SR-BII antiserum failed to detect SR-BII protein in human cells. This probably resulted from poor homology (62 %) between the mouse and human sequences in the region used to generate the anti-peptide antiserum.

1.6.5.2 Comparison of SR-BI and SR-BII

Given the fact that the majority of SR-BI and SR-BII sequences are identical, it is not surprising to discover that SR-BII shares many properties with SR-BI. For example, these two isoforms undergo the same post-translational modifications: glycosylation of the extracellular domain and myristoylation of the N-terminal [176], as well as palmitoylation, which most probably occurs on the Cys^{462} residue common to both isoforms [233]. Like mSR-BI and other palmitoylated proteins, mSR-BII was also found to localise to caveolar plasma membrane microdomains in CHO-SR-BII recombinant

cells [233]. Furthermore, Webb *et al.* [232] showed that recombinant CHO-SR-BII cells not only acquired the ability to bind DiI-labelled HDL with high affinity, but also were able to take up fluorescent lipid from these lipoprotein particles. This finding implicates SR-BII as another physiologically relevant HDL receptor.

This group went on to assess the impact of the unique C-terminal cytoplasmic tail on the ability of mSR-BII to mediate selective lipid uptake from HDL as well as FC efflux to HDL. CHO-SR-BII cells exhibited slightly higher levels of HDL CE uptake and HDL-mediated FC efflux than CHO-SR-BI cells, however the relative amounts of mSR-BI and mSR-BII protein within the recombinant cells were very different. Indeed, quantitative densitometric analysis of the transfected cells using an antibody common to the extracellular region of both isoforms revealed there to be six times more mSR-BII than mSR-BI. Therefore, when HDL CE uptake and FC efflux efficiencies were corrected for receptor levels, mSR-BII was found to be four times less efficient than mSR-BI at both cholesterol uptake and efflux [233], and it appears that the unique C-terminal cytoplasmic tail might be important for optimal lipid transfer between HDL and cells.

Webb *et al.* [233] also used a recombinant adenovirus containing the SR-BII coding sequence (AdSR-BII) in order to promote high levels of hepatic SR-BII expression in mice, and thereby determine whether SR-BII functions in a similar manner *in vivo*. Three days after treatment with AdSR-BII, a significant reduction in plasma HDL cholesterol levels was observed (52 % decrease), although this effect was not as pronounced as that observed in mice treated with AdSR-BI (75 % decrease). Lower levels of hepatic SR-BII expression were not responsible for this observation, since immunoblotting confirmed that the levels of SR-BII were 3-fold higher than SR-BI levels in the livers of the treated mice. This *in vivo* result therefore supports the earlier conclusion from recombinant CHO cells that SR-BII is less efficient than SR-BI at promoting selective lipid uptake from HDL.

In addition to the reduced efficiency of mSR-BII to mediate lipid transfer between lipoproteins and cells, the human (h) SR-BII protein failed to be detected in many different cell lines, and its significance as a physiological HDL receptor was therefore questioned [191]. However, last year Graf *et al.* [234] investigated the hormonal regulation of SR-BII to determine whether its expression, like SR-BI, is

modulated by estrogen [166]. This group treated a human liver cell line (HepG2) with physiological levels of 17β-estradiol and found that SR-BI was down regulated to undetectable levels in these cells [166]. In contrast, the hormonal treatment promoted a dramatic upregulation of SR-BII from undetectable levels in resting HepG2 cells, to levels three times greater than SR-BI at the start of the experiment. The hormone-induced switch from SR-BI to SR-BII did not inhibit selective lipid uptake, although the efficiency decreased to 75 % of that obtained by SR-BI. These findings are consistent with the estimation made by Webb *et al.* [233] that SR-BII is four times less efficient at mediating selective lipid uptake than SR-BI. The mechanism for the hormone-induced switch of expression is unclear. However, since RNAse protection assays did not detect significant changes in the amount of SR-BI and SR-BII mRNA, 17β-estradiol may therefore affect the stability of proteins, rather than regulate the splicing of the SR-BI/SR-BII transcript [234].

1.6.5.3 C-terminal cytoplasmic SR-BII interactions

Amino acid sequences:

Apart from the first 5 residues, C-terminal cytoplasmic SR-BI and SR-BII are entirely distinct [232], and it follows that any C-terminal cytoplasmic tail interactions are unique to each isoform. For example, PDZK1 binds to the C-terminal 15 amino acids of SR-BI, and is therefore not believed to interact with cytoplasmic SR-BII [219]. To date, C-terminal cytoplasmic SR-BII has not been reported to interact with any other cellular proteins. This is surprising, since my colleagues and I have identified many proline-rich, putative signalling motifs throughout the C-terminal tail sequence of hSR-BII, which have the potential to interact with signalling domains (Figure 1.11).

Within the 44-amino acid tail sequence of hSR-BII alone, there are six PXXP motifs that might serve as ligands for Src Homology 3 (SH3) domains [235], and two of these motifs are conserved in rat, mouse, and hamster sequences. An SH3 domain ligand comprises a left-handed polyproline type II helix, with three residues per turn. This structure generates a ligand with three spines: two of the spines are in contact with the SH3 domain and the third stabilises the helix [236]. In addition, a conserved consensus Src Homology 2 (SH2) domain-binding site has also been identified within this unique SR-BII tail, comprising a tyrosine residue followed by a hydrophobic amino acid at position +3 (YTPL) [237].

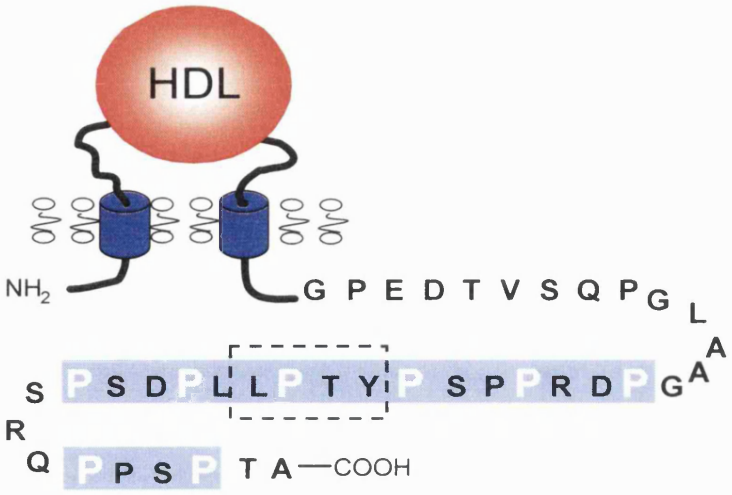

Figure 1.11 Potential signalling motifs in the cytoplasmic tail of SR-BII

I have identified a number of sites within cytoplasmic SR-BII that have the potential to bind signalling molecules upon HDL binding: six proline-rich motifs (PXXP) that might interact with SH3 domains (shaded box); and a potential SH2 recognition site, containing a tyrosine residue and a hydrophobic amino acid at position +3 (dotted box).

Implications:

SH2 and SH3 domains are small protein domains of ~100 and ~60 residues, respectively, defined by their homology to regions of the proto-oncogene c-Src. Each can fold into a compact and functional module independently of surrounding sequences. SH3 domains fold into a conserved structure of two perpendicular antiparallel β-sheets, which generate a hydrophobic pocket lined with conserved residues. These hydrophobic residues make critical contacts with proline residues in the polyproline type II helical ligand [238]. In the same way, all SH2 domains adopt an identical secondary structure: a large central antiparallel β-sheet, flanked by two α-helices. Like the SH3 domain, the SH2 domain also contains a conserved pocket, lined with basic residues that bind the phosphorylated receptor tyrosine residue (pTyr) [239]. This pocket includes the invariant arginine residue, which forms hydrogen bonds with two pTyr phosphate oxygens [236]. Furthermore, residues immediately C-terminal to pTyr contribute significantly to SH2 domain binding interactions [237], indicating that the sequence context of pTyr dictates which SH2 domain-containing signalling proteins will bind.

SH2 and SH3 regions are non-catalytic domains present in a diverse group of modular proteins, which mediate protein-protein interactions between signalling components downstream of membrane-bound receptors. Upon receptor activation, these

domains mediate the formation of heteromeric protein complexes at the plasma membrane, which in turn control signal transduction pathways, such as G-protein signalling and tyrosine kinase regulation [240]. For example, EGF binding to its receptor induces receptor dimerisation and autophosphorylation, which in turn creates high-affinity binding sites for the phospholipase C-γ1 (plc-γ1) SH2 domain [241]. Following plc-γ1 recruitment to the membrane, bound plc-γ1 is tyrosine phosphorylated by the activated receptor, leading to stimulation of its activity and hydrolysis of phosphatidylinositol 4,5-bisphosphate (PIP_2). PIP_2 cleavage generates two second messengers, DAG and inositol triphosphate, which stimulate PKC and raise intracellular calcium levels. Furthermore, SH2 and SH3 domains are also found in signalling proteins that do not contain any known catalytic element. These non-catalytic proteins may serve as adaptors to link tyrosine kinases to specific target proteins [238].

Lipoprotein receptors and signalling:

For many years, lipoprotein receptors were thought to mediate merely the exchange of lipids at the cell surface or the internalisation of lipoprotein particles. However, more recent findings implicate these multifunctional receptors to be involved in transmembrane signalling; the cytoplasmic domains of the LDL receptor family members not only mediate internalisation, but also interact with a number of signalling molecules, such as phosphotyrosine-binding domain-containing proteins [reviewed in 142,242]. These signalling domains interact with residues in the vicinity of the cytoplasmic 'NPXY' motifs. For example, the cytosolic adaptor protein Disabled-1 (Dab1) was proposed to bind to the cytoplasmic tails of VLDLR and apoER2 following loss-of-function studies in mice [243]. These studies revealed identical mutant phenotypes in Dab1-deficient mice to that of mice lacking both VLDLR and apoER2, indicating that they might be obligate components of the same biological process. The signal that binds to the extracellular domains of both receptors and initiates this signalling cascade was identified as Reelin [244,245]. Following Dab1 binding and activation, phosphorylated Dab1 is thought to activate downstream kinases and thus modulate neuronal development [142]. Furthermore, Riddell *et al.* [138] reported that apoE inhibits platelet aggregation by promoting activation of eNOS. This signal transduction pathway is most probably mediated via the apoE receptor, apoER2, which is expressed in platelets [137]. More recently, SR-BI was also found to participate in transmembrane signalling: HDL binding to SR-BI activates eNOS [192], in a ceramide-dependent manner [246]. Therefore, due to the presence of many potential signalling

motifs within the C-terminus of SR-BII, it appears that this lipoprotein receptor may not only be involved in cholesterol flux at the cell surface, but may also promote signal transduction through its unique cytoplasmic tail.

1.7 Aims of Thesis

I have hypothesised that: ***'upon HDL stimulation of SR-BII, its C-terminal cytoplasmic tail interacts with a signalling molecule to activate the CE mobilisation pathway.'*** Broadly, I aimed to investigate the role of human SR-BII in signal transduction *(Chapter 3)* and cellular cholesterol homeostasis *(Chapter 4)*. More specifically the aims of my thesis were:

Aim 1: *To generate recombinant C-terminal SR-BII fusion proteins to investigate whether signalling domains/molecules interact with this cytoplasmic tail.*

Aim 2: *To ascertain whether human SR-BII localises to caveolae (microdomains of the plasma membrane involved in both cholesterol flux and signal transduction).*

Aim 3: *To generate recombinant cells over-expressing human SR-BII in order to study the role of this receptor in cholesterol mobilisation and efflux, upon HDL stimulation.*

Chapter 2

2. MATERIALS AND METHODS

2.1 Materials

The Y190 yeast strain and yeast expression vectors were generously provided by Dr. X-M Sun (Hammersmith Hospital, UK). GST-tagged SH3 domain-containing proteins were a gift from Dr. I. Gout (Ludwig Institute, UK). Plasmid vectors expressing GST-tagged plc-γ1 SH2 and SH3 domains were provided by Dr. G. Skouteris (Royal Free & University College Medical School, London, UK). All oligonucleotide primers and the SR-BII synthetic peptide (amino acids: 493-514) were made to order by Sigma Genosys (Cambridge, UK). The DNA polymerases, *Taq* and *Pfu* Turbo were bought from Roche Diagnostics (East Sussex, UK) and Stratagene (Cambridge, UK), respectively. All restriction enzymes were purchased from Promega (Southampton, UK). [4-^{14}C]-cholesterol was obtained from Amersham Biosciences (Buckinghamshire, UK). Methanol, ethanol, diethyl ether, chloroform, hexane, glacial acetic acid and Cocktail T scintillant were supplied by BDH Laboratory Supplies (Poole, UK). All other reagents, unless otherwise stated in the text, were purchased from Sigma-Aldrich Company Ltd. (Poole, UK).

2.2 Molecular Biology Techniques

2.2.1 MESSENGER RNA EXTRACTION

Isolation of high quality, intact RNA is crucial for successful cDNA synthesis. To protect RNA from degradation by RNases, samples were processed quickly, disposable RNase-free plastic-ware was used, and water was treated with 0.1 % (v/v) diethylpyrocarbonate (DEPC) and autoclaved [247]. Disposable gloves were worn for all manipulations.

The QuickPrep Messenger RNA (mRNA) Purification Kit from Amersham Biosciences was used to isolate mRNA directly from eukaryotic cells, which obviates the need for intermediate total RNA purification. The principle behind this direct purification of mRNA is the use of complementary oligo(dT)-cellulose to separate polyadenylated mRNA from all other types of cellular RNA and contaminating genomic

DNA. This method therefore specifically isolates mRNA, which comprises only 1-2 % of a total RNA extraction.

The purification kit allows mRNA isolation from one to 1 x 10^7 cells. Having counted suspensions of HepG2 and THP-1 cells using a haemocytometer *(Section 2.4.1.2),* the cells were washed in phosphate buffered saline (PBS), and resuspended in 0.4 ml of extraction buffer and 0.8 ml of elution buffer. After each addition, a homogeneous suspension was achieved by vortexing. To prepare a cleared cellular homogenate, the samples were spun at maximum speed (13,000 rpm), for 10 min, in a bench-top microfuge. The homogenates were transferred to tubes containing oligo(dT)-cellulose and gently mixed by inversion for 3 min. The matrix was pelleted by brief centrifugation, before the supernatant was aspirated, and any contaminating proteins, nucleic acids and carbohydrates were removed by thorough washing with a high-salt buffer, followed by a low-salt buffer. The mRNA was eluted from the cellulose matrix using 0.2 ml warm (65 °C) elution buffer. In order to maximise mRNA yields, the elution step was repeated. Concentration of this dilute sample (in 400 µl) was then performed by precipitating the mRNA with 10 µl glycogen solution, 40 µl potassium acetate solution and 1 ml 95 % ethanol, and placing the sample at -20 °C for 30 min. The precipitated mRNA was collected by brief centrifugation in a microfuge at 4 °C, and re-dissolved in water. To estimate the amount of isolated mRNA, the absorbance at 260 nm (A_{260}) was measured with a UVIKON 930 spectrophotometer (Kontron Instruments, Hertfordshire, UK) and used in the following equation:

$$\textit{Isolated mRNA } (\mu g/ml) = A_{260} \textit{ x dilution factor x 40 } \mu g/ml$$

The mRNA was either reverse transcribed immediately *(Section 2.2.2),* or stored at -80 °C.

2.2.2 REVERSE TRANSCRIPTION

Isolated mRNA from HepG2 and THP-1 cells was reverse transcribed into single-stranded cDNA to create a suitable template for polymerase chain reaction (PCR) amplification *(Section 2.2.3).* Reverse transcription uses deoxynucleotide triphosphates (dNTPs; Promega), a reverse transcriptase enzyme, along with either random hexamer primers, an oligo(dT) primer, or a gene-specific primer, to produce a DNA copy of the RNA template. The cDNA then provides the necessary DNA template upon which thermostable DNA polymerases can amplify a sequence during PCR. The process, using an oligo(dT) primer, is summarised in Figure 2.1.

One μg of mRNA was converted to cDNA using SuperScript II reverse transcriptase and the 'SuperScript Preamplification System for First Strand cDNA Synthesis' Kit (Life Technologies, Paisley, UK).

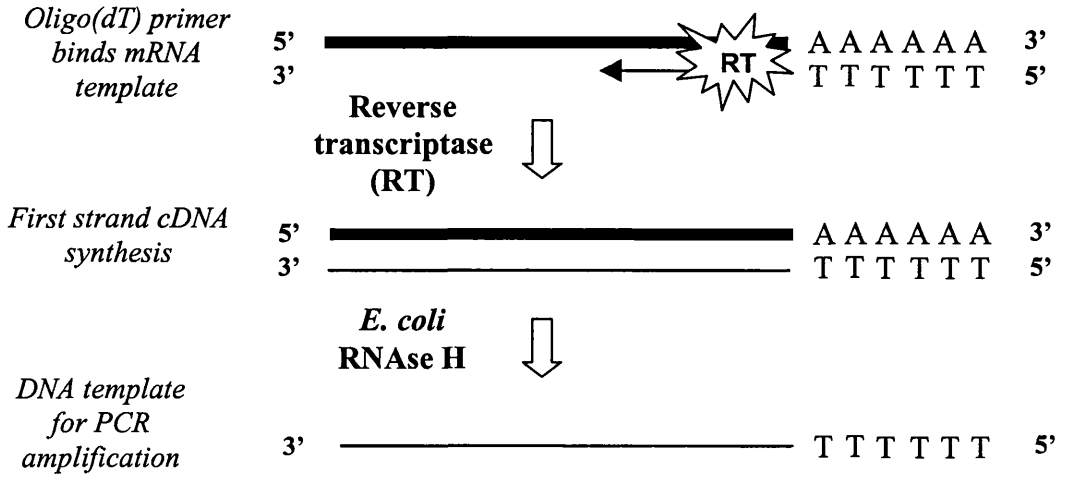

Figure 2.1 Reverse transcription of mRNA using oligo(dT) primers

RNA/primer mixtures were prepared by the addition of 0.5 μg oligo(dT)$_{12-18}$ and 1 μg mRNA to 10 μl DEPC-treated water in 0.5 ml thin-walled PCR tubes. Each sample was denatured by incubation at 70 °C for 10 min, followed by 1 min on ice. A reaction mix was prepared containing:

Component	Volume (μl)	Final Concentration (in 20 μl)
10 X PCR Buffer	2	1 X
$MgCl_2$ (25 mM)	2	2.5 mM
dNTP mix (10 mM)	1	0.5 mM
DTT (0.1 M)	2	10 mM
Total	**7**	

Following the addition of 7 μl of the reaction mix to the RNA/primer solution, the samples were incubated at 42 °C for 5 min. This allows the oligo(dT) primers to anneal to the polyadenylated RNA. Following the annealing, 1 μl (200 U) of SuperScript II reverse transcriptase was added to each of the samples. These were then mixed and incubated at 42 °C for a further 50 min to allow for first strand cDNA synthesis. Termination of the reaction occurs by denaturing the enzyme for 15 min at 70

°C. After the samples had been chilled on ice, 1 µl (2 U) of *E. coli* RNase H was added to each tube to remove any RNA. The digestion was complete after 20 min at 37 °C. For subsequent PCR amplification reactions one-tenth (2 µl) of this cDNA template was used directly.

2.2.3 PCR AMPLIFICATION OF DNA

PCR is a technique that allows rapid amplification of DNA or cDNA templates [248]. Successful PCR amplification of a target sequence will generate sufficient copies that far outnumber the strands of template cDNA. In this thesis, the amplified PCR products were visualised on agarose gels *(Section 2.2.5)* and cloned into expression vectors *(Section 2.2.8).*

Briefly, the PCR process amplifies a specific, short target sequence of nucleic acids from a longer DNA molecule. A reaction mixture typically comprises a DNA or cDNA template, a pair of specific oligonucleotide primers, dNTPs, a thermostable polymerase and a reaction buffer containing $MgCl_2$. Following thorough mixing of the reaction components, the samples are placed in a thermal cycler. This automated instrument cycles through a series of set temperatures, for varying amounts of time, allowing repetitive cycles of DNA denaturation, primer annealing and primer extension (DNA amplification).

In more detail, the first step of the PCR cycle is the production of a single-stranded DNA template by heating the sample to at least 95 °C for at least 1 min. This denaturation process separates the two intertwined strands of DNA and generates a template upon which the thermostable DNA polymerase can function. The second step allows annealing of the oligonucleotide primers to the separated DNA strands. The stable association of the primer pair with the template DNA occurs within 30–60 s, but is critically dependent upon temperature (approximately 50–70 °C). Therefore, for every primer pair and template combination, the optimal annealing temperature must first be established. This optimisation can easily be achieved using a RoboCycler 40 Gradient Cycler (Stratagene), which produces a gradient of annealing temperatures across the heating block. Finally, during the third step, the DNA polymerase begins new DNA synthesis, extending from the primers. This extension phase of the reaction occurs at the optimal temperature for the thermostable polymerase; this temperature is usually 72 °C.

The amount of time needed for this stage depends upon the length of the target sequence. Having completed one cycle of amplification, the temperature returns to 95 °C to begin the next cycle. Theoretically, for every PCR cycle, the amount of target sequence in the reaction doubles. Therefore, twenty cycles of PCR would amplify the desired sequence by a factor of more than a million. The amplified nucleic acid can then be analysed for size, sequence and quantity, followed by further experimental methods, such as cloning.

2.2.3.1 Basic PCR protocol

For each PCR reaction, a master mix was prepared by adding the reagents in the order and amounts shown below to 0.5 ml thin-walled PCR tubes:

Component	Volume (µl)	Final Concentration
10 X Cloned *Pfu* DNA Polymerase Buffer	5	1 X
dNTP Mix (10 mM)	1	200 µM
Forward Primer (10 µM)	5	1 µM
Reverse Primer (10 µM)	5	1 µM
THP-1 or HepG2 cDNA from Reverse Transcription Reaction	2	-
DEPC Water	31.5	-
Pfu Turbo (2.5 U/µl)	0.5	1.25 U
Total Volume	**50**	

To ensure that there was no contaminating DNA present in the master mix, it was necessary to set up a negative PCR control. This sample contained all the components of the PCR reaction, except for the cDNA template, which was replaced with DEPC water. The Robocycler PCR machine has a "hot-top" which prevents evaporation of the sample upon heating. This feature eliminated the need to cover the contents of the reaction tubes with a layer of mineral oil. For each primer pair combination, the conditions of the primer-annealing step were optimised (Table 2.1), by using a gradient of annealing temperatures and the following PCR program:

95 °C	5 min	
95 °C	30 s	} 30 cycles
54 – 68 °C	30 s	
72 °C	1 min	
72 °C	10 min	

The success of the PCR amplification was ascertained by running 5 µl of the reaction mixture on an agarose gel *(Section 2.2.5)*. The PCR products were either

purified directly from the reaction mixture *(Section 2.2.7),* or extracted from the agarose gel following electrophoresis *(Section 2.2.6).*

PCR target	Primer Sequence 5'→ 3' (F. Forward; R. Reverse)	Optimised Annealing Temp. (°C)
Full-length SR-BI	**F.** GAT CAA GCT TCC TGT GTC GTC TCT GTC G **R.** GAT CGG ATC CGA GGC TCA GGC TGT GG	62
Cytoplasmic SR-BII	**F.** GAT CTC CTG AGG ACA CCG TGA GC **R.** GAT CGG ATC CGA GGC TCA GGC TGT GG	60 - 65
Cytoplasmic SR-BII (pYTH9 vector)	**F.** GAT CGT CGA CGC AAA TCC GGA GCC AAG G **R.** GAT CAC TAG TAG TCA GGC TGT GGG GCT GG	64
U1A	**F.** GGC CCG GCA TGT GGT GCA TAA **R.** CAG TAT GCC AAG ACC GAC TCA GA	56

Table 2.1 Primer sequences and their optimised annealing temperatures
Restriction endonuclease sites are underlined (Section 2.2.8)

2.2.3.2 PCR protocol for amplifying GC-rich SR-BI/II sequences

Most DNA sequences can be amplified by standard PCR methods described above. However, some genes contain regions that are rich in guanines and cytosines (GC-rich), which prevent amplification by conventional PCR techniques [249]. GC-rich regions possess strong secondary structure that often fails to denature during the first step of the PCR, thereby preventing primer annealing and amplification. 75 % of the first 200 bp of SR-BI/II are either guanines or cytosines and so the 'Advantage-GC cDNA PCR' kit (Clontech, Hampshire, UK) was chosen to amplify the full-length sequence. This PCR utilises dimethylsulphoxide (DMSO) and a reagent named 'GC-melt' to help weaken base pairing in GC-rich sequences and create single strands of cDNA for primer annealing [250]. The Advantage-GC cDNA Polymerase Mix contains two DNA polymerases: one is an N-terminal deletion mutant of *Taq* DNA polymerase, which is deficient in 5' exonuclease activity, and the second provides 3'→5' proof-reading activity. The mix also contains a TaqStart Antibody, which automatically provides a "hot-start" PCR [251]. This antibody blocks any polymerase activity that might occur at room temperature whilst the PCR samples are being set up. However, polymerase activity is restored when the antibodies denature and lose their function at temperatures above 70 °C. This allows an automatic "hot-start" during the first denaturing step of the PCR.

For optimisation of PCR conditions for the amplification of full-length SR-BI/II, a temperature gradient of 56–66 °C was set up for the annealing step. To ascertain the optimal concentration of 'GC-melt' required for successful PCR amplification, increasing concentrations of GC-melt (0, 0.5, 1.0 and 1.5 M) were added to 50 µl PCR reaction mixtures *(Section 2.2.3.1)*, containing 'Advantage-GC cDNA Polymerase Mix' and its reaction buffer.

The samples were heated for 1 min at 95 °C, before amplification proceeded for 35 cycles with the denaturation step at 95 °C for 30 s, annealing of primers at 62 °C for 30 s, and extension at 68 °C for 1 min. Finally, the reaction was completed by an extension step at 68 °C for 10 min. Reaction products were then visualised and photographed under UV light following agarose gel electrophoresis *(Section 2.2.5)*.

2.2.4 ASSESSMENT OF cDNA QUALITY

Following the reverse transcription of mRNA, cDNA quality was assessed by PCR amplification of the *U1A* sequence. *U1A* is a "housekeeping" gene that encodes part of the spliceosome complex and is required by all living cells [252]. The basic PCR protocol *(Section 2.2.3.1)* was followed for amplification of this sequence, using the primers and annealing temperature listed in Table 2.1. A successful RNA preparation gave a clean PCR product of 230 bp in length [253].

2.2.5 AGAROSE GEL ELECTROPHORESIS OF DNA

After PCR amplification, the reaction products can be analysed using agarose gel electrophoresis [254]. During electrophoresis, the strands of DNA are separated according to size as they migrate through the agarose matrix towards the anode. Ethidium bromide within the gel intercalates between adjacent base pairs and can be detected and photographed under UV light. The percentage of agarose in the gel should differ according to the expected size of the DNA fragments. For clear resolution of low MW bands, such as 100 bp, a high percentage of agarose is used [2 % (w/v)], whereas higher MW bands (>1 kb) should be run on a low percentage agarose gel [1 % (w/v)].

The following protocol describes a typical minigel analysis. The minigel apparatus (Horizon minigel apparatus from Life Technologies) was set up as recommended by the manufacturer. The appropriate weight of low-melting point

agarose was dissolved in Tris-borate ethylenediaminetetra-acetate (TBE) buffer [100 mM Tris, pH 8.4, 90 mM boric acid and 1 mM ethylenediaminetetra-acetate (EDTA); diluted from a 10 X stock (Life Technologies)] by heating the mixture in a microwave oven for about 2 min on medium power. The solution was cooled to about 60 °C and, after adding ethidium bromide (0.5 μg/ml), was poured into the cast. The gel was left to set for ~30 min at room temperature and a sufficient volume of TBE buffer was added until the surface of the gel was covered. The PCR products were mixed 9:1 with 10 X loading buffer [10 mM Tris-HCl, pH 7.5, containing 50 mM EDTA, 10 % Ficoll 400 (w/v), 0.25 % (w/v) bromophenol blue and 0.25 % (w/v) xylene cyanol FF] and 10–20 μl of each sample were loaded into each well. Ten μl of a 1 kb or 100 bp DNA ladder (Life Technologies) were run in an adjacent lane for product size determination. A constant voltage of 150 V was then applied to the gel until bromophenol blue had migrated to 2 cm from the bottom of the gel. Following electrophoresis, the gel was visualised and photographed on a UV lightbox.

2.2.6 EXTRACTION OF DNA FROM AGAROSE GELS

The 'QIAquick Gel Extraction' kit (Qiagen, Crawley, UK) was used for the extraction of DNA bands from agarose gels. Briefly, the band was excised under UV light using a clean scalpel. After weighing the piece of agarose, 3 volumes of QG solution from the kit were added to 1 volume of gel (for example, 100 mg gel = 300 μl QG). This buffer served to solubilise the gel when placed at 50 °C for 10 min, with vortexing every 2 min. One gel volume of isopropanol was added to the sample before it was transferred to a QIAquick spin column and centrifuged at 13,000 rpm for 1 min to bind the DNA. Once the flow-through had been discarded, the column was washed with 0.75 ml of PE buffer (supplied with the kit) and re-centrifuged under the same conditions. The column was placed in a clean 1.5 ml microfuge tube and, following the addition of 30 μl deionised water to the column for 1 min, the DNA was eluted by centrifugation (13,000 rpm, 1 min). The concentration of purified DNA was estimated by measuring the absorbance at 260 nm (A_{260}) with a UVIKON 930 spectrophotometer (Kontron Instruments), and then using this value in the following equation:

$$\textit{Isolated DNA } (\mu g/ml) = A_{260} \times \textit{dilution factor} \times 50\ \mu g/ml$$

The DNA fragment was used immediately, or stored at –20 °C.

2.2.7 DIRECT PURIFICATION OF PCR PRODUCTS

For direct purification of DNA from a PCR reaction, the 'Wizard PCR Preps DNA Purification System' (Promega) was used. To the 50 µl PCR reaction, 100 µl of the Direct Purification Buffer were added, and mixed by brief vortexing. Next, 1 ml of resin was added, which bound the DNA during 3 episodes of vortexing over 1 min. The slurry was then pushed through a minicolumn with a syringe and washed with 2 ml of 80 % isopropanol. Centrifugation of the minicolumn at 13,000 rpm for 2 min removed traces of wash buffer, before DNA was released from the column by the addition of 30 µl deionised water (65 °C) for 1 min. After collecting the eluted DNA fragment by centrifugation, an estimation of the DNA concentration was calculated using the equation in the previous section. The DNA fragment was either used immediately, or stored at -20 °C.

2.2.8 RESTRICTION ENZYME DIGESTION

Bacterial restriction enzymes, also known as restriction endonucleases, recognise specific, short nucleotide sequences within DNA and cleave the DNA at all such sites [255]. *Eco*R1 and many other restriction enzymes cleave DNA so that overhanging, "sticky" ends remain (Figure 2.2). These single-stranded segments will readily combine with other complementary cleavage fragments and play an important role in recombinant DNA techniques. For example, following PCR amplification, DNA can be specifically cleaved with the same restriction enzyme that cuts within the multiple cloning site (MCS) of a vector. This then allows for efficient insertion of the DNA fragment into the host vector.

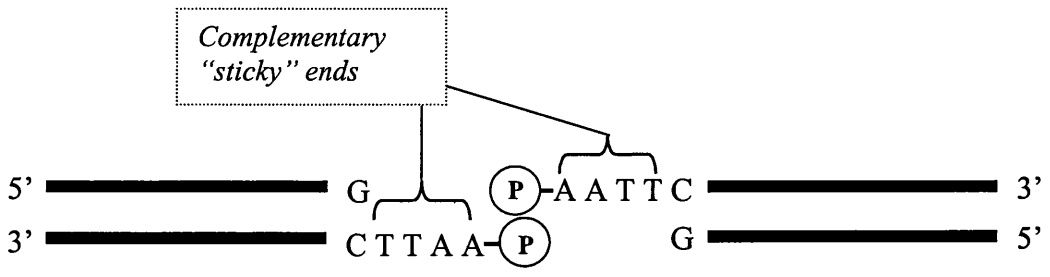

Figure 2.2 Complementary "sticky" ends of *Eco*R1. *P represents a phosphate group.*

For each restriction digest, up to 2 µg of DNA (purified PCR product or plasmid vector) was digested using the manufacturer's buffers (B-F & H) and instructions (Promega). The reaction buffers contained different concentrations of Tris-HCl (pH 7.5), NaCl and $MgCl_2$. Briefly, the restriction digests were performed for 1-2 h in 20 µl

reaction volume, using 2 U of restriction enzyme. Table 2.2 outlines the reaction conditions required by the enzymes used in this thesis. If the reaction conditions matched, two enzymes could be used in the same reaction mix. However, if they differed, the reactions were completed separately with a DNA purification step in between *(Section 2.2.7)*.

Enzyme	Cleavage Site	Reaction Conditions for 100% Activity
*Acc*III	T/CCGG A A GGCC/T	Buffer F at 65 °C
*Bam*HI	G/GATC C C CTAG/G	Buffer E at 37 °C
*Bsu*36I	CC/TNA GG GG ANT/CC	Buffer E at 37 °C
*Eco*RI	G/AATT C C TTAA/G	Buffer H at 37 °C
*Hind*III	A/AGCT T T TCGA/A	Buffer B or E at 37 °C
*Not*I	GC/GGCC GC CG CCGG/CG	Buffer D at 37 °C
*Sac*II	CC GC/GG GG/CG CC	Buffer C at 37 °C
*Sal*I	G/TCGA C C AGCT/G	Buffer D at 37 °C
*Spe*I	A/CTAG T T GATC/A	Buffer B at 37 °C
*Xba*I	T/CTAG A A GATC/T	Buffer D at 37 °C
*Xho*I	C/TCGA G G AGCT/C	Buffer D at 37 °C

Table 2.2 Restriction enzyme cleavage sites and reaction conditions

After completion of enzyme digestion, DNA fragments of interest were purified from agarose gels *(Section 2.2.6)*, or directly from the reaction mix *(Section 2.2.7)* and eluted in 30 µl of deionised water, ready for cloning into a suitable plasmid vector *(Section 2.2.9)*.

2.2.9 CONSTRUCTION OF EXPRESSION VECTORS ENCODING SR-BI/II

Cytoplasmic SR-BII expression vectors

SR-BII mRNA is detected at much lower levels than SR-BI in both THP-1 and HepG2 cells [232]. I therefore devised a cloning strategy to isolate cytoplasmic SR-BII

from either SR-BI or II cDNA, which avoided amplification of the exon unique to SR-BI. Initially, primers were designed to amplify only the unique SR-BII tail sequence (Figure 2.3).

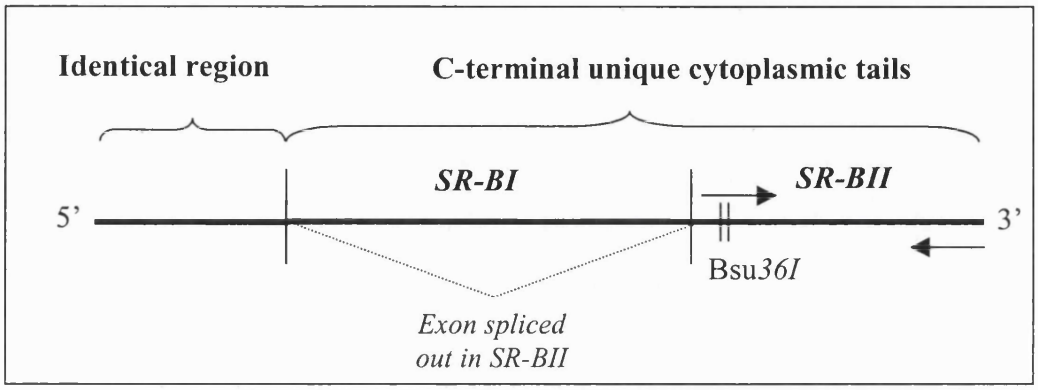

Figure 2.3 C-terminus of SR-BI cDNA. *The arrows represent PCR primers.*

Once this PCR product was cloned into a vector, the vector was manipulated in order to insert the remainder of the 5' cytoplasmic tail sequence using an oligonucleotide polylinker (adaptor; Figure 2.4). Since this adaptor spanned the cytoplasmic SR-BI exon boundary, its use avoided the amplification of PCR products containing the unique cytoplasmic SR-BI exon. The entire cytoplasmic SR-BII tail sequence was subsequently transferred to bacterial and yeast expression vectors to generate fusion proteins, which were used to investigate potential signalling interactions.

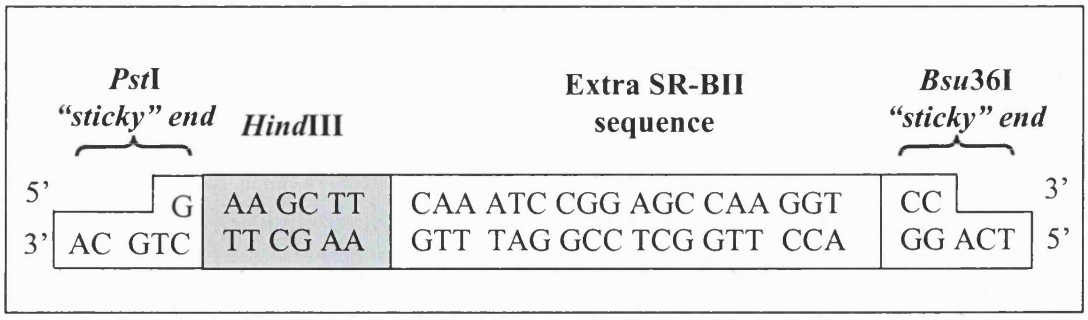

Figure 2.4 The cytoplasmic SR-BII adaptor sequence

The vector containing the 3' cytoplasmic SR-BII PCR product was digested with PstI and Bsu36I restriction enzymes. The adaptor was subsequently ligated into this vector using the same sites. The HindIII restriction site was used in future manipulations.

An overview of the cloning strategy for the generation of expression vectors containing the cytoplasmic SR-BII tail sequence is given below. Following the overview, the individual procedures are explained in more detail.

STEP 1: CLONING CYTOPLASMIC SR-BII INTO THE pGEM-T VECTOR

- PCR amplification of *unique* cytoplasmic SR-BII tail sequence.
- A/T cloning of PCR product into pGEM-T vector using single 3'-T overhangs at the fragment insertion site of vector and polyA tail of PCR product.
- Insertion of oligonucleotide polylinker containing the first 18 bp of cytoplasmic SR-BII to generate the entire tail sequence (pGEM-II).

STEP 2: TRANSFER OF CYTOPLASMIC SR-BII INTO EXPRESSION VECTORS

- *Bam*HI and *Hind*III restriction sites transferred cytoplasmic SR-BII from pGEM-II into the PPXa-3 vector to generate PPXa3-II.
- Cytoplasmic SR-BII was PCR-amplified from PPXa3-II using PCR primers containing the desired restriction sites: *Spe*I and *Sal*I. These restriction sites transferred the SR-BII tail into the yeast two-hybrid vector, pYTH9, to generate pYTH9-II.
- *Sal*I and *Not*I restriction sites transferred cytoplasmic SR-BII from pYTH9-II into the pGEX-4T-2 vector to generate pGEX-II.

The unique SR-BII cytoplasmic sequence was amplified from THP-1 cDNA using the primers listed in Table 2.1. The forward SR-BII primer was chosen so that it contained a restriction site (*Bsu*36I), which would then serve to anneal the PCR product to the adaptor sequence *(Section 2.2.9.2).* The reverse SR-BII primer was also designed to contain a restriction site at its 5' end (*Bam*HI), for future manipulations. Since amplification of the SR-BII cytoplasmic tail sequence was performed using the *Pfu* Turbo DNA polymerase, the PCR product therefore underwent A-tailing *(Section 2.2.9.1)* before it was ligated into the pGEM-T vector (pGEM-II; supplied by Promega). Following successful plasmid ligation *(Section 2.2.9.4)*, transformation *(Section 2.2.9.5),* and extraction *(Section 2.2.9.6)*, bacterial clones were sequenced to determine the orientation of the PCR product within the host vector. Automated fluoresecent sequencing was performed by 'Babraham Technix DNA Sequencing' (Cambridge, UK), using Promega sequencing primers complementary to the SP6 and T7 RNA polymerase promoter sites within the MCS of the pGEM-T vector. The pGEM-II vector was subjected to enzymatic digestion using *Bsu*36I and *Pst*I, a unique restriction site located

within the vector MCS. The adaptor molecule was then ligated into the cut vector using these same sites (Figure 2.4).

The *Bam*HI site in the reverse primer and the *Hind*III site in the adaptor were used to transfer the cytoplasmic tail from pGEM-II to the PinPoint Xa-3 bacterial expression vector (PPXa3-II; supplied by Promega). This vector expresses the inserted sequence as a biotinylated fusion protein. The "type 3" vector was chosen since it allowed the tail sequence to be ligated into the MCS without shifting the reading frame. Unfortunately, the yeast two-hybrid expression vector (pYTH9) did not contain any suitable restriction sites within its MCS for direct transfer of the SR-BII tail into this plasmid. Therefore, cytoplasmic SR-BII was PCR-amplified from PPXa3-II using forward and reverse primers containing *Sal*I and *Spe*I sites, respectively (Table 2.1). Following digestion of both the PCR product and the pYTH9 vector with these enzymes, the SR-BII tail was ligated into the yeast expression vector (pYTH9-II) for use in the yeast two-hybrid assay. Finally, the SR-BII tail was transferred from pYTH9-II to another bacterial expression vector, pGEX-4T-2 (Amersham Biosciences) using the *Sal*I and *Not*I restriction sites (pGEX-II) for the production of GST-tagged cytoplasmic SR-BII. Again, the "type 2" vector was specifically chosen to maintain the correct open reading frame. A summary of the expression vectors containing cytoplasmic SR-BII sequences is shown in Table 2.3.

Vector	Expression	Used for
pGEM-II	Bacteria	Cloning unique cytoplasmic tail of SR-BII (PCR product) and adaptor molecule insertion
PPXa3-II	Bacteria	Producing biotinylated cytoplasmic SR-BII fusion proteins
pYTH9-II	Yeast	Generating cytoplasmic SR-BII fused to GAL4 DNA binding domain for yeast two-hybrid assay
pGEX-II	Bacteria	Producing GST-tagged cytoplasmic SR-BII fusion proteins

Table 2.3 Summary of expression vectors containing the cytoplasmic SR-BII insert

Cytoplasmic SR-BI expression vectors

In order to generate expression vectors containing the SR-BI cytoplasmic tail sequence, similar methods were employed. I had previously attempted to clone the full-length SR-BI PCR product *(Section 2.2.3.2)* into pGEM-T, but unfortunately sequencing had revealed clones with many mutations throughout the SR-BI sequences. However,

one SR-BI clone had the correct cytoplasmic tail sequence, and I decided to manipulate this vector and cut out the unwanted 5' region to leave only the cytoplasmic SR-BI sequence. An overview of the cloning strategy for the generation of expression vectors containing the cytoplasmic SR-BI tail sequence is given below:

STEP 1: CLONING CYTOPLASMIC SR-BI INTO pGEM-T VECTOR

- Full-length SR-BI was amplified by PCR.
- A/T cloning of PCR product into pGEM-T vector.
- Removal of unwanted 5' sequence using *Sac*II and *Acc*III restriction sites, leaving the majority of the C-terminal SR-BI cytoplasmic tail sequence in the vector.
- Insertion of oligonucleotide polylinker containing the first 4 bp of cytoplasmic SR-BI to generate the entire SR-BI cytoplasmic tail sequence (pGEM-I).

STEP 2: TRANSFER OF CYTOPLASMIC SR-BI INTO EXPRESSION VECTORS

- *Bam*HI and *Hind*III restriction sites transferred cytoplasmic SR-BI from pGEM-I into the PPXa-3 vector to generate PPXa3-I.
- *Acc*III and *Not*I restriction sites removed cytoplasmic SR-BII from pGEX-II. Subsequently, these sites were used to transfer cytoplasmic SR-BI from PPXa3-I into the 'empty' vector to generate pGEX-I.

The mutated 5' sequence was removed from the pGEM-T vector containing full-length SR-BI using *Sac*II and *Acc*III restriction sites. An adaptor molecule was subsequently ligated into the vector in order to maintain the short sequence between the transmembrane domain and the *Acc*III site. This adaptor was similar to the one used for cytoplasmic SR-BII production: it contained a *Sac*II "sticky" end, a *Hind*III restriction site and the first 4 nucleotides of the C-terminal cytoplasmic tail, followed by an *Acc*III "sticky" end (Figure 2.5). Once again, the *Hind*III site within the adaptor and the *Bam*HI site in the PCR primer served to transfer the SR-BI tail into the PinPoint Xa-3 expression vector (PPXa3-I). Following this, the *Acc*III and *Not*I sites were used to exchange the cytoplasmic SR-BII sequence within pGEX-II for cytoplasmic SR-BI (pGEX-I). These vectors were used to generate fusion proteins as described for cytoplasmic SR-BII in Table 2.3.

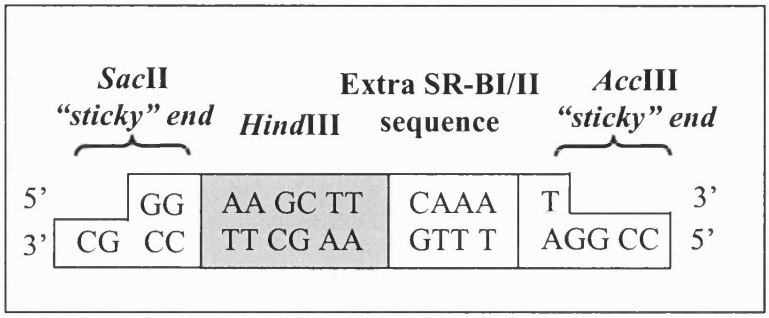

Figure 2.5 The cytoplasmic SR-BI adaptor sequence

The vector containing the 3' cytoplasmic SR-BI sequence was digested with SacII and AccIII restriction enzymes. The adaptor was subsequently ligated into this vector using the same sites. The HindIII restriction site was used in future manipulations.

Full-length SR-BI/II expression vectors

The full-length SR-BI sequence in the pT7T3D vector was kindly donated by Dr. C. Sharp (GlaxoSmithKline, UK). To transfer this fragment into the pCDNA3 mammalian expression vector (Invitrogen, The Netherlands), *Eco*RI and *Not*I sites were used. However, since there is an *Eco*RI site within SR-BI, the full-length sequence was digested from the pT7T3D vector in 2 fragments (Figure 2.6), which were subsequently ligated into pCDNA3 in a 3-way ligation *(Section 2.2.9.4)*.

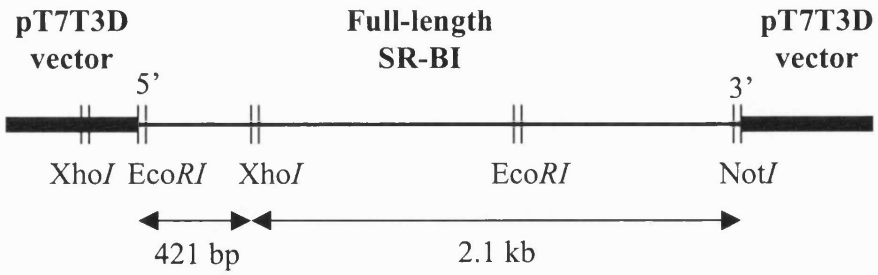

Figure 2.6 Diagram showing the relevant restriction sites in pT7T3D-SR-BI

Digestion using *Xho*I and *Not*I produced 3 fragments: the cut vector, a small fragment of about 450 bp and a 2.1 kb fragment. The 2.1 kb digestion product was then purified from the agarose gel *(Section 2.2.6)*. The second digestion involved *Eco*RI and *Xho*I, and produced the required fragment of 421 bp, which was purified from the other fragments by agarose gel extraction. These 2 purified fragments were then ligated into pCDNA3, exposing *Eco*RI and *Not*I "sticky" ends. After successfully transferring the full-length SR-BI sequence into pCDNA3 (to generate pCDNA3-I), the *Acc*III and *Not*I

sites were used to swap the cytoplasmic tails and produce the full-length SR-BII sequence ligated into pCDNA3 (i.e. pCDNA3-II).

2.2.9.1 A-tailing PCR fragments

The pGEM-T vector is a convenient vector into which PCR products can be readily inserted. Many thermostable polymerases, such as *Taq*, often add a single deoxyadenosine to the 3' ends of amplified fragments, in a template-independent manner [256]. The pGEM-T vector has been engineered to take advantage of this phenomenon and therefore contains single 3'-T overhangs at the fragment insertion site. These bases prevent recircularisation of the vector and provide a compatible overhang for the PCR product to efficiently ligate with the vector. *Pfu* turbo, however, creates blunt-ended PCR products with no 3' A-tails. Therefore, before the cytoplasmic SR-BII PCR products could be ligated into the pGEM-T vector, they had to undergo the A-tailing procedure. DNA fragments from the PCR reaction mixture were purified *(Section 2.2.7)* and used in the following reaction mix. The A-tailing occurred in 30 min at 70 °C.

Component	**Volume (µl)**	**Final Concentration**
PCR Reaction Product	2	-
10 X *Taq* Polymerase Buffer	1	1 X
$MgCl_2$ (25 mM)	1	2.5 mM
dATP (1 mM)	2	200 µM
DEPC Water	3	-
Taq Polymerase (5 U/µl)	1	5 U
Final Volume	**10**	

2.2.9.2. Adaptor molecule formation

The forward and reverse polylinker oligonucleotides were designed so that when they bound to one another, endonuclease "sticky" ends would be formed (Figures 2.4 and 2.5). In order for these adaptor molecules to ligate into the cut, dephosphorylated vector *(Section 2.2.9.3)*, the forward and reverse oligonucleotides were synthesised with 5' phosphorylation modifications (Sigma Genosys). Annealing of the oligonucleotides occurred by mixing 1 µl of each primer stock solution (10 µM), with 2 µl 10 X T4 DNA ligase buffer, and making the reaction mix up to 20 µl with deionised water. The components were then heated to 70 °C for 30 s, before reducing the temperature by 0.02 °C/s until 4 °C was reached. The adaptor molecules were either used immediately, or stored at –20 °C.

2.2.9.3 Preparing vectors for ligation

Most vectors combine with DNA fragments using complementary "sticky" ends produced by restriction endonucleases *(Section 2.2.8)*. Enzymes leave the 5' terminal bases with exposed phosphate groups. These phosphates form phosphodiester bonds with adjacent nucleic acids, and serve to link the vector and the incoming nucleic acid sequence during the ligation reaction. However, the vector may re-circularise rather than ligate to an inserted fragment. Therefore, it is necessary to perform a dephosphorylation reaction and remove all terminal 5' phosphates to prevent vector recircularisation [255]. This reaction is achieved with calf intestinal alkaline phosphatase (CIP; purchased from Roche Diagnostics).

After subjecting 1 µg of vector to specific endonuclease digestion within the MCS, the vector was purified and eluted in 30 µl deionised water *(Section 2.2.7)*. The vector was then dephosphorylated using the reaction mix listed below:

Component	**Volume (µl)**
Purified cut vector (eluted in 30 µl)	30
10 X Alkaline Phosphatase Buffer	4
Sterile Water	4
CIP (1 U/µl)	2
Total Volume	**40**

After 1 h at 37 °C, another 1 µl of CIP was added and the reaction continued for a further 30 min at 37 °C. The dephosphorylated vector was purified and concentrated using ethanol precipitation. For this procedure, one-tenth of the volume of 3 M sodium acetate (pH 5.2) was added to the reaction mix, followed by 2.5 times the combined volume of 100 % ethanol. After mixing, the tube was left overnight at –20 °C before the precipitated DNA was collected by centrifugation for 20 min at 4 °C. The supernatant was removed and the pellet was washed with 100 µl of 70 % ethanol. After another spin for 15 min at 4 °C, and removal of the ethanol, the pellet was left to air-dry. The dephosphorylated vector was resuspended in 10 µl of sterile water.

2.2.9.4 Ligation

T4 DNA ligase catalyses the formation of phosphodiester bonds between neighbouring 3'-hydroxyl- and 5'-phosphate ends in double-stranded DNA [257]. This enzyme can ligate complementary "sticky" ends from the vector and the insert. For pGEM-T ligation reactions, 1, 3 or 5 µl of A-tailed insert were added to 1 µl of vector (50 ng/µl), 7.5 µl of 2 X Rapid Ligation Buffer, 1 µl of T4 DNA Ligase (3 U/µl), and made up to a final volume of 15 µl with deionised water (Promega). The ligation took place during 16 h at 4 °C. For the other vectors used in this thesis, the following components were mixed and incubated for 16 h at 4 °C:

Components	**Volume (µl)**
Vector (< 1 µg/10µl)	1
Cut PCR Product	5 or 15
T4 DNA Ligase (1 U/µl; Roche Diagnostics)	1
10 X DNA Ligase Buffer	2
Final Volume	**Made up to 20 µl with deionised water**

It is suggested that ligation reactions use a vector DNA:insert DNA molar ratio of 1:3. When 3 different DNA fragments are to be joined in a 3-way ligation step, it is important to calculate the appropriate amounts of vector and inserts for the ligation reaction. The following equation can be used:

$$\frac{ng\ of\ vector \times kb\ size\ of\ insert}{kb\ size\ of\ vector} \times insert{:}vector\ molar\ ratio = ng\ of\ insert$$

This equation was used to determine the quantity of vector and inserts needed for the ligation reaction when the full-length SR-BI sequence was transferred into the pCDNA3 expression vector in two fragments.

2.2.9.5 Transformation of plasmid DNA into competent *E. coli*

When bacteria are treated with ice-cold solutions of calcium chloride and then briefly heated, a transient state of "competence" is induced, during which the ability of bacteria to take up recombinant DNA vectors is enhanced [258]. The DNA synthesising machinery of the host then replicates the plasmids. Following plasmid extraction *(Section 2.2.9.6)*, individual clones can be analysed to isolate successful transformants.

Dr. A. Manzano (Dept. of Medicine, Royal Free & University College Medical School, London) supplied the DH5α strain of *E. coli*, and the BL21 and JM109 strains were purchased from Stratagene and Promega, respectively. The transformation efficiency of the competent cells was assessed by transforming the bacteria with an uncut plasmid and then calculating the number of colony forming units/μg DNA. Competent cells should have an efficiency of at least 1 x 10^8 colony forming units/μg of DNA.

A 50 μl aliquot of competent cells was thawed on ice and then mixed with 2 μl of the ligation reaction (approximately 10 ng of DNA) by gentle swirling. Following incubation of the cells on ice for 30 min, the cells were transferred to a 42 °C water-bath for exactly 90 s, before being placed back on ice for another 5 min. Next, 125 μl of LB-Broth were added to the tubes, which were then shaken at ~150 rpm for 1 h at 37 °C. To select for transformants, the contents of each tube were spread onto LB agar plates (containing 100 μg/ml ampicillin) and left for 1 h at room temperature. The plates were then turned upside-down and incubated in a dry 37 °C incubator overnight. All the plasmid vectors used in this thesis contain the ampicillin resistance gene. Therefore, any successful transformants exhibit ampicillin resistance and will grow on the selection plates. These colonies were picked and grown overnight in a 50 ml tube, containing 6 ml of LB broth (with 100 μg/ml ampicillin) with constant shaking (~200 rpm) at 37 °C. For the negative control, DNA was always left out from the transformation reaction. Therefore, if any colonies were found to grow on the negative plates, then the ampicillin selection was known to have failed.

The pGEM-T vector has been designed so that successful insertion of a sequence into its MCS results in disruption of the β-galactosidase coding sequence. This allows easy colour screening of recombinant clones growing on indicator plates. The indicator plates were made by spreading 100 μl isopropyl β-D-thiogalactopyranoside (IPTG; 100 mM stock) and 20 μl 5-bromo-4-chloro-3-indolyl-β-D-galactopyranoside (X-gal; 50 mg/ml stock) over the surface of LB plates (containing 100 μg/ml ampicillin) and allowing absorption for 30 min at 37 °C prior to use. If ligation has not been successful and the β-galactosidase sequence is uninterrupted, then IPTG will promote formation of this enzyme, which will convert its colourless substrate (X-gal) into an insoluble product that turns blue upon oxidation. Successful ligation, however, will generate white colonies and these should be picked and analysed.

Bacterial clones were stored indefinitely at -80 °C as glycerol stocks. Glycerol stocks were prepared by mixing an overnight culture 1:1 with sterile glycerol, and storing them at –80 °C. After storage in glycerol, the bacterial stocks were removed from the freezer, spread onto LB plates and incubated at 37 °C. This promoted exponential growth of the bacteria again.

2.2.9.6 Extraction of plasmids

To determine whether the clones that were picked from the agar plate contain recombinant plasmids with the required PCR insert, the plasmids must first be extracted from their bacterial hosts and then analysed by endonuclease digestion and agarose gel electrophoresis. Plasmids were extracted from 3 ml of an overnight culture using Promega's 'Wizard *Plus* Minipreps DNA Purification System'. Briefly, the cells were pelleted by centrifugation at 13,000 rpm for 2 min, and resuspended in 200 µl TE buffer: 50 mM Tris-HCl, pH 7.5 and 10 mM EDTA. Next, 200 µl of cell lysis solution [0.2 M NaOH and 1 % (w/v) sodium dodecyl sulphate (SDS)] were added and the tubes were mixed by inversion. Following the addition of 200 µl 1.32 M potassium acetate (neutralisation solution), the cell debris was removed by a 5 min centrifugation step at 13,000 rpm. One ml of resin was added to the supernatant and this slurry was then pushed through a minicolumn. The DNA was washed with 2 ml 'column wash solution' before the DNA was dried by centrifuging the column at 13,000 rpm for 2 min. Finally, the DNA plasmids were eluted with 50 µl of deionised water (65 °C) and collected by brief centrifugation. The plasmids were either analysed straight away, or were stored at –20 °C.

Large-scale extraction of plasmids from 100 ml of an overnight culture was performed using the 'EndoFree Plasmid Maxi' kit (Qiagen), according to the manufacturer's instructions. This protocol extracts up to 500 µg endotoxin-free plasmid DNA, which can then be used to transfect sensitive eukaryotic cells. The steps were very similar to those described above, except on a larger scale.

2.2.10 SITE-DIRECTED MUTAGENESIS

Sequencing of pGEMT-II (*Section 2.2.9*) revealed a mis-sense mutation that would cause an amino acid change upon mRNA translation. Therefore, site-directed mutagenesis was performed to correct the mutation, using the 'QuikChange Site-Directed Mutagenesis Kit' from Stratagene. This procedure uses a double stranded DNA

vector and two synthetic oligonucleotides. These primers are complementary to opposite strands of the sequence of interest and contain the desired mutation. Following primer annealing to the vector, primer extension occurs using *Pfu* turbo DNA polymerase and a thermal cycler, during which the mutation becomes incorporated into the linearised vector sequence. Once sufficient rounds of amplification have taken place, the parental DNA template is digested using the restriction endonuclease *Dpn*I, which recognises methylated and hemimethylated DNA. The linearised vector sequences, with the mutation incorporated, are transformed into *E. coli,* which re-ligate the two ends of linear DNA to produce circular plasmids. Bacterial clones can then be analysed to confirm the presence of the desired mutation.

The pGEM-II plasmid contained a guanine (G) instead of an adenine (A). The codon therefore read GGA, rather than AGA. This would have resulted in an amino change from an arginine to a glycine. The two synthetic oligonucleotide primers were designed to contain the correct bases (forward 5'-GAC TCT CCC AGC AGA CAG C-3', and reverse 5'-GCT GTC TGC TGG GAG AGT C-3'). The vector containing the mutated sequence was purified from bacteria using the miniprep extraction procedure *(Section 2.2.9.6)*. Reaction mixtures were made up using either 5, 10, 20, 50 or 100 ng of DNA template with 125 ng of forward and reverse primers, 1 X cloned *Pfu* DNA polymerase buffer, 200 µM dNTP mix and 2.5 U *Pfu* turbo DNA Polymerase, in a final volume of 50 µl.

The cycling parameters used for denaturation, primer annealing and extension are listed below. Stratagene advises 12 cycles for point mutations and 2 min for the extension step for every kb of plasmid length.

95 °C	30 s	
95 °C	30 s	} 12 cycles
55 °C	1 min	
68 °C	7 min	

Following temperature cycling, the reaction mixtures were placed on ice for 2 min. Agarose gel electrophoresis of 10 µl of the amplified product revealed sufficient amplification *(Section 2.2.5)*. Next, 10 U of the *Dpn*I enzyme were added to each of the amplification reactions before they were incubated at 37 °C for 1 h to digest the parental DNA. One µl of the *Dpn*I-treated DNA was later transformed into *E. coli* XL1-Blue

(Stratagene) using the protocol described in *Section 2.2.9.5.* Sequencing of plasmids extracted from bacterial clones revealed the success of the mutagenesis *(Section 2.2.9).*

The manufacturer supplied a control reaction to verify that the site-directed mutagenesis system worked. The control plasmid encoded a mutated β-galactosidase gene, containing a stop codon (TAA) instead of a glutamine codon (CAA). Control primers were supplied that function to mutate the premature stop codon back to a glutamine. The control reaction mix used 10 ng of DNA template and the cycling conditions were also the same. To detect whether the mutagenesis had taken place, the transformed bacteria were plated out onto indicator plates *(Section 2.2.9.5).* If the mutation had been successfully corrected, then protein translation would continue to the end of the β-galactosidase sequence. Bacteria expressing a functional β-galactosidase enzyme would subsequently turn blue in colour.

2.3 Protein Detection and Expression

2.3.1 PROTEIN MEASUREMENT

The 'Bio-Rad Protein Assay' (Bio-Rad, Hemel Hempstead, UK) was used for all protein quantification, except when samples contained more than 0.1 % (v/v) detergent, which would interfere with the chemical-dye interactions. Therefore, when protein measurements were required from cell lysates, containing 1 % (v/v) Triton X-100, the alternative 'BCA Protein Assay Kit' (Perbio Science Ltd., Cheshire, UK) was used.

2.3.1.1 The BCA protein assay

This assay combines the biuret reaction, in which Cu^{+2} is reduced to Cu^{+1} by protein in an alkaline environment, with the sensitive colorimetric detection of cuprous cations (Cu^{+1}) by bicinchoninic acid (BCA) [259]. During the reaction, two molecules of BCA chelate each cuprous ion generated by the biuret reaction, to produce a purple-coloured product. This water-soluble complex has been found to have a strong absorbance at 560 nm, which increases linearly as the protein concentration increases, over a broad working range (20 μg/ml - 2 mg/ml).

For every assay performed, triplicate dilutions of bovine serum albumin (BSA) protein standard were prepared in distilled water to a final volume of 100 μl. A typical

standard curve ranged from 0–20 μg protein/100 μl. Triplicates of unknown samples were also made up to 100 μl with distilled water. To prepare the working reagent, BCA Reagent A was mixed with BCA Reagent B in a ratio of 50:1. One ml of the working reagent was added to each tube, before incubation at 60 °C for 30 min. The samples were transferred to disposable 1 ml microcuvettes and absorbances were measured at 562 nm relative to the water blank reference using the UVIKON 930 spectrophotometer (Kontron Instruments). The concentration of standards versus their absorbance at 562 nm (OD_{562}) was plotted, and the test sample concentrations were determined from the standard curve.

2.3.1.2 The Bio-Rad protein assay

This assay is based on the observation that protein binding to the acidic solution of Coomassie Brilliant Blue G-250 causes its absorbance maximum to shift from 465 nm to 595 nm. Bradford first demonstrated the usefulness of this principle [260], and Spector subsequently found that the extinction coefficient of a dye-albumin complex solution was constant over a 10-fold range [261]. This means that Beer's Law can be used to accurately quantify protein concentration, by selecting an appropriate ratio of dye volume to sample concentration.

This assay was conducted in a 96-well plate and analysed using a Dynex plate-reader (Jencons-PLS, East Sussex, UK) measuring absorbance at 595 nm. The standards were set up as described for the BCA method (*Section 2.3.1.1*), except the final volume was 50 μl. The unknown samples were also diluted in 50 μl of distilled water. To each well, 250 μl of freshly diluted dye reagent [20 % (v/v) solution of Bio-Rad concentrate] were added. After 10 min incubation at room temperature, the OD_{595} versus reagent blank was measured. The concentration of standards versus their OD_{595} was plotted, and the test sample concentrations were determined from the standard curve.

2.3.2 SDS-POLYACRYLAMIDE GEL ELECTROPHORESIS

The most common method for the fractionation and characterisation of proteins is sodium dodecyl sulphate-polyacrylamide gel electrophoresis (SDS-PAGE). SDS-PAGE requires only microgram amounts of proteins, and other advantages include speed and simplicity, compared to other protein separation techniques [262]. The goal of SDS-PAGE is the separation of polypeptides within a complex mixture according to molecular size. SDS-PAGE uses a buffer system, containing the ionic detergent SDS,

which dissociates all the proteins within the mixture into their individual polypeptide subunits. When proteins are heated to 100 °C in the presence of excess SDS and a reducing agent [β-mercaptoethanol or dithiothreitol (DTT)], the proteins become denatured and bind SDS in a constant SDS:weight ratio (1.4:1). This results in every polypeptide having a constant negative charge per mass unit since intrinsic charges of the polypeptide become insignificant [263]. During electrophoresis, SDS-polypeptide complexes will migrate towards the anode, and owing to the molecular-sieving properties of the gel, their mobilities are inversely proportional to the $\log_{10}$ of their molecular weights. Sample protein molecular weights can therefore be estimated if standard proteins of known molecular weight are applied to the same gel.

Polyacrylamide gels are formed as a result of acrylamide monomer polymerisation into long chains, which then become cross-linked by compounds such as N,N'-methylenebisacrylamide (bisacrylamide). The polymerisation reaction is initiated by ammonium persulphate and accelerated by N,N,N',N'-tetramethylethylenediamine (TEMED). TEMED acts by catalysing the formation of free radicals from persulphate, which then initiate polymerisation. The effective linear range of polypeptide separation of polyacrylamide gels is greatly influenced by the percentage acrylamide in the polymerisation mixture and the amount of crosslinking (Table 2.4). The cross-links created by bisacrylamide not only provide the gel with rigidity, but form pores through which the SDS-polypeptide complexes pass. As the bisacrylamide:acrylamide ratio increases, the size of the pores decrease. However, the ratio of 1:29 is most commonly used, which generates a gel capable of resolving polypeptides that differ in molecular weight by as little as 3 %.

Acrylamide Concentration % (w/v) [biscrylamide:acrylamide at a 1:29 molar ratio]	**Linear Range of Polypeptide Separation (kDa)**
3	95 – 400
5	57 – 212
7.5	36 – 94
10	16 - 68
15	12 - 43

Table 2.4 Range of polypeptide separation using SDS-polyacrylamide gels

To obtain a high resolution of polypeptide separation from a large, dilute sample applied to the gel, a discontinuous gel system is used. This system utilises both stacking and resolving gel layers that differ in salt concentration, pH, acrylamide concentration or a combination of these. The sample is applied to a stacking gel with high porosity [usually 4 % (w/v) acrylamide], which serves to concentrate the SDS-polypeptide complexes into an extremely narrow zone (or stack) at the top of the resolving gel. The resolving gel has a larger percentage of acrylamide, and therefore has greater molecular-sieving properties, and can separate the complexes into sharp polypeptide bands, according to molecular weight.

Gradient polyacrylamide gels, with increasing acrylamide concentration through the resolving gel, are now extensively used. There are a number of advantages to using gradient gels, over single percentage gels; gradient gels resolve proteins covering a wide range of molecular weights on a single gel and also promote sharpening of protein bands during migration. The SDS-polypeptide complexes migrate through the pores until the decreasing pore sizes impede their progress [264].

In this thesis, SDS-PAGE was used to estimate protein purity in a solution *(Section 2.3.2.3)*, to reveal protein-protein interactions *(Section 2.3.7)* and to fractionate a complex protein mixture before Western blotting *(Section 2.3.3)*.

2.3.2.1 Polyacrylamide gel preparation

Single Percentage Gels

Single percentage gels were made using the following components:

- **Acrylamide mix:** acrylamide and bisacrylamide mixed in a ratio of 29:1.
- **Tris buffers:** the resolving gel buffer is 1.5 M Tris-HCl (pH 8.8) and the stacking gel buffer is 1.0 M Tris-HCl (pH 6.8).
- **Ammonium persulphate (APS):** 10 % (w/v).
- **SDS:** 10 % (w/v).

The mini gels were cast in Bio-Rad MiniProtean II electrophoresis cassettes. Firstly, the resolving gel was made using the components and quantities listed in Table 2.5. The acrylamide solution was then quickly poured into the cassette, until the meniscus was at the correct distance from the top of the plate to allow for the comb length plus 0.5 cm. To produce a level resolving gel, the acrylamide solution was

overlaid with water-saturated isobutanol and then left to set. After about 30 min, the isobutanol was removed and the gel washed a few times with distilled water. The stacking gel acrylamide solution was then prepared (Table 2.5) and added on top of the resolving gel. Once a comb with the appropriate number of wells had been inserted, the stacking gel was allowed to set. The comb was subsequently removed and the wells were washed with distilled water, followed by 1 X running buffer; 25 mM Tris, pH 8.3, 192 mM glycine and 0.1 % (w/v) SDS (diluted from a 10 X stock purchased from National Diagnostics, Leicestershire, UK).

Solution Components (enough for 1 x 10 ml gel) *Solutions were added last to initiate polymerisation	**4 % Stacking**	**8 % Resolving**	**15 % Resolving**
Water	6.1 ml	4.6 ml	2.3 ml
30 % Acrylamide Mix	1.3 ml	2.7 ml	5.0 ml
Tris Buffer	2.5 ml *(pH 6.8)*	2.5 ml *(pH 8.8)*	2.5 ml *(pH 8.8)*
10 % SDS	100 µl	100 µl	100 µl
* 10 % APS	100 µl	100 µl	100 µl
* TEMED	10 µl	6 µl	4µl

Table 2.5 Components required for preparing gels for SDS-PAGE

In addition to casting single percentage gels in the laboratory, 'Novex' Tris-glycine pre-cast gels (8 and 16 %) were also purchased from Invitrogen, and used to produce high quality figures. The gels were supplied in plastic cassettes and a packaging buffer containing 0.02 % (w/v) sodium azide. Before use, the 12-well comb was removed and the wells were washed with distilled water, followed by 1 X running buffer.

Gradient Percentage Gels

All pre-cast Tris-glycine gradient 'Novex gels' (4-20 % and 8-16 %) were purchased from Invitrogen and prepared for electrophoresis in the same way as described above.

2.3.2.2 Electrophoresis

Sample preparation for all gels was the same: samples were mixed 3:1 with 4 X SDS-PAGE sample buffer [200 mM Tris-HCl, pH 6.8, 8 % (w/v) SDS, 0.2 % (w/v) bromophenol blue and 20 % (v/v) glycerol]. For reduced samples, β-mercaptoethanol

was added to a final concentration of 2 % (v/v), and the samples were heated in a boiling water bath for 5 min. For non-reducing conditions, β-mercaptoethanol was omitted and the samples were heated only. The broad range molecular weight marker (6-175 kDa; New England Biolabs, Hertfordshire, UK) was also heated for 3 min prior to loading on to the gel. After loading up to 30 µl of sample and 15 µl of marker into the wells, the electrophoresis chamber was filled with 1 X running buffer. Novex gels were run in the 'Mini-cell Xcell II' gel tank (Invitrogen), according to the manufacturer's instructions. Electrophoresis using the mini gels cast in the laboratory was performed in the Bio-Rad MiniProtean II electrophoresis chamber at a constant voltage of 125 V. When the dye front had migrated to the bottom of the gel, the gel was removed from its cassette and then subjected to either Coomassie or silver staining *(Section 2.3.2.3)*, or Western blotting *(Section 2.3.3).*

2.3.2.3 Staining SDS-PAGE polyacrylamide gels

Coomassie staining

Protein bands on gels can be detected using an easily visualised reagent that reacts with any protein irrespective of biological activity. The most simple and most commonly used technique is Coomassie blue staining, which has a sensitivity of 0.1-0.5 µg protein per band. This method was used to detect the purity of proteins that had been isolated using affinity chromatography. Following polypeptide separation by SDS-PAGE, the gel was transferred to a container holding about 50 ml of Coomassie stain: 0.25 % (w/v) Coomassie brilliant blue R-250, 50 % (v/v) methanol and 10 % (v/v) glacial acetic acid. Staining took place at room temperature over 30 min with shaking. Following gel staining, excess stain was removed by destaining in successive volumes of destain: 30 % (v/v) methanol and 10 % (v/v) glacial acetic acid. The destained gel was then washed and stored in distilled water, before it was dried using the Bio-Rad 'GelAir Drying Frame'.

Silver staining

Silver staining is a hundred times more sensitive than Coomassie blue staining, which is advantageous for the detection of nanograms of protein per band. After electrophoresis, gels were fixed for 3 x 20 min in a solution of 30 % (v/v) ethanol and 10 % (v/v) glacial acetic acid, to prevent diffusion of the protein bands. The gels were then washed for 3 x 10 min in distilled water before being subjected to silver staining using the Sigma 'Silver Stain Kit for Polyacrylamide Gels'. This method can also be used to

stain gels previously stained with Coomassie blue. Following staining, gels were dried as described for Coomassie stained gels.

2.3.3 WESTERN BLOTTING

Antibodies have a crucial role to play in the specific detection of small quantities of antigen within a complex mixture of proteins. Two immunodetection methods frequently used in this thesis were immunoprecipitation *(Section 2.3.5)* and Western blotting. The latter method involves antibody detection of antigens already fractionated from the complex mixture of proteins by electrophoresis. Following gel separation, the proteins are transferred to a nitrocellulose membrane, which then has its protein binding sites blocked before exposure to the specific primary antibody. This reduces the amount of non-specific binding of the primary antibody to the membrane. After washing away any unbound primary antibody with extensive washing, secondary antibodies directed against the primary antibody and labelled with horseradish peroxidase (HRP) are then incubated with the membrane. Following further washing, chemiluminescence is used to visualise the antigens. Luminescence describes the emission of light resulting from the release of energy from a substance in an excited state. In chemiluminescence, the excitation results from a chemical reaction. The ECL detection system (Amersham Biosciences) involves the oxidation of luminol by HRP in the presence of chemical enhancers, such as phenols [265]. The light emitted is at a wavelength of 428 nm and can be detected by a short exposure to blue-light sensitive autoradiography film. The Western blotting procedure is summarised below:

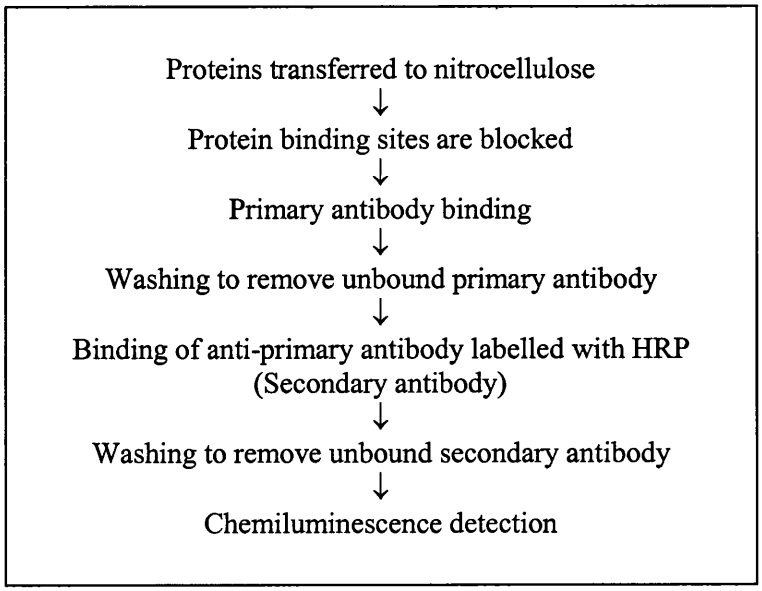

2.3.3.1 Sample transfer

Proteins were transferred from polyacrylamide gels to Hybond ECL nitrocellulose membranes (Amersham Biosciences) using two different methods. The first method involved a Bio-Rad Trans-Blot Semi-Dry Transfer Cell and the second method utilised the Novex Western Transfer Apparatus. In each case, a piece of nitrocellulose membrane and 2 sheets of 3MM absorbent paper (Whatman, Maidstone, UK) were cut to the correct gel size and pre-soaked in transfer buffer: 25 mM Tris, pH 8.3, 192 mM glycine and 20 % (v/v) methanol. The gel was then placed next to the nitrocellulose membrane and surrounded by absorbent paper to create a transfer sandwich:

Cathode end
1 layer of absorbent paper
polyacrylamide gel
1 layer of nitrocellulose membrane
1 layer of absorbent paper
Anode end

For semi-dry blotting, the transfer sandwich was placed on the bottom electrode (anode) and then the upper electrode was placed on top of the stack. Blotting occurred over 90 min with a constant current of 1.5 mA/cm^2 of gel. For Novex blotting, the transfer sandwich was positioned in the centre of the Xcell II Blotting Module (Invitrogen) surrounded by pre-soaked sponges. The module was subsequently filled with transfer buffer, and deionised water was poured around it to prevent overheating. Blotting occurred over 90 min at a constant current of 125 mA. A pre-stained protein marker was always present in the polyacrylamide gels and acted as an internal control for protein transfer.

2.3.3.2 Immunoblotting

- **Tris buffered saline (TBS):** 10 mM Tris-HCl, pH 7.5 and 150 mM NaCl.
- **TBS-T washing buffer:** TBS and 0.05 % (v/v) Tween 20.
- **PBS:** 138 mM NaCl, 10 mM Na_2HPO_4, 1.75 mM KH_2PO_4 and 2.7 mM KCl.
- **PBS-T washing buffer**: PBS and 0.05 % (v/v) Tween 20.
- **Milk blocking buffer:** 5 % (w/v) Marvel milk powder in PBS-T washing buffer.
- **BSA blocking buffer:** 3 % (w/v) BSA in TBS-T washing buffer.

Before exposing nitrocellulose to the primary antibody, the membrane was blocked. Generally, this method utilised the milk blocking buffer, and took place on a shaker at room temperature for 1 h, or overnight at 4 °C. When the primary antibody to be used was directed against a phosphate group (e.g. anti-phosphotyrosine), BSA blocking buffer was used instead of milk blocking buffer, and TBS-T washing buffer was used in each of the subsequent steps. This avoids incubating the nitrocellulose membrane with phosphates, which might bind the primary antibody and increase the background of the Western blot.

Primary antibodies were optimally diluted in BSA/milk blocking buffer or PBS-T washing buffer (Table 2.6) and incubated with the membrane on a shaker for 16 h at 4 °C. In a few cases, primary antibody incubations were done within 1 h at room temperature (Table 2.6). The membrane was then thoroughly washed with 5 x 10 min washing buffer steps. Secondary antibodies were diluted in either PBS-T or TBS-T washing buffers and incubated with the membrane for 1 h at room temperature. After repeating the washing steps, the membrane was visualised using an enhanced chemiluminescence (ECL) substrate, according to the manufacturer's instructions (Amersham Biosciences). The blot was secured in a film cassette and briefly exposed to X-ray film (Hyperfilm ECL, Amersham Biosciences).

2.3.3.3 Stripping the nitrocellulose membrane

Membranes were sometimes used more than once to visualise different antigens on the same blot. Following the first immunodetection, antibodies bound to the membrane were removed by placing the blot at 55 °C for 30 min in a stripping buffer: 100 mM β-mercaptoethanol, 62.5 mM Tris-HCl, pH 6.7 and 2 % (w/v) SDS. The membrane was then washed for 2 x 10 min in washing buffer, blocked, and subjected to a second round of immunodetection.

1° Antibody & Supplier	Antigen	1° Dilution & Buffer	1° Incubation Conditions	2° Antibody & Dilution in Wash Buffer
α-caveolin-1 (mAb) Clone C060 *Transduction Labs (Lexington, KY, USA)*	caveolin-1	1:1000 Milk	4 °C 16 h	Sheep α-mouse HRP 1:5,000
α-caveolin-1 *Transduction Labs (Lexington, KY, USA)*	caveolin-1	1:3000 Milk	4 °C 16 h	Goat α-rabbit HRP 1:5,000
α-CLA-1 (mAb) Clone 25 *Transduction Labs (Lexington, KY, USA)*	extracellular SR-BI/II	1:1000 BSA	4 °C 16 h	Sheep α-mouse HRP 1:10,000
α-clathrin *Santa Cruz Biotech (Santa Cruz, CA, USA)*	clathrin heavy chain	1:1000 Milk	4 °C 16 h	Goat α-rabbit HRP 1:10,000
α-GAL4-DBD (mAb) Clone 10 *Autogen Bioclear (Wiltshire, UK)*	GAL4 DNA Binding Domain	1:10,000 Washing (PBS-T)	RT 1 h	Sheep α-mouse HRP 1:10,000
α-GST *Amersham Biosciences (Bucks, UK)*	GST tag	1:3000 Washing (PBS-T)	RT 0.5 h	Rabbit α-goat HRP 1:10,000
α-pS *Cambridge Bioscience (Cambridge, UK)*	phosphoserine	1:1000 BSA	4 °C 16 h	Goat α-rabbit HRP 1:10,000
α-pT *Cambridge Bioscience (Cambridge, UK)*	phospho-threonine	1:1000 BSA	4 °C 16 h	Goat α-rabbit HRP 1:10,000
α-pY *Cambridge Bioscience (Cambridge, UK)*	phosphotyrosine	1:10,000 BSA	4 °C 16 h	Goat α-rabbit HRP 1:10,000
α-plc-γ1 (530) *Autogen Bioclear (Wiltshire, UK)*	phospholipase C-γ1	1:1000 BSA	4 °C 16 h	Goat α-rabbit HRP 1:10,000
α-SR-BI *Dr. van der Westhuyzen (University of Kentucky Medical Centre, USA)*	cytoplasmic SR-BI	1:3000 BSA	4 °C 16 h	Goat α-rabbit HRP 1:10,000
α-SR-BII *Sigma Genosys (Cambridge, UK)*	cytoplasmic SR-BII	1:1000 BSA	4 °C 16 h	Goat α-rabbit HRP 1:10,000
Streptavidin-HRP *Sigma-Aldrich Co Ltd. (Poole, UK)*	biotin	1:1000 Washing (PBS-T)	RT 1 h	none

Table 2.6 Western blotting conditions for detecting various antigens

All antibodies were polyclonal, except where monoclonal (mAb) is stated. The symbol α denotes anti. Secondary antibodies were supplied by Sigma-Aldrich Company Ltd (Poole, UK).

2.3.4 PRODUCTION OF ANTI-PEPTIDE ANTISERUM TO HUMAN CYTOPLASMIC SR-BII (α-SR-BII)

An anti-peptide antiserum directed against the cytoplasmic tail of human SR-BII was commissioned from Sigma Genosys. The sequence of peptides in the SR-BII tail was deduced from the published cDNA sequence and the chosen polypeptide was synthesised to be identical to a sequence of 22 amino acids in the cytoplasmic tail (493-514: EDTVSQPGLAAGPDRPPSPYTP). The anti-peptide serum against the SR-BII cytoplasmic tail will be referred to as α-SR-BII. In addition, pre-immune serum was taken from the rabbits before injection of the synthetic peptide. Characterisation of α-SR-BII was conducted using Western blotting: 0.5 μg of biotinylated cytoplasmic SR-BII *(Section 2.3.6)* was subjected to 16 % SDS-PAGE under reduced and non-reduced conditions, followed by immunodetection with α-SR-BII using the conditions described in *Section 2.3.3* and Table 2.6. Further characterisation of the serum was needed to determine whether α-SR-BII could immunoprecipitate cytoplasmic SR-BII from solution: α-SR-BII antibody (diluted 1:100) was incubated in a 1 μg/ml solution of biotinylated cytoplasmic SR-BII and subjected to the immunoprecipitation method described in *Section 2.3.5.* In addition isoform specificity of the antiserum was ascertained by subjecting solubilised lysates from recombinant CHO-SR-BI/II cell *(Section 2.4.3)* to 8 % SDS-PAGE separation and subsequent immunoblotting with α-SR-BII.

2.3.5 IMMUNOPRECIPITATION

Immunoprecipitation involves the specific removal of an antigen from a complex mixture of proteins by an antibody. Following antibody/antigen complex formation, the antibody binds to a matrix and becomes immobilised, thereby separating the immune complex from the protein mixture. Dynabeads covalently bound to either sheep anti-mouse IgG or sheep anti-rabbit IgG (Dynal, Merseyside, UK) were used to bind either the mouse- or rabbit-antibody/antigen complexes, respectively. Dynabeads are superparamagnetic beads that are designed as a matrix for immunomagnetic separation. After thoroughly washing the beads, to remove any non-specific proteins, the matrix was heated in SDS-PAGE sample buffer, containing β-mercaptoethanol. This released the antigen from the immune complex, which was subsequently identified by Western blotting *(Section 2.3.3).*

For basic immunoprecipitation reactions, 1 mg/ml cell lysates *(Section 2.4.4)* were subjected to pre-clearing. This involved incubating the cell lysate with 50 µl of washed Dynabeads on a rotating wheel for at least 90 min at 4 °C. Subsequently, the beads were isolated from the lysate and discarded. This served to remove molecules that had a high non-specific binding activity. The primary antibody was then incubated with the lysate on a rotating wheel at a 1:100 dilution for 3 h at 4 °C. Following immune complex formation, 100 µl of washed dynabeads were added to the lysate and the antibody/antigen complexes bound to this matrix during 90 min on a rotating wheel at 4 °C. Immune complexes that had bound the beads were separated from the rest of the cell lysate proteins magnetically and subjected to 4 washing steps with 500 µl of lysis buffer: 50 mM Tris-HCl, pH 7.5, 150 mM NaCl, 2 mM EDTA and 1 % (v/v) Triton X-100, containing the 'Complete' Mini protease inhibitor cocktail (Roche Diagnostics). The beads were resuspended in 60 µl 1 X SDS-PAGE sample buffer and 1 µl of β-mercaptoethanol, and boiled for 5 min *(Section 2.3.2.2)*. Twenty-five µl of each boiled sample were loaded onto a polyacrylamide gel for analysis.

2.3.6 BACTERIAL EXPRESSION OF FUSION PROTEINS

Transformed *E. coli* can be exploited to generate milligrams of recombinant protein that can easily be purified from other bacterial proteins, due to the presence of a fusion tag. The two systems used in this thesis are the 'PinPoint Xa Protein Purification System' (Promega) and the 'Glutathione *S*-Transferase Gene Fusion System' (Amersham Biosciences), which produce biotinylated and GST-tagged fusion proteins, respectively. Following purification, the tags can be cleaved from the fusion proteins, or the recombinant proteins can be used directly in experiments such as 'pull-down' assays *(Section 2.3.7)*.

2.3.6.1 Production of biotinylated SR-BI and II cytoplasmic tails

The cytoplasmic tail sequences of human SR-BI and II were cloned into PinPoint Xa vectors *(Section 2.2.9)*, and the plasmids were transformed into the *E. coli* JM109 bacterial strain for fusion protein expression. This strain expresses biotin ligase holoenzyme, which catalyses the biotinylation of a specific lysine residue in the purification tag sequence. Unlike the endogenous biotinylated protein generated by the host bacterium, the biotin moiety on the recombinant fusion protein is accessible to purification with avidin. This renders downstream avidin-purification of the biotinylated protein highly specific.

For small-scale fusion protein induction and detection, overnight bacterial cultures transformed with recombinant plasmids and the control plasmid (Promega) were diluted 1:100 in 50 ml of fresh LB media containing 100 μg/ml ampicillin and 2 μM biotin. After 1 h of shaking at 37 °C, IPTG was added to a final concentration of 100 μM to induce protein expression. Cultures were then incubated in a 37 °C shaker for a further 5 h. To detect the presence of fusion proteins in the bacterial cultures, 100 μl of each culture were centrifuged, and the pelleted cells were resuspended and boiled in 50 μl of 1 X SDS-PAGE sample buffer and 1 μl of β-mercaptoethanol. Five μl of the boiled samples were run on a 16 % polyacrylamide gel, blotted onto nitrocellulose membrane and detected using a streptavidin-HRP conjugate and chemiluminescence (*Sections 2.3.2* and *2.3.3;* Table 2.6).

For large-scale cultures, the quantity of cells was scaled up by a factor of 40 to produce 2 litres of bacterial culture. Following centrifugation of the cells for 10 min at 20 °C and 8,000 *g* using a 6 x 300 ml rotor (43115-112) and a Europa 24M centrifuge, cytosolic proteins were released from the bacterial cells by ultrasonic disruption. Cells were resuspended in 10 volumes of ice-cold, glycerol lysis buffer [50 mM Tris-HCl, pH 7.5, 50 mM NaCl and 5 % (v/v) glycerol, containing the 'Complete' Mini protease inhibitor cocktail] and sonicated on ice, using a Sanyo Soniprep 150 (10 x 15 s pulses at 10 μm amplitude, with 15 s pauses between pulses). Cellular debris was removed from the crude lysate by a 15 min centrifugation step at 10,000 *g* and 4 °C.

Purification of the biotinylated fusion proteins from the mixture of cytosolic proteins was performed at 4 °C using affinity chromatography. This process utilised an affinity column connected to an Uvicord SII spectrophotometer and recorder, which monitored and recorded the amount of protein leaving the column (flow-through). A fraction collector was situated downstream of the spectrophotometer to collect the flow-through. The affinity column was generated by filling a column with 1 ml of 'SoftLink Soft Release Avidin Resin' (Promega) and equilibrating the resin with glycerol lysis buffer, until a stable OD_{280} reading from the spectrophotometer was obtained (baseline). Following the equilibration step, cell lysate was applied to the affinity column using a peristaltic pump, at a rate of <1 ml/min to allow for efficient capture of the biotinylated proteins. The resin was subsequently washed with glycerol lysis buffer until the OD_{280} reading had returned to baseline, and any non-specific proteins that had bound the

column had been washed away. Elution of the biotinylated fusion proteins was achieved during a 15 min incubation of the affinity resin with 1.5 ml of 5 mM biotin in glycerol lysis buffer. Avidin-biotin interactions are very strong and usually require denaturing conditions to separate the components. However, use of the 'Soft Release Avidin Resin' allowed recombinant proteins to be eluted from the avidin matrix using the nondenaturing biotin solution. Fractions of eluted protein were subsequently collected and quantified using the Bio-Rad protein assay *(Section 2.3.1.2).* The fractions containing protein were pooled and dialysed in PBS using a 10,000 Da molecular weight cut-off (MWCO) dialysis cassette (Perbio Science Ltd.). Following concentration of the samples using a 500 µl Vivaspin concentrator (10,000 MWCO; Vivascience Ltd., Binbrook, UK), the eluted proteins were then subjected to SDS-PAGE, followed by Coomassie staining to verify protein purity *(Section 2.3.2).*

2.3.6.2 Production of GST-tagged fusion proteins

The cytoplasmic tail sequences of human SR-BI and II were cloned into the pGEX-4T-2 vector *(Section 2.2.9),* which is designed for inducible, intracellular expression of gene fragments as fusions with *Schistosoma japonicum* GST [266]. The recombinant vectors, along with an empty pGEX-4T-2 control vector, were subsequently transformed into the BL21 *E. coli* strain *(Section 2.2.9.5).* GST-tagged expression vectors containing sequences for plc-γ1 SH2 and SH3 domains were also transformed into this bacterial strain [267]. One pGEX-2TK vector contained all three plc-γ1 SH2 and SH3 domain sequences (SH223; nucleotides 1597-2553), and the other vector contained only the two SH2 domain sequences (SH22; nucleotides 1597-2274). Following transformation, clones were screened for fusion protein expression. Individual colonies were picked and transferred into separate tubes containing 6 ml of 2 X YTA media (16 g/l Tryptone, 10 g/l Yeast Extract and 5 g/l NaCl, containing 100 µg/ml ampicillin). The cultures were grown overnight in a 37 °C shaker and then diluted 1:100 in the desired volume of 2 X YTA media. Growth of the bacteria continued at 37 °C until the absorbance of the culture had reached an OD_{600} reading of 0.6-0.8 (between 3-5 h). At this stage, fusion protein expression was induced, by the addition of IPTG to a final concentration of 0.35 mM. Incubation of the culture continued for a further 2 h, before 6 ml was pelleted at 13,000 rpm and resuspended in 300 µl of ice-cold PBS (50 µl PBS/ml culture). Sonication using a Sanyo Soniprep 150 (5 x 15 s pulses at 10 µm amplitude, with 15 s pauses between pulses) was then performed to disrupt the cells, the cellular debris was pelleted at 13,000 rpm, and the supernatant was incubated on a

rotating wheel for 90 min at 4 °C with 50 µl of glutathione-agarose beads (pre-washed in PBS). The beads were washed twice with 1 ml PBS, before they were boiled for 5 min in 60 µl 1 X SDS-PAGE sample buffer containing 1 µl β-mercaptoethanol. Twenty µl of each of the samples were subjected to SDS-PAGE (using a 16 % gel) and the proteins were then detected by Western blotting with the α-GST primary antibody and chemiluminescence (*Sections 2.3.2* and *2.3.3*; Table 2.6).

For large-scale production of GST-tagged fusion proteins, the experimental procedure was almost entirely the same as described above, except for the following points:

- The overnight cultures were diluted 1:100 to produce 4 litres of induced culture.
- Sonication took place in PBS containing 1 % Triton X-100 to facilitate solubilisation of the fusion protein.
- Pelleting of the cells occurred by centrifuging at a speed of 8,000 *g* for 10 min using a 6 x 300 ml rotor (43115-112) and a Europa 24M centrifuge.
- Purification was performed using a 'RediPack' column (Amersham Biosciences) containing 2 ml of glutathione-sepharose.

Large-scale affinity purification of GST-tagged proteins was performed using 'RediPack' columns, according to the manufacturer's instructions. Briefly, the bacterial lysate was applied to the matrix, followed by extensive matrix washing with 3 x 20 ml of PBS. The fusion protein was eluted by incubating the matrix at room temperature for 10 min in 2 ml Glutathione Elution buffer: 50 mM Tris-HCl, pH 8.0 and 10 mM glutathione. The eluate was collected before the elution step was repeated twice more, followed by protein quantification of each fraction, using the Bio-Rad protein assay *(Section 2.3.1.2)*. As for biotinylated fusion proteins, the protein-containing fractions were pooled, dialysed against PBS and concentrated. The eluted proteins were then subjected to SDS-PAGE, followed by Coomassie staining to verify protein purity *(Section 2.3.2.3)*.

2.3.7 PULL-DOWN ASSAYS

'Pull-down' assays are designed to detect whether an immobilised protein interacts with another protein in solution, allowing it to be isolated from the solution during matrix separation. This method was used to screen for potential binding interactions between the biotinylated cytoplasmic tails of SR-BI and II and GST-tagged

SH3 domains from a variety of modular signalling proteins (src, crk, plc-γ1, fyn, csk and grb-2). It was also used to detect whether larger quantities of GST-tagged cytoplasmic SR-BII could interact with, and therefore pull-down, any cellular proteins from cell lysates.

2.3.7.1 Example method

For each assay, 2 μg of GST-tagged SH3 domains were immobilised on 50 μl of glutathione-agarose beads during 90 min incubation on a rotating wheel at 4 °C. The agarose was then washed twice with 1 ml PBS, before 2 μg of biotinylated cytoplasmic tail (in a total volume of 200 μl PBS) were mixed with the matrix. The negative controls comprised beads alone, and beads bound to the GST tag. The 'pull-down' reaction took place over 2 h on a rotating wheel at 4 °C. The samples were then transferred to a microfuge spin column and subjected to 5 x 0.5 ml washes with PBS, using a refrigerated microfuge at 4 °C. During the last wash, the samples were pipetted into microfuge tubes and the beads were resuspended in 60 μl 1 X SDS-PAGE sample buffer and 1 μl of β-mercaptoethanol, to disrupt any interactions. The samples were separated on a 16 % polyacrylamide gel, immunoblotted using a streptavidin-HRP conjugate, and detected with chemiluminescence (*Sections 2.3.2* and *2.3.3*; Table 2.6). To verify that the generation of affinity matrices had been successful, the blots were stripped *(Section 2.3.3.3)* and re-probed with the α-GST primary antibody.

2.3.7.2 Assay variations

Method 1

The 'pull-down' assay was reversed by immobilising 2 μg of biotinylated cytoplasmic tails on 50 μl of TetraLink Tetrameric Avidin Resin (Promega), followed by incubation of the resin with 200 μl of PBS containing 2 μg of GST-tagged SH3 domains. In this case, avidin resin alone served as the negative control. The α-GST primary antibody was used to detect interacting proteins, and the blot was re-probed with a streptavidin-HRP conjugate to ensure that the generation of each affinity matrix had been successful.

Method 2

The 'pull-down' assay was repeated using affinity matrices bound to GST-tagged plc-γ1 SH3 domains, with 2 μg biotinylated cytoplasmic SR-BII in 200 μl of the following

protein-rich solutions: PBS, 1 % (w/v) BSA, 10 % (v/v) fetal bovine serum (FBS) and 1 mg/ml HepG2 lysate *(Section 2.4.4)*.

Method 3

Two mg of GST alone or GST-SR-BII were coupled to 1 ml NHS-Sepharose HiTrap columns, as described by the manufacturers (Amersham Biosciences). This obviated the need to use glutathione-agarose beads to create an affinity matrix, and therefore allowed the 'pull-down' assay to involve GST-tagged proteins both in solution and attached to the affinity matrix. Once the coupling efficiencies for each column had been estimated, beads bound to 50 μg protein were incubated with 25 μg of GST-tagged plc-γ1 SH2 and SH3 domains (GST-SH22 and GST-SH223; *Section 2.3.6.2*) in 200 μl PBS. Interacting proteins were separated using 4-20 % SDS-PAGE and immunoblotted with α-GST.

Method 4

Cell lysate 'pull-down' assays involved immobilising 25 μg of GST-tagged cytoplasmic tail or GST alone on 50 μl glutathione-agarose, and incubating the beads with 1 ml of THP-1 cell lysate, at a concentration of 1 mg/ml *(Section 2.4.4)*. In this case, the proteins were separated using 16 % or 4-20 % polyacrylamide gels, and detected using Western blotting or silver staining *(Section 2.3.2.3)*.

2.3.7.3 'Pull-down' assays with SR-BII immunoprecipitation

Method 1

To investigate whether plc-γ1 binds cytoplasmic SR-BII in response to receptor activation, the following 'pull-down' assay with SR-BII immunoprecipitation was employed. Confluent cultures of recombinant Chinese hamster ovary (CHO) cells expressing human SR-BII (CHO-SR-BII; *Section 2.4.3*) were stimulated for 30 min with 10 % (v/v) 'HDL plasma' prior to cell lysis *(Sections 2.3.10.6* and *2.4.4)*. One ml of stimulated cell lysate (0.5 mg/ml) was subsequently incubated for 2 h with 25 μg of GST alone, or the GST-tagged plc-γ1 SH2 and SH3 domains, GST-SH22 or GST-SH223 *(Section 2.3.6.2)*. The receptor was isolated by immunoprecipitation with α-CLA-1 *(Section 2.3.5)*, and any bound GST-tagged proteins were separated by 4-20 % SDS-PAGE and detected by immunoblotting with α-GST.

Method 2

HDL-stimulated tyrosine phosphorylation of cytoplasmic SR-BII was monitored using the following method. CHO-SR-BII cells *(Section 2.4.3)* were grown to confluency in 90 mm plates, washed with PBS, and then subjected to 5 or 30 min incubations in serum-free media with and without 10 % (v/v) 'HDL plasma' *(Section 2.3.10.6)*. One plate of cells was left 'resting' (i.e. no change of media). Cells were washed in ice-cold PBS and lysed in 1 ml lysis buffer, containing 0.1 mM sodium vanadate and 1 mM DTT *(Section 2.4.4)*. Cell lysate protein concentrations were quantified using the BCA protein assay *(Section 2.3.1.1)*. Up to 0.8 ml of 1 mg/ml lysates were subjected to immunoprecipitation with α-CLA-1 *(Section 2.3.5)*. Successful isolation of the receptor and the state of cytoplasmic tail phosphorylation were detected by immunoblotting with α-SR-BII and α-phosphotyrosine, respectively.

2.3.8 YEAST TWO-HYBRID SYSTEM

The 'Matchmaker GAL4 Two-Hybrid System' (Clontech) was used to identify whether there are any cellular protein-protein interactions between the cytoplasmic tail of SR-BII and the SH3 domain of plc-γ1. This system is based on the method first described by Fields and Song [268]. Yeast express two regulatory proteins, GAL4 and GAL80, which control galactose metabolism. When galactose is present in the medium, the GAL4 protein binds to the responsive elements within the upstream activating sequences of many genes involved in galactose metabolism, and activates their transcription. When galactose is absent, GAL80 binds to GAL4 and transcriptional activation is blocked. In the yeast two-hybrid system, the GAL4 protein is divided into two domains: the DNA-binding domain (GAL4-DBD) and the activation domain (GAL4-AD). The GAL4-DBD binds to its conserved activation sequence within the DNA, but alone cannot promote transcription; the GAL4-AD must be complexed to GAL4-DBD in order for the gene to be transcribed. In this procedure, yeast are transformed with expression vectors encoding GAL4-DBD and GAL4-AD fused to peptide sequences of interest. If an interaction occurs between the fusion proteins, the GAL4-AD is brought into close proximity with the GAL4-DBD and a complete activation complex is generated. This active complex binds upstream of the *lacZ* reporter gene and activates its transcription. The production of the β-galactosidase enzyme can then be monitored using a colorimetric assay.

The Y190 yeast strain was chosen for the two-hybrid experiment. This host strain carries a deletion of the *gal4* and *gal80* genes, which means that induction of the reporter gene only occurs in response to a two-hybrid interaction. Briefly, the host was transformed with the pGAD10-plc-γ1 expression vector (containing the GAL4-AD and plc-γ1 SH3 domain sequences) and the pYTH9-II expression vector (containing the GAL4-DBD and cytoplasmic SR-BII sequences; for construction of this vector see *Section 2.2.9*). Successful transformants were subsequently isolated using selection plates and analysed for the presence of the β-galactosidase enzyme. The positive control plasmids, pSE1111 and pSE1112, were a kind gift from Dr. A. Robertson (Royal Free & University College Medical School, London, UK) and encode for SNF1 and SNF4 proteins fused to GAL4-DBD and GAL4-AD domains, respectively. SNF1 and SNF4 proteins interact in yeast and therefore serve as positive controls for this system [269].

2.3.8.1 Culturing and handling yeast

The yeast strain was grown in YPD medium and on YPD agar medium plates (Clontech). The YPD medium is a blend of peptone, yeast extract and glucose in the correct proportions for the growth of most *S. cerevisae* strains. The medium was adjusted to pH 5.8 and then autoclaved. Once the medium had cooled to 55 °C, adenine hemisulphate was added to a final concentration of 0.003 % (w/v). The Y190 host strain carries the *ade-101* mutation and its growth is therefore enhanced by the addition of adenine hemisulphate.

Synthetic dropout (SD) medium is a minimal medium used to select for specific phenotypes following yeast transformation. SD medium consists of a minimal SD base (which provides a nitrogen base and a carbon source) and a 'dropout' solution that contains a specific mixture of amino acids and nucleosides. The minimal SD Base, SD Agar and 10 X dropout solutions were purchased from Clontech. The selection medium was adjusted to pH 5.8, autoclaved and adenine hemisulphate was added in the same way as described for YPD medium.

The Y190 strain was stored indefinitely as a glycerol stock culture at –80 °C. To prepare a new glycerol stock culture, a colony was picked and resuspended in 0.5 ml of YPD medium. Once the cells had been dispersed by vortexing, sterile glycerol was added to a final concentration of 25 % (v/v), and the cells were stored at –80 °C. To recover frozen strains, a small amount of the glycerol stock was streaked onto YPD

plates and incubated at 30 °C for 3-4 days, until the colonies reached 2 mm diameter. This plate was described as the 'working stock' plate. It was wrapped in parafilm and stored at 4 °C for up two months. Transformed yeast strains were maintained in the same way, except that SD medium was used.

To prepare an overnight liquid culture, a large colony (2-3 mm diameter) was transferred from the working stock plate to 5 ml YPD medium, followed by vortexing for 1 min to disperse the cells. The cultures were then incubated at 30 °C for 16 h with shaking (250 rpm) to produce a stationary phase culture with an absorbance at 600 nm (OD_{600}) greater than 1.5. Enough overnight culture was transferred to fresh medium to produce an OD_{600} value in the range of 0.2–0.3, before the culture was incubated at 30 °C for a further 3-5 h with shaking. This produced a mid-log phase culture with an OD_{600} ~ 0.5. The absorbance measurements were made using a UVIKON 930 spectrophotometer (Kontron Instruments).

2.3.8.2 Transformation and selection

DNA was introduced into yeast using the lithium acetate (LiAc)-mediated method [270]. This method is simple and thought to be highly reproducible. To prepare competent cells for transformation, a 300 ml yeast culture was grown to mid-log phase and the cells were pelleted by 5 min centrifugation at 1,000 *g* and room temperature. The supernatant was discarded and the cells were resuspended in 1.5 ml of freshly prepared, sterile LiAc solution: 100 mM LiAc, 10 mM Tris-HCl, pH 7.5 and 1 mM EDTA. This provided enough competent cells for 15 different transformations. Generally, competent cells were co-transformed with both plasmids at the same time. However, sequential transformation, with colony selection in between transformations, was also used.

Co-transformation reactions were prepared by mixing 5 μg of each plasmid and 0.1 mg of herring testes carrier DNA with 100 μl of competent cells. For the positive control, 2.5 μg of each of the plasmids were used, and for the negative control, plasmids were omitted. To each tube 0.6 ml of sterile polyethylene glycol/LiAc solution [40 % (w/v) polyethylene glycol 3350, in LiAc solution] was added and mixed well by vortexing for 10 s. The cells were then incubated at 30 °C for 30 min with shaking at 200 rpm, before 70 μl of DMSO were added and mixed by gentle inversion. The

competent cells were subjected to a heat shock at 42 °C for 15 min, to allow the DNA to enter the cells. The cells were then cooled on ice for 2 min and pelleted at 13,000 rpm and room temperature. The supernatant was discarded and the cells were resuspended in 0.5 ml TE buffer: 10 mM Tris-HCl, pH 7.5 and 1 mM EDTA. One hundred µl of each transformation reaction was plated onto SD selection plates, which were incubated upside-down at 30 °C for 2-4 days, to allow for growth of successful transformants.

Yeast-two hybrid expression vectors contain nutritional markers for the selection of cells successfully transformed with the plasmids. The pGAD10 plasmid contains the leucine sequence, whereas the pYTH9 plasmid contains the tryptophan sequence. Therefore, cells transformed with both plasmids were selected by growth on SD plates containing the leucine/tryptophan dropout solution. Following the selection of successful transformants, the β-galactosidase assay determined whether these cells expressed fusion proteins that were interacting with one another.

2.3.8.3 β-Galactosidase assay

- Z buffer: 16.1 g/L $Na_2HPO_4.7H_2O$, 5.5 g/L $NaH_2PO_4.H_2O$, 0.75 g/L KCl and 0.246 g/L $MgSO_4.7H_2O$.
- X-gal stock solution: 20 mg/ml X-gal in N,N-dimethylformamide.
- Z buffer/X-gal solution: 100 ml Z buffer, 1.67 ml X-gal solution and 0.27 ml β-mercaptoethanol.

A colony-lift filter assay was used to detect whether the transformed yeast cells were expressing the *lacZ* gene. For each plate to be assayed, a sterile Whatman #5 filter was presoaked in 2.5 ml of Z buffer/X-gal solution in a 100-mm plate. A clean, dry filter was placed over the surface of the plate containing the colonies to be assayed. The filter was then transferred to a pool of liquid nitrogen for 10 s, followed by thawing at room temperature. The freeze/thaw cycle served to permeabilise the cells and cause the β-galactosidase enzyme to be released. This filter was then placed on top of the presoaked filter, containing the substrate for β-galactosidase, and incubated at 30 °C until blue colonies appeared. The blue colouration indicated the expression of β-galactosidase, which had resulted directly from the interaction of GAL4-DBD and GAL4-AD fusion proteins within the yeast cell.

2.3.8.4 Yeast protein extracts

In order to verify expression of the two fusion proteins within the transformed yeast, the cell walls were disrupted by a combination of chemical and physical means, and the proteins were subsequently isolated. For every transformed yeast strain that was to be assayed in a Western blot, a 50 ml mid-log phase culture was prepared *(Section 2.3.8.1)* and the total number of OD_{600} units was calculated for future use (e.g. OD_{600} = 0.6 x 55 ml = 33 total OD_{600} units). A larger culture of the untransformed yeast strain (Y190) was also prepared as a negative control. Each culture was poured into two pre-chilled 50 ml centrifuge tubes (halfway filled with ice), before the tubes were centrifuged in a pre-chilled 8 x 50 ml rotor (43114-143) for 5 min at 1,000 *g* and 4 °C, using the Europa 24M centrifuge (Kontron Instruments). The cell pellet was washed in 50 ml ice-cold distilled water and stored at -80 °C until the next stage of the experiment.

- 100 X PMSF (phenylmethyl-sulphonyl fluoride) stock solution: 0.1742 g in 10 ml isopropanol.
- TCA buffer: 20 mM Tris-HCl, pH 8.0, 50 mM ammonium acetate, 2 mM EDTA and 1 X PMSF. The PMSF and 'yeast protease inhibitor cocktail' were added immediately prior to use.

Each cell pellet was thawed on ice and then resuspended in 100 µl of ice-cold TCA buffer per 7.5 OD_{600} units of cells. The cell suspension was then transferred to a 1.5 ml tube containing 100 µl of glass beads, and 100 µl of ice-cold 20 % (w/v) trichloracetic acid (TCA), per 7.5 OD_{600} units of cells. The tube was vortexed at 4 °C for 10 min and the supernatant (the first cell extract) was transferred to a fresh tube. The glass beads were washed by adding 500 µl of an ice-cold 1:1 mixture of 20 % (w/v) TCA and TCA buffer, followed by vortexing at 4 °C for 5 min. The supernatant was added to the first cell extract and the proteins were pelleted at 13,000 rpm for 10 min at 4 °C. The pellet was resuspended in 10 µl of 1 X SDS-PAGE sample buffer (containing β-mercaptoethanol) per OD_{600} unit of cells, and boiled for 10 min. The samples were centrifuged for 10 min at 13,000 rpm and room temperature, and then 35 µl of each supernatant were loaded onto a 4-20 % Novex gel for SDS-PAGE *(Section 2.3.2)*. Once the proteins had been separated by SDS-PAGE, they were transferred to a nitrocellulose membrane and immunoblotted with the following antibodies, to detect fusion protein expression: α-SR-BII, α-plc-γ1 and α-GAL4-DBD *(Section 2.3.3)*.

2.3.9 ISOLATION OF CAVEOLAE LIGHT MEMBRANES FROM CELL LYSATES

2.3.9.1 Sucrose gradient ultracentrifugation

Due to their low buoyant density, caveolin-rich light membranes (CLM) can be isolated from cells using density gradient ultracentrifugation. CLM were prepared using a detergent-free method as described by Waugh *et al.* [271]. Recombinant CHO cell monolayers were grown to confluence in 175 cm^2 flasks *(Section 2.4.1)* and scraped into 2 ml MBS buffer [25 mM morpholinoethane sulphonic acid, 150 mM NaCl, 10 mM EDTA and 10 mM EGTA, pH 6.5] containing 500 mM sodium carbonate and protease inhibitors. Cells were sonicated on ice using a Sanyo Soniprep 150 (5 x 10 s pulses at 12 μm amplitude, with 10 s pauses between pulses) and the cell homogenate was then mixed with 2 ml of 90 % (w/v) sucrose in MBS buffer. After transferring each sample to a 12 ml (14 x 89 mm) ultracentrifuge tube (Beckman Coulter, Buckinghamshire, UK), a 5-35 % discontinuous sucrose gradient was formed above the homogenate. Firstly, a 4 ml layer of 35 % (w/v) sucrose in MBS was gently pipetted onto the sample, followed by a second 4 ml layer of 5 % (w/v) sucrose in MBS. The sucrose gradient was centrifuged in a Beckman SW41 swing-out rotor for 18 h at 39,000 rpm and 4 °C (Beckman Optima LE-80). Following the overnight spin, a light-scattering CLM band was seen at the 5-35 % sucrose interface.

Twelve 1 ml fractions were collected from the Beckman tubes and their protein content was determined using the Bio-Rad protein assay *(Section 2.3.1.2)*. Twenty μl samples from fractions 2-12 were subjected to SDS-PAGE (using 4-20 % Novex gels), followed by immunoblotting with α-caveolin-1 (pAb), α-clathrin, α-SR-BII and α-CLA-1 *(Sections 2.3.2* and *2.3.3)*.

2.3.9.2 Co-immunoprecipitation

To determine whether human SR-BII co-immunoprecipitated with caveolin-1, 250 μl of the CLM fraction were mixed 1:1 with Tris buffered saline (TBS), and the sample was subjected to immunoprecipitation with polyclonal α-caveolin-1 *(Section 2.3.5)*. The sample was eluted from the beads in 100 μl of SDS-PAGE sample buffer (containing 2 μl β-mercaptoethanol), separated by SDS-PAGE and analysed by immunoblotting with α-SR-BII *(Sections 2.3.2* and *2.3.3)*. In order to ascertain the

proportion of SR-BII that co-immunoprecipitated with caveolin-1, another sample of the starting material, as well as the flow-through from the immunoprecipitation, were concentrated 10-fold using a 500 µl Vivaspin concentrator (10,000 MWCO; Vivascience Ltd.). These samples were mixed 1:1 with 2 X SDS-PAGE sample buffer and 2 µl of β-mercaptoethanol. The concentrated starting material and flow-through were run alongside the immunoprecipitation reaction samples on the Novex gel. Following transfer of the proteins onto nitrocellulose, the blot was cut into two parts and appropriate sections were probed with SR-BII antiserum or α-caveolin-1 monoclonal antibody.

Finally, to investigate whether plc-γ1, or any other signalling molecule, co-immunoprecipitates with the α-caveolin-1/SR-BII complex in response to HDL binding, the CLM fraction was isolated from HDL-stimulated CHO-SR-BII cells and subjected to the co-immunoprecipitation reaction described above. Recombinant cells were HDL-stimulated by incubation in serum-free media containing 10 % (v/v) 'HDL plasma' *(Section 2.3.10.6)* for 20 min, whereas resting cells were incubated in serum-free media alone. Both silver staining and immunoblotting with α-plc-γ1 *(Sections 2.3.2.3* and *2.3.3)* were subsequently performed to assess whether plc-γ1, or any other signalling protein, is recruited to caveolae following HDL stimulation.

2.3.10 ISOLATION OF PLASMA LIPOPROTEINS FROM HUMAN PLASMA

Several procedures exist to separate lipoproteins into their various classes [reviewed in 272]. The two lipoprotein separation techniques used in this thesis are precipitation and ultracentrifugation. The latter procedure is the preferred method for large-scale lipoprotein preparation, and was used to isolate large quantities of LDL. A combination of both procedures provided a fast and economical way to isolate total HDL. These two techniques are described in detail below.

2.3.10.1 Blood sampling

For all lipoprotein isolations, 50 ml of blood was taken from the antecubital vein of a donor, and added to tubes containing 0.8 ml of 0.2 M EDTA (pH 7.4) and 1.4 ml of 0.3 M sodium chloride (pH 7.4) [273]. The blood was immediately centrifuged for 20 min at 1,800 *g* and 4 °C using a bench-top centrifuge (Heraeus Megafuge 1.0R) to separate the plasma from the blood cells.

2.3.10.2 Sequential preparative ultracentrifugation

Lipoproteins have lower hydrated densities than other plasma proteins, which permit their isolation from plasma by flotation ultracentrifugation [274]. The density of plasma can be increased by the addition of NaCl and/or NaBr. Subsequently, during ultracentrifugation, lipoproteins will float to the surface depending on their density and the overall density of the solution. By sequentially increasing the density of the plasma solution, the individual lipoprotein classes can be isolated in a stepwise manner. The density range of plasma lipoproteins is given in Table 2.7.

Lipoprotein Class	**Density Range (g/ml)**
Chylomicrons	< 0.940
VLDL	0.940 – 1.006
Intermediate-density lipoprotein (IDL)	1.006 – 1.019
LDL	1.019 – 1.063
HDL_2	1.063 – 1.125
HDL_3	1.125 – 1.21

Table 2.7 Density classes of plasma lipoproteins

The sodium bromide density solutions required for sequential preparative ultracentrifugation were prepared by Dr. D. Riddell (Royal Free & University College Medical School, London, UK). Briefly, a base density solution of 1.006 g/ml was generated by adding 57 g anhydrous NaCl, 0.5 g EDTA, 5 ml 1 M NaOH, and 0.5 g sodium azide to 5.015 litres of distilled water. This solution gave a refractive index value of 1.3345 at 20 °C. All the other density solutions required for lipoprotein isolation were prepared by adding a known weight of solid NaBr to the base density solution. For accurate density determination, the refractive index value for each solution was measured using a refractometer. Fine adjustments to the density solutions were achieved by adding d=1.478 g/ml and d=1.006 g/ml solutions to increase and decrease the overall density, respectively.

The following equation was used to calculate the volume of density solution required to float lipoproteins:

$$v_1.d_1 + v_2.d_2 = (v_1 + v_2).d_3$$

Where: v_1 = Volume of plasma (or ultrafiltrate)

v_2 = Volume of density solution to be added

d_1 = Density of plasma (or ultrafiltrate)

d_2 = Density solution used for adjustment

d_3 = Density required

All the following centrifugation steps took place at 16 °C, using a 12 x 38.5 ml rotor (Kontron TFT 50.38) in a Kontron Centrikon T-2060 ultracentrifuge. Screw-capped polycarbonate centrifuge tubes with a working capacity of 29 ml were used for all of the centrifugations (Kontron Instruments Ltd.)

2.3.10.3 Chylomicron, VLDL and IDL preparation

The first step in LDL and HDL purification was the isolation of all the lipoproteins with lower densities than LDL (d<1.019 g/ml): chylomicrons, VLDL and IDL. Firstly, 19.333 ml of plasma were placed in the centrifuge tube and its density was adjusted to 1.019 g/ml by adding 9.667 ml of 1.045 g/ml density solution. The samples were centrifuged for 20 h at 37,000 rpm (105,000 *g*). The lipoproteins that floated to the top of the tube were collected using a syringe and a needle.

2.3.10.4 LDL preparation

The solution below the chylomicron, VLDL and IDL fraction was removed, wiping clean the inner surface of the tube, until only 19.333 ml remained. The density of this solution was then adjusted to 1.065 g/ml with the addition of 9.667 ml of 1.157 g/ml density solution. The samples were mixed and centrifuged under the same conditions as described in *Section 2.3.10.3.* The LDL fraction was isolated from the top 4 ml and dialysed against 2 x 4 litres of PBS using dialysis cassettes (10,000 MWCO; Perbio Science Ltd.). Finally, its concentration was determined using the Bio-Rad protein assay *(Section 2.3.1.2).*

2.3.10.5 Isolation of HDL by ultracentrifugation

After LDL removal, HDL_2 and HDL_3 were sequentially isolated. Firstly, the solution below the LDL fraction was adjusted to 19.333 ml, and its density was changed to 1.125 g/ml with the addition of 3.29 ml of 1.478 g/ml and 6.38 ml of 1.125 g/ml

density solutions. The samples were centrifuged for 40 h at 37,000 rpm (105,000 *g*) and the HDL_2 was isolated. Secondly, the solution below the HDL_2 fraction was removed such that 19.333 ml was left in the tube. Its density was adjusted to 1.21 g/ml by adding 6.13 ml of 1.478 g/ml and 3.54 ml of 1.21 g/ml density solutions. Following another centrifugation step at 37,000 rpm (105,000 *g*) for 40 h, the HDL_3 was isolated. Dialysis and protein quantification subsequently took place in the same way as described for LDL.

2.3.10.6 Isolation of HDL by precipitation

Apolipoprotein B (apoB) interacts with a number of precipitating agents, such as magnesium and phosphotungstic acid, causing apoB-containing lipoproteins to be separated from non-apoB-containing lipoproteins in a single step. This creates an easy method for separating HDL particles from chylomicrons, VLDL, IDL and LDL. For the precipitation reaction, 100 µl of 0.5 M $MgCl_2$ and 100 µl of 4 % (w/v) phosphotungstic acid (in 0.19 M NaOH) were added to every 1 ml of fresh plasma and mixed well [272]. The plasma was then centrifuged immediately for 20 min at 2,000 *g* and 20 °C in a bench-top centrifuge (Heraeus Megafuge 1.0R). All the apoB-containing lipoproteins were precipitated, leaving plasma with HDL as the sole lipoprotein component. In some cases, HDL_2 and HDL_3 were isolated from the apoB-free plasma by raising its density (still at 1.006 g/ml) and performing ultracentrifugation, essentially as described above. The apoB-free plasma was dialysed and quantified in the same way as for LDL, and used directly as a rich source of total HDL ('HDL plasma').

2.3.10.7 Agarose gel electrophoresis for lipoprotein detection

Following the isolation of plasma lipoprotein subclasses by sequential ultracentrifugation, the success of the separation was verified using agarose gel electrophoresis. During agarose gel electrophoresis, lipoproteins migrate to different positions according to their charge. Figure 2.7 represents the migration pattern of the major plasma lipoproteins that can be clearly visualised following electrophoretic separation: LDL particles remain close to the application point and migrate in the beta position; VLDL particles migrate further than LDL particles to the pre-beta position; HDL particles comprise the fastest fraction and migrate to the alpha position; finally chylomicrons remain at the application point. Furthermore, when plasma is separated using this method and lipoprotein (a) or Lp(a) particles are present at a sufficiently high

concentration, they can be seen migrating between VLDL and HDL (fast pre-beta position).

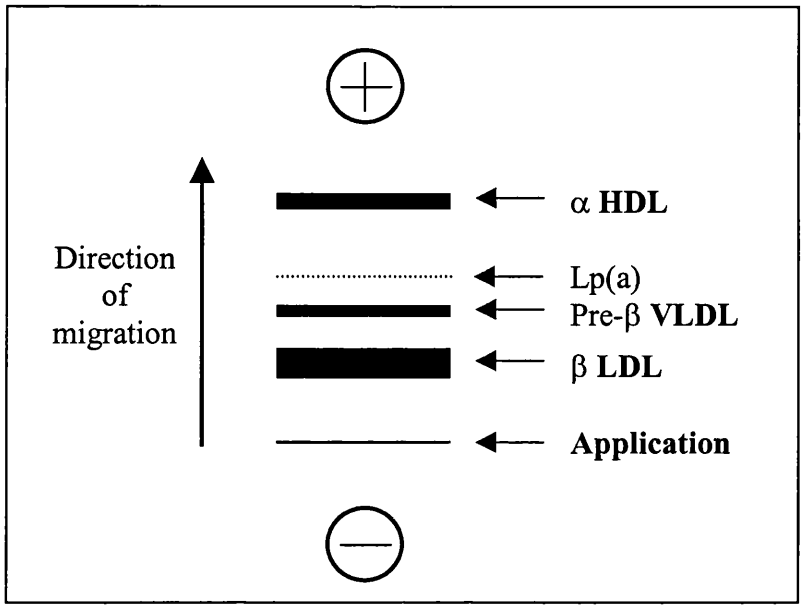

Figure 2.7 Migration pattern of plasma lipoproteins following electrophoresis

Lipoprotein separation using agarose gel electrophoresis was performed using the 'HYDRAGEL LIPO + Lp(a)' kit from Sebia (Issy-les-Moulineaux, France) according to the manufacturer's instructions. Briefly, up to 5 µl of each lipoprotein sample was applied to the bottom of the 8 % (w/v) agarose gel. Samples of fresh plasma (3 µl per lane) were used as controls to monitor lipoprotein migration in the gel. The gel was subsequently placed into the electrophoresis chamber (Sebia K20) containing 300 ml of Tris-barbital running buffer (pH 9.2; supplied with the kit), and migration took place over 90 min with a constant voltage of 50 V. Once the gel had dried it was subjected to staining with a lipid specific Sudan black stain to reveal the migration patterns of the lipoproteins (typically 10 min). The Sudan black stain was prepared fresh before use: 0.044 % (w/v) in 53 % ethanol. Once the gel had been destained with a solution of 45 % (v/v) ethanol, the purity of individual lipoprotein fractions was determined.

2.4 Cell Culture

2.4.1 GENERAL CELL CULTURE AND CRYOPRESERVATION

HepG2 (hepatoblastoma) cells and THP-1 (monocytic) cells were the two human cell lines used in this thesis. The CHO-K1 hamster epithelial cell line was chosen to

transfect and over-express human SR-BI or II. HepG2, THP-1 and CHO-K1 cell lines were purchased from the European Collection of Animal Cell Culture (ECACC, Wiltshire, UK), with ECACC numbers of 85011430, 88081201 and 85051005, respectively.

2.4.1.1 Cell maintenance

All cell types were cultured in 75 cm^2 and 175 cm^2 tissue culture flasks at 37 °C, in a humidified atmosphere of 5 % CO_2 and 95 % air (Jencons Millenium CO_2 incubator, Jencons-PLS). In each case, the growth medium was supplemented with the following components: 2 mM glutamine, 10 % (v/v) heat inactivated FBS, 100 µg/ml streptomycin and 100 U/ml penicillin. All cell culture work was performed in a class II microbiological safety cabinet (Envair Ltd., Lancashire, UK), using sterile, disposable plastic ware.

HepG2 hepatoblastoma cells

HepG2 cells were maintained as adherent cells in Dulbecco's Modified Eagle's Medium (Life Technologies). The cells were passaged every 7 days by brief trypsinisation: HepG2 cell monolayers were washed in PBS, removed using a 2 min incubation with 0.25 % (v/v) trypsin-EDTA at 37 °C, and then neutralised in fresh media. The resuspended cells were passed through a 21 G needle to form a single cell suspension and split 1:8.

THP-1 monocytic cells

THP-1 cells were grown as a suspension culture in RPMI-1640 media (Life Technologies). The cells were seeded at a density of 1 x 10^5 cells/ml and allowed to grow until their density reached 1 x 10^6 cells/ml (about 7 days).

CHO-K1 epithelial cells

CHO-K1 cells were maintained as adherent cells in Ham's F12 media (Life Technologies). The cells were passaged every 3-4 days by brief trypsinisation, as described for HepG2 cells, and split 1:7 using fresh media.

2.4.1.2 Viable cell counting

Trypan Blue stain was used to stain dead cells and determine cell viability during counting. A 30 µl aliquot of the cell suspension was diluted 1:1 with Trypan Blue stain,

and pipetted under the coverslip of a haemocytometer. The number of viable cells present in eight 1 mm^2 squares, and a total volume of 10^{-4} cm^3, was counted using an inverted phase-contrast microscope (Nikon TMS, Jencons-PLS). After calculating the average number of viable cells per square, the concentration of the cell suspension was calculated using the following equation:

$$Viable\ cell\ count/ml = Dilution\ factor \times Average\ count\ per\ square \times 10^4$$

2.4.1.3 Cryopreservation

Cryopreservation is a technique that allows cells to be stored for a long period under liquid nitrogen. To prepare cells for storage, 1-5 x 10^6 cells were resuspended in 1 ml freezing solution [10 % (v/v) DMSO in normal culture medium]. Immediately, the cells were transferred to a 1.8 ml cryovial (Life Technologies) and placed in a freezing chamber (Nalgene Cryo 1 °C Freezing Container, Fisher Scientific, Leicestershire, UK) at -80 °C. When the isopropanol-containing freezing chamber is placed at -80 °C, its temperature is reduced by 1 °C every minute. Once the cells had reached -80 °C, the cryovials were transferred to liquid nitrogen containers for long-term storage.

When required, cells were rapidly thawed by immersing the bottom of the cryovial in a 37 °C water bath, before transferring the vial contents to an excess of media. The cells were pelleted at 300 *g* for 5 min in a bench-top centrifuge (Heraeus Megafuge 1.0R), resuspended in fresh media, and transferred to a 75 cm^2 flask. Cells were subsequently subcultured as described previously *(Section 2.4.1.1).*

2.4.2 MONOCYTE DIFFERENTIATION AND CHOLESTEROL LOADING

2.4.2.1 Monocyte differentiation

The phorbol ester, phorbol 12-myristate 13-acetate (PMA) was used to differentiate THP-1 monocytes into macrophages. The phorbol binds to the cell membrane and activates the protein kinase C signal transduction pathway. This causes the cells to stop proliferating and form an adherent monolayer [275]. In order to differentiate cells into macrophages, 1.75 x 10^7 THP-1 cells in 35 ml of RPMI-1640 media were seeded into 175 cm^2 flasks. PMA was added to the cells at a final concentration of 250 nM (from a 1 mM stock dissolved in DMSO), and the flasks were incubated in a humidified atmosphere of 5 % CO_2 and 95 % air at 37 °C. The media containing PMA was replaced every two days. After 7 days, the differentiated

macrophages had developed irregular shaped nuclei and contained many phagocytotic vacuoles. The THP-1 macrophages were then cell surface biotinylated to isolate membrane proteins *(Section 2.4.5.1),* or they were incubated with Ac-LDL to accumulate cellular cholesterol (see section below).

2.4.2.2 Cholesterol loading of macrophages

Scavenger receptors expressed on the cell surface of macrophages are responsible for the uptake of modified forms of LDL in cell culture, such as Ac-LDL. In the presence of Ac-LDL, THP-1 macrophages rapidly accumulate cellular cholesterol and the resultant lipid-laden macrophages are found to closely resemble atherosclerotic foam cells [7,276]. The addition of acetyl groups to positive lysine and arginine residues of apolipoprotein B abolishes their ability to bind to the LDL receptor and promotes their rapid uptake by macrophage scavenger receptors [277].

Native LDL (nLDL) was acetylated by a protocol based on the method of Basu *et al.* [278]. Following isolation of nLDL from plasma, using sequential ultracentrifugation *(Section 2.3.10)* its protein concentration was determined, before the lipoprotein was subjected to chemical modification by saturated sodium acetate and acetic anhydride. To a volume of nLDL (6-10 mg/ml), an equal volume of saturated sodium acetate was added. The mixture was stirred constantly at 4 °C. Six aliquots of 10 M acetic anhydride were then added over a period of an hour, with a final 30 min stirring after the last addition. The total volume (μl) of acetic anhydride to be added was equal to 1.5 times the total mg nLDL used. The mixture was then dialysed against PBS, using a dialysis cassette (Perbio Science Ltd.), sterile filtered, and the protein concentration was measured once again *(Section 2.3.1).* To verify that the acetylation procedure had been successful, equal amounts of Ac-LDL and nLDL were loaded onto an agarose gel and separated by electrophoresis *(Section 2.3.10.7).* The addition of acetyl groups to positive lysine and arginine residues of apolipoprotein B causes the LDL particles to become more negatively charged, which increases their mobility by agarose gel electrophoresis.

Once it was established that the acetylation procedure had been successful, the differentiated macrophages were cholesterol-loaded. Firstly, the cells were serum-starved overnight in media containing 1 % (w/v) BSA, before the cells were incubated for 24 h in serum-free media containing 75 μg/ml Ac-LDL. The cholesterol-loaded

THP-1 macrophages were subsequently cell surface biotinylated to isolate membrane proteins *(Section 2.4.5.1)*.

2.4.3 TRANSFECTION AND SELECTION OF STABLE CLONES

Full-length SR-BI and II sequences were cloned into the pCDNA3 vector to generate pCDNA3-I and pCDNA3-II, respectively *(Section 2.2.9)*. These plasmids were used to transfect CHO-K1 cells. Subsequently, stable clones over-expressing SR-BI or II (CHO-SR-BI and CHO-SR-BII cells) were isolated and analysed.

2.4.3.1 Transfection protocol

The day before transfection, 4 x 10^5 CHO-K1 cells were seeded into each well of a 6-well plate, and incubated overnight to produce a monolayer at 70 % confluency. For each transfection reaction, 2 μg of plasmid DNA was diluted in 100 μl of culture media, containing no serum or antibiotics. Ten μl of 'Superfect Transfection Reagent' (Qiagen) were then mixed with each plasmid, and the tubes were subsequently left for 10 min at room temperature to allow transfection complex formation. 'Superfect' is a polyamidoamine dendrimer that possesses a defined spherical architecture, with branches radiating from a central core that terminate at charged amino groups [279]. Negatively charged DNA is rapidly assembled into a compact structure within the 'Superfect'-DNA transfection complexes. These complexes possess a net positive charge, which enables them to bind to negatively charged receptors, such as sialylated glycoproteins, on the surface of eukaryotic cells. Following endocytosis, and fusion of the endosome with a lysosome, the 'Superfect' reagent inhibits lysosomal nucleases by buffering the lysosome, and thereby promotes delivery of plasmid DNA into the cell. CHO-K1 cells were prepared for transfection by aspirating their growth medium and washing them with 4 ml of warm PBS. The transfection complexes were mixed gently with 600 μl of normal growth medium and transferred immediately to the cells. The plates were incubated for 3 h at 37 °C and 5 % CO_2 to allow for cellular uptake of the DNA. The transfection medium was then removed and the cells were washed three times with 4 ml of PBS. The cells were incubated overnight in normal media.

The transfection protocol described above was also performed using two controls, 'Superfect Transfection Reagent' alone and DNA alone, in parallel wells to check for cytotoxicity of the procedure. As a positive control, 2 μg of pCDNA3-GFP containing the green fluorescent protein (GFP) sequence were transfected into cells. This vector

was generously provided by Dr. A. Manzano (Royal Free & University College Medical School, London, UK). When the transfection was successful, cells expressed the fluorescent protein after 24-48 h. GFP fluorescence was detected with an inverted fluorescent microscope (Nikon Eclipse TE200) at 20X magnification, using the NB 2EC filter and incident light of wavelength 465-495 nm.

2.4.3.2 Selection and analysis of clones

The pCDNA3 vector contains the neomycin selectable marker (Figure 2.8), which confers cellular resistance to geneticin G418 sulphate (Life Technologies). Twenty-four hours after transfection, selection of the transfected cells began, with the addition of geneticin to the culture media at a final concentration of 600 μg/ml. This concentration was chosen following a geneticin dose-response experiment using untransfected CHO-K1 cells *(Section 4.2.2.1)*. Cells that had successfully taken up pCDNA3-I/II expressed neomycin, as well as SR-BI or II, and therefore survived. The surviving cells were expanded and maintained under selection pressure and are described as the 'mixed population' of cells.

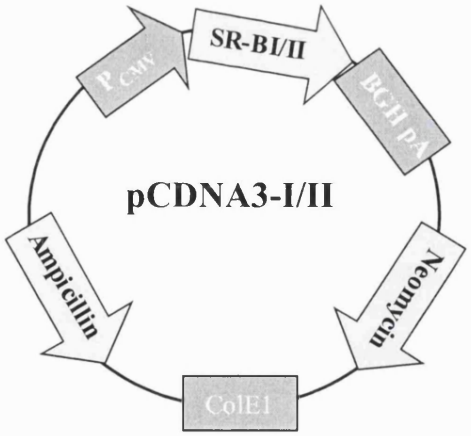

Figure 2.8 Plasmid map of pCDNA3-I/II

The cytomegalovirus (CMV) enhancer-promoter generates high-level SR-BI/II expression and the bovine growth hormone (BGH) polyadenylation signal and transcription termination sequence enhance mRNA stability. The neomycin-selectable marker confers resistance to geneticin, whereas the ampicillin resistance gene and ColE1 origin select and maintain the plasmid in E. coli.

Individual cells from the mixed population were subsequently isolated and clones were expanded and analysed. Firstly, cells underwent serial dilutions and were seeded into 90 mm plates at a very low density (~ 20 cells/plate). Once the cells had adhered to

the plate, positions of single cells were marked on the underside of the dish. Following 5 cell divisions, the clones were gently trypsinised and picked, using an inverted light microscope and a 200 µl pipette tip. Over the next few weeks, the clones were expanded and cell lysates were analysed for SR-BI/II protein expression using SDS-PAGE and Western blotting *(Sections 2.4.4, 2.3.2* and *2.3.3)*. Following analysis, one CHO-SR-BI clone and two CHO-SR-BII clones (high- and low-expressing) were selected for subcloning. This extra cloning step was performed in order to increase the chance of isolating a pure clone (method as described above). Finally, flow cytometric analysis and densitometry of autoradiographs were used to compare the levels of cell surface receptor expression in each of the clones *(Section 2.4.5)*.

2.4.4 PREPARING CELL LYSATES

In order to lyse cultured cells and isolate cellular proteins, a combination of chemical and physical techniques was used. Firstly, the cells were scraped into a detergent-containing lysis buffer, which solubilised the cell membranes. Secondly, the cells were physically disrupted using shear stress forces. The lysis buffer contained the 'Complete' Mini protease inhibitor cocktail (Roche Diagnostics) and throughout the whole procedure ice-cold buffers were used and tubes were kept on ice. Taken together, these steps reduced the amount of protein degradation caused by cellular proteases.

Monolayer cultures were grown to confluency and washed in warm PBS, followed by ice-cold PBS. One ml of lysis buffer [50 mM Tris-HCl, pH 7.5, 150 mM NaCl, 2 mM EDTA and 1 % (v/v) Triton X-100, containing the 'Complete' protease inhibitor added immediately prior to use] was pipetted into each 75 cm^2 flask. The cells were quickly scraped and collected in a 1.5 ml tube. A 19 G needle and syringe was used to create shearing forces as the cells were drawn up and down five times through the needle. The lysates were then left on ice for 30 min before the detergent-insoluble cellular fraction was pelleted by centrifugation for 10 min at 13,000 rpm and 4 °C. The supernatant was subsequently transferred to a fresh tube and assayed for protein concentration using the BCA protein assay *(Section 2.3.1.1)*.

In order to prevent protein dephosphorylation during lysate production, two extra components were added to the lysis buffer immediately prior to use: sodium vanadate and DTT, to a final concentration of 0.1 mM and 1 mM, respectively. This buffer was

used in experiments to investigate cytoplasmic SR-BII phosphorylation and cytoplasmic SR-BII binding interactions.

2.4.5 ANALYSIS OF CELL SURFACE RECEPTOR EXPRESSION

Two methods were used for comparing the levels of SR-BI and II cell surface expression in human cell lines and recombinant clones. The first method involved biotinylating cell surface proteins and isolating them using streptavidin beads. The biotinylated proteins were then subjected to SDS-PAGE and immunoblotting, followed by densitometric analysis of the autoradiograph. The second method involved flow cytometry.

2.4.5.1 Biotinylation of cell membranes

Cells were grown to confluency in 175 cm^2 flasks and washed twice with warm PBS. The cells were then incubated at room temperature for 30 min in 4 ml of 0.5 mg/ml 'EZ-Link Sulpho-NHS-LC-Biotin' (Perbio Science Ltd; dissolved in PBS). After washing the cells twice more with PBS, they were incubated at room temperature for 20 min in 4 ml of 10 mM glycine (dissolved in PBS). The glycine served to quench any biotin that had not been washed away. The cells were finally washed with PBS, before they were scraped into 2 ml ice-cold lysis buffer and lysed *(Section 2.4.4)*.

After determining the protein concentration of each cell lysate, an equal amount of protein (0.7–1.0 mg protein/ml) was incubated with 150 µl of pre-washed streptavidin superparamagnetic iron oxide particles. Binding of biotinylated proteins to the streptavidin beads occurred overnight on a rotating wheel at 4 °C. The particles were then washed with 5 x 500 µl of lysis buffer and resuspended in 60 µl SDS-PAGE sample buffer (containing 1 µl of β-mercaptoethanol). The samples were boiled for 10 min and the released proteins were subjected to SDS-PAGE and immunoblotting. The α-CLA-1 antibody bound to both isoforms of the receptor and its use in immunoblotting *(Section 2.3.3)* allowed the levels of SR-BI and II to be compared from the same autoradiograph, using densitometric analysis (Bio-Rad Imaging Densitometer, Model GS-670).

This method was also used for isolation of the SR-BII from HepG2 cells and THP-1 monocytes, macrophages and cholesterol-loaded macrophages. The receptor was detected by immunoblotting with α-SR-BII *(Section 2.3.3)*.

2.4.5.2 Flow cytometry

Flow cytometry is a rapid and sensitive technique used for making physical or biological measurements of a large number of individual suspended cells as they interact with a focused laser beam of defined wavelength. Cells are forced into serial cell flow (by a process of hydrodynamic focussing) and at the time of laser-intercept, each cell generates scattered incident light; forward scatter light depends upon cell size and side scatter light is dependent on cellular internal granularity/complexity. Cells subjected to fluorescent immunolabelling of antigenic epitopes also generate a fluorescence light emission impulse following laser light excitation. Lenses in the detection zone collect all optical signals generated by a single cell and photomultiplier tubes convert the optical signals into electrical pulses. The voltage pulse is amplified and passed to a computer to be processed into digital format and saved in Listmode data files, which can be recalled for further analysis.

Flow cytometric analyses were carried out on CHO-SR-BI/II cells to determine cell surface receptor expression. The α-RED-1 antibody (Novus Biologicals, Littleton, CO) was chosen for this experiment as it binds to the extracellular domain, common to both isoforms, and is suitable for use in immunofluorescent techniques. Adherent cells were grown to confluency in 6-well plates and the traces of media were washed away with warm PBS. One ml of ice-cold PBS was then added to the cells, which were incubated at 4 °C for 15 min. This step caused the cells to become cool and contract, thereby allowing intact cells to be recovered by gentle scraping in PBS using a cell lifter (Corning Costar, Buckinghamshire, UK). After pelleting the cells by pulse centrifugation at 13,000 rpm and 4 °C, they were resuspended in 150 µl of α-RED-1 primary antibody, diluted 1:1000 in ice-cold 0.1 % (w/v) BSA/PBS and incubated for 45 min at 4 °C. Following two washing steps with 0.25 ml ice-cold PBS, cells were resuspended in 150 µl of goat α-rabbit secondary antibody conjugated to fluorescein isothiocyanate (FITC; Molecular Probes Europe, Leiden, The Netherlands), diluted 1:800 in ice-cold 0.1 % (w/v) BSA/PBS. The incubation conditions and washing steps were the same as for the primary antibody. For experimental controls, cells were incubated with pre-immune rabbit serum (diluted 1:1000) instead of the primary antibody (with secondary antibody as normal), while other samples were only exposed to the secondary antibody (with the primary antibody omitted). Finally, the cells were fixed

in 200 µl of 1 % (w/v) paraformaldehyde in PBS as a single-cell suspension (confirmed by phase-contrast microscopy), and stored in the dark at 4 °C overnight.

FITC fluorescence resulting from antibody binding to cell surface SR-BI and II was measured using a fluorescence-activated cell sorter (FACS; FACS Calibur, Becton Dickinson, Oxford, UK) equipped with an argon ion laser providing an excitation wavelength of 488 nm, and standard computer and electronics. In this experiment, the flow cytometer was only used to observe individual characteristics of cells, and the cell-sorting function of the FACS was not required. Initially, the cell population (excluding debris) was gated on a dual parameter display of side and forward scattered light using linear amplifications. FITC fluorescent emissions between 520-530 nm were collected and analysis was performed on 5,000 gated events per sample. Log fluorescence signals were stored as Listmode data files, median fluorescence values were calculated, and figures were created using WinMDI Version 2.8 software *(internet address: http:\\facs.scripps.edu).*

2.4.6 MEASURING CELLULAR FREE [^{3}H]-CHOLESTEROL EFFLUX

Radioisotopes have important roles as tracer molecules, and have widespread use in metabolic investigations. The atomic nucleus of tritium is unstable and decays to emit an electron (β-emitting radioisotope). The number of decay events that occur in a given time interval is related only to the number of radioactive atoms present. Therefore, if the number of decay events is accurately measured by liquid scintillation counting (LSC), the number of radioactive atoms present in the sample can be quantified. Scintillant contains fluorescent organic compounds ("fluors"), which become excited upon bombardment with radiation, including electrons, and emit photons of light. This fluorescence can be detected by photomultiplier tubes and quantified. To determine whether SR-BII functions to promote efflux in response to HDL stimulation, recombinant CHO-SR-BII cells were loaded with tritiated [^{3}H]-cholesterol, incubated with HDL particles, and the amount of [^{3}H]-cholesterol effluxed into the media was measured using LSC. The methodology for measuring FC efflux was based on the protocol described by Gu *et al.* [196].

On day 1, CHO control cells and CHO-SR-BII cells (mixed population; *Section 2.4.3.2*) were seeded into 12-well plates at a density of 175,000 cells/well. For each experimental condition, triplicate wells were seeded. Following aspiration of media on

day 2, cells were loaded with 1 ml media containing 5 % (v/v) FBS and 1 μCi [^{3}H]-cholesterol. The cells were incubated at 37 °C for at least 24 h to allow for radiolabelled cholesterol uptake. On day 3, the labelling media was removed and the cells were washed twice with serum-free media. The cells were then incubated for 16 h with 1 ml of equilibration media; serum-free media containing 1 % (w/v) fatty acid free BSA. Following aspiration of equilibration media on day 4, cells were washed with serum-free media and efflux was subsequently stimulated by adding 1 ml serum-free media containing either 200 μg HDL_3 protein, 5 % (v/v) 'HDL plasma', or 5 % (v/v) plasma. Background efflux was ascertained by incubating cells with 1 ml serum-free media. Cells were then incubated at 37 °C for 4 h, or a time course (0.5, 1, 2 and 4 h) was performed.

The experiment was terminated by removing the media containing any [^{3}H]-cholesterol that had effluxed from the cells. This media was centrifuged for 2 min at 13,000 rpm and room temperature to pellet any floating cells. A 100 μl aliquot of the supernatant was taken from each media sample and mixed thoroughly with 8 ml Cocktail T scintillation fluid in scintillation vials. A liquid scintillation counter (Beckman LS 6500, Beckman Coulter Ltd.) was used to measure the number of decay events occurring in each vial over a period of 1 min. This value was recorded in disintegrations per minute (dpm). Cell monolayers were lysed in 1 ml of 0.1 M NaOH and an aliquot of 100 μl was then taken from each sample. The cellular dpm values were determined using LSC and the total [^{3}H]-cholesterol dpm in the cells and media was then calculated. Once the mean background value (no HDL stimulation) had been subtracted, the percentage [^{3}H]-cholesterol efflux was calculated for each experimental condition (see equation below). The abilities of different recombinant cells to efflux FC were then compared.

$$\textit{Percentage FC efflux} = \frac{\textit{[}^3\textit{H]-cholesterol in media above background (dpm) X 100}}{\textit{[}^3\textit{H]-cholesterol in media (dpm)+ [}^3\textit{H]-cholesterol in cells (dpm)}}$$

In order to compare the levels of FC efflux promoted by HDL versus its major apolipoprotein constituent, apoA-I, [^{3}H]-cholesterol efflux was also performed using 10 μg lipid-free apoA-I protein per ml serum-free media [199]. Delipidated apoA-I purified from human plasma was generously provided by Dr. G. Sperber (Royal Free & University College Medical School, London, UK).

2.4.7 MEASURING CELLULAR CHOLESTERYL [^{3}H]-OLEATE STORES FOLLOWING HDL STIMULATION

Tritium was used as a tracer molecule in CE mobilisation studies. Briefly, recombinant CHO cells took up [9,10-^{3}H]-oleic acid, which subsequently became esterified and generated pools of stored radiolabelled cholesteryl oleate. Once HDL had stimulated the cells, radiolabelled stores were monitored, by thin layer chromatography (TLC) and LSC, to determine whether HDL promoted a reduction in cholesteryl oleate pools.

On day 1, CHO control cells and recombinant CHO cells were seeded into 12-well plates at a density of 200,000 cells/well. For each experimental condition, triplicate wells were plated. After 24 h, the cells were serum-starved by an overnight incubation in serum-free media containing 1 % (w/v) BSA. On day 3, the cells were incubated for 36 h with 1 ml of loading media: serum-free media containing LDL (100 μg protein/ml) and 40 μM BSA/[^{3}H]-oleic acid (0.5 μCi/ml). The oleic acid/albumin complex was prepared according to the method of Ellsworth *et al.* [280]. On day 4, after 36 h of loading, the media was removed, and the cells were incubated overnight in equilibration media: serum-free media containing 1 % (w/v) BSA. On day 5, the cells were washed once with PBS, followed by incubation with 1 ml of efflux medium: serum-free media containing either 200 μg HDL_3 protein or 5 % (v/v) 'HDL plasma' *(Section 2.3.10)*. Serum-free media alone was used as a control to monitor background changes to the radiolabelled pools. The mobilisation experiment either took place over 5 h, or over a time course of 2, 4, 6, 10, 24 and 48 h. Radiolabelled cells were also analysed at time point zero to determine the level of radiolabelled CE at the start of the experiment.

Removal of the efflux media terminated the mobilisation experiment. The cells were washed once with PBS and subjected to lipid extraction with 1 ml of 3:2 hexane:isopropanol. After 1 h, the solvent containing the lipid extract was removed from the cells and spiked with 100,000 dpm of [4-^{14}C]-cholesterol. This acted as an internal control within the experiment and allowed for losses to be calculated. The solvent was then dried down at 40 °C under nitrogen and the lipids were resuspended in 25 μl chloroform. The lipid samples and a lipid standard were subsequently spotted onto the application strip of a TLC plate (Silica gel 60 Å; 20 x 20 cm, layer thickness 250 μm; Whatman, USA). To prepare the TLC chamber, the solvent mixture [hexane:diethyl ether:glacial acetic acid (90:20:1)] was added to a tank lined with filter paper and left to

equilibrate. The TLC plate was then placed into the solvent vapour-filled chamber. Once the solvent front had reached 2-3 cm from the top, the plate was removed and dried, before it was placed in an iodine chamber to stain for 5-10 min. The boundary positions of the required bands (CE and FC) were marked and scraped into scintillation vials containing 8 ml of Cocktail T scintillant. The cholesteryl oleate pools were quantified using a Beckman LS 6500 scintillation counter (Beckman Coulter Ltd.) and the values were corrected for experimental losses (using the internal [4-^{14}C]-cholesterol control). The cellular material remaining after the lipid extraction was solubilised in 1 ml of 0.1 M NaOH, and its protein concentration was determined using the Bio-Rad protein assay *(Section 2.3.1.2)*. The stores of radiolabelled CE were corrected for protein levels and expressed as dpm/μg protein. Each value was then used to calculate the percentage of the mean amount of CE present at the start of the experiment. Finally, this value was subtracted from 100 % to determine the percentage of mobilised CE. For each of the cell types (CHO control cells, CHO-SR-BI and CHO-SR-BII recombinant cells), the mean percentages of mobilised CE were compared.

2.5 Statistical Analysis

Values in text and figures were expressed as the mean ± S.E.M. Statistical differences between means were determined using Student's *t*-test and considered significant if $p<0.05$. All analyses were performed using Microsoft Excel (Microsoft Office 2000).

Chapter 3

3. SR-BII AND SIGNAL TRANSDUCTION

3.1 Introduction

As outlined in *Chapter 1 (Section 1.6.5.3)* I have identified a number of conserved proline-rich, putative signalling motifs in the C-terminal cytoplasmic tail of SR-BII, which have the potential to interact with specific domains within modular signalling proteins (Figure 1.11). Within the 44-amino acid C-terminal SR-BII tail sequence alone, there are six PXXP motifs that might serve as ligands for SH3 domains [235]. Furthermore, I have also identified a potential SH2 domain recognition site; it is well established that SH2 ligands comprise a phosphotyrosine residue followed by a hydrophobic amino acid at position +3 [237], and within the C-terminus of SR-BII such a motif (YTPL) is present. Potentially, phosphorylation of the cytoplasmic tyrosine residue within the tail of SR-BII might result from activation of the receptor when HDL binds to its extracellular region.

Due to the proline-rich nature of cytoplasmic SR-BII and the presence of a potential tyrosine phosphorylation site within it, I proposed that HDL binding to the extracellular domain of SR-BII promotes signal transduction via intracellular protein-protein interactions. One such signalling pathway that may involve SR-BII-mediated signalling is the stimulation of cellular cholesterol mobilisation in response to HDL binding at the cell surface [47]. Since SR-BII is able to bind HDL and also contains many potential signalling motifs, I hypothesised that upon HDL stimulation, SR-BII acts as a signal transducer to promote intracellular CE hydrolysis.

This chapter describes investigations into the potential role of SR-BII in signal transduction. Firstly, I generated cytoplasmic SR-BI and II fusion proteins and used them in a variety of 'pull-down' binding assays to determine whether these cytoplasmic sequences have the potential to interact with a panel of SH3 domain-containing signalling proteins. Subsequently, cytoplasmic SR-BII interactions were examined within more physiological cellular environments using either recombinant CHO cells over-expressing human SR-BII (CHO-SR-BII) or the yeast two-hybrid system. In addition, the phosphorylation state of the tyrosine residue within cytoplasmic SR-BII was monitored upon HDL stimulation of CHO-SR-BII cells. Finally, I isolated caveolae

from CHO-SR-BII cells to establish the localisation of human SR-BII within the plasma membrane. Caveolae are sites of cholesterol flux between lipoproteins and cells, as well as microdomains within the plasma membrane that concentrate signalling intermediates [50,54]. Murine SR-BII has been found to localise in these cholesterol-rich microdomains, which suggests that human SR-BII might also localise in caveolae, from where it may serve to transduce signals and promote cholesterol flux [233]. The role of SR-BII in cholesterol homeostasis was also investigated and these results are discussed in *Chapter 4*.

3.2 Results

3.2.1 GENERATION OF CYTOPLASMIC SR-BI AND II EXPRESSION VECTORS

In order to generate GST- and biotin-tagged cytoplasmic tails, C-terminal cytoplasmic sequences of SR-BI and II were PCR-amplified from a human cDNA template and cloned into fusion protein expression vectors. The fusion proteins would subsequently be used for analysing binding interactions with peptides from signalling protein domains. The cloning strategies for the production of cytoplasmic SR-BI and II expression vectors are outlined in *Section 2.2.9*. In this chapter, 'cytoplasmic tail' refers to the entire C-terminal tail sequence.

3.2.1.1 Synthesis of cDNA templates

The human HepG2 (hepatoblastoma) and THP-1 (monocytic) cell lines have been reported to express both SR-BI and II mRNA [232]. Messenger RNA was therefore isolated from these two cell lines and used for generating a cDNA template by reverse transcription *(Section 2.2.2)*. The quality of the cDNA template was assessed by PCR-amplifying the *U1A* 'housekeeping gene' using specific primers (*Section 2.2.3* and Table 2.1). The PCR products were subsequently separated by agarose gel electrophoresis *(Section 2.2.5)* and bands of the correct size (230 bp) were observed in samples from both cell lines and not in the negative control, indicating successful cDNA synthesis (Figure 3.1).

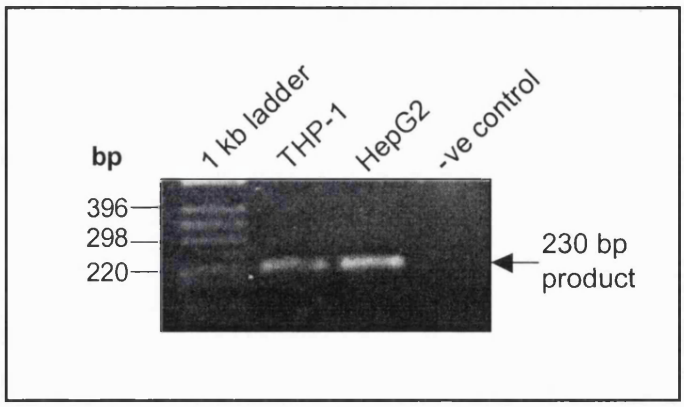

Figure 3.1 Successful generation of human cDNA templates

Messenger RNA was isolated from THP-1 and HepG2 human cell lines and used for cDNA synthesis with reverse transcriptase. The integrity of the synthesised cDNA was confirmed by a U1A RT-PCR (Section 2.2.3), followed by separation of the amplified products on a 1.5 % agarose gel (Section 2.2.5). This figure shows results from a representative UIA RT-PCR, with the method being performed following every cDNA synthesis.

3.2.1.2 Cytoplasmic SR-BII expression vectors

The 3' SR-BII cytoplasmic tail sequence was PCR-amplified from a cDNA template using the primers and conditions described in Table 2.1 and *Section 2.2.3*, respectively. The predicted amplification product of 140 bp was generated over a primer annealing temperature range of 59–65 °C, indicating that the optimum annealing temperature for this set of primers is broad (Figure 3.2, *panel A*). The 140 bp PCR product was directly purified from the reaction mix according to the method described in *Section 2.2.7*, before it was ligated into the pGEM-T vector (pGEM-II) and transformed into competent bacteria *(Sections 2.2.9.4* and *2.2.9.5)*. Plasmids were subsequently extracted from six bacterial clones and analysed by restriction endonuclease digestion with *Sac*II and *Pst*I *(Sections 2.2.9.6* and *2.2.8)*. These unique restriction sites are situated in the MCS of pGEM-T, either side of the cytoplasmic tail insertion site. Generation of a digestion product of ~160 bp would indicate that the bacterial clone had been successfully transformed with the 3' SR-BII cytoplasmic tail sequence. Digested samples were separated on an agarose gel *(Section 2.2.5)* and the correctly sized digestion products were detected in clones designated 1, 4, 5 and 6 (Figure 3.2, *panel B*). Since PCR products are able to ligate into the pGEM-T cloning vector in either orientation, the clones were sent for automated fluorescent sequencing *(Section 2.2.9)*.

Analysis of the sequencing chromatograms allowed the orientation of each cytoplasmic tail within its vector to be ascertained.

The cloned PCR product comprised only the unique SR-BII tail sequence. Therefore, in order to generate the entire tail sequence, including the five amino acids that are common to both isoforms, an oligonucleotide polylinker was inserted (Figure 2.4). Firstly, the pGEM-II vector was subjected to digestion with *Bsu*36I and *Pst*I endonucleases *(Section 2.2.8)* and dephosphorylation *(Section 2.2.9.3)*. Secondly, the polylinker with *Bsu*36I and *Pst*I "sticky ends" was ligated into the cut vector using these restriction sites *(Section 2.2.9.4)*. Following transformation of competent bacteria with the ligation reaction, plasmids were isolated from six bacterial clones *(Sections 2.2.9.5* and *2.2.9.6)*. Successful insertion of the oligonucleotide polylinker was confirmed by digesting plasmids with *Bam*HI and *Hind*III restriction enzymes. The *Bam*HI and *Hind*III restriction sites were located in the reverse primer and the polylinker, respectively. Generation of a digestion product of ~140 bp revealed that all six clones contained the entire SR-BII cytoplasmic tail sequence (Figure 3.2, *panel C*).

Sequencing data not only revealed the orientation of the tail sequence within the pGEM-II vector, but the presence of a point mutation (T→C) within each of the clones that would result in an amino acid change (Arg→Gly; Figure 3.3, *panel A*). It was therefore necessary to perform site-directed mutagenesis to correct the mutation *(Section 2.2.10)*. After 12 cycles of PCR amplification using primers containing the correct sequence, PCR products were separated on an agarose gel *(Section 2.2.5)* to verify that sufficient amplification had taken place (Figure 3.3, *panel B*). A PCR product of the correct size was seen in all samples, except the negative control. However, as the amount of vector DNA template increased, a smaller PCR product was also observed. This could have resulted from incomplete vector replication during one of the amplification cycles. Therefore, only the PCR samples containing one pure product were subjected to *Dpn*I enzyme digestion to remove any parental DNA. Competent bacteria were subsequently transformed with the desired sequence *(Section 2.2.9.5)*.

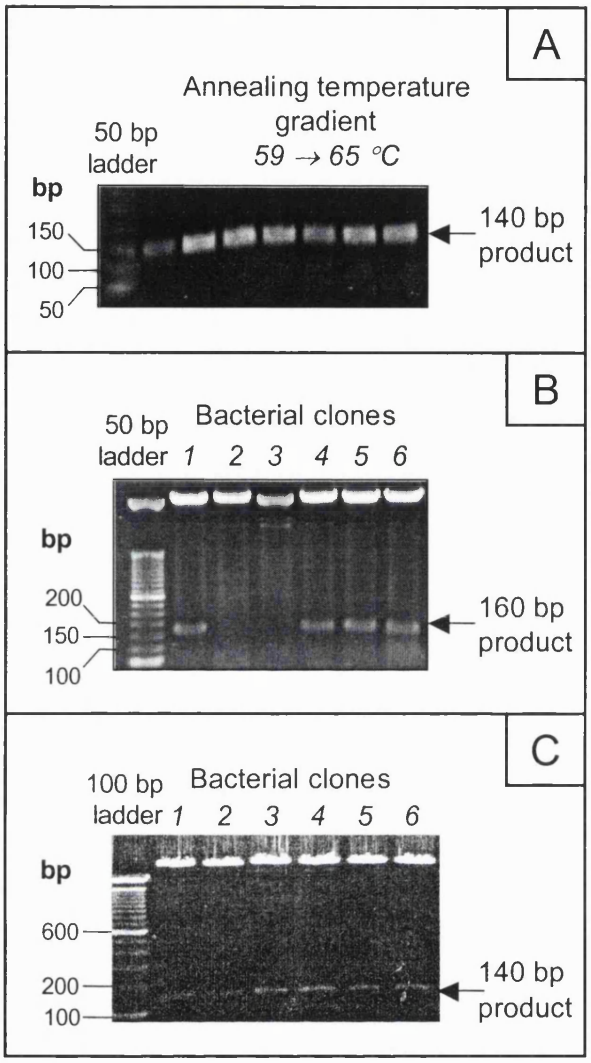

Figure 3.2 Cloning the SR-BII cytoplasmic tail sequence

Panel A, *A viable cDNA template (as assessed in Figure 3.1) was used for PCR amplification of the 3' C-terminal SR-BII tail sequence. The PCR reaction was performed over a primer annealing temperature range of 59–65 °C (Table 2.1 and Section 2.2.3), followed by separation of the amplification products using a 1.5 % agarose gel.* ***Panel B,*** *Following transformation of competent bacteria with pGEM-II, six clones were picked for analysis. Plasmids were isolated from each of the clones and subjected to restriction endonuclease digestion with SacII and PstI for 1 h, using the conditions described in Section 2.2.8. Digestion products were separated using a 1.5 % agarose gel.* ***Panel C,*** *Plasmids were extracted from six bacterial clones and analysed by restriction digestion to confirm that the oligonucleotide polylinker had been successfully inserted. Endonuclease digestion with BamHI and HindIII was performed for 1 h and digestion products were separated using a 1.5 % agarose gel.*

Successful site-directed mutagenesis of the positive control plasmid changed the premature stop codon (TAA) into a glutamine codon (CAA), resulting in the production of full-length β-galactosidase. When bacteria transformed with this plasmid were grown on indicator plates containing IPTG and X-Gal *(Section 2.2.9.5)*, blue colonies were observed. This colour screen verified the presence of β-galactosidase and the success of the control mutagenesis reaction. Sequencing was employed to reveal the success of SR-BII tail mutagenesis: two bacterial clones were confirmed to contain the corrected SR-BII tail sequence (Figure 3.3, *panel C*).

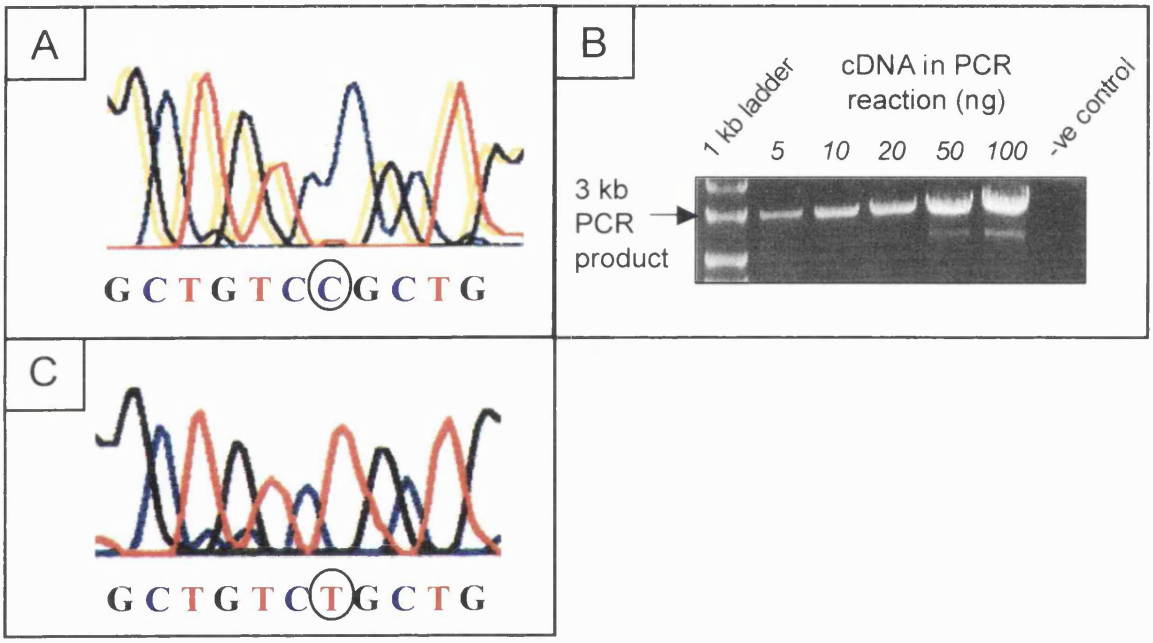

Figure 3.3 Correction of a mutation within cloned cytoplasmic SR-BII by site-directed mutagenesis

Panel A, *Chromatogram revealing part of the sequencing data from one of the pGEM-II bacterial clones. The data revealed a T→C point mutation (circled). This mutation was observed in each of the analysed clones.* ***Panel B,*** *Site-directed mutagenesis was used to correct the point mutation. PCR amplification was performed using a range of template concentrations (5-100 ng) and the conditions described in Section 2.2.10. Following 12 cycles of PCR, amplification products were separated using a 1 % agarose gel.* ***Panel C,*** *Chromatogram revealing the same region as shown in Panel A. The original point mutation had been corrected (C→T) by site-directed mutagenesis (circled).*

This corrected sequence was subsequently transferred into the pGEX-4T-2 and PPXa-3 expression vectors to produce pGEX-II and PPXa3-II, respectively *(Section 2.2.9)*. In each case, successful cytoplasmic tail transfer was confirmed by subjecting plasmids from each bacterial clone to restriction endonuclease digestion with the appropriate enzymes (data not shown). These expression vectors were subsequently used to generate GST-tagged and biotinylated cytoplasmic SR-BII fusion proteins *(Section 3.2.2)*.

3.2.1.3 Cytoplasmic SR-BI expression vectors

The full-length SR-BI sequence was amplified by PCR and ligated into the pGEM-T vector, as described in *Sections 2.2.3.2* and *4.2.1*. Following transformation of competent bacteria, plasmids were purified from four bacterial clones and sequenced *(Sections 2.2.9.5* and *2.2.9.6)*. Sequencing data revealed that all of the four clones had many mutations throughout the SR-BI sequences. One clone, however, contained the correct SR-BI cytoplasmic tail sequence, which was manipulated in the following way to isolate the cytoplasmic tail *(Section 2.2.9)*. The unwanted 5' SR-BI sequence was digested from the pGEM-T vector using *Sac*II and *Acc*III restriction enzymes *(Section 2.2.8)*. *Sac*II cuts at a unique site in the MCS of pGEM-T, upstream of the SR-BI sequence, and *Acc*III cuts at a unique site in the cytoplasmic tail sequence, a few nucleotides downstream from the transmembrane region. The digestion reaction was separated on an agarose gel *(Section 2.2.5)* and a digestion product of the expected length (~1500 bp) was observed (Figure 3.4, *panel A*). This indicated that the mutated 5' SR-BI sequence had been successfully removed. The cut vector was then purified from the gel *(Section 2.2.6)* and an oligonucleotide polylinker with *Sac*II and *Acc*III sticky ends was subsequently ligated into the vector (Figure 2.5; *Section 2.2.9.4*). This served to replace the first four cytoplasmic tail nucleotides and thereby complete the cytoplasmic tail sequence. Following transformation of competent bacteria with the re-circularised vector, plasmids were purified from five bacterial clones and subjected to endonuclease digestion with *Bam*HI and *Hind*III *(Sections 2.2.9.5, 2.2.9.6* and *2.2.8)*. As already described for cytoplasmic SR-BII, the *Bam*HI and *Hind*III sites were located in the reverse primer and oligonucleotide polylinker, respectively. The cytoplasmic tail sequence of ~140 bp was successfully digested from plasmids extracted from each of the five bacterial clones, confirming successful polylinker insertion in all of the analysed clones (Figure 3.4, *panel B*). Cytoplasmic SR-BI was transferred into the pGEX-4T-2 and PPXa-3 expression vectors to produce pGEX-I and PPXa3-I, respectively *(Section*

2.2.9). These expression vectors were subsequently used to generate GST-tagged and biotinylated cytoplasmic SR-BI fusion proteins *(Section 3.2.2).*

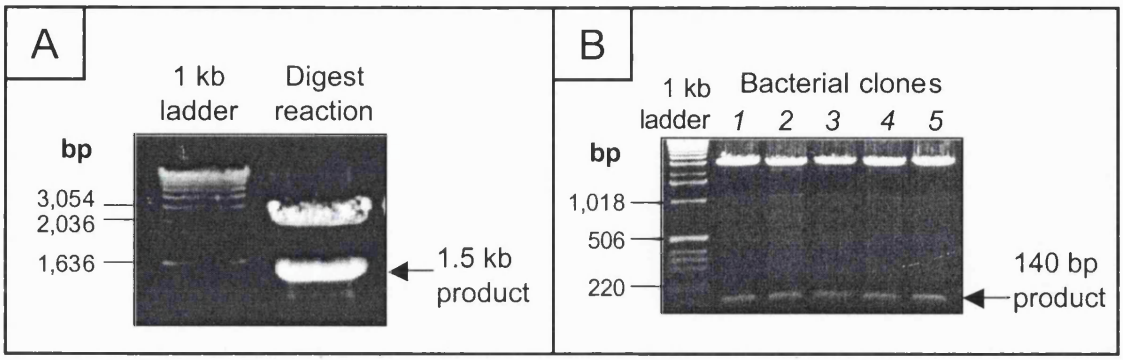

Figure 3.4 Cloning the SR-BI cytoplasmic tail sequence

Panel A, *The mutated 5' SR-BI sequence was digested from a plasmid containing the full-length sequence during 1 h incubation with AccIII and SacII restriction enzymes (Section 2.2.8). The digestion products were separated on a 1 % agarose gel.* ***Panel B,*** *Plasmids were extracted from six bacterial clones and analysed by restriction digestion to confirm that the oligonucleotide polylinker had been successfully inserted. Endonuclease digestion with BamHI and HindIII was performed for 1 h, and digestion products were separated on a 1.5 % agarose gel.*

3.2.2 PRODUCTION OF FUSION PROTEINS TO INVESTIGATE POTENTIAL SIGNALLING INTERACTIONS OF SR-BI/II CYTOPLASMIC TAILS

3.2.2.1 Small-scale production of biotinylated cytoplasmic SR-BI/II

The PinPoint Xa Protein Purification System was used to generate biotinylated SR-BI and II cytoplasmic tails *(Section 2.3.6.1).* The PPXa-3 expression vector carries a segment encoding a peptide that is biotinylated on a specific lysine residue in *E. coli* strains expressing biotin ligase. Due to the strong binding interaction that occurs between biotin and avidin, this biotinylated residue subsequently functions as a purification tag when bacterial proteins are exposed to avidin.

PPXa-3 expression vectors containing cytoplasmic SR-BI and SR-BII sequences (PPXa3-I and PPXa3-II; *Sections 2.2.9* and *3.2.1*) and the positive control expression plasmid were transformed into the *E. coli* JM109 bacterial strain for biotinylated fusion protein expression *(Section 2.2.9.5).* Small-scale recombinant bacterial cultures were grown overnight and induced to express either biotinylated cytoplasmic SR-BI/II or the control fusion protein *(Section 2.3.6.1).* Following induction with IPTG, a small aliquot

of cells was pelleted, boiled in SDS-PAGE sample buffer and analysed by SDS-PAGE and Western blotting *(Sections 2.3.2* and *2.3.3)* with a streptavidin-HRP conjugate (Figure 3.5, *panel A*). The autoradiograph shows the successful generation of biotinylated fusion proteins of the expected molecular weights: control fusion protein of 40 kDa and biotinylated cytoplasmic SR-BI/II of ~20-25 kDa. Unexpectedly, two biotinylated fusion proteins of slightly different molecular weights were detected in recombinant bacteria expressing cytoplasmic SR-BI. It appears that the major (lower) band represents the correctly sized fusion protein (~20 kDa), since the length of the two cytoplasmic tails differ only by 3 residues and its molecular weight is similar to that of the SR-BII fusion protein. It remained unclear what the minor (upper) band represented. A faint band of ~20 kDa was also observed in cellular extracts from the JM109 host strain and the cells expressing the control fusion protein. This extra band represents the single 22.5 kDa biotinylated protein generated endogenously by the *E. coli* JM109 strain. Compared to the large amount of recombinant fusion protein expression, the endogenous biotinylated protein is only expressed at low levels. The 22.5 kDa *E. coli* protein would have also been observed in the cellular extracts from recombinant cells expressing SR-BI and II cytoplasmic tails if their molecular weights had been more dissimilar. Despite the low levels of endogenous biotinylated protein generated by the host bacterium, it cannot be purified by avidin since the biotin moiety is not accessible. Therefore, when avidin-based purification methods were employed, only recombinant fusion proteins were isolated.

The next step was to verify that the two cytoplasmic peptides were recognised by their respective antibodies using Western blotting with isoform-specific antibodies. This experiment would confirm that the sequences had been inserted into their expression vectors so as to maintain their correct open reading frames. Recombinant bacterial proteins were separated as described above by SDS-PAGE, followed by immunoblotting with an isoform-specific antibody directed against the C-terminal cytoplasmic tail of human SR-BI (Dr. van der Westhuyzen, University of Kentucky Medical Centre, USA). The cytoplasmic SR-BI fusion protein was readily detected by α-SR-BI, indicating that this fusion protein had been successfully generated (Figure 3.5, *panel B*). Furthermore, the minor (upper) band that was detected with streptavidin-HRP had disappeared, indicating that this unknown biotinylated peptide does not cross-react with α-SR-BI. Unfortunately, there are no isoform-specific human SR-BII antibodies commercially available, and no reports have been published using an antibody against the C-terminal

tail of this isoform. Therefore, in order to confirm SR-BII cytoplasmic tail expression in recombinant *E. coli*, it was necessary for me to produce a specific antiserum against SR-BII *(Section 3.2.2.2)*.

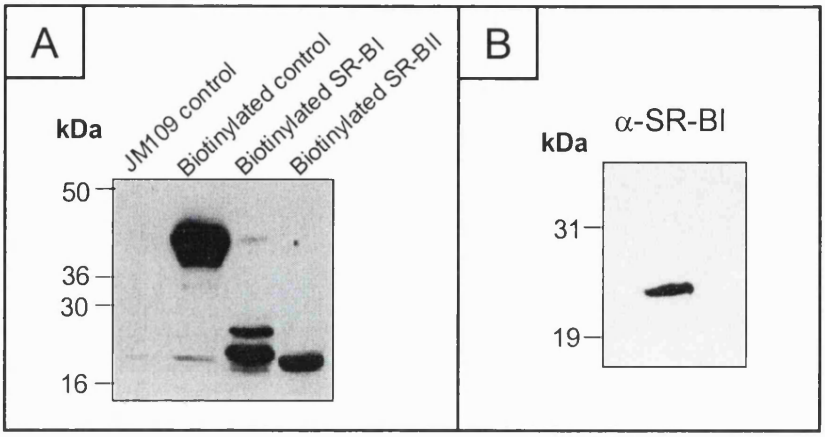

Figure 3.5 Generation of biotinylated cytoplasmic SR-BI and II fusion proteins

Panel A, *Control JM109 cultures and recombinant JM109 cultures expressing either a 40 kDa biotinylated control protein or biotin-tagged cytoplasmic SR-BI/II were boiled under reducing conditions (Section 2.3.6.1). Following protein separation by 16 % SDS-PAGE, the fusion proteins were detected by immunoblotting with a streptavidin-HRP conjugate.* ***Panel B,*** *The experiment was repeated using recombinant cultures expressing biotinylated cytoplasmic SR-BI and immunoblotting with the α-SR-BI isoform-specific antibody.*

3.2.2.2 Anti-peptide antiserum to cytoplasmic human SR-BII

The unique cytoplasmic SR-BII tail sequence is very short (only 39 amino acids), which therefore limits the choice of immunogenic region. Having assessed the hydrophilicity of the tail sequence [281,282], the most antigenic region was estimated to be a stretch of 22-amino acids two residues downstream from the common SR-BI and II region (residues 493-514: EDTVSQPGLAAGPDRPPSPYTP). A rabbit anti-peptide antiserum directed against this peptide (α-SR-BII) was subsequently commissioned *(Section 2.3.4)*. Although anti-peptide antisera are invariably immunoreactive with their synthetic peptides, it is not guaranteed that this will be the case for the 'native' protein. Therefore, it was necessary to characterise the antibody and to ascertain the conditions in which the antibody could recognise its antigen *(Section 2.3.4)*.

The majority of human SR-BII antiserum characterisation was performed under my supervision by Camilla Reed, a Wellcome Trust vacation student from the Royal Holloway University of London (Surrey, UK). Firstly, 0.5 μg of biotinylated

cytoplasmic SR-BII fusion protein *(Section 3.2.2.1)* was separated by 16 % SDS-PAGE under reduced and non-reduced conditions *(Section 2.3.2).* Following protein transfer to a nitrocellulose membrane, the membrane was incubated with SR-BII antiserum diluted 1:1,000 in BSA blocking buffer, using the optimised conditions described in *Section 2.3.3.2* and Table 2.6. As shown in panel A of Figure 3.6, α-SR-BII was found to be strongly immunoreactive towards cytoplasmic SR-BII (~25 kDa) under both conditions. Pre-immune serum that was taken from the same rabbits before antigen injection failed to react with the fusion protein (data not shown), indicating that the antiserum is specific to cytoplasmic SR-BII. This result also confirmed that the biotinylated cytoplasmic SR-BII fusion protein had been generated successfully. Secondly, the ability of the antiserum to immunoprecipitate the cytoplasmic SR-BII fusion protein from solution was investigated: SR-BII antiserum or pre-immune serum was diluted 1:100 in a 1 μg/ml solution of biotinylated cytoplasmic SR-BII and subjected to the immunoprecipitation method described in *Section 2.3.5.* Precipitated proteins were separated by 16 % SDS-PAGE and immunoblotted with streptavidin-HRP. SR-BII antiserum, but not the pre-immune serum, was found to precipitate biotinylated cytoplasmic SR-BII from the solution (Figure 3.6, *panel B*).

In addition, I verified that the antiserum was isoform-specific and able to recognise the full-length type II receptor by subjecting clarified cell lysates from recombinant CHO cells over-expressing full-length SR-BI and II (described in *Sections 2.4.3* and *2.4.4)* to Western blotting. SR-BII protein was readily detected by α-SR-BII in recombinant cells expressing low and high amounts of receptor, yet this antiserum did not cross-react with SR-BI protein (Figure 3.6, *panel C*). This result confirmed that α-SR-BII was indeed specific for the full-length type II isoform. Due to the properties of α-SR-BII, this antiserum would serve as a vital tool for detecting SR-BII expression in recombinant CHO cells by Western blotting *(Section 4.2.2.2)*, as well as isolating SR-BII from human cell lines *(Section 4.2.8).*

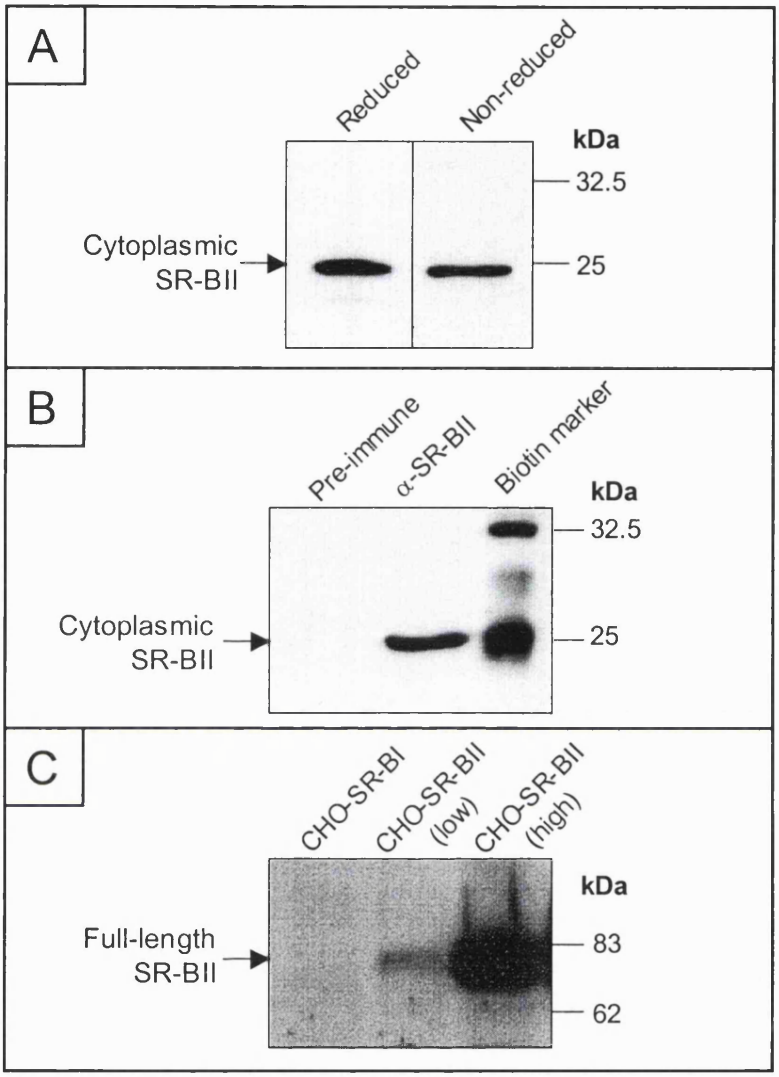

Figure 3.6 Characterisation of the antipeptide antiserum to cytoplasmic SR-BII

Panel A, *Biotinylated cytoplasmic SR-BII protein (0.5 μg) was subjected to 16 % SDS-PAGE under both reducing and non-reducing conditions, prior to Western blotting using the antipeptide antiserum to cytoplasmic SR-BII (α-SR-BII; Section 2.3.3).* ***Panel B,*** *Biotinylated cytoplasmic SR-BII protein in solution was subjected to immunoprecipitation with either pre-immune serum or α-SR-BII. Precipitated biotinylated peptides were subsequently reduced, separated by 16 % SDS-PAGE, transferred onto nitrocellulose, and detected with streptavidin-HRP and chemiluminescence (Section 2.3.3.2).* ***Panel C,*** *Recombinant CHO cells over-expressing full-length SR-BI or SR-BII (at high and low levels) were lysed and equal quantities of cell extracts were separated by 8 % SDS-PAGE (Sections 2.4.1 and 2.4.4). The full-length SR-BII protein was detected by immunoblotting with α-SR-BII (for isoform-specific identification).*

3.2.2.3 Large-scale production of biotinylated cytoplasmic SR-BI/II

Having established that the recombinant JM109 cultures could be induced to express detectable quantities of biotinylated cytoplasmic SR-BI and II tails and that these fusion proteins cross-react with isoform-specific antibodies, I then used affinity chromatography with an avidin column for large-scale fusion protein production *(Section 2.3.6.1)*. For large-scale purifications, cell extracts from two litres of recombinant JM109 cultures were applied to the avidin affinity column. During chromatography, a UV spectrophotometer (OD_{280}) and recorder constantly measured and traced the protein absorbance of the column outflow. An example of an absorbance trace is shown in Figure 3.7.

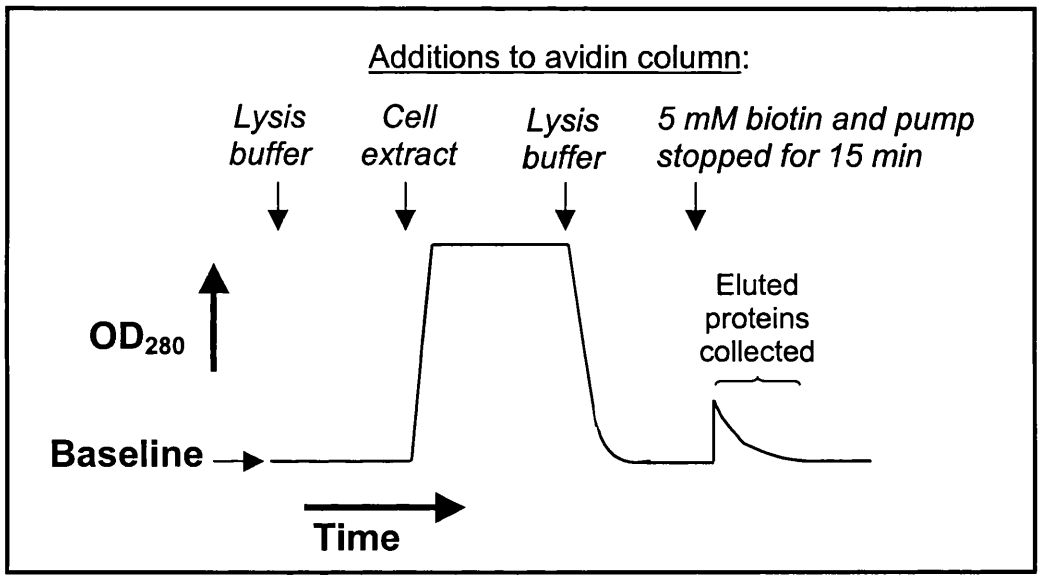

Figure 3.7 Representative protein absorbance (OD_{280}) trace during biotinylated cytoplasmic SR-BI/II purification using avidin affinity chromatography

Lysis buffer was pumped through the system to allow the avidin column to equilibrate and a stable baseline to be achieved (Section 2.3.6.1). When the cell extract was applied to the column, the biotinylated fusion proteins bound to the avidin resin. The spectrophotometer absorbance reading increased as unbound cellular proteins passed through the column. This value subsequently decreased to baseline when the column was washed with lysis buffer to remove traces of unbound protein. At this point, 5 mM biotin was introduced to the column and the pump was turned off for 15 min to allow biotin to compete with the fusion proteins for avidin resin binding sites and thereby release biotinylated fusion proteins from the column. When the pump was switched on again, the eluted proteins were collected.

To verify that the avidin resin had efficiently captured the biotinylated proteins, the column flow-through was collected. Firstly, equal volumes of starting cell extract and column flow-through were separated by SDS-PAGE, along with an aliquot of the column eluate *(Section 2.3.2)*. Secondly, the proteins were transferred to nitrocellulose and immunoblotted with streptavidin-HRP *(Section 2.3.3)*. Despite finding biotinylated fusion proteins in the starting material and in the eluate as expected, there were no biotinylated proteins detected in the flow-through (Figure 3.8, *panel A*). This result suggested that the avidin column had sufficient capacity and was efficient at binding all the biotinylated protein available. However, the band detected in the starting cell lysate was quite weak, and in order to confirm that the column was indeed capturing the biotinylated proteins efficiently, I should have concentrated both the starting material and flow-through by 10 times before repeating the Western blot.

Finally, the eluted proteins were separated by SDS-PAGE, and the gel was Coomassie stained to analyse protein purity and check for degradation products *(Section 2.3.2.3)*. Pure biotinylated fusion proteins were isolated using this method of purification (Figure 3.8, *panel B*), and since no bands of lower molecular weight were detected, it appeared that no fusion protein degradation had taken place.

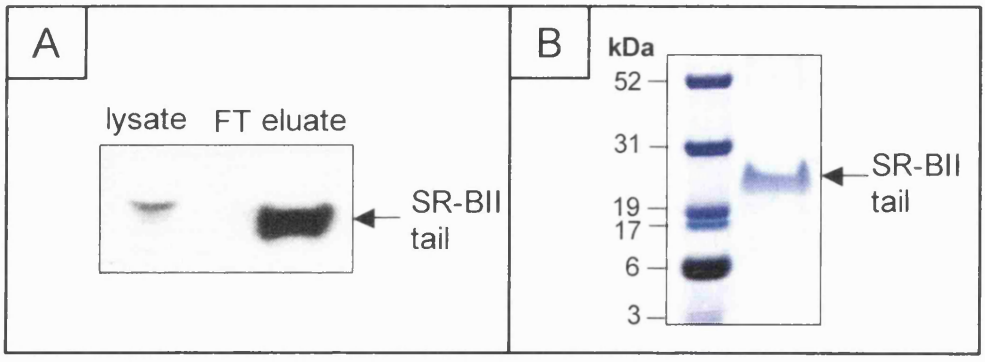

Figure 3.8 Binding efficiency of the avidin column and purity of the eluted biotinylated cytoplasmic SR-BII fusion protein

Panel A, *Equal volumes of bacterial cell lysate and column flow-through (FT) were separated by 16 % SDS-PAGE, along with an aliquot of the eluted fusion protein (Section 2.3.2). Immunoblotting with streptavidin-HRP detected the biotin-tagged cytoplasmic tail.* ***Panel B,*** *Two μg of protein eluted from the affinity column were separated by 16 % SDS-PAGE and detected by Coomassie staining (Section 2.3.2.3). The stained gel shows pure cytoplasmic SR-BII fusion protein obtained from a typical preparation; additional affinity purifications gave similar results.*

Following biotinylated protein elution, fractions were collected and those containing protein (as quantified by the Bradford assay; *Section 2.3.1.2*) were pooled and dialysed against PBS. Although the manufacturer claimed that this system would typically yield 1-5 mg of purified fusion protein per litre of starting culture, the largest quantity of SR-BI/II cytoplasmic tail that I managed to purify from nine different preparations was only 50 μg. Since no fusion protein degradation products were observed using either immunoblotting or Coomassie staining (Figures 3.5 and 3.8), it appeared likely that the problem was low fusion protein expression, rather than specific degradation of cytoplasmic SR-BI/II by the host strain of *E. coli*.

3.2.2.4 GST-tagged cytoplasmic SR-BI/II

Because my recombinant bacteria only expressed biotinylated cytoplasmic SR-BI/II at low levels, it was necessary to find another system for generating larger quantities of cytoplasmic tail fusion proteins. Firstly, bacteria were transformed with the empty GST expression vector (pGEX) and the expression vector containing the cytoplasmic SR-BII tail sequence (pGEX-II; *Sections 3.2.1.2* and *2.2.9.5*). Subsequently, two clones from each type of recombinant bacteria were expanded into small-scale cultures. These cultures were grown overnight and induced to express GST alone or GST-tagged cytoplasmic SR-BII with the addition of IPTG *(Section 2.3.6.2)*. Clarified bacterial cell lysates were incubated with glutathione-agarose beads to isolate the GST-tagged proteins. The beads were boiled in SDS-PAGE sample buffer and samples were immunoblotted with α-GST *(Sections 2.3.2* and *2.3.3)*. Panel A of Figure 3.9 shows that each clone expressed either the GST tag (27 kDa) or a larger GST-tagged cytoplasmic SR-BII fusion protein (~32 kDa). Immunoblotting with α-SR-BII was performed to confirm successful production of GST-SR-BII (Figure 3.9, *panel B*). The same approach was employed to detect whether recombinant bacteria transformed with the pGEX-I vector were expressing GST-tagged cytoplasmic SR-BI. The α-GST blot (Figure 3.9, *panel C*) revealed that one of the bacterial clones expressed a GST-tagged protein of the correct molecular weight (~32 kDa). Unfortunately, I was unable to use Western blotting to verify that the cytoplasmic tail had been accurately generated, due to insufficient α-SR-BI antibody. However, since the protein was the correct size and sequencing data had previously shown that the expression plasmid contained the correct tail sequence 'in-frame', I concluded that GST-SR-BI had been successfully generated.

Following large-scale purification of GST-tagged proteins using glutathione-sepharose columns, the eluted protein was quantified. The GST-tagged fusion proteins were expressed at extremely high levels in the recombinant bacteria; 4 litres of starting culture generated over 30 mg of fusion protein. A Coomassie stained gel revealed the purity of the isolated fusion proteins (Figure 3.9, *panel D*). The GST tag alone and the GST-SR-BII fusion protein were pure, but the GST-SR-BI sample contained a minor band with the same molecular weight as GST alone. This extra band may have resulted from use of the same glutathione-sepharose column after purification of GST alone (i.e. the GST tag may not have been completely eluted from the column during the elution and regeneration procedures) or GST-SR-BI may have degraded. However, since both the GST tag and the GST-SR-BI fusion protein would serve as negative controls in future experiments *(Sections 3.2.4* and *3.2.5),* it was not necessary to purify GST-SR-BI any further.

3.2.2.5 GST-tagged plc-γ1 SH2 and SH3 domains

Small-scale recombinant bacterial cultures were induced with IPTG to express plc-γ1 SH2 and SH3 domains as fusion proteins with the GST tag (GST-SH223 and GST-SH22; *Section 2.3.6.2).* GST-tagged proteins were isolated from cell lysates using glutathione-agarose beads and analysed by 4-20 % SDS-PAGE. Immunoblotting with α-GST showed strong bands at 55 and 64 kDa, the correct molecular weights for GST-SH22 and GST-SH223, respectively (Figure 3.10, *panel A*). Bound antibodies were stripped from the membrane *(Section 2.3.3.3)*, which was subsequently re-probed with α-plc-γ1 *(Section 2.3.3* and Table 2.6). This antibody was raised against a recombinant protein corresponding to amino acids 530-850, mapping within the SH2-SH2-SH3 domains of plc-γ1. Immunoblotting with α-plc-γ1 revealed that the GST-SH223 fusion protein had been successfully generated (Figure 3.10, *panel B*). This antibody was not predicted to bind to the GST-SH22 fusion protein (as the SH3 domain is absent), yet a faint band was detected. The most likely explanation for the presence of this faint band is incomplete stripping of the membrane. Despite failing to verify successful production of plc-γ1 SH2 domains by immunoblotting, I was confident to use the GST-SH22 fusion protein in future binding assays, since the expression vector had been used previously by Finan *et al.* [283,284] to generate a functionally active protein.

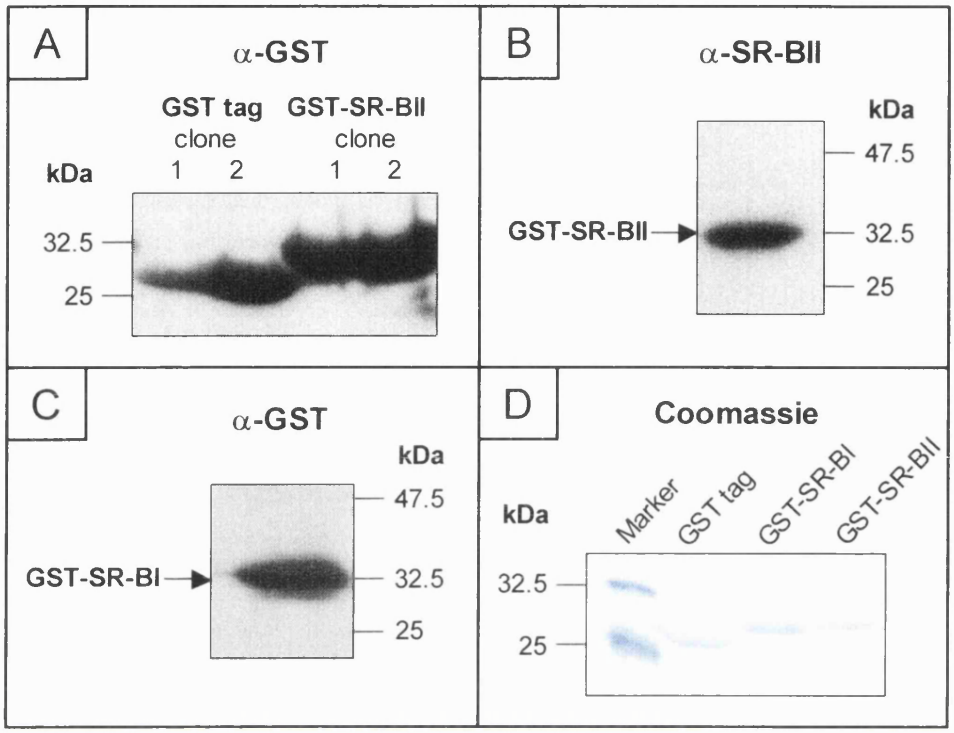

Figure 3.9 Generation of the GST tag and GST-tagged cytoplasmic SR-BI and II fusion proteins

Recombinant bacterial clones induced to express the GST tag or GST-tagged cytoplasmic SR-BII were cultured and lysed. The GST-tagged proteins were subsequently separated from the clarified lysates by incubation with glutathione-agarose beads, as described in Section 2.3.6.2. The beads were boiled under reducing conditions to release bound proteins, which were then separated using 16 % SDS-PAGE (Section 2.3.2) and immunoblotted with α-GST ***(Panel A),*** *or α-SR-BII* ***(Panel B).*** *The experiment was repeated using recombinant bacteria induced to express GST-tagged cytoplasmic SR-BI and α-GST for detection* ***(Panel C).*** *The purity of eluted peptides from the large-scale glutathione-sepharose columns was determined by separating 1 μg of each GST-tagged protein by 16 % SDS-PAGE, followed by Coomassie staining (Section 2.3.2.3) of the gel* ***(Panel D).***

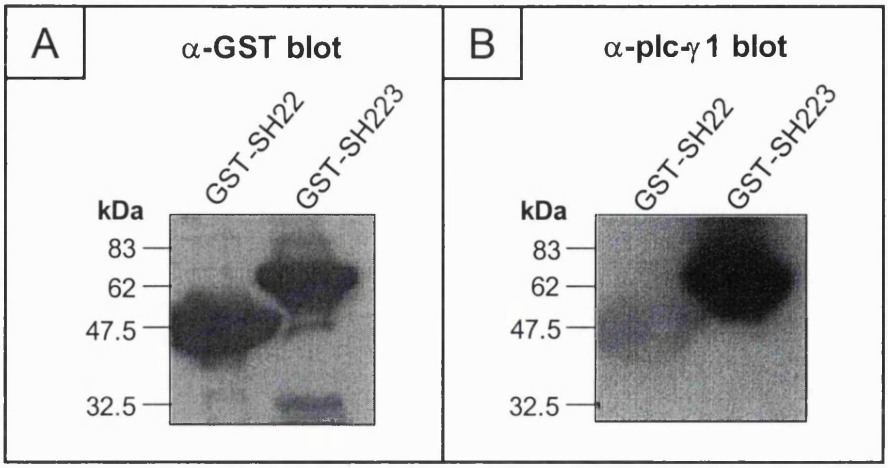

Figure 3.10 Generation of GST-tagged plc-γ1 SH2 and SH3 domains

Recombinant bacterial cultures were induced to express GST-tagged plc-γ1 SH2 domains with and without the SH3 domain (GST-SH223 and GST-SH22, respectively). The GST-tagged proteins were subsequently separated from clarified bacterial cell lysates by incubation with glutathione-agarose beads, as described in Section 2.3.6.2. The beads were boiled under reducing conditions to release bound proteins, which were then separated using 4-20% SDS-PAGE. Immunoblotting with α-GST revealed the purified GST-tagged proteins ***(Panel A),*** *while detection with α-plc-γ1 confirmed the successful generation of a GST-tagged peptide containing the SH2 and SH3 domains of plc-γ1* ***(Panel B, right hand lane).***

3.2.3 'PULL-DOWN' ASSAYS INDICATE AN INTERACTION BETWEEN THE SH3 DOMAIN OF PLC-γ1 AND CYTOPLASMIC SR-BII

To investigate the potential of cytoplasmic SR-BII to interact with signalling domains, a number of 'pull-down' assays were performed. In the first instance, the 'pull-down' binding screen involved immobilising equal quantities (2 μg) of GST-SH3 domain fusion proteins on glutathione-agarose beads to generate a variety of affinity matrices. GST-tagged SH3 domains from the following modular signalling proteins were used: crk, csk, fyn, grb-2, plc-γ1 and src. The type 1 isoenzyme of plc-γ was chosen as this is constitutively expressed, whereas the type 2 isoenzyme is only found in the lymphoid system [285]. The affinity matrices were subsequently incubated with biotinylated cytoplasmic SR-BII. After substantial washing of the matrices, the beads were boiled in SDS-PAGE sample buffer to release any bound proteins. The presence of cytoplasmic SR-BII in each of the samples was detected by Western blotting with a streptavidin-HRP conjugate *(Section 2.3.7.1).* Panel A of Figure 3.11 shows the

autoradiograph from the preliminary binding screen: the SH3 domain of plc-γ1 bound more cytoplasmic SR-BII than any of the other SH3 domains. Furthermore, this binding interaction was detected when the screen was repeated on two other occasions. This autoradiograph also reveals weak interactions between the SH3 domains of csk and src, and cytoplasmic SR-BII. However, these interactions were not observed in any of the other binding screens. As expected, the negative controls (either beads or GST alone) failed to interact with cytoplasmic SR-BII. Finally, to ensure that each of the affinity matrices had successfully bound the GST-tagged fusion proteins, the antibodies were stripped from the blot and the membrane was subsequently re-probed with an antibody directed against the GST tag (α-GST). GST-tagged fusion proteins were observed in each lane (apart from beads alone), revealing that the generation of each affinity matrix had been successful. Furthermore, this autoradiograph revealed that the interaction between cytoplasmic SR-BII and the SH3 domain of plc-γ1 was a valid result, as overloading of GST-plc-γ1 onto the beads had not caused it.

In order to confirm that this interaction was specific to the SR-BII isoform, avidin affinity matrices bound to biotinylated SR-BI or II cytoplasmic tails were generated, and incubated with GST-tagged plc-γ1 SH3 domains (*Section 2.3.7.2; method 1*). Any bound proteins were detected by immunoblotting with α-GST (Figure 3.11, panel B). Avidin beads alone and the SR-BI cytoplasmic tail affinity matrix failed to bind to GST-plc-γ1, yet interactions between cytoplasmic SR-BII and the plc-γ1 SH3 domain were still detected. This result revealed that the protein-protein interaction is specific to cytoplasmic SR-BII and that the interaction does not involve the first five residues in the C-terminal tail that are present in both isoforms. This finding was expected as no potential proline-rich signalling motifs were present in either the unique cytoplasmic SR-BI sequence or in the tail sequence common to SR-BI and II. The results shown here demonstrate the ability of cytoplasmic SR-BII to bind to the SH3 signalling domain of plc-γ1. However, the conditions of this 'pull-down' assay were not physiological, as two pure proteins were incubated together in isolation from any other proteins. It was therefore necessary to ascertain the significance of the preliminary binding screen result and demonstrate that cytoplasmic SR-BII and plc-γ1 still interact within a more physiological environment.

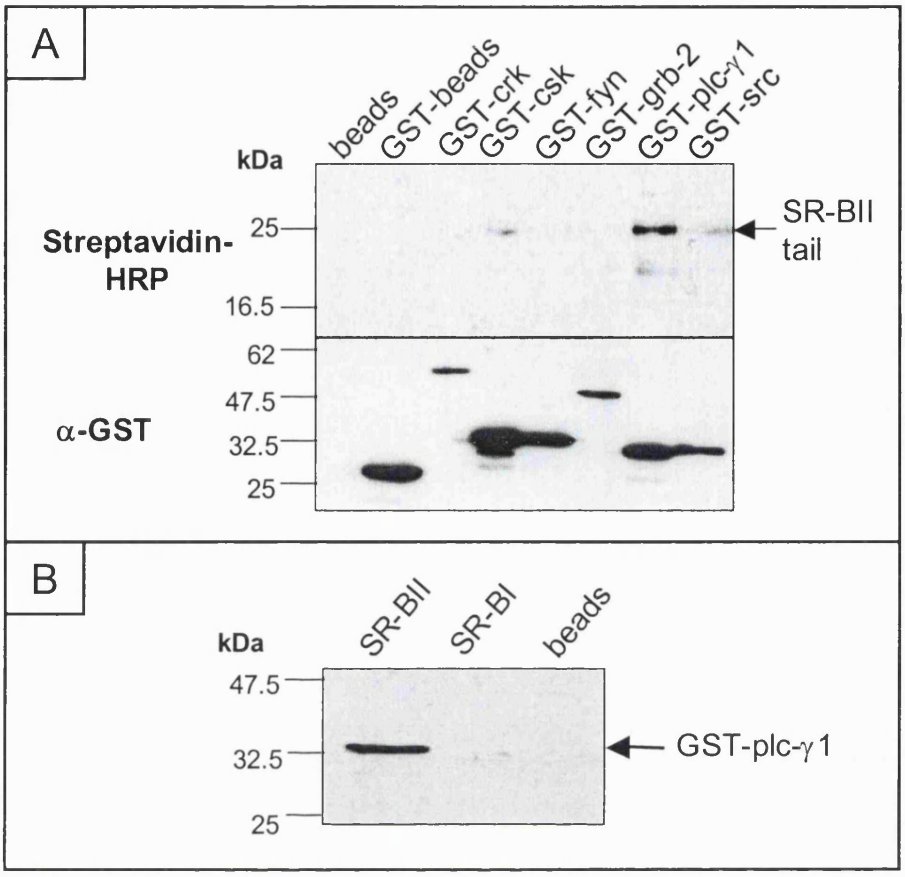

Figure 3.11 'Pull-down' assays showing an interaction between the cytoplasmic tail of SR-BII and the plc-γ1 SH3 domain

Panel A, *Two μg of GST-tagged SH3 domains from a variety of signalling proteins were immobilised on 50 μl of glutathione-agarose beads and incubated with a solution containing 2 μg of biotinylated cytoplasmic SR-BII. The beads were washed and boiled in SDS-PAGE sample buffer, containing β-mercaptoethanol, to elute any bound cytoplasmic SR-BII. After separating the samples by 16 % SDS-PAGE, the interacting proteins were detected by immunoblotting with a streptavidin-HRP conjugate. The blot was stripped and probed with α-GST to ensure that each GST-tagged SH3 domain had successfully bound to the matrix. These blots represent one 'pull-down' binding screen, but the same results were obtained on two other occasions.* ***Panel B,*** *The 'pull-down' assay was reversed in order to investigate whether the interaction between cytoplasmic SR-BII and the SH3 domain of plc-γ1 was specific to the SR-BII isoform. Affinity matrices, comprising 50 μl avidin beads bound to 2 μg biotinylated cytoplasmic SR-BI or II, were incubated in a solution containing 2 μg GST-tagged plc-γ1 SH3 domains. Interacting proteins were detected as described for panel A, except that an α-GST antibody was used.*

3.2.4 CYTOPLASMIC SR-BII FAILS TO BIND PLC-γ1 USING A 'PULL-DOWN' ASSAY UNDER MORE PHYSIOLOGICAL CONDITIONS

The initial 'pull-down' binding screen revealed a binding interaction between the following two pure proteins: the SH3 domain of plc-γ1 and cytoplasmic SR-BII *(Section 3.2.3)*. In order to establish whether these two proteins specifically interact under more physiological conditions (i.e. in the presence of many other proteins), the 'pull-down' assay was repeated using GST-plc-γ1 affinity matrices incubated with cytoplasmic SR-BII in the following protein-rich solutions: 1 % (w/v) BSA, 10 % (v/v) FBS and 1 mg/ml HepG2 cell lysate *(Section 2.3.7.2; method 2)*. Figure 3.12 shows the autoradiograph generated from immunoblotting with a streptavidin-HRP conjugate. It was evident that the protein-protein interaction between the SH3 domain of plc-γ1 and cytoplasmic SR-BII only took place when the two pure proteins were present alone in solution. When albumin, FBS or cellular proteins were introduced to the system, cytoplasmic SR-BII failed to bind the plc-γ1 SH3 domain.

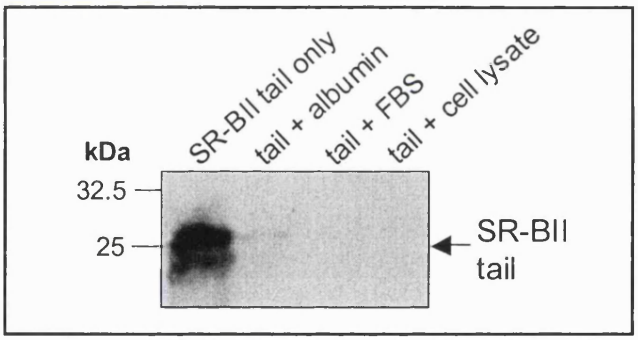

Figure 3.12 Cytoplasmic SR-BII fails to interact with plc-γ1 SH3 domain in the presence of other proteins

Two μg of GST-tagged plc-γ1 SH3 domains were immobilised on 50 μl of glutathione-agarose beads. The affinity matrices were incubated with 2 μg biotinylated cytoplasmic SR-BII in 200 μl of the following solutions: PBS, 1 % (w/v) BSA, 10 % (v/v) FBS and 1 mg/ml HepG2 cell lysate (Section 2.3.7.2). Interacting proteins were detected by boiling the beads in SDS-PAGE sample buffer under reducing conditions, and any eluted proteins were separated by 4-20 % SDS-PAGE and immunoblotted with a streptavidin-HRP conjugate.

If a strong binding interaction exists between cytoplasmic SR-BII and the plc-γ1 SH3 domain, one would have expected these proteins to interact in the presence of other proteins. However, the additional proteins introduced into the system might have been used in too great excess, thereby blocking the binding sites non-specifically. In addition,

the HepG2 cell lysate contains full-length native plc-γ1, which might have competed with the GST-tagged SH3 domain of plc-γ1 for cytoplasmic SR-BII binding.

Despite this discouraging finding, I proceeded to determine whether there is a stronger interaction between cytoplasmic SR-BII and the SH3 domain of plc-γ1 when either its two adjacent SH2 signalling domains are present, or the plc-γ1 SH3 domain is correctly folded within the full-length signalling molecule. For both of these experiments, larger quantities (25 μg) of GST-tagged proteins were used for the generation of affinity matrices (as described by Finan *et al.* [284]). Firstly, 'pull-down' experiments were performed using affinity matrices bound to GST-tagged cytoplasmic SR-BII or GST alone, in the presence of GST-tagged plc-γ1 SH2 and SH3 domains in solution (GST-SH22 and GST-SH223; *Section 2.3.7.2; method 3).* Since both the cytoplasmic tail and plc-γ1 domains were GST-tagged, the cytoplasmic SR-BII affinity matrix was generated using NHS-activated sepharose, which obviated the use of glutathione-agarose beads. Immunoblotting with α-GST confirmed that equal quantities of GST tag and GST-SR-BII had been used in the experiment (Figure 3.13, *panel A*). This antibody also revealed that both the GST alone control beads and GST-SR-BII beads had interacted with the plc-γ1 signalling domains. These interactions were therefore non-specific and had most likely resulted from the dimerisation of GST tags [286]. One way to avoid the dimerisation of GST tags would have been to cleave this tag from cytoplasmic SR-BII before using it in the assay. An alternative method would have been to generate a cytoplasmic SR-BII fusion protein with a different tag (e.g. histidine tag), using another expression system.

Secondly, to establish whether the cytoplasmic tail of SR-BII is able to 'pull-down' full-length, native plc-γ1 from solution, more physiological 'pull-down' experiments were performed using cytoplasmic SR-BII affinity matrices incubated in the presence of human THP-1 cell lysates. Glutathione-agarose affinity matrices bound to GST-SR-BI/II or GST tag were incubated with the whole THP-1 cell lysate *(Section 2.3.7.2; method 4).* Any bound proteins were eluted and subjected to SDS-PAGE and immunoblotting with α-plc-γ1. The positive control verified that plc-γ1 was detectable in the THP-1 cell lysate, yet no full-length, native plc-γ1 had been 'pulled-down' down by GST-tagged cytoplasmic SR-BII (Figure 3.13, *panel B*).

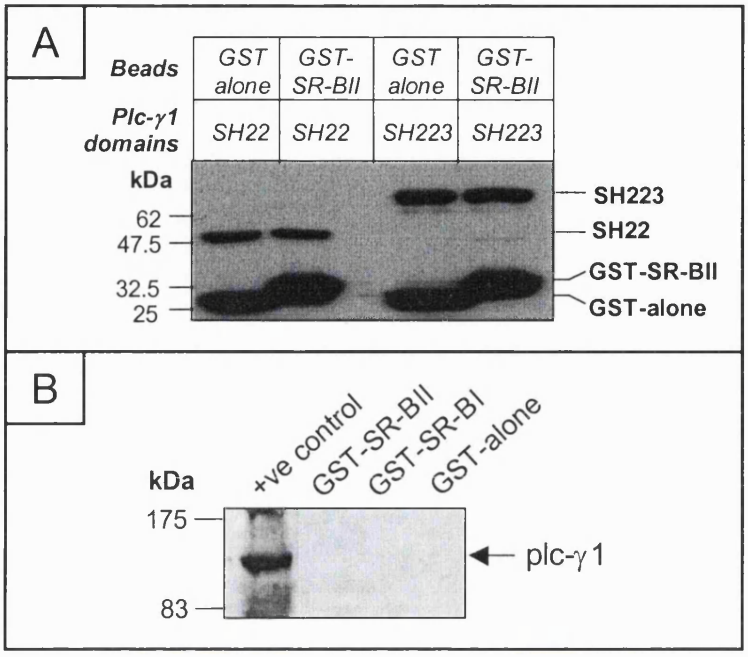

Figure 3.13 Cytoplasmic SR-BII fails to interact with full-length plc-γ1

Panel A, *NHS-Sepharose beads bound to 50 μg GST-SR-BI/II or GST tag were incubated in 200 μl PBS containing 25 μg of GST-tagged plc-γ1 SH2 and SH3 domains (SH22 and SH223). Any interacting proteins were detected using the method described in Figure 3.12 and immunoblotting with α-GST.* ***Panel B,*** *Twenty-five μg of GST-tagged cytoplasmic SR-BI/II or GST tag alone were immobilised on 50 μl of glutathione-agarose beads. The affinity matrices were incubated with 1 ml of THP-1 cell lysate (1 mg protein/ml). Eluted proteins were separated by 8 % SDS-PAGE and immunoblotted with α-plc-γ1. The positive control was 25 μg protein from the THP-1 cell lysate.*

Therefore, using this cell lysate 'pull-down' assay, I failed to demonstrate an interaction between cytoplasmic SR-BII and full-length plc-γ1. However, at this stage I was unable to conclude that cytoplasmic SR-BII does not bind plc-γ1, since the binding capabilities of the cytoplasmic tail had been studied in isolation from the rest of the receptor. Moreover, although this experiment used a cell lysate, none of the experiments had studied binding interactions within a cellular environment.

3.2.5 CELLULAR SIGNALLING MOLECULES THAT BIND CYTOPLASMIC SR-BII REMAIN ELUSIVE

In order to widen the search for signalling molecules that bind cytoplasmic SR-BII, a 'pull-down' experiment using a cytoplasmic SR-BII affinity matrix incubated with a human THP-1 cell lysate was performed *(Section 2.3.7.3; method 4).* The human monocytic THP-1 cell line was chosen because these cells contain SR-BII mRNA transcripts [232]. Cellular proteins that bound the affinity matrix were subjected to SDS-PAGE and immunoblotted with antibodies against serine, threonine or tyrosine phosphorylated residues (α-pS/T/Y), to detect any interacting phosphorylated cellular proteins. Many signalling cascades are known to involve proteins containing these phosphorylated residues, such as pathways involving receptor tyrosine kinases [241]. The α-pY antibody bound to proteins containing phosphorylated tyrosines within the cell lysate positive control, but no proteins containing phosphotyrosines were found to interact with cytoplasmic SR-BII (Figure 3.14, *panel A*). No cellular proteins containing phosphorylated serines/threonines were detected to interact with cytoplasmic SR-BII, however even the α-pS and α-pT antibodies failed to bind the cell lysate positive controls (data not shown). Therefore, no conclusion can be made as to whether cytoplasmic SR-BII interacts with cellular proteins containing phosphorylated serine or threonine residues. This finding was probably not due to dephosphorylation of the residues during the experiment, as a phosphatase inhibitor was included in the cell lysis buffer.

The same samples were subjected to silver staining for the sensitive detection of any cellular binding proteins. The initial silver stain result looked promising, as there was a protein of ~80 kDa repeatedly found in the GST-SR-BII sample that was absent from the GST alone control (Figure 3.14, *panel B*). Since SR-BII has a molecular weight of 82 kDa, I immunoblotted the samples with α-SR-BII, to establish whether dimerisation of the cytoplasmic tails had caused cytoplasmic SR-BII to bind the whole receptor and thereby isolate it from the rest of the cell lysate (Figure 3.14, *panel C*). Despite verifying the presence of cytoplasmic SR-BII at the same position as the unknown ~80 kDa protein, there were also many other bands in the lane and it appeared likely that the antibody was binding to dimers of GST-tagged cytoplasmic SR-BII and not to the cellular receptor itself. The experiment was then repeated with a better experimental control: GST-SR-BII affinity matrix incubated with cell lysis buffer.

Immunoblotting with α-GST confirmed that the ~80 kDa band was most probably generated from dimerisation of the GST-tagged SR-BII cytoplasmic tails (Figure 3.14, *panel D*).

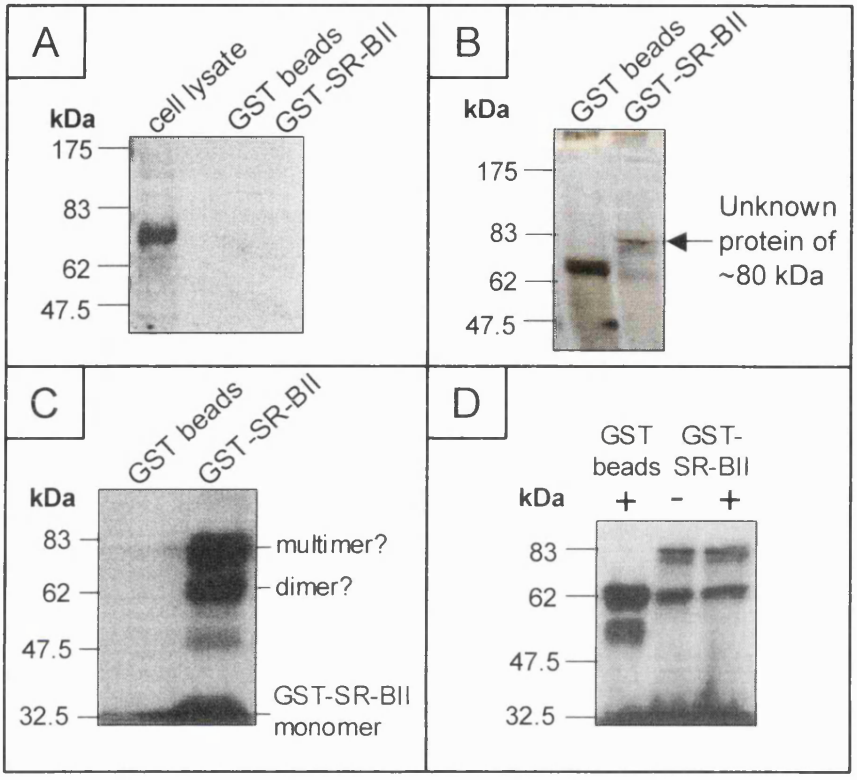

Figure 3.14 The interaction of cytoplasmic SR-BII and cellular proteins as investigated by cell lysate 'pull-down' assays

Twenty-five μg of GST-tagged cytoplasmic SR-BII or GST alone were immobilised on 50 μl of glutathione-agarose beads and the affinity matrices were incubated with 1 ml of THP-1 cell lysate (1 mg/ml). Interacting proteins were detected by boiling the beads in SDS-PAGE sample buffer under reducing conditions, and any proteins eluted from the affinity beads were separated by 4-20 % SDS-PAGE (Section 2.3.7.2). ***Panel A,*** *The proteins were transferred to a nitrocellulose membrane and probed with α-phosphotyrosine.* ***Panel B,*** *Samples were separated by SDS-PAGE and silver stained.* ***Panel C,*** *The proteins were transferred to a nitrocellulose membrane and probed with α-SR-BII.* ***Panel D,*** *The experiment was repeated to include the following control reaction: GST-SR-BII affinity matrix incubated with cell lysis buffer (-). The samples with cell lysate present are indicated with a + sign. The proteins were transferred to a nitrocellulose membrane and probed with α-GST.*

Having failed to elucidate the identity of any signalling proteins that bind to cytoplasmic SR-BII alone, it was necessary to explore whether the cytoplasmic tail binds

signalling molecules in response to activation of the whole receptor. My next experiments *(Section 3.2.6)* therefore involved CHO cells over-expressing recombinant human SR-BII *(Section 2.4.3)*.

3.2.6 INCUBATION OF CHO-SR-BII CELLS WITH HDL DOES NOT STIMULATE PLC-γ1 TO INTERACT WITH CYTOPLASMIC SR-BII

To establish whether the cytoplasmic tail of SR-BII binds plc-γ1 in response to HDL binding to its extracellular domain, recombinant CHO cells over-expressing SR-BII *(Section 2.4.3)* were subjected to a short exposure with HDL, prior to cell lysis. Subsequently, GST-tagged plc-γ1 SH2 and SH3 domains were incubated with the activated cell lysates *(Section 2.3.7.3, method 1)*. The receptor was successfully immunoprecipitated from the lysate using an antibody directed against the extracellular region (data not shown). Any GST-tagged proteins interacting with the activated receptor were detected by immunoblotting with α-GST (Figure 3.15, *panel A*). The antibody successfully bound to the GST alone positive control, yet neither of the two plc-γ1 fusion proteins, GST-SH22 or GST-SH223, were found to have been recruited by the activated receptor. As with many immunoprecipitation reactions, the heavy chain IgG (53 kDa) is clearly visible in all the immunoprecipitated samples. Although, any interaction between cytoplasmic SR-BII and plc-γ1 appears unlikely, the strong IgG heavy chain band may have obscured any signal from the GST-SH22 fusion protein, which has a molecular weight of 55 kDa.

Finally, there is one tyrosine residue in the cytoplasmic tail of SR-BII, which is positioned three residues upstream of a hydrophobic residue. If the tyrosine residue was to become phosphorylated, then this motif would comprise a potential SH2 domain recognition site [237]. I therefore investigated cytoplasmic SR-BII tyrosine phosphorylation in response to HDL stimulation *(Section 2.3.7.3, method 2)*. Recombinant CHO-SR-BII cells were incubated for 5 or 30 min in serum-free media with or without HDL. Subsequently, the cells were lysed and the receptor was immunoprecipitated from cell lysates using α-CLA-1. On three separate occasions, immunoblotting with α-SR-BII verified the successful isolation of SR-BII (Figure 3.15, *panel B*), but probing with α-pY failed to detect phosphorylation of the cytoplasmic tyrosine residue, with or without HDL stimulation. This result was not caused by

dephosphorylation of the tyrosine residue, as a phosphatase inhibitor was included in the lysis buffer. Although α-pY is used routinely in our laboratory, regrettably, I failed to run an immunoblotting positive control in an adjacent lane on the gel. I am unable, therefore, to confirm that the immunoblotting reaction was successful on each occasion, and so cannot conclude unequivocally that the tyrosine residue within cytoplasmic SR-BII fails to become phosphorylated upon receptor activation.

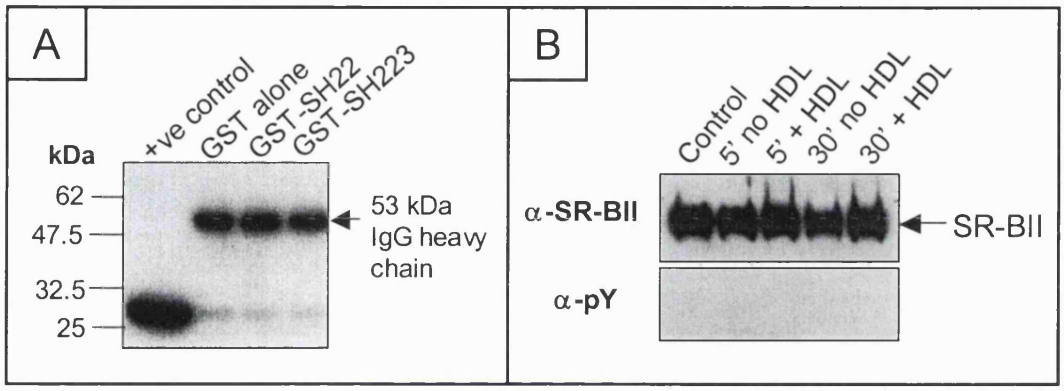

Figure 3.15 Cytoplasmic SR-BII activation in response to HDL stimulation

Panel A, *Confluent cultures of recombinant CHO cells expressing SR-BII (CHO-SR-BII) were stimulated for 30 min with 10 % (v/v) 'HDL plasma' prior to cell lysis (Sections 2.3.7.3 and 2.3.10.6). One ml of stimulated cell lysate (0.5 mg/ml) was subsequently incubated for 2 h with 25 μg of GST alone, or GST-tagged plc-γ1 SH2 and SH3 domains (GST-SH22 or GST-SH223). The receptor was isolated by immunoprecipitation using α-CLA-1 (Section 2.3.5). After boiling the immunocomplexes in SDS-PAGE sample buffer under reducing conditions, any eluted GST-tagged proteins were separated by 4-20% SDS-PAGE and detected by immunoblotting with α-GST. GST alone was included in the first lane of the gel as an immunoblotting positive control.* ***Panel B,*** *Recombinant CHO-SR-BII monolayers were grown to confluency in 100 mm dishes and incubated for 5 and 30 min in serum-free media with and without 5 % (v/v) 'HDL plasma'. Control cells remained in Ham's F12 media containing 5 % (v/v) FBS. Following treatments, the cells were lysed and the protein concentration of each lysate was quantified. Equal amounts of cell lysate were subjected to receptor immunoprecipitation with α-CLA-1, before precipitated proteins were analysed by 4-20 % SDS-PAGE and immunoblotting. Probing with SR-BII antiserum verified the success of the precipitation, while α-phosphotyrosine (α-pY) detected the state of cytoplasmic tail tyrosine phosphorylation.*

3.2.7 THE YEAST TWO-HYBRID SYSTEM FAILS TO DETECT CYTOPLASMIC SR-BII AND PLC-γ1 CELLULAR INTERACTIONS

The yeast two-hybrid system was performed to establish whether the SH3 domain of plc-γ1 and cytoplasmic SR-BII interact within a cellular environment *(Section 2.3.8)*. The pYTH9 yeast expression vector containing the GAL4 DNA binding domain (GAL4-DBD) sequence, and the pGAD10 vector containing the plc-γ1 SH3 domain and GAL4 activation domain (GAL4-AD) sequences, were generously provided by Dr. X-M. Sun (MRC Lipid Group, Hammersmith Hospital, UK). In order to generate the correct restriction sites for insertion of the cytoplasmic SR-BII tail sequence into pYTH9, cytoplasmic SR-BII was re-amplified by PCR, using the PPXa3-II plasmid as a template and the primers and conditions described in *Section 2.2.3* and Table 2.1. After separating the PCR products by agarose gel electrophoresis *(Section 2.2.5)*, the correctly sized amplification product of ~140 bp was detected over a wide annealing temperature range of 56-68 °C (Figure 3.16, *panel A*). However, at lower annealing temperatures (e.g. 56-62 °C), two faint bands were also observed, which meant that the desired PCR product was not completely pure. Thus, the correctly sized product was cut and purified directly from the gel *(Section 2.2.6)*, and subjected to restriction endonuclease digestion with *Spe*I and *Sal*I *(Section 2.2.8)*. This digestion reaction created the correct 'sticky ends' to enable cytoplasmic SR-BII to be inserted into the MCS of pYTH9 in the correct orientation (pYTH9-II). Following ligation and transformation, plasmids were isolated from 6 bacterial clones *(Section 2.2.9)* and analysed by restriction digestion with *Spe*I and *Sal*I to verify correct insertion of the tail sequence (Figure 3.16, *panel B*). Digestion products of ~140 bp were observed in all 6 samples, revealing the high efficiency of the ligation reaction. Plasmids from two of the pYTH9-II clones were sequenced to confirm that the tail had been inserted 'in-frame' and that no mutations had been introduced by PCR amplification. The pGAD10-plc-γ1 expression vector was also sequenced to verify that it contained the correct SH3 domain sequence and that it had been ligated into the MCS so as to maintain the correct reading frame.

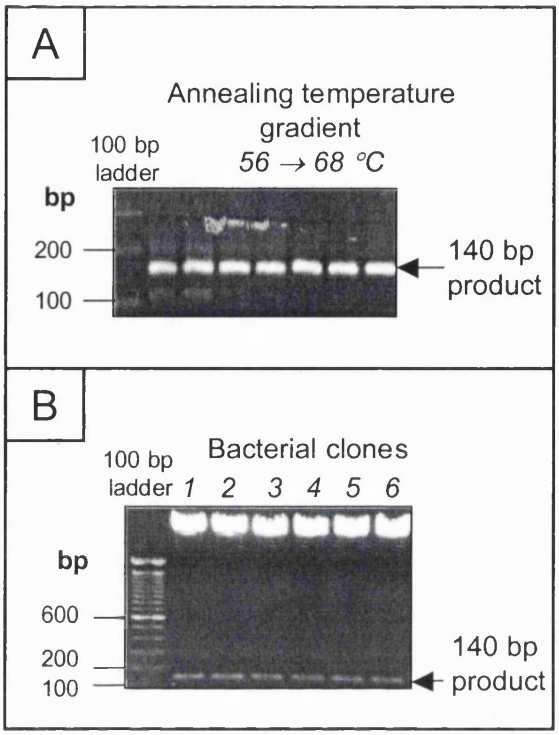

Figure 3.16 Generation of a yeast two-hybrid expression vector containing cytoplasmic SR-BII

Panel A, *The SR-BII cytoplasmic tail sequence was re-amplified from the PPXa3-II DNA template over a primer annealing temperature range of 56–68 °C, using the primers and conditions described in Table 2.1 and Section 2.2.3. Amplification products were separated using a 1.5 % agarose gel.* ***Panel B,*** *Following transformation of competent bacteria with pYTH9-II, six clones were picked for analysis. Plasmids were isolated from each of the clones and subjected to restriction endonuclease digestion with SpeI and SalI, for 1 h, using the conditions described in Section 2.2.8. Digestion products were separated using a 1.5 % agarose gel.*

Competent yeast cells were co-transformed with pGAD10-plc-γ1 and pYTH9-II expression vectors *(Section 2.3.8.2)*. The pGAD10-plc-γ1 and pYTH9-II contain the leucine and tryptophan nutritional markers, respectively, which allow cells that have been successfully transformed with both plasmids to be selected overnight on plates lacking leucine and tryptophan amino acids. The transformation reaction looked promising, since many transformed cells formed colonies on the selection plates, whereas untransformed cells failed to grow. The next step was to determine whether the two peptides of interest (cytoplasmic SR-BII and the plc-γ1 SH3 domain) were

interacting within the yeast cells. For this, β-galactosidase expression was measured *(Section 2.3.8.3)*. Expression of β-galactosidase would indicate that the two fusion proteins were interacting, thereby bringing the GAL4 activation domain into close proximity with the GAL4 DNA binding domain to create a functional transcriptional activator. The SNF1 and SNF4 fusion proteins are known to interact within yeast [269], therefore yeast that I had transformed with plasmids encoding these proteins served as a positive control for this assay. Indeed, following the β-galactosidase assay, the positive control colonies turned blue, verifying that the assay had been successful (Figure 3.17, *panel A*). Unfortunately, no blue colour was observed from colonies transformed with cytoplasmic SR-BII and the plc-γ1 SH3 domain, indicating that the cells were not expressing β-galactosidase. This result meant that either the fusion proteins were not interacting, or that they had not been successfully expressed in the first place.

The selected transformants continued to grow on selection plates, suggesting that the yeast cells contained both expression plasmids. However, it was necessary to confirm that the required fusion proteins were being expressed using Western blotting. Proteins were therefore extracted from transformed yeast *(Section 2.3.8.4)*, and subjected to immunoblotting with antibodies against the SH3 domain of plc-γ1, cytoplasmic SR-BII, GAL4-AD and GAL4-DBD. Despite performing three Western blots to detect each fusion protein, I was unable to verify the presence of either of the two fusion proteins within the transformed yeast. This was also the case when the yeast were transformed with only one of the expression vectors. Panels B and C of Figure 3.17 are examples of the α-plc-γ1 and α-GAL4-DBD blots obtained. In both cases, the positive immunoblotting controls, of pure GST-plc-γ1 and a GAL4-DBD-containing protein, bound their respective antibodies (lanes 4), although there was a high level of non-specific binding to proteins in the yeast lysate. No specific bands of the expected molecular weights were detected in the transformed yeast protein extracts that were absent from the negative control (untransformed yeast protein extracts). The same findings were obtained when the GAL4-AD and α-SR-BII antibodies were used, indicating that neither GAL4-DBD/cytoplasmic SR-BII nor GAL4-AD/plc-γ1 (SH3 domain) fusion proteins were detectable by Western blotting.

It appears as though the transformation reaction was successful and that leucine and tryptophan were being expressed, which allowed the transformed cells to grow on

selection plates. Unfortunately, the fusion proteins were either not being expressed at sufficiently high levels for detection, or else the proteins were rapidly degraded. Since neither GAL4-DBD/cytoplasmic SR-BII nor GAL4-AD/plc-γ1 (SH3 domain) fusion proteins were detected in the transformed yeast, the negative β-galactosidase assay result is invalid, and I am unable to conclude whether or not these two peptides interact within the yeast cell.

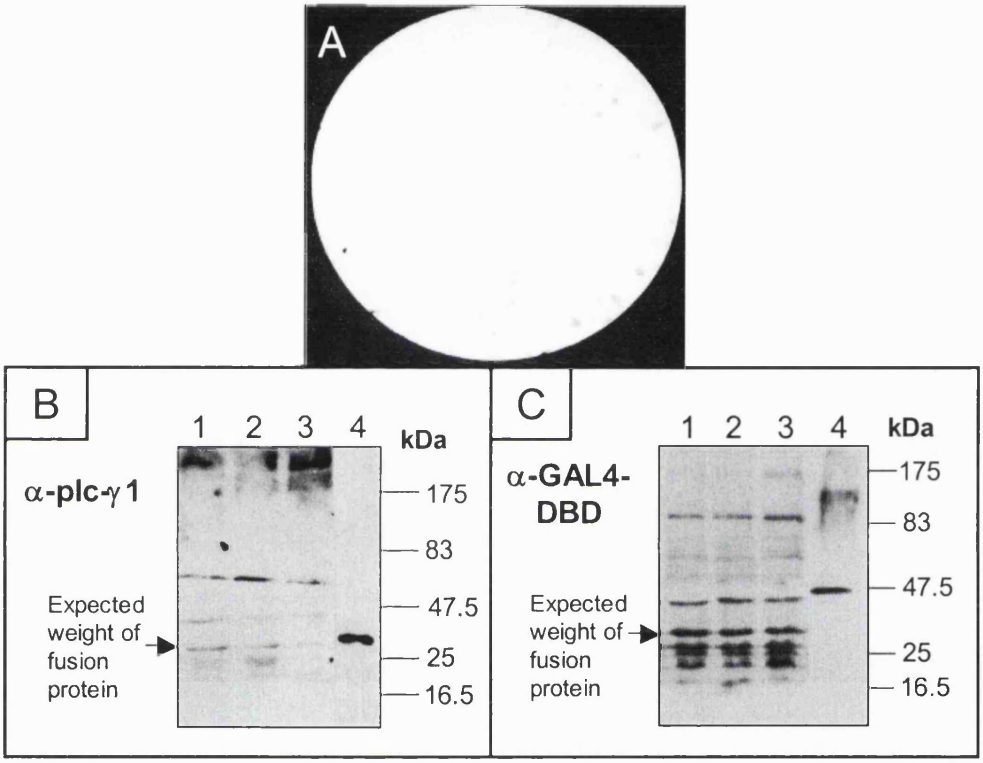

Figure 3.17 Generation of yeast two-hybrid fusion proteins was unsuccessful

The Y190 yeast strain was co-transformed with pSE1111 and pSE1112 positive control plasmids. Selected colonies were analysed using the β-galactosidase assay to confirm lacZ gene expression ***(Panel A)****. Proteins were extracted from yeast transformed with expression vectors encoding the cytoplasmic SR-BII and plc-γ1 SH3 domain sequences (Section 2.3.8.4). Equal quantities of cellular proteins were separated by 4-20 % SDS-PAGE and immunoblotted with antibodies against the SH3 domain of plc-γ1* ***(Panel B)*** *and the GAL4-DNA binding domain (GAL4-DBD;* ***Panel C****). Each autoradiograph is representative of three blots obtained using the same procedure.* ***Key:*** *1 = double transformants; 2 = single transformants [plc-γ1 SH3 domain (B) and cytoplasmic SR-BII (C)]; 3 = negative control (untransformed); 4 = positive control [GST- plc-γ1 SH3 domain (B) and GAL4-DBD-containing protein (C)].*

3.2.8 HUMAN SR-BII CO-IMMUNOPRECIPITATES WITH CAVEOLIN-1, REVEALING TRUE CAVEOLAR LOCALISATION

Caveolin-rich light membranes (CLM) were prepared from recombinant CHO cells expressing human SR-BI or II (CHO-SR-BI/II). After lysing the cells by sonication in a buffer containing 0.5 M Na_2CO_3, pH 11.0, cell extracts were fractionated by discontinuous sucrose density gradient ultracentrifugation *(Section 2.3.9.1)*. Samples from each of the twelve fractions were separated by SDS-PAGE and the proteins were detected by silver staining *(Section 2.3.2)*. A distinct protein population comprising the CLM fraction was seen in fractions 4 and 5, while the remaining protein was found at the bottom of the density gradient in fractions 8-12 (Figure 3.18, *panel A*). Protein quantification of each fraction using the Bio-Rad protein assay *(Section 2.3.1.2)* indicated that the CLM fraction comprised about 5 % of total cellular protein [271]. Confirmation of CLM in fractions 4 and 5 at the 5/35 % (w/v) sucrose interface was achieved by immunoblotting the gradient fractions for caveolin-1, an integral membrane protein marker for caveolae (Figure 3.18, *panel B*). Furthermore, immunoblotting with an antibody against the clathrin heavy chain confirmed the presence of this clathrin-coated pit associated protein in the bottom fractions (*panel B*). When gradient fractions from CHO-SR-BII recombinant cells were probed with SR-BII antiserum, human SR-BII was found to be present in the CLM fractions that contained caveolin-1. Immunoblotting with the α-CLA-1 antibody verified the presence of human SR-BI in CLM fractions isolated from recombinant CHO-SR-BI cells (*panel B*). Caveolae membrane invaginations are a subset of lipid rafts, which are generated by the polymerisation of caveolin proteins [287]. The data presented here confirms only the presence of human SR-BII within these plasma membrane lipid rafts, and it cannot be concluded that this receptor has true caveolar localisation. It was necessary, therefore, to demonstrate co-immunoprecipitation of SR-BII with caveolin proteins in order to confirm the presence of SR-BII within caveolae.

Immunoisolation of caveolae from CLM was performed using polyclonal α-caveolin-1 serum and magnetic Dynabeads covered in anti-rabbit secondary antibody *(Section 2.3.5)*. Immunoblotting with a monoclonal α-caveolin-1 antibody verified that caveolin-1 had been successfully immunoprecipitated from the CLM fraction (Figure 3.18, *panel C*).

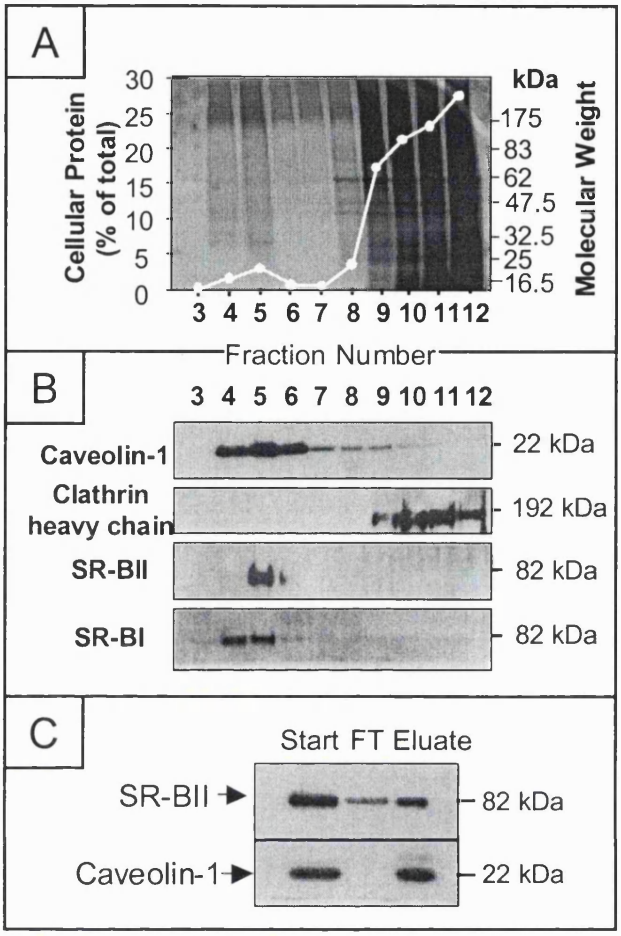

Figure 3.18 Human SR-BII localises to CLM and co-immunoprecipitates with caveolin-1

Confluent monolayers of recombinant CHO cells expressing either human SR-BI or II from one 175-cm^2 flask were sonicated in 2 ml of buffer containing 500 mM Na_2CO_3, and the homogenates were subsequently fractioned on a 5/35 % (w/v) discontinuous sucrose density gradient. ***Panel A,*** *Fractions (12 x 1 ml) were collected and assayed for protein concentration followed by reduced SDS-PAGE and silver staining (4-20 % acrylamide gels; the position of the molecular weight markers is shown on the right).* ***Panel B,*** *Replicate gels were immunoblotted with antibodies against caveolin-1, clathrin heavy chain, SR-BII and SR-BI as indicated.* ***Panel C,*** *250 µl of the CLM fraction (fractions 4 & 5) were incubated sequentially with α-caveolin-1 polyclonal antibody and magnetic beads coated with secondary antibody. Equivalent volumes of the starting CLM fraction, the post-adsorption flow-through (FT), and the adsorbed proteins eluted from the beads (Eluate) were analysed by SDS-PAGE and immunoblotting on nitrocellulose membranes. The blot was cut into two parts and appropriate sections were probed with SR-BII antiserum or α-caveolin-1 monoclonal antibody.*

The immunocomplexes were subsequently immunoblotted with SR-BII antiserum, which demonstrated that the majority of this isoform co-immunoprecipitated with caveolin-1 (Figure 3.18, *panel C*). This finding confirms SR-BII localization to caveolae, a plasma membrane microdomain involved in cholesterol homeostasis and signal transduction [50,54].

3.2.9 HDL STIMULATION OF CHO-SR-BII CELLS DOES NOT RECRUIT PLC-γ1 TO CAVEOLAE

Having successfully co-immunoprecipitated caveolin-1 and SR-BII, I then proceeded to determine whether plc-γ1 is recruited to caveolae upon HDL stimulation, and therefore precipitates with caveolin-1 and SR-BII. CLM fractions were isolated from resting and HDL-stimulated CHO-SR-BII cells, and subjected to immunoprecipitation with polyclonal α-caveolin-1 *(Section 2.3.9.2)*. Western blotting with α-SR-BII and a monoclonal α-caveolin-1 antibody confirmed that the receptor had successfully co-immunoprecipitated with caveolin-1 (Figure 3.19, *panel A*). Samples were subsequently immunoblotted with α-plc-γ1 to detect whether plc-γ1 also co-immunoprecipitates with the caveolin-1/SR-BII complex. The α-plc-γ1 antibody successfully bound to the two positive controls: the GST-tagged plc-γ1 SH3 domain and the full-length hamster plc-γ1 from CHO-SR-BII cell lysates (Figure 3.19, *panel B*). This result verified that the human antibody was able to detect hamster plc-γ1 and would therefore be able to recognise any precipitated plc-γ1 from CHO-SR-BII cells. Short exposure autoradiographs failed to detect any interactions between caveolar SR-BII and hamster plc-γ1 (data not shown). However, after exposing the film to the blot for longer, faint bands of the correct molecular weight for plc-γ1 were observed in both lanes representing resting and HDL-stimulated cells (Figure 3.19, *panel B*). Following HDL stimulation of the recombinant cells, no upregulation of plc-γ1 precipitation with caveolin-1 was detected, indicating that plc-γ1 is not recruited to caveolae in response to HDL. It therefore seems unlikely that plc-γ1 is stimulated to interact with SR-BII once the receptor is activated. This experiment provides evidence that human SR-BII does not interact with full-length hamster plc-γ1 in response to HDL activation.

Finally, the samples were also analysed by silver staining to identify any other cellular proteins that might co-immunoprecipitate with caveolar SR-BII in response to

HDL stimulation (Figure 3.19, *panel C*). The stained gel revealed an identical pattern of bands at a similar intensity in both resting and stimulated cells, and no specific band was detected in the +HDL lane, that was not present in the -HDL lane. It therefore appears that no specific protein precipitates with SR-BII and caveolin-1 as a result of HDL activation.

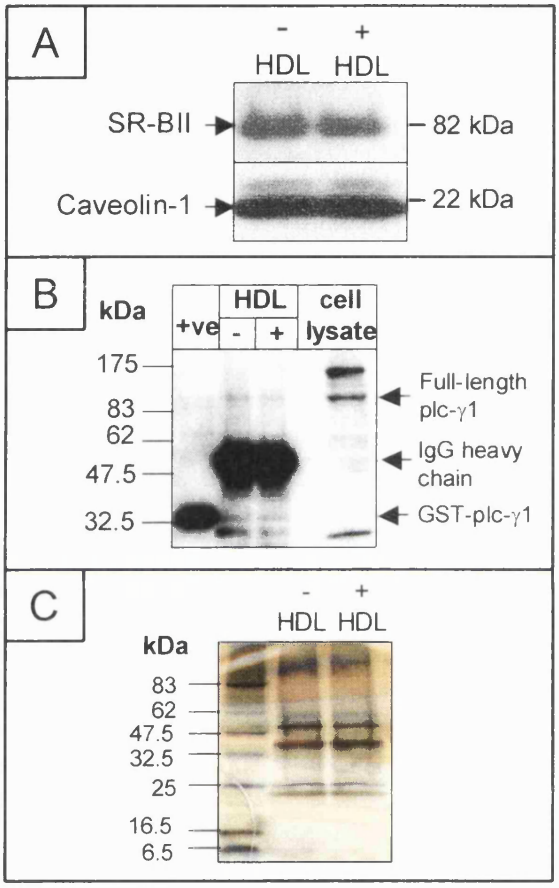

Figure 3.19 Co-immunoprecipitation of signalling molecules with caveolin-1 following stimulation of CHO-SR-BII cells with HDL

The CLM fraction was isolated from HDL-stimulated and resting CHO-SR-BII monolayers (Section 2.3.9.2) and subjected to immunoprecipitation with the α-caveolin-1 polyclonal antibody as described for Figure 3.18. Proteins eluted from the beads were analysed by 4-20 % SDS-PAGE and the following methods: immunoblotting with SR-BII antiserum, and α-caveolin-1 monoclonal antibody ***(Panel A)****; immunoblotting with α-plc-γ1* ***(Panel B)****; and silver staining* ***(Panel C)****.*

3.3 Discussion

3.3.1 CYTOPLASMIC SR-BII HAS THE POTENTIAL TO INTERACT WITH SIGNALLING MOLECULES

Following the identification of many putative signalling motifs within the C-terminal cytoplasmic tail of SR-BII (Figure 1.11), my initial aim in this study was to determine the signalling potential of SR-BII. Despite very few reports regarding the characteristics of the type II splice variant, we have a great deal of information regarding its extracellular binding interactions, since this region is identical to that of its well-characterised isoform, SR-BI [232]; SR-BII therefore binds HDL via its major apolipoprotein, apoA-I [201]. However, in contrast to SR-BI, its physiological significance as an HDL receptor has been questioned [191]. In this chapter, I investigated whether cytoplasmic SR-BII binds cellular signalling molecules in response to HDL stimulation, in order to establish whether this isoform might function as the unidentified HDL receptor involved in signal transduction and the activation of cellular cholesterol mobilisation [47].

'Pull-down' assays were employed to screen SH3 domains from a variety of modular signalling proteins for cytoplasmic SR-BII protein-protein interactions. Preliminary results revealed a binding interaction between the SH3 domain of plc-γ1 and cytoplasmic SR-BII. Initially, I considered plc-γ1 to be an attractive candidate for SR-BII signalling as it associates with caveolae, plasma membrane microdomains involved in signal transduction [54], and mediates the activation of PKC, via phospholipid hydrolysis and DAG production. Indeed, HDL binding to the cell surface of cholesterol-loaded fibroblasts is known to promote PKC activation [47]. However, signalling pathways involving plc-γ1 are reported to be transduced in response to interactions between the SH2 domains of plc-γ1 and autophosphorylation sites on activated receptor tyrosine kinases [241]. In contrast, SH3 domains mediate association with proline-rich sequences in partner proteins and, for many years, proteins that interact with this domain in plc-γ1 had not been convincingly identified *in vivo*. Last year, Yablonski *et al.* [288] identified the SLP-76 adaptor protein as a physiological ligand for the SH3 domain of plc-γ1. This adaptor is believed to play a vital role in T-cell receptor signalling by promoting the phosphorylation and activation of plc-γ1. Indeed, association of the proline-rich region of SLP-76 with the SH3 domain of plc-γ1, within a complex of

adaptor proteins, results in the optimal activation of plc-γ1. It therefore appears as though the SH3 domain in plc-γ1 might promote signal transduction by recruiting adaptor proteins to signalling complexes, which serve to stabilise the complex and optimise the enzyme's activation.

The discovery of an interaction between cytoplasmic SR-BII and the SH3 domain of plc-γ1 highlighted the potential of cytoplasmic SR-BII to bind signalling molecules and promoted its role in signal transduction. However, this interaction had occurred when two pure peptides were present in solution; therefore this finding was not indicative that a selective cellular binding interaction occurs. Binding assays were repeated in the presence of many other proteins to ascertain whether the interaction occurs under more physiological conditions. The results were disappointing, since the protein-protein interaction between cytoplasmic SR-BII and the plc-γ1 SH3 domain only appeared to take place when the two purified peptides were present in solution. After the addition of other proteins to the assay, including BSA, FBS and cell lysates, the interaction between the SH3 domain of plc-γ1 and cytoplasmic SR-BII was not detected. Despite using larger quantities of cytoplasmic SR-BII to generate an affinity matrix, as described in 'pull-down' assays by Finan *et al.* [284], the matrix was unable to 'pull-down' full-length plc-γ1 from a cell lysate. Therefore, although I demonstrated an interaction between cytoplasmic SR-BII and the SH3 domain of plc-γ1 in an artificial environment, it appeared unlikely that this signalling domain in plc-γ1 is the physiological ligand for cytoplasmic SR-BII.

The subsequent set of experiments served to establish whether the SH3 domain of plc-γ1 binds cytoplasmic SR-BII under the following conditions: firstly, within a cellular environment (using the yeast two-hybrid system); and secondly, when the cytoplasmic tail is activated as part of the whole receptor (using HDL-stimulated recombinant CHO cells over-expressing SR-BII).

Firstly, the yeast two-hybrid system was chosen to investigate binding interactions between the SR-BII cytoplasmic tail and the SH3 domain of plc-γ1 within a cell. Transformation of the yeast with the two fusion protein expression vectors appeared to have been successful as the yeast expressed the plasmid nutritional markers and were therefore able to grow on selection plates. However, this system failed to shed

light on the binding interaction between cytoplasmic SR-BII and plc-γ1 SH3 domain, as the two peptides of interest were not expressed at high enough levels for detection by Western blotting. The fusion proteins may not have been detected for one of the following reasons: inefficient transcription of the expression plasmid due to a weak promoter, or rapid degradation of the fusion proteins and their transcripts. It is more likely that inefficient transcription was responsible for the lack of GAL4-AD/plc-γ1 (SH3 domain) production, since pGAD10 contains a truncated 410 bp *ADH1* promoter. This truncated promoter was once thought to be the only portion necessary for high-level expression [289]. However, in most vector constructs, this promoter has been found to result in very low levels of fusion protein expression [290]. The high-level of expression reported by Beier and Young [289] appears to be caused by a small segment of DNA derived from pBR322, which was later found to act as a transcriptional enhancer in yeast [291]. No details are available as to whether the pYTH9 vector contains the truncated *ADH1* promoter, but this could also explain why the GAL4-DBD/cytoplasmic SR-BII fusion protein was not detected. Therefore, despite successfully showing a binding interaction between the two positive control peptides, I was unable to use this cellular system to confirm a cellular binding interaction between cytoplasmic SR-BII and the SH3 domain of plc-γ1.

Secondly, recombinant CHO cells over-expressing SR-BII (CHO-SR-BII) were generated in order to study the whole SR-BII protein and not just its cytoplasmic tail in isolation *(Section 4.2.2)*. Moreover, the recombinant cells were used to investigate whether plc-γ1 co-immunoprecipitates with SR-BII upon HDL stimulation. Firstly, HDL-stimulated CHO-SR-BII cell lysates were incubated with GST-tagged plc-γ1 SH2 and SH3 domains, but no fusion proteins were found to co-immunoprecipitate with the activated receptor. Secondly, co-immunoprecipitation of native full-length plc-γ1 with SR-BII was investigated; caveolar SR-BII was successfully immunoisolated with caveolin-1 from HDL-stimulated CHO-SR-BII cells using α-caveolin-1, but Western blotting revealed that upon HDL stimulation there was no increase in plc-γ1 precipitation with the caveolin-1/SR-BII complex. It therefore appears unlikely that plc-γ1 binds to the cytoplasmic tail of SR-BII in response to HDL activation of the receptor.

My evidence was accumulating against a cellular binding interaction between cytoplasmic SR-BII and plc-γ1, therefore the search was widened to identify the true

cellular ligand for cytoplasmic SR-BII: silver stained gels were analysed following cell lysate 'pull-down' assays and co-immunoprecipitation of HDL-stimulated SR-BII with caveolin-1. This sensitive technique for detecting only nanograms of protein failed, however, to identify any specific proteins interacting with cytoplasmic SR-BII. Furthermore, immunoblotting for any potential signalling proteins containing phosphorylated tyrosine residues also failed to highlight any phosphorylated cellular proteins interacting with cytoplasmic SR-BII. Unfortunately, I was unable to make the same conclusions for cellular proteins containing phosphorylated serine and threonine residues, as the α-pS and α-pT antibodies failed to detect their antigens in the immunoblotting positive control.

Finally, I looked at cytoplasmic tail phosphorylation in response to receptor activation by HDL stimulation. I monitored the state of tyrosine phosphorylation of the potential SH2 binding site within the cytoplasmic tail of SR-BII following HDL stimulation. SR-BII was successfully immunoprecipitated from stimulated CHO-SR-BII cell lysates and then immunoblotted with anti-phosphotyrosine antibodies, but I repeatedly failed to demonstrate tyrosine phosphorylation in activated SR-BII. These data suggest that SR-BII does not transduce signals via SH2 domain interactions. Nevertheless, this conclusion is not unequivocal since proteins containing phosphorylated tyrosine residues were not included in the immunoblotting experiment as a positive control.

In summary, I have identified many potential proline-rich signalling motifs in cytoplasmic SR-BII and have demonstrated their potential to interact with an SH3 domain from a modular signalling molecule when studied in isolation. Unfortunately, under more physiological conditions, I was unable to confirm this interaction, or identify another signalling domain/molecule that binds to the C-terminal cytoplasmic tail of SR-BII, even when the receptor is activated by HDL.

3.3.2 CAVEOLAR LOCALISATION OF SR-BII SUGGESTS A ROLE IN BOTH SIGNALLING AND CHOLESTEROL HOMEOSTASIS

Caveolae were isolated from recombinant CHO cells expressing human SR-BII using sucrose density gradient ultracentrifugation. Co-immunoprecipitation of SR-BII with caveolin-1, an integral membrane protein marker for caveolae, revealed the presence of the majority of the human receptor in caveolar plasma membrane

microdomains. These data are the first confirmation that human SR-BII localises to the same plasma membrane microdomain as its splice variant, SR-BI [176], and is also consistent with a study on mSR-BII [233]. It therefore appears that the targeting signal for caveolar localisation resides in the homologous region present in both isoforms, and not in their distinct C-terminal cytoplasmic tails. Indeed, fatty acylation of SR-BI and II is thought to target these isoforms to caveolar microdomains of the plasma membrane [182-184], most probably by the palmitoylation of Cys^{462}, which is common to both isoforms [233].

Caveolae are thought to have two principal functions: firstly, to concentrate signalling proteins and promote signal transduction from transmembrane receptors via second messengers [54]; and secondly, to act as a conduit for cellular cholesterol flux [50]. Caveolar SR-BI is known to promote both HDL CE selective lipid uptake [176,190] and HDL-mediated cholesterol efflux [116], as well as signal transduction. SR-BI was recently discovered to activate the caveolar protein eNOS, in response to HDL binding its extracellular domain [192]. Furthermore, the cytoplasmic tail of SR-BI has been found to interact with a PDZ domain-containing protein, named PDZK1 [219]. Therefore, my detection of SR-BII in caveolae not only highlights the potential involvement of this isoform in signal transduction, but also promotes a role for SR-BII in mediating cholesterol flux between cells and lipoproteins. The roles of SR-BII in mobilising stored cholesterol and promoting cellular cholesterol efflux are investigated in *Chapter 4*.

Chapter 4

4. SR-BII AND CELLULAR CHOLESTEROL HOMEOSTASIS

4.1 Introduction

As outlined in *Chapter 1 (Section 1.6.3.1)*, SR-BI was the first physiological HDL receptor to be identified [103]. It is highly expressed in the liver and steroidogenic tissues where it functions to bind mature HDL particles, and selectively remove CE from the lipoprotein core [162,164]. In addition to mediating HDL lipid uptake, SR-BI expression also correlates with HDL-mediated cellular cholesterol efflux from cultured cells [116]. Since low levels of SR-BI are found in many tissues and cell types, including macrophages [191], this receptor is thought to contribute to cellular cholesterol homeostasis by promoting FC efflux. Despite finding significant proportions of mRNA transcripts encoding the type II splice variant of SR-BI (SR-BII) in mouse tissues [233], there has been little characterisation of SR-BII expression in human tissues. In the human monocytic (THP-1) and hepatoblastoma (HepG2) cell lines, SR-BII represents 31 % and 21 % of total SR-BI/II mRNA, respectively [232], but SR-BII protein has not been detected in THP-1 cells or untreated HepG2 cells, and its physiological significance has been questioned [191,234]. Studies with CHO cells transfected with murine SR-BII revealed that this isoform shares many properties with SR-BI; SR-BII binds HDL with high-affinity, and mediates both selective lipid uptake from HDL and HDL-dependent cellular cholesterol efflux, albeit to a lesser extent than SR-BI [233]. The role of *human* SR-BII in cellular cholesterol homeostasis, however, has not yet been determined.

This chapter investigates the role of human SR-BII in cellular cholesterol homeostasis. Once excess cellular FC has been esterified and deposited as cytosolic lipid droplets, it cannot leave the cell directly but must first undergo hydrolysis to FC before cellular efflux can occur. The mobilisation of stored cholesterol is promoted by HDL binding to an unidentified cell surface receptor, activation of signalling pathways and FC translocation to the plasma membrane [36,44-47]. Having revealed that human SR-BII localises to membrane caveolae and explored its potential to bind signalling molecules *(Chapter 3)*, I investigated whether SR-BII functions as the unidentified HDL receptor that promotes CE mobilisation and hence regression of atherosclerotic plaques, containing lipid-laden macrophages. Initially, I generated recombinant CHO cells over-expressing full-length human SR-BI or II, and aimed to select recombinant clones with

similar levels of cell surface receptor expression. I then compared the abilities of each isoform to mediate HDL-stimulated FC efflux. Prior to investigating whether human SR-BII functions to promote the mobilisation of stored CE, I confirmed SR-BII protein expression in THP-1 monocyte/macrophages, and subsequently monitored whether macrophage SR-BII expression is upregulated upon cholesterol loading. Finally, the recombinant cells were used to investigate whether SR-BII mediates labelled cholesteryl oleate hydrolysis in response to HDL stimulation.

4.2 Results

4.2.1 GENERATION OF EXPRESSION VECTORS ENCODING SR-BI AND II

The first step in generating recombinant cells over-expressing SR-BI/II was to clone the full-length SR-BI and II sequences into a mammalian expression vector. The strategy used for obtaining both sequences was firstly to isolate the type I sequence, and secondly to swap the cytoplasmic tails and thereby generate the type II sequence *(Section 2.2.9).*

4.2.1.1 Full-length SR-BI expression vectors

Due to the high GC content (~75 %) of the first 200 bp of the SR-BI/II sequence, the sequence was PCR-amplified from a THP-1 cDNA template using the 'Advantage-GC cDNA PCR' kit *(Section 2.2.3.2),* and the primers listed in Table 2.1. Firstly, it was necessary to optimise the PCR primer annealing temperature: identical PCR reactions containing 0.5 M 'GC-melt' were subjected to PCR amplification using a range of primer annealing temperatures (56–66 °C). Following the separation of PCR products using agarose gel electrophoresis, the predicted amplification product of ~1650 bp was observed in the sample with an annealing temperature of 62 °C (Figure 4.1, *panel A*). Secondly, it was necessary to optimise the concentration of 'GC-melt' added to the reaction samples. The PCR amplification reaction was repeated using the optimised primer annealing temperature of 62 °C and a range of 'GC-melt' concentrations (0, 0.5, 1.0 and 1.5 M). As shown in panel B of Figure 4.1, the largest quantity of amplification product was obtained using a 'GC-melt' concentration of 0.5 M. Little product was observed when 'GC-melt' was absent, and when its concentration increased to 1.0 M, no amplification product was detected at all. These findings highlight the sensitivity of this particular PCR amplification.

The correctly sized PCR product was extracted from the agarose gel, ligated into the pGEM-T vector and transformed into competent bacteria *(Sections 2.2.9.4* and *2.2.9.5)*. The transformed bacteria were grown overnight on selection plates containing IPTG and X-Gal, in addition to ampicillin (indicator plates). Following an overnight incubation, any blue colonies were ignored and white colonies were picked for analyses; the white colour was due to interruption of the β-galactosidase sequence, by successful ligation of the SR-BI sequence into the pGEM-T MCS. Plasmids were subsequently extracted from five bacterial clones and analysed by restriction endonuclease digestion with *Sac*II and *Sal*I *(Sections 2.2.9.6* and *2.2.8)*. These restriction sites are situated in the MCS of pGEM-T, either side of the SR-BI sequence insertion site. Digestion reaction samples were separated on an agarose gel *(Section 2.2.5)* and the correctly sized digestion product of ~1600 bp was detected in clones 1, 3, 4, and 5 (Figure 4.1, *panel C*). Sequencing data from each of these four clones not only revealed the orientation of the SR-BI sequence within the vector, but a large number of mutations throughout the sequences. It was not possible, therefore, to use any of these sequences to generate a mammalian SR-BI expression vector. However, one of the plasmids was subsequently manipulated in order to isolate the correct SR-BI cytoplasmic tail sequence, which did not contain any mutations *(Section 3.2.2.3)*.

The full-length SR-BI sequence was kindly given to me in a pT7T3D vector by Dr. C. Sharp (GlaxoSmithKline, UK). The *Eco*RI and *Not*I restriction sites were chosen as suitable sites to transfer the SR-BI fragment into the pCDNA3 mammalian expression vector (Figure 2.6). However, due to the presence of an additional *Eco*RI site within the SR-BI sequence, it was necessary to digest the SR-BI sequence from the pT7T3D vector in 2 fragments. The two endonuclease digestion reactions involved *Not*I/*Xho*I and *Xho*I/*Eco*RI pairs of enzymes, with the predicted digestion products of ~2.1 kb & ~450 bp and ~420 bp & ~640 bp, respectively. The digestion products were separated on an agarose gel and all the predicted fragments were observed (Figure 4.2, *panel A*). The bands of ~2.1 kb and ~420 bp were then purified from the gel and inserted into the pCDNA3 vector in a 3-way ligation using a vector DNA:insert DNA molar ratio of 1:3 *(Sections 2.2.6* and *2.2.9.4)*. Following transformation of competent bacteria, plasmids were purified from nine bacterial clones and analysed for correct SR-BI sequence insertion. Analysis was performed using *Xba*I and *Hind*III restriction enzymes, which have cleavage sites within the MCS of pCDNA3. The digestion products were

subsequently separated on an agarose gel to reveal that clones 3, 4, 7 and 8 contained the full-length SR-BI sequence (Figure 4.2, *panel B*). Finally, another restriction digest with *Eco*RI was performed to confirm that the 3-way ligation had indeed been successful in these four clones: the predicted digestion product of ~1050 bp was observed in each sample (Figure 4.2, *panel C*). The pCDNA3 vector containing full-length SR-BI (pCDNA3-I) was not sequenced, as the inserted fragment had already been checked for mutations in the pT7T3D vector.

4.2.1.2 Full-length SR-BII expression vectors

The generation of pCDNA3 containing full-length SR-BII was relatively simple as it only involved exchanging the type I cytoplasmic tail for the type II tail. The *Acc*III restriction site is a unique site that cuts in the cytoplasmic tail region common to both isoforms. The type I tail and 3' UTR was therefore easily removed from pCDNA3-I using *Acc*III and an enzyme that cuts downstream in the pCDNA3 MCS (*Not*I). Following separation of the ~1100 bp digestion product from the cut vector using agarose gel electrophoresis, the cut vector was purified from the gel (Figure 4.3, *panel A*). Likewise, the pGEX-II vector (*Section 2.2.9* and Table 2.3) was subjected to exactly the same digestion to remove the type II tail. The SR-BII cytoplasmic tail sequence was separated from the cut vector using agarose gel electrophoresis and then purified from the gel (Figure 4.3, *panel B*). This sequence was ligated into the cut pCDNA3 vector and transformed into competent cells. Subsequently, plasmids were isolated from six bacterial clones and analysed by *Xho*I restriction endonuclease digestion. *Xho*I was chosen to determine which isoform was present, as it cuts within the SR-BI/II sequence and the 3' MCS: the presence of SR-BII would therefore result in a digestion product of ~1.2 kb, whereas SR-BI would give a product of over 2 kb as it contains the 3' UTR. Panel C of Figure 4.3 revealed that the tail transfer had been successful, since digestion products of ~1.2 kb were observed in all six clones.

pCDNA3 expression vectors containing full-length SR-BI or II sequences (pCDNA3-I and pCDNA3-II) were isolated from large-scale bacterial cultures using the 'EndoFree Plasmid Maxi' kit *(Section 2.2.9.6)*. This procedure extracted 500 μg of endotoxin-free plasmid DNA, which was then used to transfect eukaryotic CHO-K1 cells.

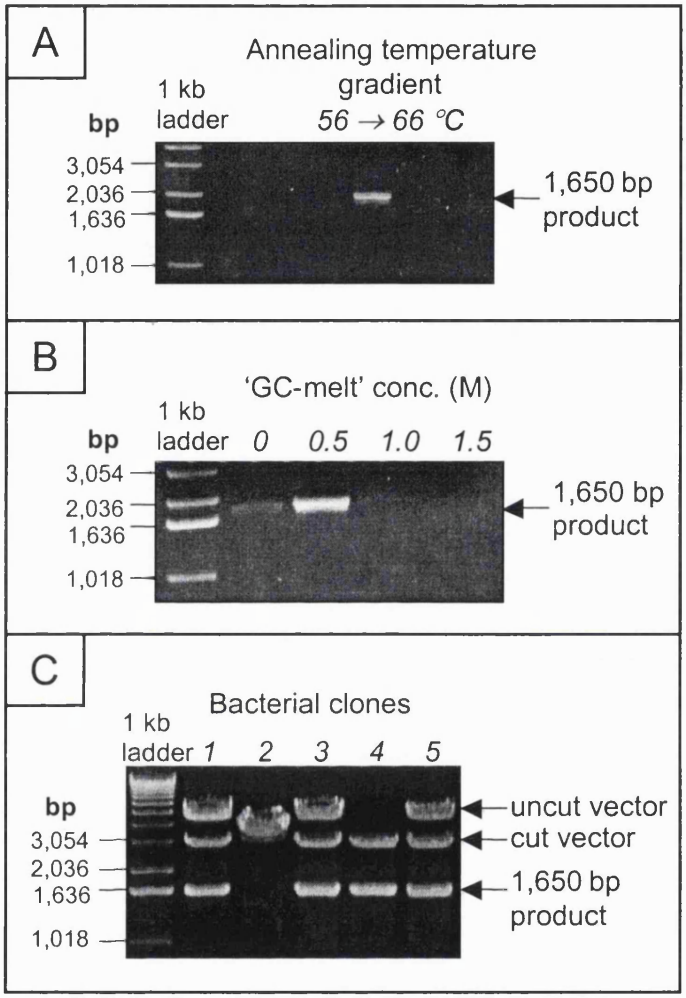

Figure 4.1 Cloning the full-length SR-BI sequence into the pGEM-T vector

Panel A, *Amplification of the full-length SR-BI sequence was performed by gradient PCR using a primer annealing temperature range of 56–66 °C (Table 2.1 and Section 2.2.3.2).* ***Panel B,*** *The PCR reaction was repeated using a range of 'GC-melt' concentrations and a primer annealing temperature of 62 °C.* ***Panel C,*** *Following ligation of the amplified SR-BI sequence into pGEM-T and transformation of competent bacteria, five clones were picked for analysis. Plasmids were isolated from each of the clones and subjected to restriction endonuclease digestion with SacII and SalI, for 1 h, using the conditions described in Section 2.2.8. In each case, the PCR amplification products and the digestion products were separated using 1.0 % agarose gels.*

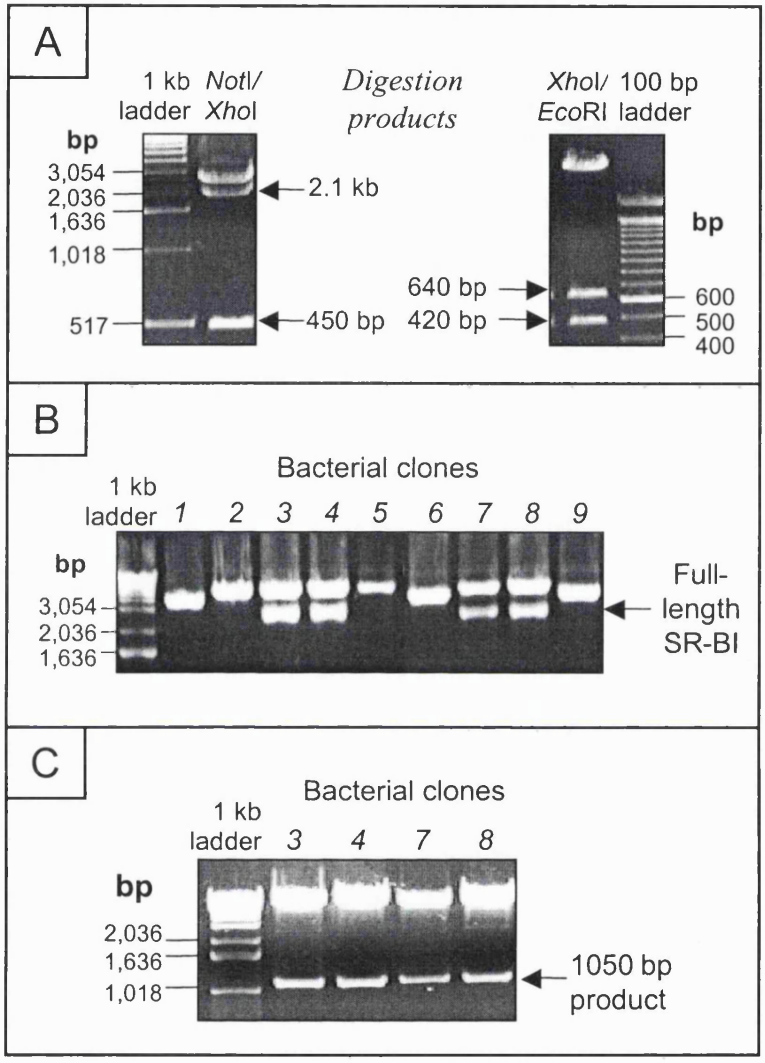

Figure 4.2 Successful transfer of the full-length SR-BI sequence into the pCDNA3 expression vector

The full-length SR-BI sequence was removed from pT7T3D in two fragments, generated from endonuclease digestion (Section 2.2.8) with the following pairs of enzymes: NotI/XhoI and XhoI/EcoRI ***(Panel A).*** *Following ligation of these two fragments into pCDNA3 and transformation of competent bacteria, nine bacterial clones were analysed (Sections 2.2.9.4 and 2.2.9.5). Plasmids were extracted from each clone and subjected to restriction endonuclease digestion with HindIII and XbaI* ***(Panel B)****, followed by digestion of clones 3, 4, 7 and 8 with EcoRI* ***(Panel C).*** *In each case, the digestion products were separated using 1.0 % agarose gels.*

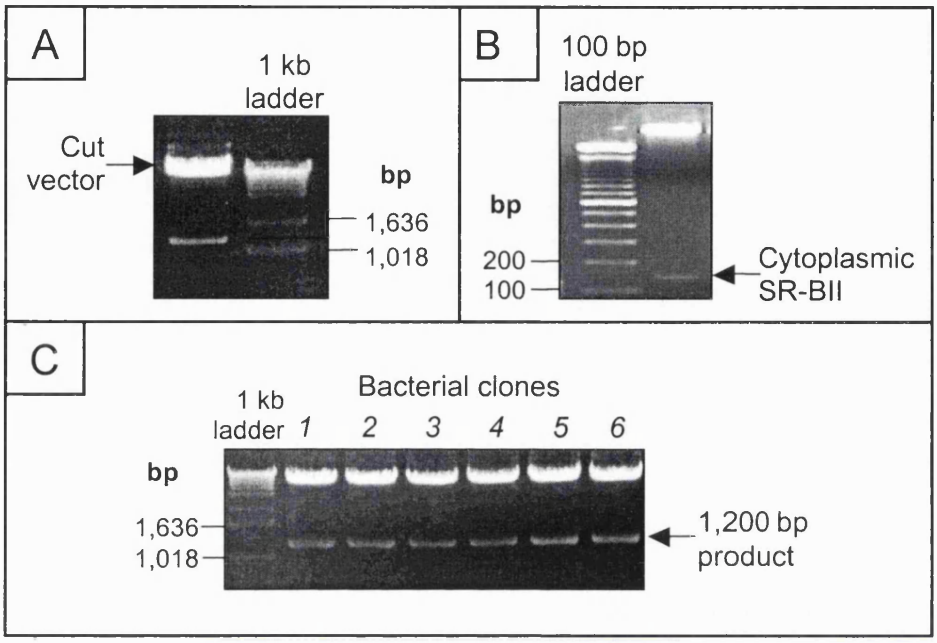

Figure 4.3 Cloning the full-length SR-BII sequence into the pCDNA3 expression vector

Panel A, *The cytoplasmic tail sequence and 3' UTR of SR-BI was digested from pCDNA3-I using NotI and AccIII restriction endonucleases and the conditions described in Section 2.2.8. Digestion products were separated using a 1.0 % agarose gel.* ***Panel B,*** *Cytoplasmic SR-BII was removed from the pGEX-II vector using the same enzymes and conditions as described for panel A. In this case a 1.5 % agarose gel was used.* ***Panel C,*** *Following ligation of the cytoplasmic SR-BII sequence into the cut pCDNA3-I vector (Section 2.2.9.4), competent bacteria were transformed (Section 2.2.9.5), and six clones were analysed. Extracted plasmids were subjected to endonuclease digestion with XhoI and digestion products were separated using a 1.0 % agarose gel.*

4.2.2 SUCCESSFUL TRANSFECTIONS OF CHO-K1 CELLS WITH SR-BI AND II

4.2.2.1 Selection of transfected cells

The pCDNA3 plasmid carries the neomycin-selectable marker, which allows its host cell to survive in the presence of geneticin G418 sulphate. Before commencing CHO-K1 transfections with pCDNA3 expression plasmids, it was necessary to perform a

dose-response experiment in order to establish the correct dose of geneticin that would cause untransfected cells to die, yet would leave the transfected cells growing. CHO-K1 cells were seeded into 6-well plates and incubated in media containing 0–1000 μg/ml geneticin. After 4 days, the percentage of cells alive was estimated and the results are shown in Figure 4.4. Very few cells survived exposure to geneticin at a concentration of 600 μg/ml, and at 800 μg/ml, all the cells had died. I therefore decided to use geneticin at a concentration of 600 μg/ml for the selection process, which was similar to the concentration described in relevant publications (500 μg/ml) [233].

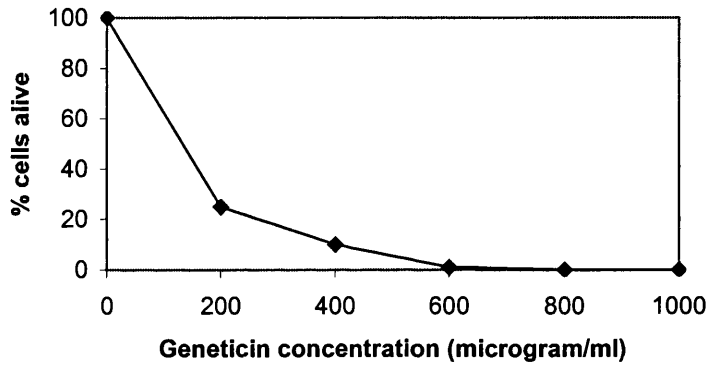

Figure 4.4 Geneticin G418 sulphate dose-response curve

CHO-K1 cells were transfected with pCDNA3-I and pCDNA3-II expression vectors according to the method described in *Section 2.4.3.1.* As a positive control reaction for the transfection protocol, CHO-K1 cells were also transfected with a pCDNA3 plasmid encoding the green fluorescent protein (pCDNA3-GFP). Twenty-four hours following transfection, the cells were observed, using phase-contrast microscopy and fluorescence microscopy with excitation light of wavelength 465-495 nm (Figure 4.5, *panels A and B*, respectively). Roughly 5 % of the cells fluoresced green, indicating that the transfection had been successful. Having confirmed this, the selection of cells transfected with pCDNA3-I/II commenced with the addition of 600 μg/ml geneticin to the culture media. After 7 days, all the untransfected CHO-K1 control cells had died, yet ~5 % of the transfected cells were growing and dividing in the selection media, indicating that the selection process was complete. The surviving cells were expanded and maintained under selection pressure and are described as the 'mixed population' of cells.

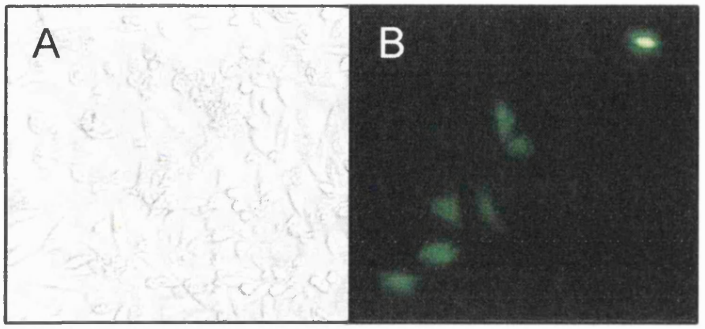

Figure 4.5 Successful transfection of CHO-K1 cells with pCDNA3-GFP

CHO-K1 cells were transfected with the pCDNA3-GFP expression plasmid using 'Superfect Transfection Reagent' as described in Section 2.4.3.1. The cells were observed 24 h post-transfection using phase-contrast microscopy ***(Panel A),*** *and fluorescence microscopy, with incident blue light of wavelength 465-495 nm* ***(Panel B),*** *both with 20X magnification.*

4.2.2.2 Confirmation of receptor expression in the transfected cells

Having selected cells containing pCDNA3 plasmids, it was necessary to confirm that these recombinant cells were producing SR-BI/II protein. Initially, CHO-K1 cells expressing SR-BII (CHO-SR-BII) were analysed: CHO-SR-BII and control CHO-K1 cells were lysed *(Section 2.4.4)* and equal quantities of cellular protein were separated by SDS-PAGE and immunoblotted with SR-BII antiserum *(Sections 2.3.2* and *2.3.3)*. As shown in panel A of Figure 4.6, a strong band was observed at ~80 kDa that was absent from the control cells, indicating that the recombinant cells were generating the full-length type II isoform. This experiment was then repeated using CHO-K1 cells expressing SR-BI (CHO-SR-BI) with the α-CLA-1 antibody against the extracellular domain of SR-BI/II, and exactly the same results were obtained (Figure 4.6, *panel A*). In order to verify that this was indeed the type I isoform, and that neither the cells nor plasmids had been mixed up during the transfection, the blot was stripped of its antibodies and re-probed with α-SR-BII *(Section 2.3.3.3)*. No band at 80 kDa was observed in this case, which allowed me to conclude that CHO-SR-BI cells were generating the full-length type I isoform (data not shown).

Since the α-CLA-1 antibody binds to SR-BI/II in the extracellular region common to both isoforms, this antibody was subsequently used to compare protein levels of both isoforms within the mixed population of recombinant cells. Equal quantities of cellular protein from recombinant lysates were subjected to Western blotting with α-CLA-1 *(Sections 2.3.2* and *2.3.3)*. The autoradiograph revealed that SR-BII was being expressed to a much greater extent than SR-BI in the recombinant cells (Figure 4.6, *panel B*). This difference would certainly interfere with subsequent experiments comparing the role of each isoform in cholesterol homeostasis. It was therefore necessary to clone the recombinant cells and attempt to match CHO-SR-BI and II clones for similar receptor expression levels *(Sections 4.2.2.3* and *4.2.3)*.

This experiment also highlighted the fact that the SR-BI/II "band" at ~80 kDa was not a single band but comprised either a doublet or a triplet. Previous studies using CHO cells over-expressing mSR-BI had found the apparent mass of this receptor to be ~82 kDa, yet the predicted mass from its primary amino acid sequence is only ~57 kDa [103,176]. Babitt *et al.* [176] subsequently studied the post-translational modification of mSR-BI, and confirmed that this isoform is indeed extensively *N*-glycosylated in its extracellular region. This finding accounts for the difference in predicted and apparent molecular weights of mSR-BI. Since this region is common to both isoforms, we can assume that mSR-BII is also modified in this way. It therefore appeared likely that the lower molecular weight bands observed in the CHO-SR-BI/II whole cell lysates represented immature forms of the receptor. In order to confirm that this was the case, cell surface proteins were biotinylated and isolated from recombinant cell lysates by precipitation with streptavidin beads *(Section 2.4.5.1)*. These membrane proteins, as well as whole cell lysates, were subsequently separated by SDS-PAGE and immunoblotted with α-CLA-1 (Figure 4.6, *panel C*). The extra receptor bands were easily observed in both CHO-SR-BI and II whole cell lysates, yet the lower bands had disappeared in the membrane protein fraction. This indicated that the lower bands were indeed immature intracellular SR-BI/II proteins and that only the larger, fully modified receptors were present at the cell surface.

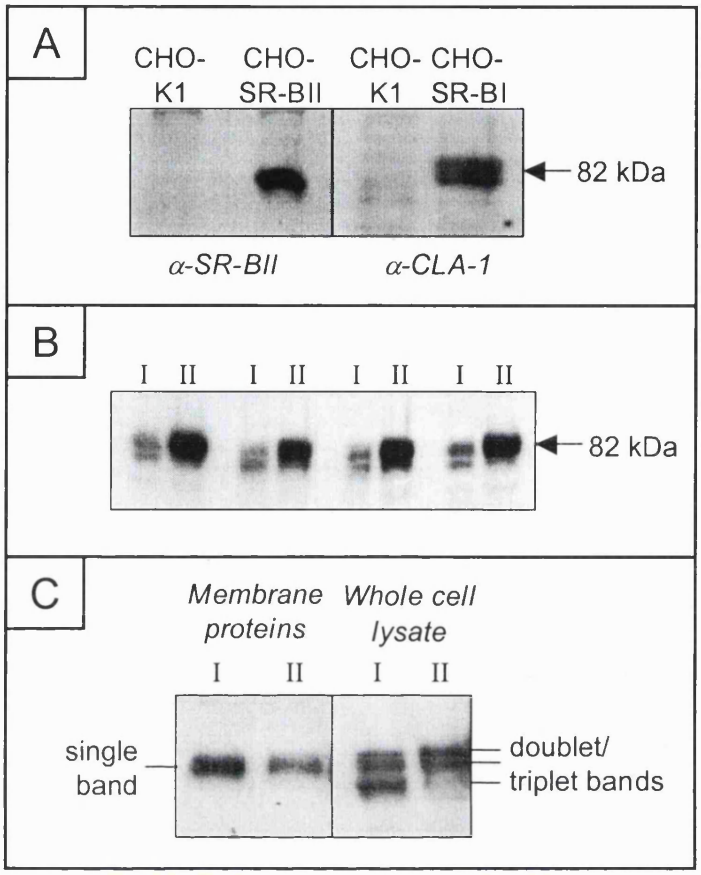

Figure 4.6 Confirmation of SR-BI or II expression by recombinant CHO-K1 cells

Panel A, *Untransfected CHO-K1 and recombinant CHO-SR-BI/II cells were lysed (Section 2.4.4) and assayed for protein concentration. Twenty μg of cellular protein from each cell lysate were separated by 8 % SDS-PAGE, followed by immunoblotting with α-SR-BII and α-CLA-1.* ***Panel B****, Thirty μg of cellular protein from CHO-SR-BI (I) and CHO-SR-BII (II) cell lysates were separated by 8 % SDS-PAGE in quadruplicate and probed with α-CLA-1.* ***Panel C,*** *Cell surface proteins were isolated from recombinant CHO-SR-BI/II cells, following cell surface biotinylation and streptavidin bead precipitation (Section 2.4.5.1). The beads were boiled under reducing conditions and the eluted membrane proteins were subjected to 8 % SDS-PAGE and immunoblotting with α-CLA-1. Whole cell lysates were also separated on the same gel, as described for panel B.*

4.2.2.3 Isolation of CHO-SR-BI and II clones

The aim of this cloning procedure was to generate CHO-SR-BII clones with high, medium and low levels of SR-BII expression, to enable this receptor to be linked to a particular function in future cholesterol efflux and mobilisation studies. Furthermore, in order to compare the roles of SR-BI and II in cholesterol homeostasis, I wanted to match one of the CHO-SR-BII clones with a CHO-SR-BI clone expressing similar levels of cell surface receptor. Individual CHO-SR-BI/II cells were isolated for cloning by serial dilution, as described in *Section 2.4.3.2.* Following 4/5 cell divisions of marked cells, 24 clones of each recombinant cell type were picked and expanded under selection pressure. Subsequently, equal amounts of cellular protein from ten of the fastest growing CHO-SR-BI/II clones were analysed by Western blotting with α-CLA-1 and α-SR-BII to detect type I and II receptor expression, respectively (Figure 4.7, *panels A and B*). The results of the initial screen revealed one high- and one low-expressing CHO-SR-BI clone, and a few CHO-SR-BII clones with varying levels of receptor expression. However, at this stage it was not possible to directly compare SR-BI and II expression levels in the recombinant clones, since different antibodies had been used for receptor detection. When the experiment was repeated using the same antibody (α-CLA-1) for SR-BI/II detection, and equal amounts of cellular protein, the type II receptor was found to be expressed at much higher levels in the high CHO-SR-BII clone than the type I receptor in the high CHO-SR-BI clone (Figure 4.7, *panel C*). Indeed, it appeared that the high CHO-SR-BI clone most closely matched the lowest CHO-SR-BII clone for levels of receptor expression.

Following analysis, three clones were chosen to undergo a further round of sub-cloning to ensure that pure clones were isolated: CHO-SR-BI (clone 10), and high- and low-expressing CHO-SR-BII (clones 1 and 21, respectively). Ten sub-clones of each recombinant cell type were expanded and equal quantities of cell lysate protein were analysed again by Western blotting with α-CLA-1 and α-SR-BII antibodies (Figure 4.8, *panels A-C*). Within each cell type, not all the sub-clones were found to express identical levels of SR-BI/II, indicating that pure clones had not been isolated in the first cloning step. From these Western blots, 1S and 21F sub-clones were chosen as high- and low-expressing CHO-SR-BII clones, respectively. I also chose 1J sub-clone as a 'medium' CHO-SR-BII clone. Finally, it was necessary to identify CHO-SR-BI and CHO-SR-BII clones with similar receptor expression levels. This was achieved by subjecting equal quantities of cellular protein from many different sub-clones to Western

blot analysis with the α-CLA-1 common antibody (Figure 4.8, *panel D*). CHO-SR-BI clone 10B and CHO-SR-BII clone 21F were subsequently matched for similar levels of receptor protein expression.

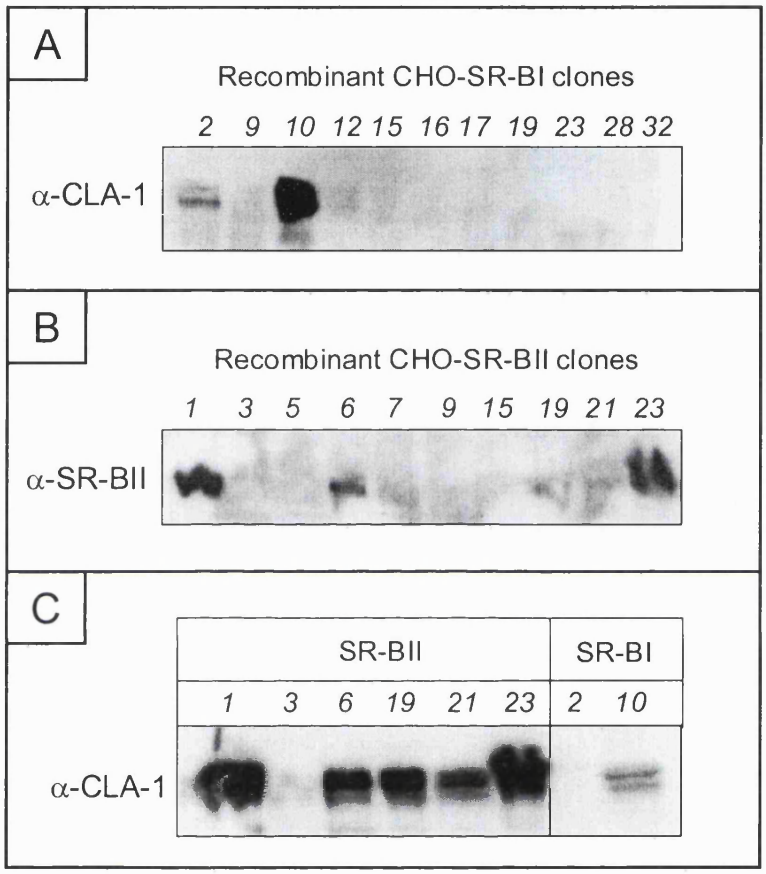

Figure 4.7 Identification of recombinant clones expressing SR-BI/II protein

Ten confluent CHO-SR-BI and CHO-SR-BII clones were lysed (Section 2.4.4) and 50 μg of cellular protein from each clone were separated by 8 % SDS-PAGE and immunoblotted with α-CLA-1 ***(Panel A)*** *and α-SR-BII* ***(Panel B)****. Equal quantities of cellular protein (50 μg) from six CHO-SR-BII and two CHO-SR-BI clones were subsequently separated on the same 8 % gel using SDS-PAGE. The proteins were transferred to nitrocellulose and probed with α-CLA-1 to compare levels of receptor expression* ***(Panel C)****.*

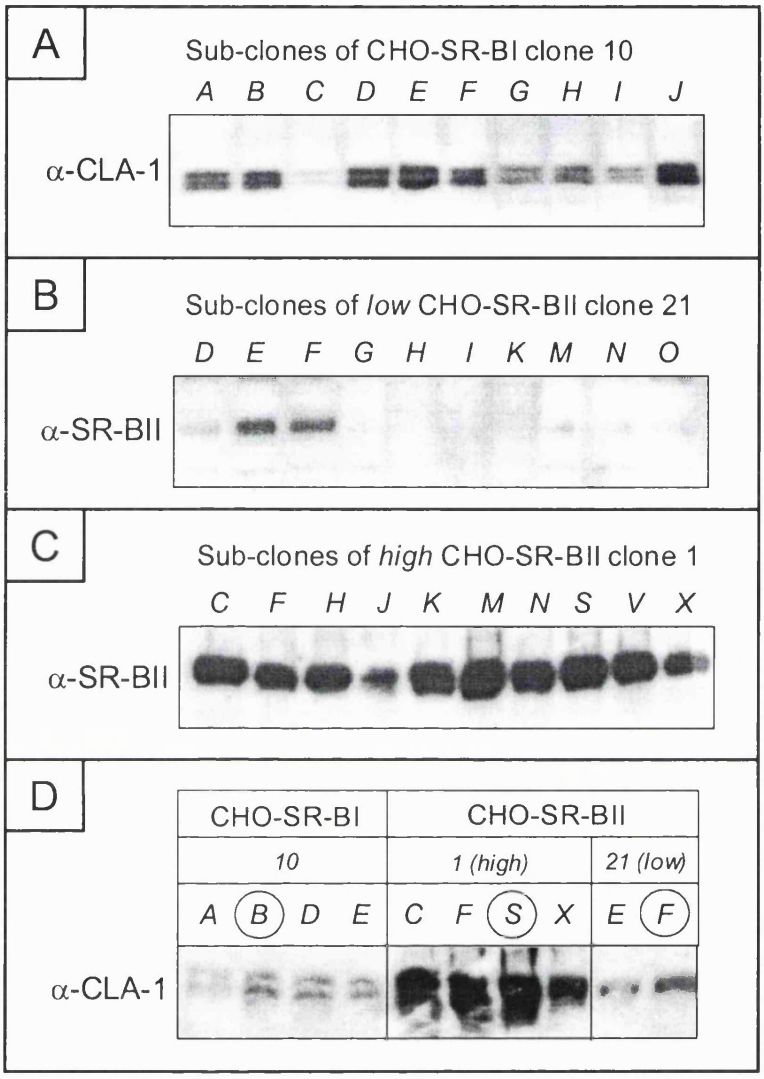

Figure 4.8 Identification of recombinant CHO sub-clones expressing SR-BI/II protein

Panels A-C, *Ten sub-clones of CHO-SR-BI clone 10 and CHO-SR-BII clones 1 and 21 were expanded and lysed. 20 μg of cellular protein from each cell lysate were separated by 8 % SDS-PAGE and immunoblotted with α-CLA-1 or α-SR-BII, for SR-BI and SR-BII expression, respectively.* ***Panel D,*** *20 μg of cellular protein from a mixture of CHO-SR-BI and II sub-clones were subsequently separated on the same 8 % gel by SDS-PAGE and immunoblotted with α-CLA-1 to compare SR-BI/II expression levels. The circled clones were chosen and expanded for future cholesterol homeostasis experiments.*

4.2.3 COMPARING LEVELS OF CELL SURFACE SR-BI AND II IN RECOMBINANT CLONES BY FLOW CYTOMETRY AND DENSITOMETRY

Western blotting analysis of whole cell lysates was used to match two CHO-SR-BI and II clones expressing similar levels of SR-BI/II protein, designated clones 10B and 21F *(Section 4.2.2.3)*. However, in order to be able to directly compare the abilities of these two clones to mediate cholesterol efflux and mobilisation in response to HDL, it was necessary to compare receptor levels at the plasma membrane. This was performed using two different methods: firstly, by flow cytometry, and secondly by immunoblotting membrane proteins followed by autoradiograph densitometry.

4.2.3.1 Flow cytometry

Confluent cultures of CHO-SR-BI clone 10B, CHO-SR-BII clone 21F, and CHO-K1 control cells were incubated with the α-RED-1 antibody according to the method described in *Section 2.4.5.2*. This antibody binds to the extracellular domain, common to both isoforms, and is suitable for use in immunofluorescent techniques. Any primary antibody binding was detected using a secondary antibody conjugated to fluorescein isothiocyanate (FITC). The experiment was performed in triplicate for each of the cell types, and included the following two controls: pre-immune serum (used instead of primary antibody) and omission of the primary antibody (but still using secondary antibody). Fixed cells in a single suspension were then analysed by flow cytometry. Firstly, the CHO-K1 cell population was gated on forward- and side-scattered laser light, to avoid debris and any cell clumps. The log FITC fluorescence, resulting from antibody binding to cell surface SR-BI and II, was then measured for 5,000 gated cells from each sample. Triplicate analyses for each cell type were made and the average median values were subsequently calculated using WinMDI software. Panels A and B of Figure 4.9 are examples of 2-parameter histograms showing CHO-SR-BI and II log FITC fluorescence profiles, respectively. The median values from the triplicate analyses are shown in Table 4.1.

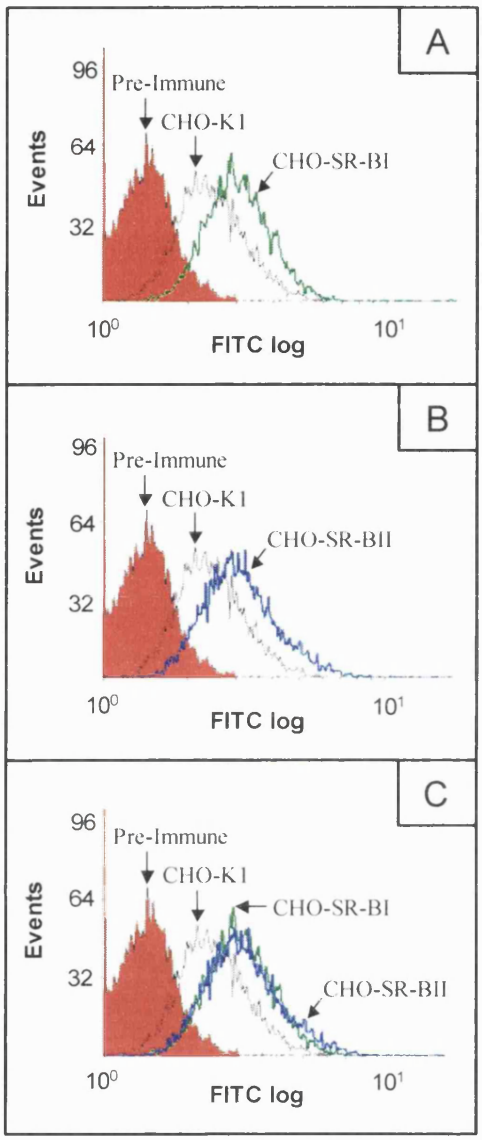

Figure 4.9 CHO-SR-BI and II clones have equivalent cell surface receptor expression as assessed by flow cytometry

CHO-SR-BI clone 10B, CHO-SR-BII clone 21F and CHO-K1 control cells were incubated with the α-RED-1 primary antibody (or pre-immune serum as a negative control), followed by a FITC-conjugated secondary antibody, as described in Section 2.4.5.2. FITC fluorescence of 5,000 intact gated cells or 'events' was detected using flow cytometry and fluorescence data was displayed as a 2-parameter histogram (showing a one decade log_{10} FITC scale against the number of events with corresponding fluorescence values). The experiment was performed in triplicate but only representative histograms for each cell type are shown. ***Panels A & B,*** *The fluorescence profile for the pre-immune negative control is shaded in red, the CHO-K1 control cell profile is outlined in black, CHO-SR-BI clone 10B outlined in green, and CHO-SR-BII clone 21F outlined in blue.* ***Panel C,*** *The fluorescence profiles for both recombinant clones were overlaid.*

Cell type	Treatment	Average median log FITC fluorescence (arbitrary fluorescence units)
CHO-K1 control	α-RED-1	4.28
CHO-SR-BI *(clone 10B)*	α-RED-1	**5.17**
	No 1°	3.65
	PI serum	3.52
CHO-SR-BII *(clone 21F)*	α-RED-1	**5.19**
	No 1°	3.72
	PI serum	3.72

Table 4.1 Comparison of SR-BI/II cell surface expression by flow cytometry

CHO-SR-BI clone 10B, CHO-SR-BII clone 21F and CHO-K1 control cells were subjected to flow cytometry (as described in Figure 4.9). The experimental controls included pre-immune (PI) serum and no primary (1°) antibody. The experiment was performed in triplicate and the average median FITC fluorescence was calculated for each treatment and cell type, using WinMDI software.

The experimental controls were performed to determine the level of non-specific binding of the primary and secondary antibodies. When the fluorescence profiles of the control samples and the recombinant CHO-SR-BI/II clones were compared, there was a clear right shift in each recombinant CHO-SR-BI/II profile away from the control profiles. Moreover, the average median FITC fluorescence values of the control cells and treatments were calculated to be significantly lower than the recombinant clones ($p<0.01$). These findings indicated that the log FITC fluorescence detected in the recombinant clones was due to receptor expression and not due to non-specific binding of the antibodies. The matched clones appeared to be expressing very similar levels of SR-BI and II, as the profiles, when overlaid, were almost identical (Figure 4.9, *panel C*). Furthermore, there was no significant difference between the median FITC fluorescence values of CHO-SR-BI and II clones ($p=0.59$), thereby confirming that these clones were equally matched.

This technique was also used to confirm that low-, medium-, and high-expressing CHO-SR-BII clones had been chosen using Western blotting analysis. The average values of median log FITC fluorescence obtained for each clone are listed in Table 4.2. Flow cytometry revealed a slight increase in log FITC fluorescence between the low and medium CHO-SR-BII clones, and the medium and high CHO-SR-BII clones, confirming that low-, medium-, and high-expressing CHO-SR-BII clones had indeed been selected.

Cell type	Treatment	Average median log FITC fluorescence (arbitrary fluorescence units)
CHO-K1 control	PI serum	1.38
	No 1°	1.50
	α-RED-1	3.35
Low CHO-SR-BII *clone 21F*	α-RED-1	**4.46**
Medium CHO-SR-BII *clone 1J*	α-RED-1	**6.43**
High CHO-SR-BII *clone 1S*	α-RED-1	**8.63**

Table 4.2 Flow cytometric analysis of SR-BII cell surface expression in low-, medium-, and high-expressing CHO-SR-BII clones

CHO-K1 control cells and CHO-SR-BII clones expressing different levels of SR-BII were subjected to flow cytometry (as described in Figure 4.9). The experimental controls included pre-immune (PI) serum and no primary (1°) antibody. The experiment was performed in triplicate and the average median FITC fluorescence was calculated for each cell type and treatment, using WinMDI software.

Surprisingly, the FITC fluorescence values generated from the high CHO-SR-BII clone were still within the first decade of log FITC fluorescence, even though the fluorescence detection of the cytometer was at maximum sensitivity; one might usually expect positive cytometric data to be within the second and third decade of log FITC fluorescence. The α-RED-1 antibody was titrated for optimal detection but consistent low fluorescence values revealed that either the receptors were poorly expressed

(although this seemed unlikely from previous Western blotting analysis), or more probably that the antibody was poor at binding its antigen for this immunofluorescent technique. Therefore, the flow cytometric data for the matched CHO-SR-BI and II clones was verified using another method for detecting levels of receptor expressed at the cell surface: immunoblotting cell surface proteins followed by densitometric analysis.

4.2.3.2 Densitometry

The aim of this experiment was to isolate plasma membrane proteins from each of the 'matched' CHO-SR-BI and II clones in triplicate and then compare levels of SR-BI and II using Western blotting and densitometric analysis. Briefly, cell surface proteins were biotinylated and lysed, and the cell lysates were adjusted to contain equal amounts of cellular protein. The biotinylated membrane proteins were subsequently isolated from each cell lysate using streptavidin beads *(Section 2.4.5.1)*. The presence of SR-BI or II in the eluted proteins was determined by separating triplicate samples on the same 8 % SDS-PAGE gel, followed by immunoblotting with α-CLA-1. The nitrocellulose membrane was then exposed to X-ray film for varying lengths of time (5–45 s) so that film saturation could be ascertained. The autoradiograph generated from a 10 s exposure is shown in panel A of Figure 4.10. The triplicate SR-BI and II bands on each of the four autoradiographs were subsequently measured by densitometry. Having subtracted the local background from each of the values, the mean 'adjusted volume' for each clone was calculated and plotted versus film exposure time (Figure 4.10, *panel B*).

The densitometry data from all four autoradiographs revealed significantly more cell surface expression of SR-BI than SR-BII in the 'matched' recombinant clones ($p<0.01$). The graph also showed that saturation of the film was reached after only 10 s exposure with the nitrocellulose membrane. I chose, therefore, to determine the difference in receptor expression levels using the data obtained from the 5 s autoradiograph. SR-BI cell surface expression was calculated to be 5.8 times that of SR-BII in the 'matched' recombinant clones. This was a surprising result that differed markedly from the flow cytometry data. However, as similar densitometry results were obtained on separate occasions, this led me to believe that the 5.8-fold difference in receptor expression between the CHO-SR-BI and II clones was real. I concluded that clones 10B and 21F were not matched and that I would therefore have to take the differences in SR-BI and II levels into account in future comparative experiments *(Section 4.2.6)*.

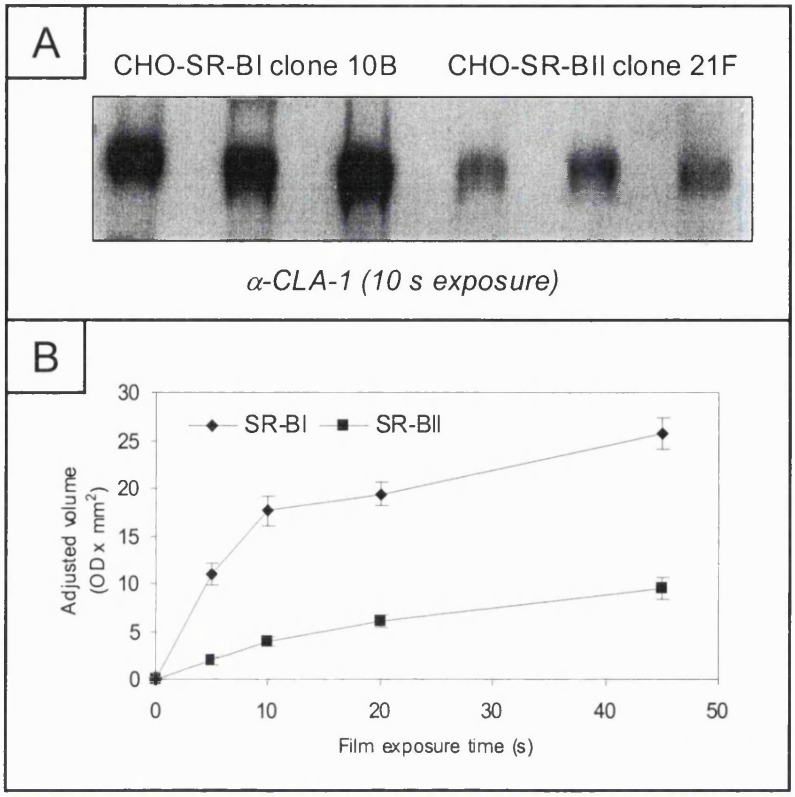

Figure 4.10 Western blotting reveals higher levels of cell surface SR-BI expression than SR-BII in the 'matched' recombinant clones

*Biotinylated membrane proteins were isolated from CHO-SR-BI and II 'matched' clones in triplicate using streptavidin beads (Section 2.4.5.1). Eluted proteins were separated by 8 % SDS-PAGE, immunoblotted with α-CLA-1, and the nitrocellulose membrane was subsequently exposed to the X-ray film for 5-45 s (**Panel A**; 10 s exposure). The SR-BI/II triplicate bands were analysed by densitometry. Having subtracted the local background from each of the values, the mean 'adjusted volume' ± S.E.M. for each clone was calculated and plotted versus film exposure time **(Panel B).***

4.2.4 LIPOPROTEIN PREPARATION

High- and low-density lipoprotein (HDL and LDL) particles were isolated from fresh human plasma using sequential ultracentrifugation *(Section 2.3.10)*. As the density of the plasma solution was increased by the addition of NaCl-NaBr, the densities of the lipoprotein particles that could be floated to the top of the tube during ultracentrifugation also increased. This method therefore allowed sequential isolation of plasma

lipoproteins in the following order: VLDL, followed by LDL, HDL_2 and HDL_3. Isolation of LDL using this method was relatively quick and easy, although isolation of HDL_3 was a much lengthier procedure. Therefore in order to isolate HDL_3 particles more quickly, this method was used in conjunction with a precipitation procedure: the first step involved precipitation of apoB-containing lipoproteins from the plasma by magnesium and phosphotungstic acid, leaving a supernatant with HDL as the sole lipoprotein component ('HDL plasma'). In some experiments, the 'HDL plasma' was dialysed and used as a rich source of HDL, although it was also possible to separate HDL_2 and HDL_3 from the 'HDL plasma' using the ultracentrifugation method described above. Following the isolation of lipoproteins from human plasma, their purities were ascertained using agarose gel electrophoresis with Sudan black staining *(Section 2.3.10.7)*. An example of one such gel is given in panel A of Figure 4.11. This gel reveals the high level of lipoprotein purity achieved using both the precipitation and ultracentrifugation methods. As expected, two distinct HDL populations were observed in the HDL_2 and HDL_3 lanes, whereas 'HDL plasma' contained both of these particles. This method was also employed to confirm that HDL_3 particles had been successfully isolated from plasma donated by three volunteers (Figure 4.11, *panel B*). Indeed, the stained gel revealed that for each donor, purified HDL_3 particles had been separated from the plasma. These particles were subsequently used to compare donor HDL_3 variability in cholesterol efflux experiments *(Section 4.2.7)*.

Finally, in order to generate a source of cholesterol that would be rapidly taken up by THP-1 macrophages during cholesterol loading, LDL particles were subjected to acetylation *(Section 2.4.2.2)*. The LDL particles were chemically modified using saturated sodium acetate and acetic anhydride. The success of the acetylation procedure was determined by separating equal amounts of Ac-LDL and native (n) LDL using agarose gel electrophoresis, followed by gel staining with Sudan black: addition of acetyl groups to the positive lysine and arginine residues of apolipoprotein B causes the LDL particles to become more negatively charged, which increases the mobility of the lipoprotein particles. As shown in panel C of Figure 4.11, the LDL acetylation procedure had been completed successfully as the Ac-LDL exhibited increased mobility on the agarose gel.

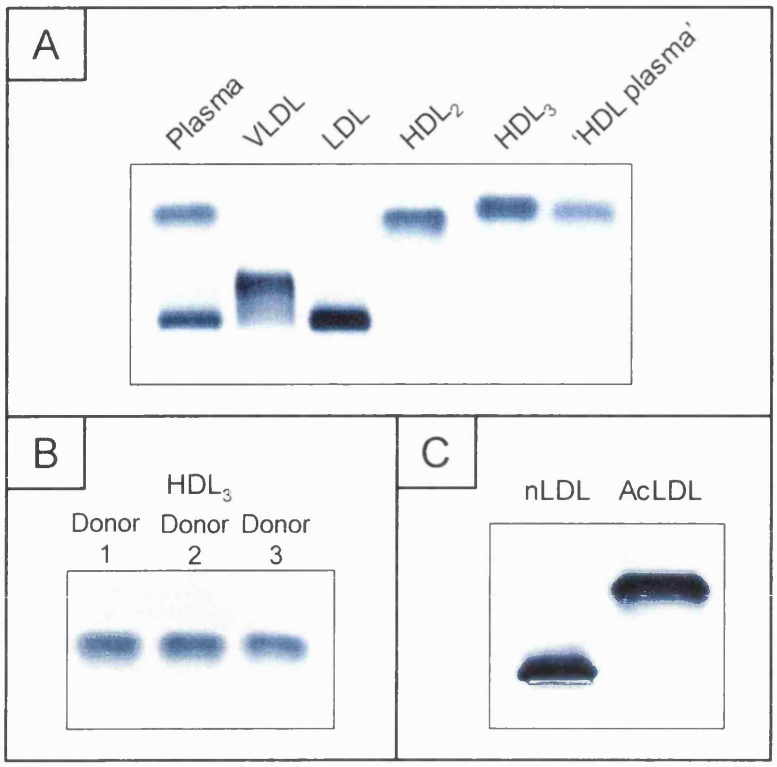

Figure 4.11 Purity of isolated lipoproteins by agarose gel electrophoresis

In each of these figures, 1-6 µl of plasma/lipoproteins were applied to agarose gels. Following electrophoresis, the gels were stained with Sudan black (Section 2.3.10). ***Panel A,*** *Lipoproteins were isolated from human plasma by sequential ultracentrifugation in the following order: VLDL, LDL, HDL_2 and HDL_3. 'HDL plasma' was generated by precipitation of the apo-B containing lipoproteins from plasma, leaving HDL as the sole lipoprotein component.* ***Panel B,*** *HDL_3 particles were purified from plasma from 3 donors and 9 µg protein was subjected to agarose gel electrophoresis.* ***Panel C,*** *native (n) LDL particles were chemically modified to produce acetylated (Ac) LDL (Section 2.4.2.2). Equal quantities of nLDL and Ac-LDL protein (7 µg) were subsequently run on an agarose gel.*

4.2.5 SR-BII PROMOTES HDL-DEPENDENT FC EFFLUX FROM RECOMBINANT CELLS

Experiments were performed to characterise the recombinant CHO-SR-BII cells and to determine whether SR-BII functions to promote HDL-mediated FC efflux. Initially, the abilities of CHO-K1 control cells and the mixed population of CHO-SR-BII cells to efflux cholesterol in response to HDL stimulation were compared *(Section 2.4.6)*. Cellular FC plasma membrane pools were labelled overnight with [^{3}H]-cholesterol. For each cell type, 40-50 % of the [^{3}H]-cholesterol was taken up from the labelling media, indicating that radiolabelling had been successful. Following the stimulation of cells

with 'HDL plasma', the level of [^{3}H]-cholesterol in the media and the cells was determined using LSC. The amount of [^{3}H]-cholesterol efflux was expressed as a percentage of total [^{3}H]-cholesterol in both the media and the cells. Background percentage efflux values were also measured by exposing radiolabelled cells of each cell type to serum-free media.

The first FC efflux experiment was performed over a 4 h time-course to determine the most suitable duration for the experiment. For each cell type, the average percentage cholesterol efflux values from duplicate wells were calculated, background efflux values were then subtracted, and the corrected efflux values were plotted versus time (Figure 4.12). This experiment revealed a clear difference between the abilities of CHO-K1 control and CHO-SR-BII cells to efflux FC: the percentage of FC efflux from the recombinant cells was higher than the control cells at every time point measured. Since this difference was the greatest at 4 h, I decided to terminate future cellular FC efflux experiments following 4 h of HDL stimulation.

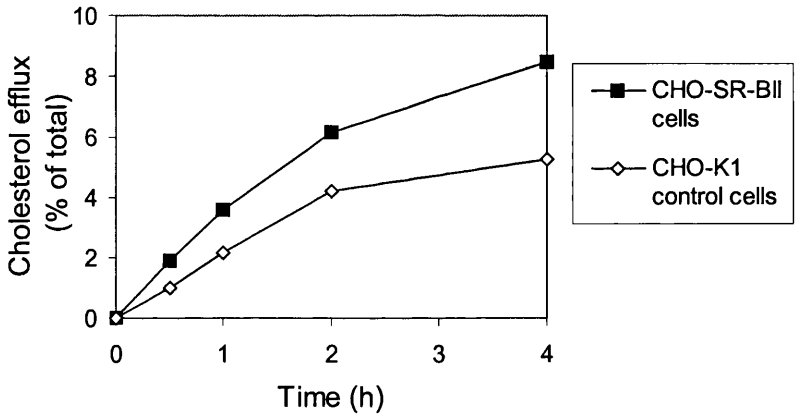

Figure 4.12 FC efflux time course for optimising experimental conditions

The FC plasma membrane pools of CHO-K1 control and CHO-SR-BII cells were labelled overnight with [^{3}H]-cholesterol, followed by efflux stimulation with 5 % (v/v) 'HDL plasma' over a 4 h time course, as described in Section 2.4.6. Radiolabelled FC efflux was measured and expressed as a percentage of total radiolabelled FC in both the media and cells. Average percentage cholesterol efflux values from duplicate wells were calculated, background efflux values from cells exposed to serum-free media were then subtracted, and the corrected efflux values were plotted versus time.

Subsequently, three further experiments were performed in triplicate to determine whether recombinant CHO-SR-BII cells were significantly better than control CHO-K1 cells at effluxing FC upon plasma and 'HDL plasma' stimulation. Panel A of Figure

4.13 shows the mean percentage cholesterol efflux values ± S.E.M. obtained from one experiment. The trends observed on this occasion were also seen in each of the other experiments: there were no significant differences between CHO-K1 and CHO-SR-BII background cholesterol efflux values, however CHO-SR-BII cells were found to be significantly better than CHO-K1 control cells at effluxing FC upon both plasma and 'HDL plasma' stimulation ($p<0.05$ and $p<0.01$, respectively). Data were combined from all three experiments by expressing the mean CHO-K1 control efflux values as a percentage of maximal CHO-SR-BII FC efflux (Figure 4.13, *panel B*).

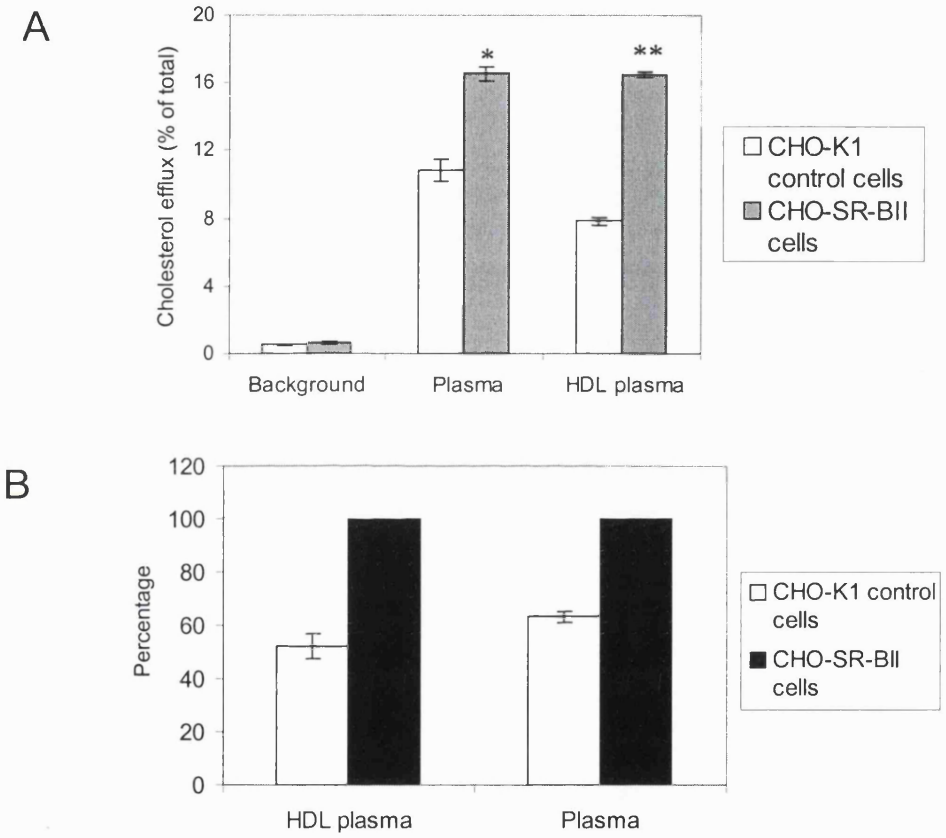

Figure 4.13 CHO-SR-BII cells are significantly better at HDL-stimulated FC efflux than control CHO-K1 cells

CHO-K1 control and CHO-SR-BII cells were labelled overnight with [^{3}H]-cholesterol, followed by efflux stimulation with plasma, 'HDL plasma', or serum-free media (background) for 4 h (Section 2.4.6). Radiolabelled FC efflux was measured and expressed as a percentage of total radiolabelled FC in both the media and cells. ***Panel A,*** *The experiment was performed in triplicate and the mean FC efflux values ± S.E.M. were calculated. The difference between the means of the control and recombinant cells was assessed by Student's t-test (*$p < 0.05$;**$p < 0.01$).* ***Panel B,*** *Data from three experiments were combined by expressing the mean FC efflux values of CHO-K1 control cells as a percentage of maximal CHO-SR-BII FC efflux (100 %).*

The combined data revealed that recombinant CHO-SR-BII cells efflux almost twice as much FC as control CHO-K1 cells in response to 'HDL plasma' stimulation. This ratio was not as high when cells were stimulated with whole plasma as the control CHO-K1 cells effluxed more FC in the presence of whole plasma than 'HDL plasma'. This indicated that apoB-containing lipoproteins in whole plasma also contribute to cellular FC efflux to a small extent.

In the last set of FC efflux experiments, CHO-K1 control cells and CHO-SR-BII clones expressing SR-BII at low, medium and high levels were incubated with purified HDL_3 for 4 h in order to definitively link SR-BII protein with HDL-stimulated FC efflux. Following overnight labelling, the control cells and recombinant clones had been successfully labelled with similar levels of [^{3}H]-cholesterol (36-47 % uptake). For each cell type, the average percentage FC efflux values were calculated from quadruplicate wells, background efflux values were then subtracted, and the corrected percentage efflux values ± S.E.M. were plotted (Figure 4.14, *panel A*). Analysis of the data using Student's *t*-test revealed that recombinant clones expressing even low levels of SR-BII were significantly better at effluxing FC than control CHO-K1 cells (*low* CHO-SR-BII clone: 12.30 ± 0.45 % efflux and CHO-K1 control: 10.95 ± 0.34 % efflux; $p<0.05$). As the level of cellular SR-BII expression increased, the percentage of FC leaving the cell and its significance also increased (*high* CHO-SR-BII: 42.17 ± 0.64 % efflux; $p<0.001$). It therefore appears that human SR-BII functions to promote HDL-mediated FC efflux.

Finally, it was necessary to confirm that this data could be reproduced using HDL_3 particles from a variety of donors. HDL_3 particles were isolated from fresh human plasma from three volunteers and the purity of the lipoprotein separation was determined *(Section 4.2.4)*. The HDL_3 particles were used to stimulate cellular FC efflux from the low CHO-SR-BII clone over a 4 h time course. For each type of donor HDL_3 and time point, the mean percentage efflux values were calculated from triplicate wells, and the background efflux value was then subtracted. The corrected percentage efflux values ± S.E.M. were plotted versus time (Figure 4.14, *panel B*). At each time point, there were no significant differences between the mean FC efflux values generated by stimulation with different HDL_3 particles ($p>0.05$), indicating that donor variability was not contributing to the percentage FC efflux values. It was therefore possible to conclude that human SR-BII functions in the same way as SR-BI and mSR-BII to promote HDL-dependent cellular cholesterol efflux.

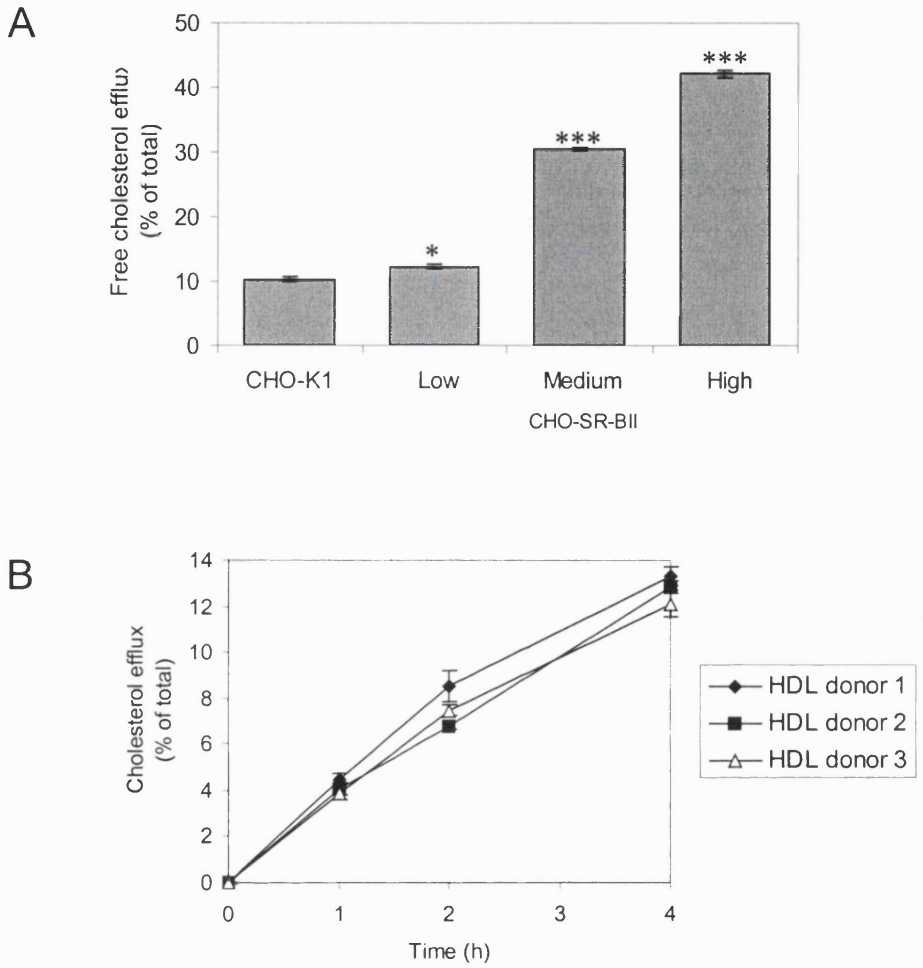

Figure 4.14 Human SR-BII promotes HDL-stimulated FC efflux from recombinant cells

In both experiments, the amount of free [^{3}H]-cholesterol efflux was expressed as a percentage of total [^{3}H]-cholesterol in the media and cells. Average percentage cholesterol efflux values from quadruplicate wells were calculated, background efflux values from cells exposed to serum-free media were then subtracted, and the corrected efflux values ± S.E.M. were plotted. The differences between the means were assessed by Student's t-test ($p<0.05$; ***$p<0.001$).* ***Panel A,*** *Control CHO-K1 cells and recombinant clones expressing low, medium and high levels of SR-BII were radiolabelled with [^{3}H]-cholesterol and subjected to stimulation with 200 μg/ml HDL_3 protein for 4 h.* ***Panel B,*** *Cells from the low CHO-SR-BII clone (21F) were radiolabelled with [^{3}H]-cholesterol and subjected to stimulation with 200 μg/ml HDL_3 protein from three donors over a 4 h time course.*

4.2.6 HUMAN SR-BII IS MORE EFFICIENT THAN SR-BI AT HDL-DEPENDENT CELLULAR FC EFFLUX

Comparisons of cell surface SR-BI/II protein expression in CHO-SR-BI and II clones by densitometry revealed that the two clones 'matched' by flow cytometry (clones 10B and 21F) had significantly different levels of receptor in the plasma membrane: cell surface SR-BI expression was 5.8 times greater than SR-BII expression *(Section 4.2.3.2).* Therefore, in order to compare the abilities of SR-BI and II in these recombinant clones to promote HDL-stimulated FC efflux, it would be necessary to correct the final percentage efflux values for receptor expression.

Firstly, cells from CHO-SR-BI clone 10B and CHO-SR-BII clone 21F were successfully labelled with similar levels of [^{3}H]-cholesterol (38-47 % uptake), before stimulation with HDL_3 from 3 donors over a 4 h time course *(Sections 2.4.6* and *4.2.4).* For each clone and type of HDL_3, the mean percentage FC efflux value was calculated from triplicate wells, and the background efflux was subtracted. Student's *t*-test was then employed to ascertain whether stimulation with HDL_3 particles from different donors had generated any significant differences between the mean percentage efflux values. Within each cell type, this statistical test always resulted in a *p*-value greater than 0.05, indicating that there were no significant differences between FC efflux values due to donor HDL_3 variability (data not shown). Once this was established, the percentage FC efflux values ± S.E.M. for each clone were combined. Subsequently, the values were corrected for the basal efflux by control CHO-K1 cells to generate specific SR-BI/II-mediated FC efflux values, which were plotted versus time (Figure 4.15, *panel A*). At each time point, the CHO-SR-BI clone was found to be significantly better at FC efflux than the CHO-SR-BII clone ($p<0.001$).

The percentage efflux values, however, had not been corrected for levels of cell surface SR-BI and II expression *(Section 4.2.3.2).* Indeed, when the percentage efflux values from the CHO-SR-BI clone were divided by 5.8, the situation had reversed: SR-BII was found to be significantly better at effluxing cellular FC than SR-BI (CHO-SR-BII: 1.83 ± 0.04 % efflux; CHO-SR-BI: 0.94 ± 0.02 % at 4 h; $p<0.001$; Figure 4.15, *panel B*). At each time point, the recombinant cells expressing SR-BII had effluxed almost two times more radiolabelled cholesterol than cells expressing SR-BI. When this

experiment was repeated on a separate occasion using HDL_3 from just one donor, the same statistical conclusions were made.

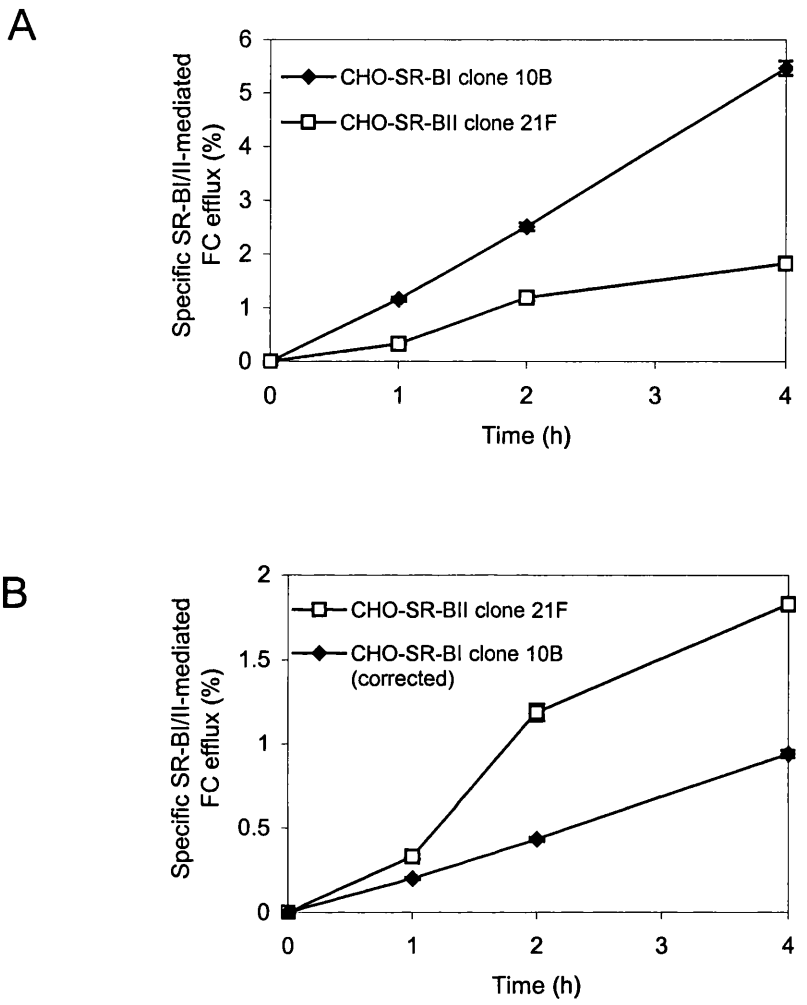

Figure 4.15 SR-BII promotes FC efflux to a greater extent than SR-BI

Cells from CHO-SR-BI clone 10B and CHO-SR-BII clone 21F were radiolabelled with [^{3}H]-cholesterol and subjected to stimulation with 200 μg/ml HDL_3 protein from three donors over a 4 h time course. The amount of free [^{3}H]-cholesterol efflux was expressed as a percentage of total [^{3}H]-cholesterol and the average background efflux was subtracted. Since there were no significant differences ($p>0.05$) between FC efflux values within each cell type due to donor HDL_3 variability, the data were combined. Basal efflux values, generated by control CHO-K1 cells, were subtracted from the mean FC efflux values to give specific SR-BI/II-mediated cholesterol efflux values ± S.E.M., which were plotted versus time ***(Panel A).*** *The values generated from the CHO-SR-BI clone were subsequently corrected for the larger amount of receptor expression (i.e. divided by 5.8)* ***(Panel B).***

4.2.7 HDL STIMULATES MORE FC EFFLUX FROM CHO-SR-BII CELLS THAN LIPID-FREE APOLIPOPROTEIN A-I

Since the extracellular binding regions of SR-BI and SR-BII are identical, we can assume that their ligand-binding interactions are also identical. Therefore, despite little characterisation of the human SR-BII protein, we have a great deal of information about this receptor, since its alternative isoform has been studied in much more detail. We know that SR-BI binds HDL via its major apolipoprotein, apoA-I [201]. Previously, I demonstrated that SR-BII mediates cellular FC efflux in response to HDL stimulation *(Section 4.2.5)*. In the following experiment, I wanted to determine whether lipid-free apoA-I was able to promote SR-BII-mediated FC efflux to the same extent as HDL.

CHO-K1 control cells and the mixed population of CHO-SR-BII cells were labelled overnight with [^{3}H]-cholesterol, before FC efflux was stimulated for 4 h with the addition of apoA-I or 'HDL plasma' to the media *(Section 2.4.6)*. The mean percentage efflux values ± S.E.M. from triplicate wells were calculated for each experimental condition. The experiment was performed on two separate occasions and the data were combined and analysed together (Figure 4.16). As expected, 'HDL plasma' stimulated CHO-SR-BII cells to efflux ~10 % of their radiolabelled FC, which was significantly higher than CHO-K1 control cells (CHO-K1 control: 6.86 ± 0.29 % efflux; CHO-SR-BII: 10.01 ± 0.36 % efflux; $p<0.001$). More importantly, CHO-SR-BII cells stimulated with 'HDL plasma' exhibited significantly higher levels of FC efflux than CHO-SR-BII cells stimulated with lipid-free apoA-I (HDL: 10.01 ± 0.36 % efflux; apoA-I: 1.85 ± 0.10 % efflux; $p<0.001$). This result reveals that apoA-I within HDL is able to promote significantly more FC efflux from CHO-SR-BII cells than lipid-free apoA-I.

However, lipid-free apoA-I stimulated significantly more FC efflux from the CHO-SR-BII and control cells than serum-free media ('background'; $p<0.001$), indicating that apoA-I does indeed promote FC efflux, albeit to a lesser extent than HDL. As there was no statistical difference in FC efflux between the two cell types in response to apoA-I stimulation, I can therefore conclude that apoA-I promotes cellular FC efflux using an alternative mechanism that does not involve binding SR-BII.

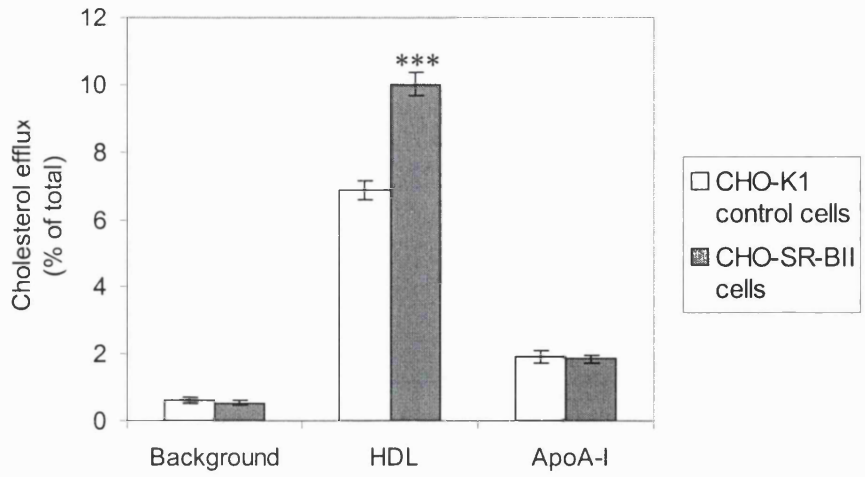

Figure 4.16 SR-BII mediates FC efflux upon stimulation with HDL but not lipid-free apoA-I

*CHO-K1 control and CHO-SR-BII cells were radiolabelled with [^{3}H]-cholesterol and subjected to stimulation with 5 % (v/v) 'HDL plasma', 10 μg/ml apoA-I protein, or serum-free media (background) for 4 h. The experiment was performed on two occasions in triplicate. The percentage FC efflux values for each experiment were combined and analysed together. The mean FC efflux values ± S.E.M. were calculated and the differences between the means were assessed by Student's t-test (***$p<0.001$).*

4.2.8 HUMAN SR-BII IS DETECTED IN BOTH MONOCYTIC (THP-1) AND HEPATOMA (HEPG2) HUMAN CELL LINES

Prior to investigating the role of SR-BII in CE mobilisation, it was necessary to confirm that the human receptor was indeed present in macrophages. THP-1 monocytes were differentiated into macrophages over 7 days with the addition of phorbol ester to the culture medium *(Section 2.4.2.1)*. Firstly, confluent cultures of THP-1 monocytes and macrophages, as well as HepG2 cells, were cell surface biotinylated. The biotin-labelled membrane proteins were subsequently isolated from cell lysates, containing equal quantities of protein, using streptavidin-coated magnetic beads *(Section 2.4.5.1)*. Proteins eluted from the beads were subjected to SDS-PAGE and immunoblotting with SR-BII antiserum *(Sections 2.3.2* and *2.3.3)*. This technique detected the protein in resting HepG2 cells, as well as at lower levels in THP-1 monocytes and macrophages (Figure 4.17). The molecular weight of SR-BII was found to be slightly higher in the recombinant CHO-SR-BII cells compared to the human cell lines, which may have

resulted from a small difference in the extent of receptor glycosylation. In addition, an extra band with a lower molecular weight was also detected in the HepG2 and THP-1 cell lines, but it remains uncertain what this band represents. However, one possibility is that this band might represent SR-BII that has undergone fewer post-translational modifications, such as glycosylation.

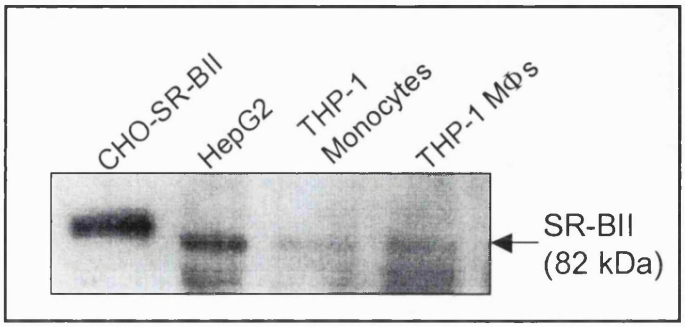

Figure 4.17 Confirmation of human SR-BII cell surface expression in THP-1 monocytes/macrophages and HepG2 cells

Confluent cultures of HepG2 hepatoma cells, THP-1 monocytes and macrophages (MΦ) were surface-labelled with biotin and lysed (Sections 2.4.5.1 and 2.4.4). Biotinylated membrane proteins were subsequently isolated from cell lysates, containing equal quantities of protein, using streptavidin superparamagnetic iron oxide particles. The adsorbed proteins were eluted from the beads and were separated by 8 % SDS-PAGE; receptor expression was detected by immunoblotting with SR-BII antiserum. The CHO-SR-BII lysate served as a positive control for the immunoblotting.

Finally, confirmation of the presence of SR-BII within the plasma membrane of THP-1 macrophage promoted the hypothesis that SR-BII might function to mobilise stored CE, thereby causing the regression of macrophage foam cells within atherosclerotic lesions.

4.2.9 MACROPHAGE SR-BI AND II EXPRESSION IN RESPONSE TO CHOLESTEROL LOADING

In human macrophages, both ABCA1 mRNA and protein expression are upregulated upon cholesterol loading with Ac-LDL [292]. This result is not surprising, as the ABCA1 transporter is known to indirectly promote cholesterol efflux from cells [91,92]. Having demonstrated the ability of human SR-BII to promote FC efflux *(Section 4.2.5)* and confirmed its presence in human THP-1 macrophages *(Section 4.2.8)*,

I then investigated whether cell surface SR-BII expression is also upregulated when macrophages are lipid-loaded. Indeed, if human SR-BII does function to promote the mobilisation of stored CE, one might expect to see upregulation of its expression in macrophages upon cholesterol loading. Membrane receptor expression was determined using two different methods: firstly, by flow cytometry and secondly, by Western blotting.

4.2.9.1 Flow cytometry

THP-1 monocytes were differentiated into macrophages and half of these cells were exposed to Ac-LDL for cholesterol loading in parallel wells *(Section 2.4.2)*. Flow cytometry was performed on both normal and lipid-laden macrophages after incubation with the α-RED-1 antibody and the FITC-conjugated secondary antibody *(Section 2.4.5.2)*. The primary antibody binds to the extracellular domain of SR-BII, and therefore also recognises SR-BI. Unfortunately, it was not possible to specifically measure the levels of SR-BII protein expression since the isoform-specific SR-BII antiserum was not found to be suitable for immunofluorescence detection. The experiment was performed in triplicate, and included the following two controls: pre-immune serum (used instead of primary antibody) and omission of the primary antibody (but still using secondary antibody). For each sample the log FITC fluorescence of 5,000 intact and gated cells was measured. Figure 4.18 is an example of a 2-parameter histogram showing log FITC fluorescence of normal and lipid-laden macrophages. The histogram shows a right shift in fluorescence profile indicating an increase in cell surface SR-BI and/or II expression in response to cholesterol loading.

The average median log FITC fluorescence values ± S.E.M. were ascertained for both normal and lipid-laden macrophages. The cholesterol-loaded macrophages were found to express significantly more SR-BI/II than normal resting macrophages (normal macrophages: 2.44 ± 0.14; cholesterol-loaded macrophages: 3.84 ± 0.03; $p<0.01$). The median log FITC fluorescence values for each of the experimental controls were less than 1.05, confirming that non-specific antibody binding was only contributing to the overall FITC fluorescence to a small extent. Finally, it was necessary to exclude the possibility that the increase in FITC fluorescence had resulted purely from an increase in macrophage size, and accompanying rise in cell surface constituents per cell, upon cholesterol loading. Thus, the fluorescence:cell size ratio for both types of macrophages was determined (Table 4.3).

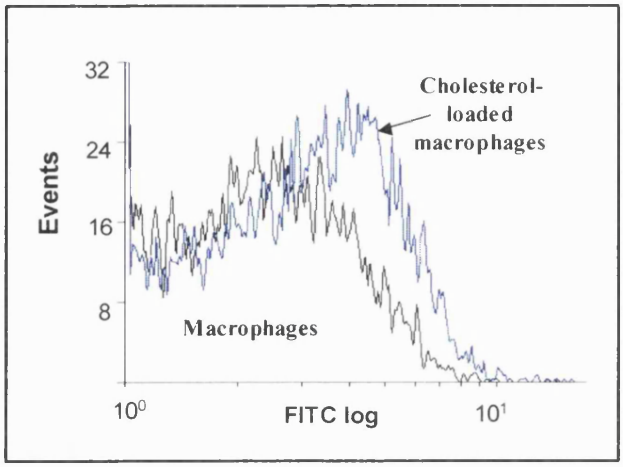

Figure 4.18 Cholesterol loading THP-1 macrophages increases cell surface SR-B (I and/or II) expression as assessed by flow cytometry

Cholesterol-loaded and resting THP-1 macrophages were incubated with α-RED-1 followed by a FITC-conjugated secondary antibody, as described in Section 2.4.5.2 and Figure 4.9. The log FITC fluorescence of 5,000 intact and gated cells was then measured by flow cytometry and displayed as a 2-parameter histogram. The fluorescence profile of normal macrophages is shaded grey, and the lipid-laden macrophage profile is outlined in blue.

Cell type (THP-1)	Average median log FITC fluorescence (arbitrary fluorescence units ± S.E.M.)	Average size (forward scattered incident light in arbitrary fluorescence units ± S.E.M.)	Fluorescence:cell size ratio
MΦ	2.44 ± 0.14	431.5 ± 11.5	5.66×10^{-3}
Lipid-laden MΦ	3.84 ± 0.03	458.0 ± 7.2	8.39×10^{-3}

Table 4.3 Cholesterol loading of THP-1 macrophages (MΦ) causes cell surface expression of SR-BI/II to increase independently of increasing cell size

The fluorescence:cell size ratio was larger for cholesterol-loaded macrophages than for normal macrophages, indicating that the increase in FITC fluorescence in cholesterol-loaded cells was not due to an overall increase in cell size, but to an increase in cell surface receptor expression. Therefore, there was indeed a significant increase in cell surface macrophage SR-BI/II expression upon cholesterol loading. However, it remained unclear which of the isoforms was contributing to this observation, as the antibody used for the immunofluorescence binds to SR-BI and II. Western blotting was

subsequently used in order to ascertain whether SR-BII expression was specifically upregulated in response to an increase in cellular cholesterol *(Section 4.2.9.2)*.

4.2.9.2 Immunoblotting

THP-1 monocytes were differentiated into macrophages and half of the cells were cholesterol-loaded with Ac-LDL in parallel wells *(Section 2.4.2)*. Normal and lipid-loaded macrophages, as well as THP-1 monocytes and HepG2 cells, were then cell surface biotinylated, before the cells were lysed and cell lysates adjusted for equal cellular protein content. Biotinylated membrane proteins were subsequently isolated from the cell lysates using streptavidin beads *(Section 2.4.5.1)*. Proteins eluted from the beads were separated by 8 % SDS-PAGE and immunoblotted with SR-BII antiserum (Figure 4.19). From this autoradiograph, it did not appear as though SR-BII expression in macrophages was upregulated in response to cholesterol loading. Unfortunately, it was not possible to perform densitometry using any of the autoradiographs generated from this experiment, as the bands were too faint compared to the high level of background. Therefore, although immunofluorescence detected a significant increase in cell surface SR-BI/II expression in macrophages upon cholesterol loading, it remains unclear whether SR-BII is contributing to this effect.

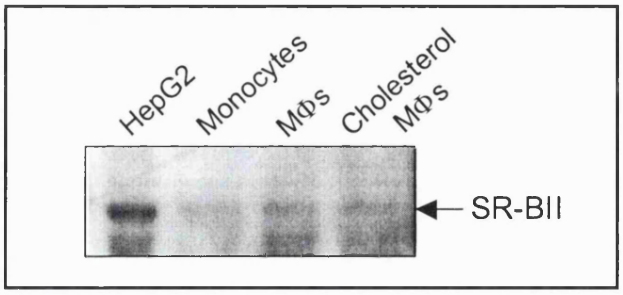

Figure 4.19 Cell surface SR-BII expression in normal and lipid-laden macrophages

Confluent cultures of HepG2 cells, THP-1 monocytes, and THP-1 macrophages (MΦ; both resting and cholesterol-loaded), were surface-labelled with biotin and lysed. Biotinylated plasma membrane proteins were subsequently isolated from cell lysates, containing equal quantities of cellular protein, using streptavidin superparamagnetic iron oxide particles. Eluted plasma membrane proteins were separated by 8 % SDS-PAGE and receptor expression was detected by immunoblotting with α-SR-BII.

4.2.10 SR-BII FAILS TO PROMOTE HDL-STIMULATED MOBILISATION OF STORED CHOLESTEROL

The final set of experiments investigated the role of SR-BII in the mobilisation of cholesterol from CEs. FC efflux experiments had previously established that the recombinant CHO-SR-BI/II cells were expressing functional receptors *(Section 4.2.5)*. I was therefore able to use these recombinant cells in order to monitor the reduction of stored CE in response to HDL stimulation. Each CE mobilisation experiment involved labelling cultured cells for 36 h with [^{3}H]-oleate, followed by an overnight equilibration step to allow intracellular radiolabelled CE stores to accumulate *(Section 2.4.7)*. The labelled cells were subsequently stimulated with HDL, before cellular lipids were extracted, and cellular protein was quantified. A [^{14}C]-cholesterol internal control was used to determine any losses during the lipid extraction and separation procedures. Having corrected for these losses, the number of [^{3}H]-CE dpm were measured.

The first experiment involved stimulation of the uncloned 'mixed population' of CHO-SR-BII cells *(Section 2.4.3.2)* with 'HDL plasma' or serum-free media over a 24 h time course, in order to determine the time point at which HDL-stimulated CE mobilisation was significantly higher than background mobilisation. The experiment was performed in 12-well plates and for each time point quadruplicate wells were measured. At time zero, the CHO-SR-BII cells had deposited around 6,000 dpm of [^{3}H]-oleate into CE stores, which confirmed that the radiolabelling had been successful. Measurements were subsequently made at 2, 4, 6, 10 and 24 h time points to monitor the reduction of labelled CE pools. The average dpm values ± S.E.M. were calculated and plotted versus time (Figure 4.20, *panel A*). After 4 h, there was a significant reduction of labelled [^{3}H]-CE stores in HDL-stimulated CHO-SR-BII cells compared to unstimulated cells (HDL plasma: 4237 ± 122 dpm; background: 5959 ± 274 dpm; $p<0.01$). After 6 h, the decrease in [^{3}H]-CE stores had become even more significant ($p<0.001$). One criticism of this initial experiment was that the CE dpm values were not corrected for the amount of cellular protein. The reduction in CE stores might have resulted from reduced numbers of adherent cells during the time course. Therefore, future CE mobilisation experiments measured CE dpm/μg cellular protein, and cells were stimulated with HDL for at least 4 h.

The second experiment compared the abilities of CHO-K1 control cells and the uncloned populations of recombinant CHO-SR-BI and CHO-SR-BII cells to mobilise CE over 4 h and 24 h of 'HDL plasma' stimulation. The uptake of [^{3}H]-oleate from the labelling medium by each cell type was found to be very similar (59-62 %). In addition, the average values of radiolabelled CE (dpm) per microgram of cellular protein ± S.E.M. generated by each cell type at the start of the experiment were calculated. The recombinant CHO-SR-BI/II cells were found to have generated significantly larger pools of radiolabelled CE than the control CHO-K1 cells (*CHO-K1*: 163.7 ± 4.6 CE dpm/μg protein; *CHO-SR-BI*: 198.3 ± 7.1 CE dpm/μg protein; *CHO-SR-BII*: 188.5 ± 7.4 CE dpm/μg protein; $p<0.05$). Therefore, in order to directly compare these cell types, it was necessary, at each time point, to express the amount of mobilised CE (dpm) per microgram of cellular protein as a percentage of the mean amount present at the start of the experiment. This experiment was performed in triplicate and for each cell type and treatment the average percentage of CE mobilised ± S.E.M. was calculated and plotted (Figure 4.20, *panel B*). When 'background' reductions in CE stores were analysed using Student's *t*-test, no significant differences were detected between CHO-K1 control cells and recombinant CHO-SR-BI/II cells ($p>0.05$). This allowed me to directly compare HDL-stimulated CE mobilisation in each cell type. Unfortunately, the mean percentages of mobilised CE at 4 and 24 h time points were found to be very similar for each cell type, with no statistically significant differences between the values ($p>0.05$). From this experiment, it appeared unlikely that either SR-BI or II functions to promote HDL-mediated CE mobilisation.

Until this point, all the CE mobilisation experiments had been performed using the 'mixed population' of CHO-SR-BII cells, which overall have lower levels of receptor expression compared to the high CHO-SR-BII clone. For the last CE mobilisation experiment, I therefore compared low- and high-expressing CHO-SR-BII clones *(Section 4.2.2.3)* in order to verify the above findings. This experiment was performed in triplicate using purified HDL_3 to stimulate the cells for 4, 8 and 24 h. For each clone and time point, the average percentage of CE mobilised ± S.E.M. was calculated and plotted (Figure 4.21). Over the time course, data generated from the low CHO-SR-BII clone were not found to be significantly different from data generated by the control CHO-K1 cells ($p>0.05$). Surprisingly, after 8 and 24 h, the high CHO-SR-BII clone was calculated to be significantly worse ($p<0.05$) than both the low CHO-SR-BII clone and CHO-K1 control cells at mobilising stored cholesterol. This finding was also observed

in a repeat experiment with 24 and 48 h time points (data not shown), which provides yet more evidence against a positive role for SR-BII in CE mobilisation. In summary, SR-BII does not accelerate CE mobilisation, indeed high levels appear inhibitory, which therefore contradicts my initial hypothesis.

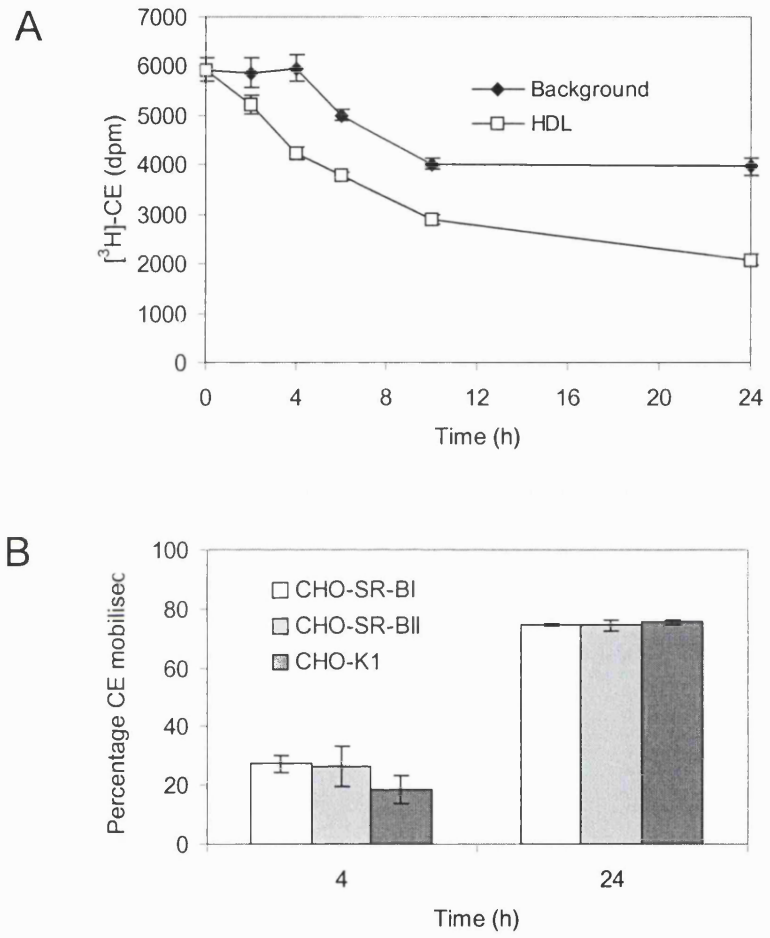

Figure 4.20 HDL-stimulated reduction of CE stores in recombinant cells

Panel A, *The mixed population of CHO-SR-BII cells were radiolabelled with [^{3}H]-oleate and stimulated with either 5 % (v/v) 'HDL plasma' or serum-free media ('background') over 24 h. Triplicate [^{3}H]-CE dpm values were measured at different time points and the mean [^{3}H]-CE dpm values ± S.E.M. were plotted versus time.* ***Panel B,*** *The same experiment as described for panel A was performed, except CHO-SR-BII cells were compared to CHO-K1 control and CHO-SR-BI cells over 4 and 24 h of 'HDL plasma' stimulation. For each time point, triplicate measurements of CE (dpm) were corrected for cellular protein (μg), and expressed as a percentage of the mean amount present at the start of the experiment. Subsequently, the average percentages of mobilised CE ± S.E.M. were calculated and plotted versus time.*

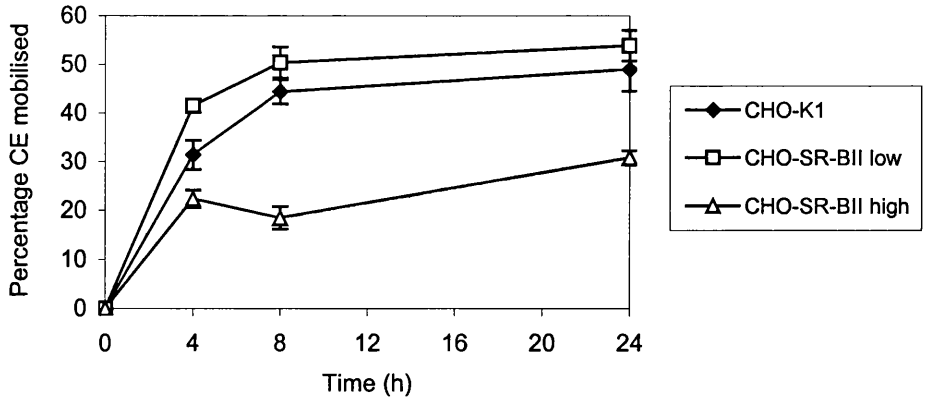

Figure 4.21 High levels of cellular SR-BII inhibit CE mobilisation

CHO-K1 control cells and recombinant CHO-SR-BII clones expressing high and low levels of SR-BII were radiolabelled with [^{3}H]-oleate and stimulated with 200 μg/ml HDL_3 over 24 h. For each time point, triplicate measurements of CE (dpm) were corrected for cellular protein (μg), and expressed as a percentage of the mean amount present at the start of the experiment. Subsequently, the average percentages of mobilised CE ± S.E.M. were calculated and plotted versus time.

4.3 Discussion

4.3.1 COMPARISON OF CELL SURFACE RECEPTOR EXPRESSION IN CHO-SR-BI AND II CLONES

The aim of this study was to produce recombinant cells over-expressing human SR-BI or II to investigate whether the role of SR-BII in cellular cholesterol homeostasis is distinct from that of SR-BI. Firstly, I generated mammalian expression vectors encoding full-length SR-BI or II sequences and used them to successfully transfect CHO-K1 cells. Western blotting techniques were subsequently employed to verify cellular expression of both isoforms of the receptor. The type II receptor was found to be expressed in the recombinant cells to a much greater extent than the type I receptor. This finding contrasts what is observed *in vivo*, where the levels of SR-BI far outweigh SR-BII [233]. However, it is consistent with data produced by Webb *et al.* [233], who repeatedly detected 4-6 times higher levels of mSR-BII expression than mSR-BI in recombinant CHO cells. The reason for such a difference in expression levels of each isoform remains unclear. Therefore, in order to directly compare the roles of SR-BI and

II in HDL-stimulated cholesterol mobilisation and efflux, it was necessary to produce recombinant clones expressing very similar amounts of plasma membrane receptor. Initially, immunoblotting was used to pick two clones with roughly equal levels of receptor expression for sub-cloning. However, a direct quantitative comparison of membrane receptor expression in each of the sub-clones was necessary to confirm that the sub-clones were indeed matched.

Flow cytometry was the preferred method for accurate comparison of membrane receptor expression levels. This is a rapid and sensitive technique for measuring individual characteristics of a large number of cells. Since there was no significant difference between the median FITC fluorescence values of the CHO-SR-BI and II sub-clones, this technique appeared to confirm that equally matched sub-clones had been chosen. However, although the α-RED-1 primary antibody was titrated for optimal SR-BI/II detection and the fluorescence detection of the cytometer was at maximum sensitivity, the FITC fluorescence values generated from both clones were all within the first decade of log FITC fluorescence. It appeared likely that this antibody was poor at binding its antigen for this immunofluorescent technique and therefore exhibited low sensitivity. This theory was endorsed by cytometric data generated from the high-expressing CHO-SR-BII clones, in which the FITC fluorescence values were again within the first decade of log FITC fluorescence. In addition, the high- and the low-expressing CHO-SR-BII clones only differed by ~4 arbitrary fluorescence units. I therefore used an alternative, but less accurate, method for detecting levels of SR-BI/II expressed at the cell surface to verify that these two sub-clones were indeed matched: immunoblotting cell surface proteins followed by densitometric analysis.

To overcome many factors that contribute to the inaccuracy of densitometry, I isolated cell surface proteins from CHO-SR-BI/II cells in triplicate, probed the eluted membrane proteins on the same blot with the same antibody, and exposed the blot to the X-ray film for varying amounts of time to determine film saturation. Unfortunately, this technique revealed that the sub-clones were far from 'matched', as SR-BI expression was found to be 5.8 times higher than SR-BII expression in the recombinant sub-clones. Since similar data was generated using this technique on separate occasions, it therefore appeared that this finding was a real result. This meant that either the lengthy sub-cloning procedure would have to be repeated (in order to isolate more equally matched CHO-SR-BI/II sub-clones), or I would have to correct for this large difference in SR-

BI/II levels in future cholesterol homeostasis comparative experiments. Time pressures forced me to choose the latter option.

4.3.2 HUMAN SR-BII PROMOTES HDL-DEPENDENT CELLULAR FC EFFLUX

It was likely that human SR-BII would function in the same way as SR-BI and mSR-BII to mediate HDL-stimulated FC efflux from cells [116,233]. Indeed, recombinant cells expressing SR-BII were found to be significantly better than CHO-K1 control cells at effluxing radiolabelled FC in response to HDL stimulation. The type II receptor was subsequently linked to this particular function using CHO-SR-BII clones with low, medium and high levels of receptor expression: as SR-BII expression increased, so did the ability of the cells to efflux FC upon HDL stimulation. The previous discovery in *Chapter 3* that human SR-BII is localised to caveolar microdomains in recombinant cell plasma membranes is therefore consistent with its role in cholesterol efflux.

As expected, human SR-BII was found to promote FC efflux in response to stimulation with HDL, but not lipid-free apoA-I. Experimental data revealed that FC efflux by CHO-SR-BII cells in response to stimulation with apoA-I was significantly lower than HDL. However, apoA-I-induced FC efflux was found to be significantly higher than background efflux levels in both CHO-SR-BII and CHO-K1 control cells, indicating that apoA-I is able to stimulate cellular FC efflux from these cells, but to a lesser extent than HDL. Furthermore, since there was no statistical difference in FC efflux between CHO-SR-BII and CHO-K1 control cells in response to apoA-I stimulation, I was able to conclude that apoA-I promotes cellular FC efflux using an alternative mechanism that does not involve binding SR-BII. It is likely that apoA-I promoted FC efflux from CHO-K1 control and recombinant cells using the following mechanism: firstly, lipid-poor apoA-I particles bind to cellular phospholipids, that have been actively flipped across the plasma membrane by the ABCA1 transporter, to form discoidal phospholipid-apoA-I complexes [91]; secondly, these complexes rapidly sequester excess plasma membrane cholesterol that traverses the membrane by diffusion.

Finally, I compared the abilities of CHO-SR-BI and CHO-SR-BII sub-clones to promote HDL-stimulated FC efflux over a 4 h time course. Initial experimental data revealed that at each time point, CHO-SR-BI cells were significantly better than CHO-

SR-BII cells at FC efflux in response to HDL. However, when the specific SR-BI-mediated efflux values were corrected for the difference in membrane receptor expression (as measured by Western blotting and densitometry), the CHO-SR-BI cells were estimated to efflux about 50 % less cholesterol than CHO-SR-BII cells. Human SR-BII therefore appears to contribute more significantly to cholesterol efflux than mSR-BII, which was found to be four times less effective than mSR-BI [233].

4.3.3 HUMAN SR-BII FAILS TO PROMOTE HDL-STIMULATED CE MOBILISATION

Despite finding SR-BII mRNA in both THP-1 and HepG2 human cell lines [232], the receptor has only been detected in hormone-induced HepG2 cells [234]. I therefore wanted to use the human type II-specific antiserum to confirm the presence of SR-BII in macrophages before investigating whether SR-BII has a role in CE mobilisation. SR-BII was clearly detected in cell surface proteins isolated from HepG2 cells, and the receptor was also expressed in the plasma membrane of THP-1 monocytes and macrophages, albeit at lower levels. This finding supported the hypothesis that SR-BII might function in macrophages to promote the reduction of CE stores in response to HDL binding; in which case, one might expect an increase in expression levels as a result of THP-1 macrophage cholesterol loading. Indeed, expression of ABCA1 mRNA and protein is upregulated in human macrophages upon cholesterol loading [292]. Flow cytometry was therefore employed to assess whether plasma membrane levels of SR-BII increase upon lipid loading. Unfortunately, the human SR-BII antiserum was not found suitable for use in this technique, and an antibody that binds the extracellular region of both isoforms was used instead. Flow cytometric data revealed a significant increase in SR-BI and/or II expression in cholesterol-loaded THP-1 macrophages compared to resting macrophages. Subsequent Western blotting data suggested that SR-BII was not contributing to this finding, although densitometric analysis was not sensitive enough to confirm this conclusion. Ideally, an α-SR-BI isoform-specific antibody would have been used to detect specific SR-BI upregulation by Western blotting, however this antibody was not available.

The final set of experiments used the recombinant CHO-SR-BII cell culture model to test the second part of the hypothesis, and thereby establish whether SR-BII functions to promote the mobilisation of stored intracellular cholesterol in response to HDL stimulation. I was confident that the CHO-SR-BII recombinant cells were

expressing functional type II receptors, since I had previously characterised their ability to promote HDL-stimulated FC efflux. Subsequently, I used these recombinant cells to study the mobilisation of radiolabelled cholesteryl oleate in response to HDL stimulation. Unfortunately, I failed to demonstrate a role for SR-BII in the mobilisation of stored cholesterol using this cell culture model. In fact, over 8 and 24 h, the CHO-SR-BII clone expressing the largest amount of SR-BII was found to be significantly worse than control CHO cells at mobilising radiolabelled CE. Although further studies are required to verify this finding, it appears as though high levels of SR-BII might prevent CE mobilisation, which therefore contradicts my initial hypothesis.

In summary, the results presented in this chapter reveal for the first time the presence of human SR-BII in THP-1 monocytes and macrophages, and its ability to promote HDL-dependent FC efflux from recombinant CHO-K1 cells. Using this cell culture model I have also demonstrated that SR-BII does not function to promote the mobilisation of cholesterol from CE stores, in response to HDL stimulation. This finding enables me to conclude that the ability of SR-BII to promote HDL-dependent FC efflux is not simply due to increased mobilisation of stored cholesterol. Therefore, although I failed to demonstrate the potential of this receptor to mobilise CE within macrophage foam cells, my findings suggest an important role of human SR-BII in HDL-dependent FC efflux and cellular cholesterol homeostasis.

Chapter 5

5. GENERAL DISCUSSION

5.1 Hypothesis

A key feature of atherosclerotic lesions is the presence of CE-engorged macrophages within the arterial intima [5]. One important aspect of this pathological imbalance in cellular cholesterol homeostasis is the uncontrolled uptake of modified LDL by macrophages [7]. Over the 2-3 last decades, much scientific interest has focussed on gaining a deeper understanding of foam cell development, with the goal of slowing atherogenesis and controlling risk factors. In contrast, fewer studies have investigated the other equally important aspect of cholesterol imbalance: ineffective clearance of excess stored cholesterol by HDL-mediated reverse cholesterol transport. Therapeutic upregulation of this mechanism would not only slow disease progression but would also promote the regression of pre-existing atherosclerotic lesions. Atheroprotective HDL, in addition to its role in collecting excess plasma membrane cholesterol from peripheral cells, binds to an unidentified cell surface receptor and activates signalling molecules, as well as CE mobilisation and FC translocation to the plasma membrane [40,44-47]. Having identified potential signalling motifs in the newly described HDL-binding protein, SR-BII, I tested the novel hypothesis that: ***'upon HDL stimulation of SR-BII, its C-terminal cytoplasmic tail interacts with a signalling molecule to activate the CE mobilisation pathway.'***

5.2 Role of human SR-BII in signal transduction

As outlined in *Chapter 1 (Section 1.6.5.3)*, lipoprotein receptors are not only involved in lipid exchange at the cell surface and lipoprotein internalisation, but also mediate transmembrane signal transduction, via cytoplasmic tail interactions with signalling molecules. Interestingly, SR-BI has also been found to interact with a signalling domain via its C-terminal cytoplasmic tail. In 2000, Ikemoto *et al.* [219] reported an interaction between the C-terminus of SR-BI and a PDZ domain-containing protein, PDZK1. Although PDZ domains are known to be involved in protein complex formation at the plasma membrane and signalling pathways, it is likely that the interaction of PDZK1 with the C-terminus of SR-BI promotes the stability of this receptor in the plasma membrane, rather than signal transduction [219]. However, last year Yuhanna *et al.* [192] published data confirming that this multifunctional HDL receptor does indeed have a role in signal transduction; upon binding of HDL to SR-BI,

the caveolar protein eNOS was activated. More recently, this signalling pathway was found to involve an increase in intracellular levels of ceramide [246]. One theory is that HDL binding to SR-BI activates a caveolar sphingomyelinase to generate ceramide; alternatively, HDL ceramide may be internalised by SR-BI along with HDL CE [246]. The discovery that SR-BI activates signalling molecules in response to ligand binding further promotes the role of its alternative isoform, SR-BII, as a signal transducer.

Following the identification of a number of potential SH3 domain recognition sites in the C-terminal cytoplasmic tail of SR-BII, I generated cytoplasmic SR-BII fusion proteins and screened several SH3 domains from a variety of modular signalling proteins for binding interactions. The initial binding screen, involving 'pull-down' assays, revealed an interaction between cytoplasmic SR-BII and the plc-γ1 SH3 domain within this artificial environment. I subsequently used the yeast two-hybrid system to determine whether or not my initial binding screen result was significant; this system is widely used for screening protein-protein interactions within a cellular environment [293]. Unfortunately, I failed to confirm or dispute my earlier finding using this technique, as the recombinant fusion proteins were not expressed in the yeast at high enough levels for detection. An alternative cellular system for studying binding interactions would have been to transfect the plc-γ1 SH3 domain sequence into recombinant cells already expressing SR-BII. Since further binding experiments using more physiological conditions failed to detect an interaction between the plc-γ1 SH3 domain and cytoplasmic SR-BII, it appears unlikely that this signalling molecule is the physiological ligand for cytoplasmic SR-BII. Despite widening the search for cellular cytoplasmic SR-BII binding proteins using cell lysate 'pull-down' assays (with α-phospho-tyrosine, -serine, and -threonine antibodies, or silver staining, for detection), I failed to elucidate the identity of a physiological ligand. Further studies, possibly using the yeast two-hybrid system to screen a cDNA library, will hopefully shed light on C-terminal cytoplasmic SR-BII binding interactions.

It appears likely that certain residues on the C-terminus of cytoplasmic SR-BII might become phosphorylated upon receptor activation. For example, I identified a potential SH2 domain recognition site within cytoplasmic SR-BII, and then investigated whether the tyrosine residue becomes phosphorylated upon HDL stimulation. However, due to the lack of an experimental positive control, I failed to conclusively demonstrate the state of tyrosine phosphorylation following HDL stimulation. Interestingly, as well

as being recognised by SH3 domains, polyproline-rich sequences also bind proteins containing WW domains [294]. WW domains are composed of 38 amino acids, with two conserved tryptophan (W) residues [295]. The WW domain is found in a diverse group of proteins, and like the SH2 and SH3 domains, it functions as a modular protein interaction site in each of its host proteins. WW domains were originally divided into three groups, based on their binding specificity, but recently, a fourth group of WW domains has been characterised, which bind proline-rich sequences containing phosphorylated serine and threonine residues [296]. The polyproline-rich C-terminal tail of SR-BII contains eight of these residues, which have the potential to become phosphorylated upon receptor activation, and bind to group IV WW domains. The identification of additional potential signalling motifs within the C-terminal tail of SR-BII further promotes the involvement of this HDL receptor in signal transduction. Future experiments, using α-phosphoserine/threonine antibodies with better immunoreactivities and perhaps alternative cell types, such as macrophages, will provide further insight into the state of cytoplasmic SR-BII phosphorylation following HDL stimulation.

In this thesis, I have investigated the role of SR-BII in signal transduction in response to HDL stimulation. However SR-BII, like SR-BI, is described as a multi-ligand receptor as its extracellular domain binds a variety of ligands, including LDL, modified lipoproteins and discoidal apolipoprotein-containing phospholipid particles [155,200,202]. It is therefore possible that SR-BII might be activated to function as a signal transducer in response to binding an alternative ligand to HDL. Future studies involving SR-BII stimulation with a variety of ligands will hopefully elucidate both the identity of the true second messenger(s) for this receptor, as well as its extracellular ligand.

5.3 Role of human SR-BII in cellular cholesterol homeostasis

5.3.1 RECOMBINANT CELL CULTURE MODEL

To study the role of human SR-BII in cellular cholesterol homeostasis, CHO cells were transfected with expression vectors encoding SR-BI or II sequences, and stable clones over-expressing these receptors were selected. This particular cell culture model was chosen for the following reasons: firstly, recombinant CHO cells over-expressing *murine* SR-BI/II sequences have been used previously to investigate the role of each

isoform in HDL cholesterol uptake and HDL-dependent cellular cholesterol efflux [233]; secondly, this hamster cell line is widely used to generate recombinant cells expressing human receptors to determine signalling pathways [297-300]; and thirdly, CHO cells are adherent cells that are easily maintained and transfected.

In order to directly compare the abilities of SR-BI and II to promote cholesterol mobilisation and efflux in response to HDL stimulation, I aimed to select recombinant clones with equal levels of receptor expression. I chose to compare the level of SR-BI and II expression on the cell surface of intact cells rather than total receptor expression in whole cell lysates, as this is a better indicator of the number of type I and II receptors that have the potential to bind HDL and influence cholesterol efflux. The preferred method for measuring cell surface SR-BI and II expression was flow cytometry, but unfortunately the sensitivity of detection using the antibody common to both isoforms (α-RED-1) was very low. Indeed, flow cytometry data revealed that two of the clones were expressing equal amounts of SR-BI or II, yet when cell surface proteins from each of the 'matched' clones were analysed by immunoblotting, I consistently detected larger amounts of SR-BI than SR-BII.

An alternative method for comparing SR-BI and SR-BII expression on each of the recombinant clones would have been to use a ligand-binding assay (conducted at 4°C) [232,233]. For example, by measuring the specific binding of ^{125}I-labelled HDL or fluorescently labelled HDL to recombinant cells (using scintillation counting and flow cytometry, respectively), the relative number of HDL binding sites on each of the clones could be determined. However, this method is far less accurate compared to immunofluorescence, as every cell surface HDL binding site is included in the measurements, not just the type I and II receptors. Despite the fact that I used the same batch of CHO-K1 cells to generate the CHO-SR-BI and CHO-SR-BII recombinant cells, the isolated sub-clones may not have expressed the same number of native HDL receptors, which would have decreased the accuracy of the measurements. Since I required accurate comparisons of SR-BI and II expression levels, I chose not to perform ligand-binding assays. Instead, I chose to employ densitometric analysis of Western blots. This involved isolating cell surface proteins from each clone in triplicate using biotinylation and streptavidin purification, followed by immunoblotting with an antibody common to both isoforms. Densitometric data revealed 5.8 times higher levels of cell surface SR-BI than SR-BII in the recombinant clones. Due to the significant difference

in cell surface SR-BI and II levels, data from cholesterol efflux experiments were therefore corrected for receptor expression, before comparisons were made.

5.3.2 HUMAN SR-BII IS PRESENT IN MACROPHAGES BUT FAILS TO MOBILISE STORED CHOLESTEROL

In addition to investigating whether SR-BII functions to promote CE mobilisation, it was also necessary to confirm the presence of the human receptor in relevant cells, such as macrophages. Despite reports of SR-BII mRNA transcripts in the HepG2 and THP-1 human cell lines [232], SR-BII protein has yet to be identified in untreated cells. Indeed, Matveev *et al.* [191] failed to detect SR-BII protein in THP-1 monocytes or macrophages. Therefore, following the production of an anti-peptide SR-BII antiserum, I used this isoform-specific antibody to reveal for the first time that SR-BII is expressed in the cell surface of resting HepG2 cells, as well as THP-1 monocytes and macrophages. If indeed its function in macrophages is to promote CE mobilisation, one might expect an increased level of receptor expression upon cholesterol loading. I subsequently used flow cytometry to determine whether membrane SR-BII protein, like ABCA1 protein [292], is significantly increased in response to macrophage cholesterol loading. Unfortunately, the SR-BII isoform-specific antibody had previously not been found suitable for immunofluorescence, as its use with CHO-K1 control cells generated high levels of background FITC fluorescence (indicating that the antibody was binding in a non-specific manner). Instead, I used an antibody that binds both SR-BI and II, which revealed that membrane levels of SR-BI and/or II are significantly increased upon cholesterol loading. However, this method was unable to determine the extent to which SR-BII was contributing to this increase. Western blotting also failed to elucidate the contribution of the type II receptor since the bands were too faint compared to the high level of background, and it was not possible to perform densitometry on the autoradiographs.

Having verified that SR-BII was present in the cell surface of macrophages, I used recombinant CHO-SR-BII clones (expressing low and high levels of the receptor) to investigate whether SR-BII functions to mobilise stored CE. Recombinant cells were labelled with [^{3}H]-oleic acid and their abilities to mobilise cellular cholesteryl oleate were monitored during HDL incubation. Unfortunately, using this cell culture model, I failed to demonstrate a role for human SR-BII in CE mobilisation: following HDL stimulation of control CHO-K1 cells and recombinant cells expressing low levels of SR-

BII over 24 h, there was no significant reduction in the levels of radiolabelled cholesteryl oleate. Unexpectedly, when cells expressing high levels of SR-BII were subjected to HDL stimulation for more than 8 h, this clone was found to be significantly worse at mobilising stored cholesterol compared to the low CHO-SR-BII clone and control cells. In contrast to my original hypothesis, the data generated from this cell culture model suggest that SR-BII inhibits the mobilisation of cholesterol from stored CE. However, as this effect was only observed with the high-expressing CHO-SR-BII clone, one could speculate that the high levels of SR-BII present in the surface of these cells promoted HDL cholesterol uptake during the experiment [232]. The resulting increase in cellular FC might then serve to switch off CE mobilisation and instead, switch on cholesterol storage. Finally, it would be interesting to elucidate whether SR-BII functions in this manner when over-expressed in cholesterol-loaded human macrophages. Indeed, this would have served as a better cell culture model for testing my hypothesis, but owing to the difficulties of transfecting monocyte/macrophages, I was unable to perform this experiment.

5.3.3 CAVEOLAR LOCALISATION OF HUMAN SR-BII

Prior to investigating the role of human SR-BII in cellular cholesterol efflux, I used the recombinant CHO-SR-BII cells to study membrane localisation of this receptor. It appeared likely that human SR-BII would localise to caveolae, as both murine SR-BI and II are found in these plasma membrane microdomains [176,233]. In this thesis, I present the first data confirming true caveolar localisation of human SR-BII. Since caveolae act as sites of cellular cholesterol flux [50], this finding promoted the involvement of human SR-BII in cholesterol efflux. Another important function of caveolae is to concentrate signalling proteins and facilitate signal transduction [54]. Indeed, within caveolae, SR-BI activates eNOS in response to HDL binding [192]. The fact that HDL activation of eNOS still occurred in isolated caveolae reveals the important role that these microdomains play in signal transduction [192]. My confirmation that human SR-BII also localises to these microdomains further promotes the potential involvement of this lipoprotein receptor in signal transduction.

5.3.4 HUMAN SR-BII PROMOTES MORE CHOLESTEROL EFFLUX THAN SR-BI

Previous studies by Webb *et al.* [233], using recombinant CHO cells over-expressing murine SR-BII, have shown this receptor to mediate both selective cellular

uptake of HDL cholesterol and HDL-dependent cholesterol efflux, although with approximately 4 times lower efficiency than SR-BI. In this thesis, I used recombinant CHO cells over-expressing human SR-BII to demonstrate for the first time that the human form of this receptor also mediates cholesterol efflux in response to HDL stimulation. As levels of SR-BII protein within the clones increased, the efficiency of the cells to mediate HDL-dependent cholesterol efflux also increased, thereby strongly linking SR-BII to this particular function.

Subsequently, I compared the abilities of human SR-BI and II to promote HDL-dependent cholesterol efflux. I was unable to accurately determine the relative efficiencies of the two isoforms, as the recombinant clones expressed different amounts of plasma membrane SR-BI/II. However, having corrected the efflux values for the different levels of cell surface receptor in each of the recombinant clones, my results demonstrate human SR-BII to have approximately two times greater efficiency than human SR-BI at HDL-mediated cholesterol efflux. From the data presented in this thesis, it therefore appears as though the type II receptor in humans has a more significant role to play in HDL-mediated cholesterol efflux than the type I receptor. Indeed, HDL lipid uptake is thought to be the most important physiological function of SR-BI, rather than HDL-mediated cholesterol efflux [301]. To date, an accurate determination of the relative efficiencies of *human* SR-BI and II to mediate HDL lipid uptake has not been reported. It would be interesting to use recombinant cells over-expressing equal levels of human SR-BI and II to directly compare the abilities of each isoform to mediate HDL-dependent cholesterol efflux, as well as HDL lipid uptake.

My findings lead me to speculate that these two HDL receptors have distinct roles in cholesterol homeostasis; perhaps SR-BII functions more effectively as a cholesterol efflux receptor, whereas the major function of SR-BI is as a cholesterol uptake receptor. Recent findings by Graf *et al.* [234] are consistent with this proposal. This group show that SR-BI protein in HepG2 cells is down regulated in response to physiological levels of 17β-estradiol, whereas SR-BII protein is upregulated from undetectable amounts in resting cells to levels three times that of SR-BI at the start of the experiment. Perhaps by an exchange of membrane SR-BI for SR-BII, HDL cholesterol uptake by the liver is replaced by HDL-mediated cholesterol efflux, thereby promoting delivery of cholesterol to steroidogenic tissues for hormone production. Certainly it would be interesting to perform cholesterol efflux studies on 17β-estradiol-treated and

resting HepG2 cells to determine whether upregulation of SR-BII protein is linked to increased HDL-dependent cholesterol efflux. Finally, it is feasible that an increase in SR-BII protein and cellular cholesterol efflux represents another mechanism by which estrogen reduces the development of atherosclerosis [302].

The cholesterol efflux data presented in this thesis differ from the results reported for murine SR-BII by Webb *et al.* [233], who found that the type II receptor was approximately 4 times less efficient at HDL-mediated cholesterol efflux that murine SR-BI. One explanation for this difference is the presence of additional potential signalling motifs in the C-terminal cytoplasmic tail of human SR-BII that are not found in murine SR-BII. As stated in my hypothesis, these putative signalling motifs in human SR-BII might be involved in intracellular signalling to promote cholesterol efflux. Since I failed to demonstrate a role for SR-BII in the mobilisation of stored CE, the target of SR-BII signalling does not appear to be CEH. However, other potential targets of human SR-BII signalling that would enhance cholesterol efflux include inhibition of ACAT and increased synthesis of cholesterol. In addition, SR-BII might increase trafficking of cholesterol to the plasma membrane, perhaps by promoting the movement of ABCA1 from endocytic vesicles to the cell surface [303]. As yet, these speculative mechanisms have not been tested.

5.3.5 SR-BII AND THE BRAIN

In 2001, an abstract was presented by Ueda *et al.* at the '14th International Symposium on Drugs Affecting Lipid Metabolism', reporting that more than 95 % of SR-BI/II transcripts in the brain of human SR-BI transgenic mice were SR-BII transcripts. This result is surprising, as SR-BII represents only 21 % of total SR-BI/II mRNA in HepG2 cells, and 12 % of the total immunodetectable SR-BI/II in mouse livers [232,233]. The high prevalence of SR-BII transcripts in the transgenic mouse brain points towards an important role for SR-BII in this organ. One might speculate that human SR-BII promotes rapid cholesterol efflux from specialised cells in the brain. Interestingly, cholesterol secreted by glial cells was recently discovered to promote synapse development in adjacent nerve cells [304]. Future cell culture studies involving neuronal and glial cells should help to decipher the role of human SR-BII in the brain, and provide an explanation for such a prevalence of type II receptor transcripts.

BIBLIOGRAPHY

1. Ross, R. (1993). The pathogenesis of atherosclerosis: a perspective for the 1990s. *Nature* **362**: 801-809.

2. Charo, I. F. (2002). Monocyte-endothelial cell interactions. *Curr.Opin.Lipidol.* **3**: 335-343.

3. Stary, H. C. (1987). Macrophages, macrophage foam cells, and eccentric intimal thickening in the coronary arteries of young children. *Atherosclerosis* **64**: 91-108.

4. Saxena, U. and Goldberg, I. J. (1994). Endothelial cells and atherosclerosis: lipoprotein metabolism, matrix interactions, and monocyte recruitment. *Curr.Opin.Lipidol.* **5**: 316-322.

5. Aqel, N. M., Ball, R. Y., Waldmann, H. and Mitchinson, M. J. (1984). Monocytic origin of foam cells in human atherosclerotic plaques. *Atherosclerosis* **53**: 265-271.

6. Peiser, L. and Gordon, S. (2001). The function of scavenger receptors expressed by macrophages and their role in the regulation of inflammation. *Microbes.Infect.* **3**: 149-159.

7. Goldstein, J. L., Ho, Y. K., Basu, S. K. and Brown, M. S. (1979). Binding site on macrophages that mediates uptake and degradation of acetylated low density lipoprotein, producing massive cholesterol deposition. *Proc.Natl.Acad.Sci.U.S.A.* **76**: 333-337.

8. von Eckardstein, A., Nofer, J. R. and Assmann, G. (2001). High density lipoproteins and arteriosclerosis. Role of cholesterol efflux and reverse cholesterol transport. *Arterioscler.Thromb.Vasc.Biol.* **21**: 13-27.

9. Beisiegel, U., Weber, W. and Bengtsson-Olivecrona, G. (1991). Lipoprotein lipase enhances the binding of chylomicrons to low density lipoprotein receptor-related protein. *Proc.Natl.Acad.Sci.U.S.A.* **88**: 8342-8346.

10. St Clair, R. W. and Beisiegel, U. (1997). What do all the apolipoprotein E receptors do? *Curr.Opin.Lipidol.* **8**: 243-245.

11. von Eckardstein, A. (1996). Cholesterol efflux from macrophages and other cells. *Curr.Opin.Lipidol.* **7**: 308-319.

12. Rumsey, S. C., Obunike, J. C., Arad, Y., Deckelbaum, R. J. and Goldberg, I. J. (1992). Lipoprotein lipase-mediated uptake and degradation of low density lipoproteins by fibroblasts and macrophages. *J.Clin.Invest.* **90**: 1504-1512.

13. Ball, R. Y., Stowers, E. C., Burton, J. H., Cary, N. R., Skepper, J. N. and Mitchinson, M. J. (1995). Evidence that the death of macrophage foam cells contributes to the lipid core of atheroma. *Atherosclerosis* **114**: 45-54.

14. Holvoet, P. and Collen, D. (1997). Thrombosis and atherosclerosis. *Curr.Opin.Lipidol.* **8** : 320-328.

15. Campbell, J. H. and Campbell, G. R. (1994). The role of smooth muscle cells in atherosclerosis. *Curr.Opin.Lipidol.* **5**: 323-330.

16. Gianturco, S. H. and Bradley, W. A. (1994). Atherosclerosis: cell biology and lipoproteins. *Curr.Opin.Lipidol.* **5**: 313-315.

17. Durrington, P. (2001). Known risk factors for coronary heart disease. *Preventive Cardiology.* Martin Dunitz Ltd. London, pp 4-29.

18. Shepherd, J. (1994). Lipoprotein metabolism. An overview. *Drugs* **47 (Suppl 2)**: 1-10.

19. Brown, M. S. and Goldstein, J. L. (1986). A receptor-mediated pathway for cholesterol homeostasis. *Science* **232**: 34-47.

20. Miller, G. J. and Miller, N. E. (1975). Plasma-high-density-lipoprotein concentration and development of ischaemic heart-disease. *Lancet* **1**: 16-19.

21. Krieger, M. (2001). Scavenger receptor class B type I is a multiligand HDL receptor that influences diverse physiologic systems. *J.Clin.Invest* **108**: 793-797.

22. Attie, A. D., Kastelein, J. P. and Hayden, M. R. (2001). Pivotal role of ABCA1 in reverse cholesterol transport influencing HDL levels and susceptibility to atherosclerosis. *J.Lipid Res.* **42**: 1717-1726.

23. Mulcahy, J. V. and Owen, J. S. (2002). HDL-C transport and atheroprotection. *Science and Medicine* **8**: 76-85.

24. Matthews, C. K. and van Holde, K. E. (1990). *Biochemistry.* The Benjamin/Cummings Publishing Company, CA, USA, pp 604-642

25. Brown, M. S., Dana, S. E. and Goldstein, J. L. (1973). Regulation of 3-hydroxy-3-methylglutaryl coenzyme A reductase activity in human fibroblasts by lipoproteins. *Proc.Natl.Acad.Sci.U.S.A.* **70**: 2162-2166.

26. Brown, M. S., Dana, S. E. and Goldstein, J. L. (1974). Regulation of 3-hydroxy-3-methylglutaryl coenzyme A reductase activity in cultured human fibroblasts. Comparison of cells from a normal subject and from a patient with homozygous familial hypercholesterolemia. *J.Biol.Chem.* **249**: 789-796.

27. Goldstein, J. L. and Brown, M. S. (1974). Binding and degradation of low density lipoproteins by cultured human fibroblasts. Comparison of cells from a normal subject and from a patient with homozygous familial hypercholesterolemia. *J.Biol.Chem.* **249**: 5153-5162.

28. Anderson, R. G., Brown, M. S. and Goldstein, J. L. (1977). Role of the coated endocytic vesicle in the uptake of receptor-bound low density lipoprotein in human fibroblasts. *Cell* **10**: 351-364.

29. Luskey, K. L., Faust, J. R., Chin, D. J., Brown, M. S. and Goldstein, J. L. (1983). Amplification of the gene for 3-hydroxy-3-methylglutaryl coenzyme A reductase, but not for the 53-kDa protein, in UT-1 cells. *J.Biol.Chem.* **258**: 8462-8469.

30. Gil, G., Faust, J. R., Chin, D. J., Goldstein, J. L. and Brown, M. S. (1985). Membrane-bound domain of HMG CoA reductase is required for sterol-enhanced degradation of the enzyme. *Cell* **41**: 249-258.

31. Brown, M. S. and Goldstein, J. L. (1975). Regulation of the activity of the low density lipoprotein receptor in human fibroblasts. *Cell* **6**: 307-316.

32. Goldstein, J. L., Dana, S. E. and Brown, M. S. (1974). Esterification of low density lipoprotein cholesterol in human fibroblasts and its absence in homozygous familial hypercholesterolemia. *Proc.Natl.Acad.Sci.U.S.A.* **71**: 4288-4292.

33. Chang, T. Y., Chang, C. C. and Cheng, D. (1997). Acyl-coenzyme A:cholesterol acyltransferase. *Annu.Rev.Biochem.* **66**: 613-638.

34. Warner, G. J., Stoudt, G., Bamberger, M., Johnson, W. J. and Rothblat, G. H. (1995). Cell toxicity induced by inhibition of acyl coenzyme A:cholesterol acyltransferase and accumulation of unesterified cholesterol. *J.Biol.Chem.* **270**: 5772-5778.

35. Rudel, L. L. and Shelness, G. S. (2000). Cholesterol esters and atherosclerosis - a game of ACAT and mouse. *Nat.Med.* **6**: 1313-1314.

36. Bernard, D. W., Rodriguez, A., Rothblat, G. H. and Glick, J. M. (1991). cAMP stimulates cholesteryl ester clearance to high density lipoproteins in J7774 macrophages. *J.Biol.Chem.* **266**: 710-716.

37. Brown, M. S., Ho, Y. K. and Goldstein, J. L. (1980). The cholesteryl ester cycle in macrophage foam cells. Continual hydrolysis and re-esterification of cytoplasmic cholesteryl esters. *J.Biol.Chem.* **255**: 9344-9352.

38. Fielding, C. J. and Fielding, P. E. (1997). Intracellular cholesterol transport. *J.Lipid Res.* **38**: 1503-1521.

39. Buhman, K. K., Accad, M., Novak, S., Choi, R. S., Wong, J. S., Hamilton, R. L., Turley, S. and Farese, R. V., Jr. (2000). Resistance to diet-induced hypercholesterolemia and gallstone formation in ACAT2-deficient mice. *Nat.Med.* **6**: 1341-1347.

40. Ho, Y. K., Brown, M. S. and Goldstein, J. L. (1980). Hydrolysis and excretion of cytoplasmic cholesteryl esters by macrophages: stimulation by high density lipoprotein and other agents. *J.Lipid Res.* **21**: 391-398.

41. Miyazaki, A., Rahim, A. T., Ohta, T., Morino, Y. and Horiuchi, S. (1992). High density lipoprotein mediates selective reduction in cholesteryl esters from macrophage foam cells. *Biochim.Biophys.Acta* **1126**: 73-80.

42. Li, Q., Tsujita, M. and Yokoyama, S. (1997). Selective down-regulation by protein kinase C inhibitors of apolipoprotein-mediated cellular cholesterol efflux in macrophages. *Biochemistry* **36**: 12045-12052.

43. Ailhaud, G. (1992). Cellular signal transductants: a new role for HDL. *Curr.Opin.Lipidol.* **3**: 222-226

44. Slotte, J. P., Oram, J. F. and Bierman, E. L. (1987). Binding of high density lipoproteins to cell receptors promotes translocation of cholesterol from intracellular membranes to the cell surface. *J.Biol.Chem.* **262**: 12904-12907.

45. Aviram, M., Bierman, E. L. and Oram, J. F. (1989). High density lipoprotein stimulates sterol translocation between intracellular and plasma membrane pools in human monocyte-derived macrophages. *J.Lipid Res.* **30**: 65-76.

46. Theret, N., Delbart, C., Aguie, G., Fruchart, J. C., Vassaux, G. and Ailhaud, G. (1990). Cholesterol efflux from adipose cells is coupled to diacylglycerol production and protein kinase C activation. *Biochem.Biophys.Res.Commun.* **173**: 1361-1368.

47. Mendez, A. J., Oram, J. F. and Bierman, E. L. (1991). Protein kinase C as a mediator of high density lipoprotein receptor-dependent efflux of intracellular cholesterol. *J.Biol.Chem.* **266**: 10104-10111.

48. Khoo, J. C., Mahoney, E. M. and Steinberg, D. (1981). Neutral cholesterol esterase activity in macrophages and its enhancement by cAMP-dependent protein kinase. *J.Biol.Chem.* **256**: 12659-12661.

49. Sakr, S. W., Williams, D. L., Stoudt, G. W., Phillips, M. C. and Rothblat, G. H. (1999). Induction of cellular cholesterol efflux to lipid-free apolipoprotein A-I by cAMP. *Biochim.Biophys.Acta* **1438**: 85-98.

50. Fielding, C. J. and Fielding, P. E. (2001). Caveolae and intracellular trafficking of cholesterol. *Adv.Drug Deliv.Rev.* **49**: 251-264.

51. Fielding, C. J. and Fielding, P. E. (2000). Cholesterol and caveolae: structural and functional relationships. *Biochim.Biophys.Acta* **1529**: 210-222.

52. Pike, L. J. and Casey, L. (1996). Localization and turnover of phosphatidylinositol 4,5-bisphosphate in caveolin-enriched membrane domains. *J.Biol.Chem.* **271**: 26453-26456.

53. Liu, P. and Anderson, R. G. (1995). Compartmentalized production of ceramide at the cell surface. *J.Biol.Chem.* **270**: 27179-27185.

54. Fielding, C. J. (2001). Caveolae and signaling. *Curr.Opin.Lipidol.* **12**: 281-287.

55. Fielding, P. E. and Fielding, C. J. (1995). Plasma membrane caveolae mediate the efflux of cellular free cholesterol. *Biochemistry* **34**: 14288-14292.

56. Smart, E. J., Ying, Y., Donzell, W. C. and Anderson, R. G. (1996). A role for caveolin in transport of cholesterol from endoplasmic reticulum to plasma membrane. *J.Biol.Chem.* **271**: 29427-29435.

57. Uittenbogaard, A., Ying, Y. and Smart, E. J. (1998). Characterization of a cytosolic heat-shock protein-caveolin chaperone complex. Involvement in cholesterol trafficking. *J.Biol.Chem.* **273**: 6525-6532.

58. Fielding, C. J. and Fielding, P. E. (2001). Cellular cholesterol efflux. *Biochim.Biophys.Acta* **1533**: 175-189.

59. Smart, E. J., Ying, Y. S., Conrad, P. A. and Anderson, R. G. (1994). Caveolin moves from caveolae to the Golgi apparatus in response to cholesterol oxidation. *J.Cell Biol.* **127**: 1185-1197.

60. Bist, A., Fielding, P. E. and Fielding, C. J. (1997). Two sterol regulatory element-like sequences mediate up-regulation of caveolin gene transcription in response to low density lipoprotein free cholesterol. *Proc.Natl.Acad.Sci.U.S.A.* **94**: 10693-10698.

61. Fielding, C. J., Bist, A. and Fielding, P. E. (1997). Caveolin mRNA levels are up-regulated by free cholesterol and down-regulated by oxysterols in fibroblast monolayers. *Proc.Natl.Acad.Sci.U.S.A.* **94**: 3753-3758.

62. Thyberg, J., Calara, F., Dimayuga, P., Nilsson, J. and Regnstrom, J. (1998). Role of caveolae in cholesterol transport in arterial smooth muscle cells exposed to lipoproteins in vitro and in vivo. *Lab Invest* **78**: 825-837.

63. von Eckardstein, A., Huang, Y. and Assmann, G. (1994). Physiological role and clinical relevance of high-density lipoprotein subclasses. *Curr.Opin.Lipidol.* **5**: 404-416.

64. Barrans, A., Jaspard, B., Barbaras, R., Chap, H., Perret, B. and Collet, X. (1996). Pre-beta HDL: structure and metabolism. *Biochim.Biophys.Acta* **1300**: 73-85.

65. Fielding, C. J. and Fielding, P. E. (1995). Molecular physiology of reverse cholesterol transport. *J.Lipid Res.* **36**: 211-228.

66. Hamilton, R. L., Williams, M. C., Fielding, C. J. and Havel, R. J. (1976). Discoidal bilayer structure of nascent high density lipoproteins from perfused rat liver. *J.Clin.Invest* **58**: 667-680.

67. Huang, Y., von Eckardstein, A., Wu, S., Maeda, N. and Assmann, G. (1994). A plasma lipoprotein containing only apolipoprotein E and with gamma mobility on electrophoresis releases cholesterol from cells. *Proc.Natl.Acad.Sci.U.S.A.* **91**: 1834-1838.

68. von Eckardstein, A., Huang, Y., Wu, S., Sarmadi, A. S., Schwarz, S., Steinmetz, A. and Assmann, G. (1995). Lipoproteins containing apolipoprotein A-IV but not apolipoprotein A-I take up and esterify cell-derived cholesterol in plasma. *Arterioscler.Thromb.Vasc.Biol.* **15**: 1755-1763.

69. Cheung, M. C., Segrest, J. P., Albers, J. J., Cone, J. T., Brouillette, C. G., Chung, B. H., Kashyap, M., Glasscock, M. A. and Anantharamaiah, G. M. (1987). Characterization of high density lipoprotein subspecies: structural studies by single vertical spin ultracentrifugation and immunoaffinity chromatography. *J.Lipid Res.* **28** : 913-929.

70. Castle, C. K., Pape, M. E., Marotti, K. R. and Melchior, G. W. (1991). Secretion of pre-beta-migrating apoA-I by cynomolgus monkey hepatocytes in culture. *J.Lipid Res.* **32**: 439-447.

71. Danielsen, E. M., Hansen, G. H. and Poulsen, M. D. (1993). Apical secretion of apolipoproteins from enterocytes. *J.Cell Biol.* **120**: 1347-1356.

72. Brewer, H. B., Jr., Fairwell, T., LaRue, A., Ronan, R., Houser, A. and Bronzert, T. J. (1978). The amino acid sequence of human APOA-I, an apolipoprotein isolated from high density lipoproteins. *Biochem.Biophys.Res.Commun.* **80**: 623-630.

73. Segrest, J. P., Jones, M. K., De Loof, H., Brouillette, C. G., Venkatachalapathi, Y. V. and Anantharamaiah, G. M. (1992). The amphipathic helix in the exchangeable apolipoproteins: a review of secondary structure and function. *J.Lipid Res.* **33**: 141-166.

74. Segrest, J. P., Jackson, R. L., Morrisett, J. D. and Gotto, A. M., Jr. (1974). A molecular theory of lipid-protein interactions in the plasma lipoproteins. *FEBS Lett.* **38**: 247-258.

75. Segrest, J. P., De Loof, H., Dohlman, J. G., Brouillette, C. G. and Anantharamaiah, G. M. (1990). Amphipathic helix motif: classes and properties. *Proteins* **8**: 103-117.

76. Nolte, R. T. and Atkinson, D. (1992). Conformational analysis of apolipoprotein A-I and E-3 based on primary sequence and circular dichroism. *Biophys.J.* **63**: 1221-1239.

77. Borhani, D. W., Rogers, D. P., Engler, J. A. and Brouillette, C. G. (1997). Crystal structure of truncated human apolipoprotein A-I suggests a lipid-bound conformation. *Proc.Natl.Acad.Sci.U.S.A.* **94**: 12291-12296.

78. Tall, A. R., Small, D. M., Deckelbaum, R. J. and Shipley, G. G. (1977). Structure and thermodynamic properties of high density lipoprotein recombinants. *J.Biol.Chem.* **252**: 4701-4711.

79. Segrest, J. P. (1977). Amphipathic helixes and plasma lipoproteins: thermodynamic and geometric considerations. *Chem.Phys.Lipids* **18**: 7-22.

80. Segrest, J. P., Jones, M. K., Klon, A. E., Sheldahl, C. J., Hellinger, M., De Loof, H. and Harvey, S. C. (1999). A detailed molecular belt model for apolipoprotein A-I in discoidal high density lipoprotein. *J.Biol.Chem.* **274**: 31755-31758.

81. Segrest, J. P., Li, L., Anantharamaiah, G. M., Harvey, S. C., Liadaki, K. N. and Zannis, V. (2000). Structure and function of apolipoprotein A-I and high-density lipoprotein. *Curr.Opin.Lipidol.* **11**: 105-115.

82. Oram, J. F. and Lawn, R. M. (2001). ABCA1. The gatekeeper for eliminating excess tissue cholesterol. *J.Lipid Res.* **42**: 1173-1179.

83. Brooks-Wilson, A., Marcil, M., Clee, S. M., Zhang, L. H., Roomp, K., van Dam, M., Yu, L., Brewer, C., Collins, J. A., Molhuizen, H. O., Loubser, O., Ouelette, B. F., Fichter, K., Ashbourne-Excoffon, K. J., Sensen, C. W., Scherer, S., Mott, S., Denis, M., Martindale, D., Frohlich, J., Morgan, K., Koop, B., Pimstone, S., Kastelein, J. J. and Hayden, M. R. (1999). Mutations in ABC1 in Tangier disease and familial high-density lipoprotein deficiency. *Nat.Genet.* **22**: 336-345.

84. Bodzioch, M., Orso, E., Klucken, J., Langmann, T., Bottcher, A., Diederich, W., Drobnik, W., Barlage, S., Buchler, C., Porsch-Ozcurumez, M., Kaminski, W. E., Hahmann, H. W., Oette, K., Rothe, G., Aslanidis, C., Lackner, K. J. and Schmitz, G. (1999). The gene encoding ATP-binding cassette transporter 1 is mutated in Tangier disease. *Nat.Genet.* **22**: 347-351.

85. Rust, S., Rosier, M., Funke, H., Real, J., Amoura, Z., Piette, J. C., Deleuze, J. F., Brewer, H. B., Duverger, N., Denefle, P. and Assmann, G. (1999). Tangier disease is caused by mutations in the gene encoding ATP-binding cassette transporter 1. *Nat.Genet.* **22**: 352-355.

86. Francis, G. A., Knopp, R. H. and Oram, J. F. (1995). Defective removal of cellular cholesterol and phospholipids by apolipoprotein A-I in Tangier Disease. *J.Clin.Invest* **96**: 78-87.

87. Owen, J. S. (1999). Role of ABC1 gene in cholesterol efflux and atheroprotection. *Lancet* **354**: 1402-1403.

88. Dean, M., Hamon, Y. and Chimini, G. (2001). The human ATP-binding cassette (ABC) transporter superfamily. *J.Lipid Res.* **42**: 1007-1017.

89. Walker, J. E., Saraste, M., Runswick, M. J. and Gay, N. J. (1982). Distantly related sequences in the alpha- and beta-subunits of ATP synthase, myosin, kinases and other ATP-requiring enzymes and a common nucleotide binding fold. *EMBO J.* **1**: 945-951.

90. Hyde, S. C., Emsley, P., Hartshorn, M. J., Mimmack, M. M., Gileadi, U., Pearce, S. R., Gallagher, M. P., Gill, D. R., Hubbard, R. E. and Higgins, C. F. (1990). Structural model of ATP-binding proteins associated with cystic fibrosis, multidrug resistance and bacterial transport. *Nature* **346**: 362-365.

91. Fielding, P. E., Nagao, K., Hakamata, H., Chimini, G. and Fielding, C. J. (2000). A two-step mechanism for free cholesterol and phospholipid efflux from human vascular cells to apolipoprotein A-1. *Biochemistry* **39**: 14113-14120.

92. Wang, N., Silver, D. L., Thiele, C. and Tall, A. R. (2001). ATP-binding cassette transporter A1 (ABCA1) functions as a cholesterol efflux regulatory protein. *J.Biol.Chem.* **276**: 23742-23747.

93. Jiang, X. C., Bruce, C., Mar, J., Lin, M., Ji, Y., Francone, O. L. and Tall, A. R. (1999). Targeted mutation of plasma phospholipid transfer protein gene markedly reduces high-density lipoprotein levels. *J.Clin.Invest* **103**: 907-914.

94. Weinstock, P. H., Bisgaier, C. L., Aalto-Setala, K., Radner, H., Ramakrishnan, R., Levak-Frank, S., Essenburg, A. D., Zechner, R. and Breslow, J. L. (1995). Severe hypertriglyceridemia, reduced high density lipoprotein, and neonatal death in lipoprotein lipase knockout mice. Mild hypertriglyceridemia with impaired very low density lipoprotein clearance in heterozygotes. *J.Clin.Invest* **96**: 2555-2568.

95. Shimada, M., Shimano, H., Gotoda, T., Yamamoto, K., Kawamura, M., Inaba, T., Yazaki, Y. and Yamada, N. (1993). Overexpression of human lipoprotein lipase in transgenic mice. Resistance to diet-induced hypertriglyceridemia and hypercholesterolemia. *J.Biol.Chem.* **268**: 17924-17929.

96. Liang, H. Q., Rye, K. A. and Barter, P. J. (1996). Remodelling of reconstituted high density lipoproteins by lecithin: cholesterol acyltransferase. *J.Lipid Res.* **37**: 1962-1970.

97. Miida, T., Kawano, M., Fielding, C. J. and Fielding, P. E. (1992). Regulation of the concentration of pre beta high-density lipoprotein in normal plasma by cell membranes and lecithin-cholesterol acyltransferase activity. *Biochemistry* **31**: 11112-11117.

98. Glomset, J. A. (1968). The plasma lecithins:cholesterol acyltransferase reaction. *J.Lipid Res.* **9**: 155-167.

99. Frank, P. G. and Marcel, Y. L. (2000). Apolipoprotein A-I: structure-function relationships. *J.Lipid Res.* **41**: 853-872.

100. Sparks, D. L., Frank, P. G. and Neville, T. A. (1998). Effect of the surface lipid composition of reconstituted LPA-I on apolipoprotein A-I structure and lecithin: cholesterol acyltransferase activity. *Biochim.Biophys.Acta* **1390**: 160-172.

101. Sakai, N., Vaisman, B. L., Koch, C. A., Hoyt, R. F., Jr., Meyn, S. M., Talley, G. D., Paiz, J. A., Brewer, H. B., Jr. and Santamarina-Fojo, S. (1997). Targeted disruption of the mouse lecithin:cholesterol acyltransferase (LCAT) gene. Generation of a new animal model for human LCAT deficiency. *J.Biol.Chem.* **272**: 7506-7510.

102. Czarnecka, H. and Yokoyama, S. (1995). Lecithin:cholesterol acyltransferase reaction on cellular lipid released by free apolipoprotein-mediated efflux. *Biochemistry* **34**: 4385-4392.

103. Acton, S., Rigotti, A., Landschulz, K. T., Xu, S., Hobbs, H. H. and Krieger, M. (1996). Identification of scavenger receptor SR-BI as a high density lipoprotein receptor. *Science* **271**: 518-520.

104. Liang, H. Q., Rye, K. A. and Barter, P. J. (1994). Dissociation of lipid-free apolipoprotein A-I from high density lipoproteins. *J.Lipid Res.* **35**: 1187-1199.

105. Barrans, A., Collet, X., Barbaras, R., Jaspard, B., Manent, J., Vieu, C., Chap, H. and Perret, B. (1994). Hepatic lipase induces the formation of pre-beta 1 high density lipoprotein (HDL) from triacylglycerol-rich HDL_2. A study comparing liver perfusion to in vitro incubation with lipases. *J.Biol.Chem.* **269**: 11572-11577.

106. Clay, M. A., Newnham, H. H., Forte, T. M. and Barter, P. I. (1992). Cholesteryl ester transfer protein and hepatic lipase activity promote shedding of apo A-I from HDL and subsequent formation of discoidal HDL. *Biochim.Biophys.Acta* **1124**: 52-58.

107. Lambert, G., Chase, M. B., Dugi, K., Bensadoun, A., Brewer, H. B., Jr. and Santamarina-Fojo, S. (1999). Hepatic lipase promotes the selective uptake of high density lipoprotein-cholesteryl esters via the scavenger receptor B1. *J.Lipid Res.* **40**: 1294-1303.

108. Brown, M. L., Inazu, A., Hesler, C. B., Agellon, L. B., Mann, C., Whitlock, M. E., Marcel, Y. L., Milne, R. W., Koizumi, J. and Mabuchi, H. (1989). Molecular basis of lipid transfer protein deficiency in a family with increased high-density lipoproteins. *Nature* **342**: 448-451.

109. Cohen, J. C., Vega, G. L. and Grundy, S. M. (1999). Hepatic lipase: new insights from genetic and metabolic studies. *Curr.Opin.Lipidol.* **10**: 259-267.

110. Krapp, A., Ahle, S., Kersting, S., Hua, Y., Kneser, K., Nielsen, M., Gliemann, J. and Beisiegel, U. (1996). Hepatic lipase mediates the uptake of chylomicrons and beta-VLDL into cells via the LDL receptor-related protein (LRP). *J.Lipid Res.* **37**: 926-936.

111. von Eckardstein, A., Jauhiainen, M., Huang, Y., Metso, J., Langer, C., Pussinen, P., Wu, S., Ehnholm, C. and Assmann, G. (1996). Phospholipid transfer protein mediated conversion of high density lipoproteins generates pre beta 1-HDL. *Biochim.Biophys.Acta* **1301**: 255-262.

112. Lagrost, L., Desrumaux, C., Masson, D., Deckert, V. and Gambert, P. (1998). Structure and function of the plasma phospholipid transfer protein. *Curr.Opin.Lipidol.* **9**: 203-209.

113. Gordon, D. J. and Rifkind, B. M. (1989). High-density lipoprotein – the clinical implications of recent studies. *N.Eng.J.Med.* **321**: 1311-1315.

114. Nofer, J. R., Kehrel, B., Fobker, M., Levkau, B., Assmann, G. and Eckardstein, A. (2002). HDL and arteriosclerosis: beyond reverse cholesterol transport. *Atherosclerosis* **161**: 1-16.

115. Wang, N., Silver, D. L., Costet, P. and Tall, A. R. (2000). Specific binding of ApoA-I, enhanced cholesterol efflux, and altered plasma membrane morphology in cells expressing ABC1. *J.Biol.Chem.* **275**: 33053-33058.

116. Ji, Y., Jian, B., Wang, N., Sun, Y., Moya, M. L., Phillips, M. C., Rothblat, G. H., Swaney, J. B. and Tall, A. R. (1997). Scavenger receptor BI promotes high density lipoprotein-mediated cellular cholesterol efflux. *J.Biol.Chem.* **272**: 20982-20985.

117. Rigotti, A., Trigatti, B. L., Penman, M., Rayburn, H., Herz, J. and Krieger, M. (1997). A targeted mutation in the murine gene encoding the high density lipoprotein (HDL) receptor scavenger receptor class B type I reveals its key role in HDL metabolism. *Proc.Natl.Acad.Sci.U.S.A.* **94**: 12610-12615.

118. Cushing, S. D., Berliner, J. A., Valente, A. J., Territo, M. C., Navab, M., Parhami, F., Gerrity, R., Schwartz, C. J. and Fogelman, A. M. (1990). Minimally modified low density lipoprotein induces monocyte chemotactic protein 1 in human endothelial cells and smooth muscle cells. *Proc.Natl.Acad.Sci.U.S.A.* **87**: 5134-5138.

119. Berliner, J. A., Territo, M. C., Sevanian, A., Ramin, S., Kim, J. A., Bamshad, B., Esterson, M. and Fogelman, A. M. (1990). Minimally modified low density lipoprotein stimulates monocyte endothelial interactions. *J.Clin.Invest* **85**: 1260-1266.

120. Holvoet, P. and Collen, D. (1998). Oxidation of low density lipoproteins in the pathogenesis of atherosclerosis. *Atherosclerosis* **137 Suppl**: S33-S38.

121. Parthasarathy, S., Barnett, J. and Fong, L. G. (1990). High-density lipoprotein inhibits the oxidative modification of low- density lipoprotein. *Biochim.Biophys.Acta* **1044**: 275-283.

122. Mackness, M. I., Arrol, S. and Durrington, P. N. (1991). Paraoxonase prevents accumulation of lipoperoxides in low-density lipoprotein. *FEBS Lett.* **286**: 152-154.

123. Watson, A. D., Berliner, J. A., Hama, S. Y., La Du, B. N., Faull, K. F., Fogelman, A. M. and Navab, M. (1995). Protective effect of high density lipoprotein associated paraoxonase. Inhibition of the biological activity of minimally oxidized low density lipoprotein. *J.Clin.Invest* **96**: 2882-2891.

124. Subbaiah, P. V. and Liu, M. (1996). Disparate effects of oxidation on plasma acyltransferase activities: inhibition of cholesterol esterification but stimulation of transesterification of oxidized phospholipids. *Biochim.Biophys.Acta* **1301**: 115-126.

125. Mackness, M. I., Mackness, B., Durrington, P. N., Connelly, P. W. and Hegele, R. A. (1996). Paraoxonase: biochemistry, genetics and relationship to plasma lipoproteins. *Curr.Opin.Lipidol.* **7**: 69-76.

126. Miyata, M. and Smith, J. D. (1996). Apolipoprotein E allele-specific antioxidant activity and effects on cytotoxicity by oxidative insults and beta-amyloid peptides. *Nat.Genet.* **14**: 55-61.

127. Uittenbogaard, A., Shaul, P. W., Yuhanna, I. S., Blair, A. and Smart, E. J. (2000). High density lipoprotein prevents oxidized low density lipoprotein-induced inhibition of endothelial nitric-oxide synthase localization and activation in caveolae. *J.Biol.Chem.* **275**: 11278-11283.

128. Tamagaki, T., Sawada, S., Imamura, H., Tada, Y., Yamasaki, S., Toratani, A., Sato, T., Komatsu, S., Akamatsu, N., Yamagami, M., Kobayashi, K., Kato, K., Yamamoto, K., Shirai, K., Yamada, K., Higaki, T., Nakagawa, K., Tsuji, H. and Nakagawa, M. (1996). Effects of high-density lipoproteins on intracellular pH and proliferation of human vascular endothelial cells. *Atherosclerosis* **123**: 73-82.

129. Fleisher, L. N., Tall, A. R., Witte, L. D., Miller, R. W. and Cannon, P. J. (1982). Stimulation of arterial endothelial cell prostacyclin synthesis by high density lipoproteins. *J.Biol.Chem.* **257**: 6653-6655.

130. Sugiyama, S., Kugiyama, K., Matsumura, T., Suga, S., Itoh, H., Nakao, K. and Yasue, H. (1995). Lipoproteins regulate C-type natriuretic peptide secretion from cultured vascular endothelial cells. *Arterioscler.Thromb.Vasc.Biol.* **15**: 1968-1974.

131. Cockerill, G. W., Rye, K. A., Gamble, J. R., Vadas, M. A. and Barter, P. J. (1995). High-density lipoproteins inhibit cytokine-induced expression of endothelial cell adhesion molecules. *Arterioscler.Thromb.Vasc.Biol.* **15**: 1987-1994.

132. Xia, P., Vadas, M. A., Rye, K. A., Barter, P. J. and Gamble, J. R. (1999). High density lipoproteins (HDL) interrupt the sphingosine kinase signaling pathway. A possible mechanism for protection against atherosclerosis by HDL. *J.Biol.Chem.* **274**: 33143-33147.

133. Stannard, A. K., Khan, S., Graham, A., Owen, J. S. and Allen, S. P. (2001). Inability of plasma high-density lipoproteins to inhibit cell adhesion molecule expression in human coronary artery endothelial cells. *Atherosclerosis* **154**: 31-38.

134. Hassall, D. G., Owen, J. S. and Bruckdorfer, K. R. (1983). The aggregation of isolated human platelets in the presence of lipoproteins and prostacyclin. *Biochem.J.* **216**: 43-49.

135. Naqvi, T. Z., Shah, P. K., Ivey, P. A., Molloy, M. D., Thomas, A. M., Panicker, S., Ahmed, A., Cercek, B. and Kaul, S. (1999). Evidence that high-density lipoprotein cholesterol is an independent predictor of acute platelet-dependent thrombus formation. *Am.J.Cardiol.* **84**: 1011-1017.

136. Desai, K., Bruckdorfer, K. R., Hutton, R. A. and Owen, J. S. (1989). Binding of apoE-rich high density lipoprotein particles by saturable sites on human blood platelets inhibits agonist-induced platelet aggregation. *J.Lipid Res.* **30**: 831-840.

137. Riddell, D. R., Vinogradov, D. V., Stannard, A. K., Chadwick, N. and Owen, J. S. (1999). Identification and characterization of LRP8 (apoER2) in human blood platelets. *J.Lipid Res.* **40**: 1925-1930.

138. Riddell, D. R., Graham, A. and Owen, J. S. (1997). Apolipoprotein E inhibits platelet aggregation through the L-arginine:nitric oxide pathway. Implications for vascular disease. *J.Biol.Chem.* **272**: 89-95.

139. Higashihara, M., Kinoshita, M., Teramoto, T., Kume, S. and Kurokawa, K. (1991). The role of apoE in inhibitory effects of apoE-rich HDL on platelet function. *FEBS Lett.* **282**: 82-86.

140. Nofer, J. R., Tepel, M., Kehrel, B., Walter, M., Seedorf, U., Assmann, G. and Zidek, W. (1996). High density lipoproteins enhance the Na+/H+ antiport in human platelets. *Thromb.Haemost.* **75**: 635-641.

141. Nofer, J. R., Walter, M., Kehrel, B., Wierwille, S., Tepel, M., Seedorf, U. and Assmann, G. (1998). HDL_3-mediated inhibition of thrombin-induced platelet aggregation and fibrinogen binding occurs via decreased production of phosphoinositide-derived second messengers 1,2-diacylglycerol and inositol 1,4,5-tris-phosphate. *Arterioscler.Thromb.Vasc.Biol.* **18**: 861-869.

142. Howell, B. W. and Herz, J. (2001). The LDL receptor gene family: signaling functions during development. *Curr.Opin.Neurobiol.* **11**: 74-81.

143. Herz, J. (2001). The LDL receptor gene family: (un)expected signal transducers in the brain. *Neuron* **29**: 571-581.

144. Davis, C. G., Goldstein, J. L., Sudhof, T. C., Anderson, R. G., Russell, D. W. and Brown, M. S. (1987). Acid-dependent ligand dissociation and recycling of LDL receptor mediated by growth factor homology region. *Nature* **326**: 760-765.

145. Pittman, R. C., Knecht, T. P., Rosenbaum, M. S. and Taylor, C. A., Jr. (1987). A nonendocytotic mechanism for the selective uptake of high density lipoprotein-associated cholesterol esters. *J.Biol.Chem.* **262**: 2443-2450.

146. Bachorik, P. S., Franklin, F. A., Virgil, D. G. and Kwiterovich, P. O., Jr. (1982). High-affinity uptake and degradation of apolipoprotein E free high-density lipoprotein and low-density lipoprotein in cultured porcine hepatocytes. *Biochemistry* **21**: 5675-5684.

147. Biesbroeck, R., Oram, J. F., Albers, J. J. and Bierman, E. L. (1983). Specific high-affinity binding of high density lipoproteins to cultured human skin fibroblasts and arterial smooth muscle cells. *J.Clin.Invest* **71**: 525-539.

148. Chen, Y. D., Kraemer, F. B. and Reaven, G. M. (1980). Identification of specific high density lipoprotein-binding sites in rat testis and regulation of binding by human chorionic gonadotropin. *J.Biol.Chem.* **255**: 9162-9167.

149. Fidge, N. H. (1999). High density lipoprotein receptors, binding proteins, and ligands. *J.Lipid Res.* **40**: 187-201.

150. Graham, D. L. and Oram, J. F. (1987). Identification and characterization of a high density lipoprotein-binding protein in cell membranes by ligand blotting. *J.Biol.Chem.* **262**: 7439-7442.

151. McKnight, G. L., Reasoner, J., Gilbert, T., Sundquist, K. O., Hokland, B., McKernan, P. A., Champagne, J., Johnson, C. J., Bailey, M. C. and Holly, R. (1992). Cloning and expression of a cellular high density lipoprotein-binding protein that is up-regulated by cholesterol loading of cells. *J.Biol.Chem.* **267**: 12131-12141.

152. Dodson, R. E. and Shapiro, D. J. (1997). Vigilin, a ubiquitous protein with 14 K homology domains, is the estrogen-inducible vitellogenin mRNA 3'-untranslated region-binding protein. *J.Biol.Chem.* **272**: 12249-12252.

153. Tozuka, M. and Fidge, N. (1989). Purification and characterization of two high-density-lipoprotein-binding proteins from rat and human liver. *Biochem.J.* **261**: 239-244.

154. Matsumoto, A., Mitchell, A., Kurata, H., Pyle, L., Kondo, K., Itakura, H. and Fidge, N. (1997). Cloning and characterization of HB_2, a candidate high density lipoprotein receptor. Sequence homology with members of the immunoglobulin superfamily of membrane proteins. *J.Biol.Chem.* **272**: 16778-16782.

155. Acton, S. L., Scherer, P. E., Lodish, H. F. and Krieger, M. (1994). Expression cloning of SR-BI, a CD36-related class B scavenger receptor. *J.Biol.Chem.* **269**: 21003-21009.

156. Vega, M. A., Segui-Real, B., Garcia, J. A., Cales, C., Rodriguez, F., Vanderkerckhove, J. and Sandoval, I. V. (1991). Cloning, sequencing, and expression of a cDNA encoding rat LIMP II, a novel 74-kDa lysosomal membrane protein related to the surface adhesion protein CD36. *J.Biol.Chem.* **266**: 16818-16824.

157. Calvo, D. and Vega, M. A. (1993). Identification, primary structure, and distribution of CLA-1, a novel member of the CD36/LIMPII gene family. *J.Biol.Chem.* **268**: 18929-18935.

158. Murao, K., Terpstra, V., Green, S. R., Kondratenko, N., Steinberg, D. and Quehenberger, O. (1997). Characterization of CLA-1, a human homologue of rodent scavenger receptor BI, as a receptor for high density lipoprotein and apoptotic thymocytes. *J.Biol.Chem.* **272**: 17551-17557.

159. Kozarsky, K. F., Donahee, M. H., Rigotti, A., Iqbal, S. N., Edelman, E. R. and Krieger, M. (1997). Overexpression of the HDL receptor SR-BI alters plasma HDL and bile cholesterol levels. *Nature* **387**: 414-417.

160. Wang, N., Arai, T., Ji, Y., Rinninger, F. and Tall, A. R. (1998). Liver-specific overexpression of scavenger receptor BI decreases levels of very low density lipoprotein ApoB, low density lipoprotein ApoB, and high density lipoprotein in transgenic mice. *J.Biol.Chem.* **273**: 32920-32926.

161. Ueda, Y., Royer, L., Gong, E., Zhang, J., Cooper, P. N., Francone, O. and Rubin, E. M. (1999). Lower plasma levels and accelerated clearance of high density lipoprotein (HDL) and non-HDL cholesterol in scavenger receptor class B type I transgenic mice. *J.Biol.Chem.* **274**: 7165-7171.

162. Varban, M. L., Rinninger, F., Wang, N., Fairchild-Huntress, V., Dunmore, J. H., Fang, Q., Gosselin, M. L., Dixon, K. L., Deeds, J. D., Acton, S. L., Tall, A. R. and Huszar, D. (1998). Targeted mutation reveals a central role for SR-BI in hepatic selective uptake of high density lipoprotein cholesterol. *Proc.Natl.Acad.Sci.U.S.A.* **95**: 4619-4624.

163. Trigatti, B., Rayburn, H., Vinals, M., Braun, A., Miettinen, H., Penman, M., Hertz, M., Schrenzel, M., Amigo, L., Rigotti, A. and Krieger, M. (1999). Influence of the high density lipoprotein receptor SR-BI on reproductive and cardiovascular pathophysiology. *Proc.Natl.Acad.Sci.U.S.A.* **96**: 9322-9327.

164. Temel, R. E., Trigatti, B., DeMattos, R. B., Azhar, S., Krieger, M. and Williams, D. L. (1997). Scavenger receptor class B, type I (SR-BI) is the major route for the delivery of high density lipoprotein cholesterol to the steroidogenic pathway in cultured mouse adrenocortical cells. *Proc.Natl.Acad.Sci.U.S.A.* **94**: 13600-13605.

165. Ueda, Y., Gong, E., Royer, L., Cooper, P. N., Francone, O. L. and Rubin, E. M. (2000). Relationship between expression levels and atherogenesis in scavenger receptor class B, type I transgenics. *J.Biol.Chem.* **275**: 20368-20373.

166. Landschulz, K. T., Pathak, R. K., Rigotti, A., Krieger, M. and Hobbs, H. H. (1996). Regulation of scavenger receptor, class B, type I, a high density lipoprotein receptor, in liver and steroidogenic tissues of the rat. *J.Clin.Invest* **98**: 984-995.

167. Wang, N., Weng, W., Breslow, J. L. and Tall, A. R. (1996). Scavenger receptor BI (SR-BI) is up-regulated in adrenal gland in apolipoprotein A-I and hepatic lipase knock-out mice as a response to depletion of cholesterol stores. In vivo evidence that SR-BI is a functional high density lipoprotein receptor under feedback control. *J.Biol.Chem.* **271**: 21001-21004.

168. Sun, Y., Wang, N. and Tall, A. R. (1999). Regulation of adrenal scavenger receptor-BI expression by ACTH and cellular cholesterol pools. *J.Lipid Res.* **40**: 1799-1805.

169. Spady, D. K., Kearney, D. M. and Hobbs, H. H. (1999). Polyunsaturated fatty acids up-regulate hepatic scavenger receptor B1 (SR-BI) expression and HDL cholesteryl ester uptake in the hamster. *J.Lipid Res.* **40**: 1384-1394.

170. Mattson, F. H. and Grundy, S. M. (1985). Comparison of effects of dietary saturated, monounsaturated, and polyunsaturated fatty acids on plasma lipids and lipoproteins in man. *J.Lipid Res.* **26**: 194-202.

171. Cao, G., Garcia, C. K., Wyne, K. L., Schultz, R. A., Parker, K. L. and Hobbs, H. H. (1997). Structure and localization of the human gene encoding SR-BI/CLA-1. Evidence for transcriptional control by steroidogenic factor 1. *J.Biol.Chem.* **272**: 33068-33076.

172. Lopez, D. and McLean, M. P. (1999). Sterol regulatory element-binding protein-1a binds to cis elements in the promoter of the rat high density lipoprotein receptor SR-BI gene. *Endocrinology* **140**: 5669-5681.

173. Mizutani, T., Yamada, K., Minegishi, T. and Miyamoto, K. (2000). Transcriptional regulation of rat scavenger receptor class B type I gene. *J.Biol.Chem.* **275**: 22512-22519.

174. Stangl, H., Cao, G., Wyne, K. L. and Hobbs, H. H. (1998). Scavenger receptor, class B, type I-dependent stimulation of cholesterol esterification by high density lipoproteins, low density lipoproteins, and nonlipoprotein cholesterol. *J.Biol.Chem.* **273**: 31002-31008.

175. Voshol, P. J., Schwarz, M., Rigotti, A., Kreiger, M., Groen, A. K. and Kuipers, F. (2001). Down-regulation of intestinal scavenger receptor class B, type I (SR-BI) expression in rodents under conditions of deficient bile delivery to the intestine. *Biochem.J.* **356**: 317-325.

176. Babitt, J., Trigatti, B., Rigotti, A., Smart, E. J., Anderson, R. G., Xu, S. and Krieger, M. (1997). Murine SR-BI, a high density lipoprotein receptor that mediates selective lipid uptake, is N-glycosylated and fatty acylated and colocalizes with plasma membrane caveolae. *J.Biol.Chem.* **272**: 13242-13249.

177. Tao, N., Wagner, S. J. and Lublin, D. M. (1996). CD36 is palmitoylated on both N- and C-terminal cytoplasmic tails. *J.Biol.Chem.* **271**: 22315-22320.

178. Resh, M. D. (1994). Myristylation and palmitylation of Src family members: the fats of the matter. *Cell* **76**: 411-413.

179. Gordon, J. I., Duronio, R. J., Rudnick, D. A., Adams, S. P. and Gokel, G. W. (1991). Protein N-myristoylation. *J.Biol.Chem.* **266**: 8647-8650.

180. Milligan, G., Parenti, M. and Magee, A. I. (1995). The dynamic role of palmitoylation in signal transduction. *Trends Biochem.Sci.* **20**: 181-187.

181. McLaughlin, S. and Aderem, A. (1995). The myristoyl-electrostatic switch: a modulator of reversible protein-membrane interactions. *Trends Biochem.Sci.* **20**: 272-276.

182. Shaul, P. W., Smart, E. J., Robinson, L. J., German, Z., Yuhanna, I. S., Ying, Y., Anderson, R. G. and Michel, T. (1996). Acylation targets endothelial nitric-oxide synthase to plasmalemmal caveolae. *J.Biol.Chem.* **271**: 6518-6522.

183. Garcia-Cardena, G., Oh, P., Liu, J., Schnitzer, J. E. and Sessa, W. C. (1996). Targeting of nitric oxide synthase to endothelial cell caveolae via palmitoylation: implications for nitric oxide signaling. *Proc.Natl.Acad.Sci.U.S.A.* **93**: 6448-6453.

184. Robinson, L. J. and Michel, T. (1995). Mutagenesis of palmitoylation sites in endothelial nitric oxide synthase identifies a novel motif for dual acylation and subcellular targeting. *Proc.Natl.Acad.Sci.U.S.A.* **92**: 11776-11780.

185. Parton, R. G. (1996). Caveolae and caveolins. *Curr.Opin.Cell Biol.* **8**: 542-548.

186. Fra, A. M., Williamson, E., Simons, K. and Parton, R. G. (1995). De novo formation of caveolae in lymphocytes by expression of VIP21- caveolin. *Proc.Natl.Acad.Sci.U.S.A.* **92**: 8655-8659.

187. Lisanti, M. P., Scherer, P. E., Vidugiriene, J., Tang, Z., Hermanowski-Vosatka, A., Tu, Y. H., Cook, R. F. and Sargiacomo, M. (1994). Characterization of caveolin-rich membrane domains isolated from an endothelial-rich source: implications for human disease. *J.Cell Biol.* **126**: 111-126.

188. Dorahy, D. J., Lincz, L. F., Meldrum, C. J. and Burns, G. F. (1996). Biochemical isolation of a membrane microdomain from resting platelets highly enriched in the plasma membrane glycoprotein CD36. *Biochem.J.* **319** (Pt 1): 67-72.

189. Anderson, R. G., Brown, M. S. and Goldstein, J. L. (1977). Role of the coated endocytic vesicle in the uptake of receptor-bound low density lipoprotein in human fibroblasts. *Cell* **10**: 351-364.

190. Graf, G. A., Connell, P. M., van der Westhuyzen, D. R. and Smart, E. J. (1999). The class B, type I scavenger receptor promotes the selective uptake of high density lipoprotein cholesterol ethers into caveolae. *J.Biol.Chem.* **274**: 12043-12048.

191. Matveev, S., van der Westhuyzen, D. R. and Smart, E. J. (1999). Co-expression of scavenger receptor-BI and caveolin-1 is associated with enhanced selective cholesteryl ester uptake in THP-1 macrophages. *J.Lipid Res.* **40**: 1647-1654.

192. Yuhanna, I. S., Zhu, Y., Cox, B. E., Hahner, L. D., Osborne-Lawrence, S., Lu, P., Marcel, Y. L., Anderson, R. G., Mendelsohn, M. E., Hobbs, H. H. and Shaul, P. W. (2001). High-density lipoprotein binding to scavenger receptor-BI activates endothelial nitric oxide synthase. *Nat.Med.* **7**: 853-857.

193. Swarnakar, S., Temel, R. E., Connelly, M. A., Azhar, S. and Williams, D. L. (1999). Scavenger receptor class B, type I, mediates selective uptake of low density lipoprotein cholesteryl ester. *J.Biol.Chem.* **274**: 29733-29739.

194. Stangl, H., Hyatt, M. and Hobbs, H. H. (1999). Transport of lipids from high and low density lipoproteins via scavenger receptor-BI. *J.Biol.Chem.* **274**: 32692-32698.

195. Gu, X., Lawrence, R. and Krieger, M. (2000). Dissociation of the high density lipoprotein and low density lipoprotein binding activities of murine scavenger receptor class B type I (mSR-BI) using retrovirus library-based activity dissection. *J.Biol.Chem.* **275**: 9120-9130.

196. Gu, X., Kozarsky, K. and Krieger, M. (2000). Scavenger receptor class B, type I-mediated [^{3}H]cholesterol efflux to high and low density lipoproteins is dependent on lipoprotein binding to the receptor. *J.Biol.Chem.* **275**: 29993-30001.

197. Llera-Moya, M., Rothblat, G. H., Connelly, M. A., Kellner-Weibel, G., Sakr, S. W., Phillips, M. C. and Williams, D. L. (1999). Scavenger receptor BI (SR-BI) mediates free cholesterol flux independently of HDL tethering to the cell surface. *J.Lipid Res.* **40**: 575-580.

198. Kellner-Weibel, G., Llera-Moya, M., Connelly, M. A., Stoudt, G., Christian, A. E., Haynes, M. P., Williams, D. L. and Rothblat, G. H. (2000). Expression of scavenger receptor BI in COS-7 cells alters cholesterol content and distribution. *Biochemistry* **39**: 221-229.

199. Chen, W., Silver, D. L., Smith, J. D. and Tall, A. R. (2000). Scavenger receptor-BI inhibits ATP-binding cassette transporter 1-mediated cholesterol efflux in macrophages. *J.Biol.Chem.* **275**: 30794-30800.

200. Xu, S., Laccotripe, M., Huang, X., Rigotti, A., Zannis, V. I. and Krieger, M. (1997). Apolipoproteins of HDL can directly mediate binding to the scavenger receptor SR-BI, an HDL receptor that mediates selective lipid uptake. *J.Lipid Res.* **38**: 1289-1298.

201. Williams, D. L., Llera-Moya, M., Thuahnai, S. T., Lund-Katz, S., Connelly, M. A., Azhar, S., Anantharamaiah, G. M. and Phillips, M. C. (2000). Binding and cross-linking studies show that scavenger receptor BI interacts with multiple sites in apolipoprotein A-I and identify the class A amphipathic alpha-helix as a recognition motif. *J.Biol.Chem.* **275**: 18897-18904.

202. Li, X., Kan, H. Y., Lavrentiadou, S. N., Krieger, M. and Zannis, V. I. (2002). Reconstituted discoidal APOE-phospholipid particles are ligands for the scavenger receptor B-1. The amino terminal 1-165 domain of APOE suffices for receptor binding. *J.Biol.Chem.* **277**: 21149-21157.

203. de Beer, M. C., Durbin, D. M., Cai, L., Jonas, A., de Beer, F. C. and van der Westhuyzen, D. R. (2001). Apolipoprotein A-I conformation markedly influences HDL interaction with scavenger receptor BI. *J.Lipid Res.* **42**: 309-313.

204. Liadaki, K. N., Liu, T., Xu, S., Ishida, B. Y., Duchateaux, P. N., Krieger, J. P., Kane, J., Krieger, M. and Zannis, V. I. (2000). Binding of high density lipoprotein (HDL) and discoidal reconstituted HDL to the HDL receptor scavenger receptor class B type I. Effect of lipid association and APOA-I mutations on receptor binding. *J.Biol.Chem.* **275**: 21262-21271.

205. Rodrigueza, W. V., Thuahnai, S. T., Temel, R. E., Lund-Katz, S., Phillips, M. C. and Williams, D. L. (1999). Mechanism of scavenger receptor class B type I-mediated selective uptake of cholesteryl esters from high density lipoprotein to adrenal cells. *J.Biol.Chem.* **274**: 20344-20350.

206. Gu, X., Trigatti, B., Xu, S., Acton, S., Babitt, J. and Krieger, M. (1998). The efficient cellular uptake of high density lipoprotein lipids via scavenger receptor class B type I requires not only

receptor-mediated surface binding but also receptor-specific lipid transfer mediated by its extracellular domain. *J.Biol.Chem.* **273**: 26338-26348.

207. Connelly, M. A., Llera-Moya, M., Monzo, P., Yancey, P. G., Drazul, D., Stoudt, G., Fournier, N., Klein, S. M., Rothblat, G. H. and Williams, D. L. (2001). Analysis of chimeric receptors shows that multiple distinct functional activities of scavenger receptor, class B, type I (SR-BI), are localized to the extracellular receptor domain. *Biochemistry* **40**: 5249-5259.

208. Connelly, M. A., Klein, S. M., Azhar, S., Abumrad, N. A. and Williams, D. L. (1999). Comparison of class B scavenger receptors, CD36 and scavenger receptor BI (SR-BI), shows that both receptors mediate high density lipoprotein- cholesteryl ester selective uptake but SR-BI exhibits a unique enhancement of cholesteryl ester uptake. *J.Biol.Chem.* **274**: 41-47.

209. Hamilton, J. A., Miller, K. W. and Small, D. M. (1983). Solubilization of triolein and cholesteryl oleate in egg phosphatidylcholine vesicles. *J.Biol.Chem.* **258**: 12821-12826.

210. Silver, D. L., Wang, N., Xiao, X. and Tall, A. R. (2001). High density lipoprotein (HDL) particle uptake mediated by scavenger receptor class B type 1 results in selective sorting of HDL cholesterol from protein and polarized cholesterol secretion. *J.Biol.Chem.* **276**: 25287-25293.

211. Delamatre, J. G., Carter, R. M. and Hornick, C. A. (1993). Evidence that a neutral cholesteryl ester hydrolase is responsible for the extralysosomal hydrolysis of high-density lipoprotein cholesteryl ester in rat hepatoma cells (Fu5AH). *J.Cell Physiol* **157**: 164-168.

212. Silver, D. L. and Tall, A. R. (2001). The cellular biology of scavenger receptor class B type I. *Curr.Opin.Lipidol.* **12**: 497-504.

213. Ohgami, N., Nagai, R., Miyazaki, A., Ikemoto, M., Arai, H., Horiuchi, S. and Nakayama, H. (2001). Scavenger receptor class B type I-mediated reverse cholesterol transport is inhibited by advanced glycation end products. *J.Biol.Chem.* **276**: 13348-13355.

214. Endemann, G., Stanton, L. W., Madden, K. S., Bryant, C. M., White, R. T. and Protter, A. A. (1993). CD36 is a receptor for oxidized low density lipoprotein. *J.Biol.Chem.* **268**: 11811-11816.

215. Hinshaw, J. E. and Schmid, S. L. (1995). Dynamin self-assembles into rings suggesting a mechanism for coated vesicle budding. *Nature* **374**: 190-192.

216. Mellman, I., Yamamoto, E., Whitney, J. A., Kim, M., Hunziker, W. and Matter, K. (1993). Molecular sorting in polarized and non-polarized cells: common problems, common solutions. *J.Cell Sci.Suppl* **17**: 1-7.

217. Uittenbogaard, A., Everson, W. V., Matveev, S. V. and Smart, E. J. (2002). Cholesteryl ester is transported from caveolae to internal membranes as part of a caveolin-annexin II lipid-protein complex. *J.Biol.Chem.* **277**: 4925-4931.

218. Ji, Y., Wang, N., Ramakrishnan, R., Sehayek, E., Huszar, D., Breslow, J. L. and Tall, A. R. (1999). Hepatic scavenger receptor BI promotes rapid clearance of high density lipoprotein free cholesterol and its transport into bile. *J.Biol.Chem.* **274**: 33398-33402.

219. Ikemoto, M., Arai, H., Feng, D., Tanaka, K., Aoki, J., Dohmae, N., Takio, K., Adachi, H., Tsujimoto, M. and Inoue, K. (2000). Identification of a PDZ-domain-containing protein that interacts with the scavenger receptor class B type I. *Proc.Natl.Acad.Sci.U.S.A.* **97**: 6538-6543.

220. Fanning, A. S. and Anderson, J. M. (1999). PDZ domains: fundamental building blocks in the organization of protein complexes at the plasma membrane. *J.Clin.Invest* **103** : 767-772.

221. Kocher, O., Comella, N., Tognazzi, K. and Brown, L. F. (1998). Identification and partial characterization of PDZK1: a novel protein containing PDZ interaction domains. *Lab Invest* **78**: 117-125.

222. Glass, C. K., Pittman, R. C., Keller, G. A. and Steinberg, D. (1983). Tissue sites of degradation of apoprotein A-I in the rat. *J.Biol.Chem.* **258**: 7161-7167.

223. Kozyraki, R., Fyfe, J., Kristiansen, M., Gerdes, C., Jacobsen, C., Cui, S., Christensen, E. I., Aminoff, M., de la, C. A., Krahe, R., Verroust, P. J. and Moestrup, S. K. (1999). The intrinsic factor-vitamin B12 receptor, cubilin, is a high-affinity apolipoprotein A-I receptor facilitating endocytosis of high-density lipoprotein. *Nat.Med.* **5**: 656-661.

224. Hammad, S. M., Stefansson, S., Twal, W. O., Drake, C. J., Fleming, P., Remaley, A., Brewer, H. B., Jr. and Argraves, W. S. (1999). Cubilin, the endocytic receptor for intrinsic factor-vitamin B_{12} complex, mediates high-density lipoprotein holoparticle endocytosis. *Proc.Natl.Acad.Sci.U.S.A.* **96**: 10158-10163.

225. Seetharam, B., Bose, S. and Li, N. (1999). Cellular import of cobalamin (Vitamin B-12). *J.Nutr.* **129**: 1761-1764.

226. Moestrup, S. K. and Kozyraki, R. (2000). Cubilin, a high-density lipoprotein receptor. *Curr.Opin.Lipidol.* **11**: 133-140.

227. Batuman, V., Verroust, P. J., Navar, G. L., Kaysen, J. H., Goda, F. O., Campbell, W. C., Simon, E., Pontillon, F., Lyles, M., Bruno, J. and Hammond, T. G. (1998). Myeloma light chains are ligands for cubilin (gp280). *Am.J.Physiol* **275**: F246-F254.

228. Moestrup, S. K., Kozyraki, R., Kristiansen, M., Kaysen, J. H., Rasmussen, H. H., Brault, D., Pontillon, F., Goda, F. O., Christensen, E. I., Hammond, T. G. and Verroust, P. J. (1998). The intrinsic factor-vitamin B12 receptor and target of teratogenic antibodies is a megalin-binding peripheral membrane protein with homology to developmental proteins. *J.Biol.Chem.* **273**: 5235-5242.

229. Gliemann, J. (1998). Receptors of the low density lipoprotein (LDL) receptor family in man. Multiple functions of the large family members via interaction with complex ligands. *Biol.Chem.* **379**: 951-964.

230. Jollie, W. P. (1990). Development, morphology, and function of the yolk-sac placenta of laboratory rodents. *Teratology* **41**: 361-381.

231. Sahali, D., Mulliez, N., Chatelet, F., Laurent-Winter, C., Citadelle, D., Roux, C., Ronco, P. and Verroust, P. (1992). Coexpression in humans by kidney and fetal envelopes of a 280 kDa-coated pit-restricted protein. Similarity with the murine target of teratogenic antibodies. *Am.J.Pathol.* **140**: 33-44.

232. Webb, N. R., de Villiers, W. J., Connell, P. M., de Beer, F. C. and van der Westhuyzen, D. R. (1997). Alternative forms of the scavenger receptor BI (SR-BI). *J.Lipid Res.* **38**: 1490-1495.

233. Webb, N. R., Connell, P. M., Graf, G. A., Smart, E. J., de Villiers, W. J., de Beer, F. C. and van der Westhuyzen, D. R. (1998). SR-BII, an isoform of the scavenger receptor BI containing an alternate cytoplasmic tail, mediates lipid transfer between high density lipoprotein and cells. *J.Biol.Chem.* **273**: 15241-15248.

234. Graf, G. A., Roswell, K. L. and Smart, E. J. (2001). 17beta-Estradiol promotes the up-regulation of SR-BII in HepG2 cells and in rat livers. *J.Lipid Res.* **42**: 1444-1449.

235. Feng, S., Chen, J. K., Yu, H., Simon, J. A. and Schreiber, S. L. (1994). Two binding orientations for peptides to the Src SH3 domain: development of a general model for SH3-ligand interactions. *Science* **266**: 1241-1247.

236. Pawson, T. (1995). Protein modules and signalling networks. *Nature* **373**: 573-580.

237. Zhou, S. and Cantley, L. C. (1995). Recognition and specificity in protein tyrosine kinase-mediated signalling. *Trends Biochem.Sci.* **20**: 470-475.

238. Koch, C. A., Anderson, D., Moran, M. F., Ellis, C. and Pawson, T. (1991). SH2 and SH3 domains: elements that control interactions of cytoplasmic signaling proteins. *Science* **252**: 668-674.

239. Cohen, G. B., Ren, R. and Baltimore, D. (1995). Modular binding domains in signal transduction proteins. *Cell* **80**: 237-248.

240. Musacchio, A., Wilmanns, M. and Saraste, M. (1994). Structure and function of the SH3 domain. *Prog.Biophys.Mol.Biol.* **61**: 283-297.

241. Anderson, D., Koch, C. A., Grey, L., Ellis, C., Moran, M. F. and Pawson, T. (1990). Binding of SH2 domains of phospholipase C gamma 1, GAP, and Src to activated growth factor receptors. *Science* **250**: 979-982.

242. Herz, J., Gotthardt, M. and Willnow, T. E. (2000). Cellular signalling by lipoprotein receptors. *Curr.Opin.Lipidol.* **11**: 161-166.

243. Trommsdorff, M., Gotthardt, M., Hiesberger, T., Shelton, J., Stockinger, W., Nimpf, J., Hammer, R. E., Richardson, J. A. and Herz, J. (1999). Reeler/Disabled-like disruption of neuronal migration in knockout mice lacking the VLDL receptor and ApoE receptor 2. *Cell* **97**: 689-701.

244. Hiesberger, T., Trommsdorff, M., Howell, B. W., Goffinet, A., Mumby, M. C., Cooper, J. A. and Herz, J. (1999). Direct binding of Reelin to VLDL receptor and ApoE receptor 2 induces tyrosine phosphorylation of disabled-1 and modulates tau phosphorylation. *Neuron* **24**: 481-489.

245. D'Arcangelo, G., Homayouni, R., Keshvara, L., Rice, D. S., Sheldon, M. and Curran, T. (1999). Reelin is a ligand for lipoprotein receptors. *Neuron* **24**: 471-479.

246. Li, X. A., Titlow, W. B., Jackson, B. A., Giltiay, N., Nikolova-Karakashian, M., Uittenbogaard, A. and Smart, E. J. (2002). High density lipoprotein binding to scavenger receptor, class B, type I activates endothelial nitric-oxide synthase in a ceramide-dependent manner. *J.Biol.Chem.* **277**: 11058-11063.

247. Sambrook, J., Fritsch, E. F. and Maniatis, T. (1989). Extraction, purification & analysis of messenger RNA from eukaryotic cells. *Molecular Cloning: A Laboratory Manual.* Cold Sping Harbor Publications, New York, pp 7.3-7.4.

248. Sambrook, J., Fritsch, E. F. and Maniatis, T. (1989). *In vitro* amplification of DNA by the polymerase chain reaction. *Molecular Cloning: A Laboratory Manual.* Cold Spring Harbor Publications, New York, pp 14.1-14.22.

249. Chenchik, A., Diachenko, L., Moqadam, F., Tarabykin, V., Lukyanov, S. and Siebert, P. D. (1996). Full-length cDNA cloning and determination of mRNA 5' and 3' ends by amplification of adaptor-ligated cDNA. *Biotechniques* **21**: 526-534.

250. Pomp, D. and Medrano, J. F. (1991). Organic solvents as facilitators of polymerase chain reaction. *Biotechniques* **10**: 58-59.

251. Kellogg, D. E., Rybalkin, I., Chen, S., Mukhamedova, N., Vlasik, T., Siebert, P. D. and Chenchik, A. (1994). TaqStart Antibody: "hot start" PCR facilitated by a neutralizing monoclonal antibody directed against Taq DNA polymerase. *Biotechniques* **16**: 1134-1137.

252. Moras, D. and Poterszman, A. (1995). RNA-protein interactions. Diverse modes of recognition. *Curr.Biol.* **5**: 249-251.

253. Brink, A. A., Oudejans, J. J., Jiwa, M., Walboomers, J. M., Meijer, C. J. and van den Brule, A. J. (1997). Multiprimed cDNA synthesis followed by PCR is the most suitable method for Epstein-Barr virus transcript analysis in small lymphoma biopsies. *Mol.Cell Probes* **11**: 39-47.

254. Sambrook, J., Fritsch, E. F. and Maniatis, T. (1989). Gel electrophoresis of DNA. *Molecular Cloning: A Laboratory Manual.* Cold Spring Harbor Publications, New York, pp 6.1-6.62.

255. Sambrook, J., Fritsch, E. F. and Maniatis, T. (1989). Enzymes used in molecular cloning. *Molecular Cloning: A Laboratory Manual.* Cold Spring Harbor Publications, New York, pp 5.3-5.32.

256. Clark, J. M. (1988). Novel non-templated nucleotide addition reactions catalyzed by procaryotic and eucaryotic DNA polymerases. *Nucleic Acids Res.* **16**: 9677-9686.

257. Weiss, B., Jacquemin-Sablon, A., Live, T. R., Fareed, G. C. and Richardson, C. C. (1968). Enzymatic breakage and joining of deoxyribonucleic acid. VI. Further purification and properties of polynucleotide ligase from Escherichia coli infected with bacteriophage T4. *J.Biol.Chem.* **243**: 4543-4555.

258. Hanahan, D. (1983). Studies on transformation of Escherichia coli with plasmids. *J.Mol.Biol.* **166**: 557-580.

259. Smith, P. K., Krohn, R. I., Hermanson, G. T., Mallia, A. K., Gartner, F. H., Provenzano, M. D., Fujimoto, E. K., Goeke, N. M., Olson, B. J. and Klenk, D. C. (1985). Measurement of protein using bicinchoninic acid. *Anal.Biochem.* **150**: 76-85.

260. Bradford, M. M. (1976). A rapid and sensitive method for the quantitation of microgram quantities of protein utilizing the principle of protein-dye binding. *Anal.Biochem.* **72**: 248-254.

261. Spector, T. (1978). Refinement of the coomassie blue method of protein quantitation. A simple and linear spectrophotometric assay for less than or equal to 0.5 to 50 microgram of protein. *Anal.Biochem.* **86**: 142-146.

262. Hames, B. D. and Rickwood, D. (1983). *Gel Electrophoresis of Proteins: A Practical Approach.* IRL press Ltd, Oxford.

263. Hames, B. D. and Rickwood, D. (1983). An introduction to polyacrylamide electrophoresis. *Gel Electrophoresis of Proteins: A Practical Approach.* IRL press Ltd, Oxford, pp 1-192.

264. Margolis, J. and Kenrick, K. C. (1967). Polyacrylamide gel-electrophoresis across a molecular sieve gradient. *Nature* **214**: 1334-1336.

265. Whitehead, T. P., Kricka, L. J., Carter, T. J. and Thorpe, G. H. (1979). Analytical luminescence: its potential in the clinical laboratory. *Clin.Chem.* **25**: 1531-1546.

266. Smith, D. B. and Johnson, K. S. (1988). Single-step purification of polypeptides expressed in Escherichia coli as fusions with glutathione S-transferase. *Gene* **67** : 31-40.

267. Smith, M. R., Liu, Y. L., Kim, S. R., Bae, Y. S., Kim, C. G., Kwon, K. S., Rhee, S. G. and Kung, H. F. (1996). PLC gamma 1 Src homology domain induces mitogenesis in quiescent NIH 3T3 fibroblasts. *Biochem.Biophys.Res.Commun.* **222**: 186-193.

268. Fields, S. and Song, O. (1989). A novel genetic system to detect protein-protein interactions. *Nature* **340**: 245-246.

269. Celenza, J. L., Eng, F. J. and Carlson, M. (1989). Molecular analysis of the SNF4 gene of Saccharomyces cerevisiae: evidence for physical association of the SNF4 protein with the SNF1 protein kinase. *Mol.Cell Biol.* **9**: 5045-5054.

270. Guthrie, C. and Fink, G. R. (1991). Guide to yeast genetics and molecular biology. *Methods Enzymol.* **194**: 1-863.

271. Waugh, M. G., Lawson, D., Tan, S. K. and Hsuan, J. J. (1998). Phosphatidylinositol 4-phosphate synthesis in immunoisolated caveolae-like vesicles and low buoyant density non-caveolar membranes. *J.Biol.Chem.* **273**: 17115-17121.

272. Mackness, M. I. and Durrington, P. N. (1992). Lipoprotein separation and analysis for clinical studies. *Lipoprotein Analysis: A Practical Approach* (Converse, C.A. and Skinner, E.R. eds). Oxford University Press, New York, pp1-42.

273. Edelstein, C. and Scanu, A. M. (1986). Precautionary measures for collecting blood destined for lipoprotein isolation. *Methods Enzymol.* **128**: 151-154.

274. Schumaker, V. N. and Puppione, D. L. (1986). Sequential flotation ultracentrifugation. *Methods Enzymol.* **128**: 155-170.

275. Tsuchiya, S., Kobayashi, Y., Goto, Y., Okumura, H., Nakae, S., Konno, T. and Tada, K. (1982). Induction of maturation in cultured human monocytic leukemia cells by a phorbol diester. *Cancer Res.* **42**: 1530-1536.

276. Brown, M. S. and Goldstein, J. L. (1983). Lipoprotein metabolism in the macrophage: implications for cholesterol deposition in atherosclerosis. *Annu.Rev.Biochem.* **52**: 223-261.

277. Innerarity, T. L., Pitas, R. E. and Mahley, R. W. (1986). Lipoprotein-receptor interactions. *Methods Enzymol.* **129**: 542-565.

278. Basu, S. K., Goldstein, J. L., Anderson, G. W. and Brown, M. S. (1976). Degradation of cationized low density lipoprotein and regulation of cholesterol metabolism in homozygous familial hypercholesterolemia fibroblasts. *Proc.Natl.Acad.Sci.U.S.A.* **73**: 3178-3182.

279. Gebhart, C. L. and Kabanov, A. V. (2001). Evaluation of polyplexes as gene transfer agents. *J.Control Release* **73**: 401-416.

280. Ellsworth, J. L., Erickson, S. K. and Cooper, A. D. (1986). Very low and low density lipoprotein synthesis and secretion by the human hepatoma cell line Hep-G2: effects of free fatty acid. *J.Lipid Res.* **27**: 858-874.

281. Hopp, T. P. and Woods, K. R. (1981). Prediction of protein antigenic determinants from amino acid sequences. *Proc.Natl.Acad.Sci.U.S.A.* **78**: 3824-3828.

282. Hopp, T. P. (1989). Use of hydrophilicity plotting procedures to identify protein antigenic segments and other interaction sites. *Methods Enzymol.* **178**: 571-585.

283. Finan, P. M., Hall, A. and Kellie, S. (1996). Sam68 from an immortalised B-cell line associates with a subset of SH3 domains. *FEBS Lett.* **389**: 141-144.

284. Finan, P. M., Soames, C. J., Wilson, L., Nelson, D. L., Stewart, D. M., Truong, O., Hsuan, J. J. and Kellie, S. (1996). Identification of regions of the Wiskott-Aldrich syndrome protein responsible for association with selected Src homology 3 domains. *J.Biol.Chem.* **271**: 26291-26295.

285. Rhee, S. G. (2001). Regulation of phosphoinositide-specific phospholipase C. *Annu.Rev.Biochem.* **70**: 281-312.

286. Tudyka, T. and Skerra, A. (1997). Glutathione S-transferase can be used as a C-terminal, enzymatically active dimerization module for a recombinant protease inhibitor, and functionally secreted into the periplasm of Escherichia coli. *Protein Sci.* **6**: 2180-2187.

287. Simons, K. and Toomre, D. (2000). Lipid rafts and signal transduction. *Nat.Rev.Mol.Cell Biol.* **1**: 31-39.

288. Yablonski, D., Kadlecek, T. and Weiss, A. (2001). Identification of a phospholipase C-gamma1 (PLC-gamma1) SH3 domain-binding site in SLP-76 required for T-cell receptor-mediated activation of PLC-gamma1 and NFAT. *Mol.Cell Biol.* **21**: 4208-4218.

289. Beier, D. R. and Young, E. T. (1982). Characterization of a regulatory region upstream of the ADR2 locus of S. cerevisiae. *Nature* **300**: 724-728.

290. Ruohonen, L., Penttila, M. and Keranen, S. (1991). Optimisation of Bacillus α-amylase production by Saccharomyces cerevisiae. *Yeast* **7**: 337-346.

291. Tornow, J. and Santangelo, G. M. (1990). Efficient expression of the Saccharomyces cerevisiae glycolytic gene ADH1 is dependent upon a cis-acting regulatory element (UASRPG) found initially in genes encoding ribosomal proteins. *Gene* **90**: 79-85.

292. Langmann, T., Klucken, J., Reil, M., Liebisch, G., Luciani, M. F., Chimini, G., Kaminski, W. E. and Schmitz, G. (1999). Molecular cloning of the human ATP-binding cassette transporter 1 (hABC1): evidence for sterol-dependent regulation in macrophages. *Biochem.Biophys.Res.Commun.* **257**: 29-33.

293. Fields, S. and Sternglanz, R. (1994). The two-hybrid system: an assay for protein-protein interactions. *Trends Genet.* **10**: 286-292.

294. Chan, D. C., Bedford, M. T. and Leder, P. (1996). Formin binding proteins bear WWP/WW domains that bind proline-rich peptides and functionally resemble SH3 domains. *EMBO J.* **15**: 1045-1054.

295. Sudol, M. (1996). Structure and function of the WW domain. *Prog.Biophys.Molec.Biol.* **65**:113-132.

296. Lu, P. J., Zhou, X. Z., Shen, M. and Lu, K. P. (1999). Function of WW domains as phosphoserine- or phosphothreonine-binding modules. *Science* **283**: 1325-1328.

297. May, L. G., Johnson, S., Krebs, S., Newman, A. and Aronstam, R. S. (1999). Involvement of protein kinase C and protein kinase A in the muscarinic receptor signalling pathways mediating phospholipase C activation, arachidonic acid release and calcium mobilisation. *Cell Signal.* **11**: 179-187.

298. Berg, K. A., Cropper, J. D., Niswender, C. M., Sanders-Bush, E., Emeson, R. B. and Clarke, W. P. (2001). RNA-editing of the 5-HT(2C) receptor alters agonist-receptor-effector coupling specificity. *Br.J.Pharmacol.* **134**: 386-392.

299. Dickenson, J. M., Blank, J. L. and Hill, S. J. (1998). Human adenosine A1 receptor and P2Y2-purinoceptor-mediated activation of the mitogen-activated protein kinase cascade in transfected CHO cells. *Br.J.Pharmacol.* **124**: 1491-1499.

300. Alderton, F., Fan, T. P. and Humphrey, P. P. (2001). Somatostatin receptor-mediated arachidonic acid mobilization: evidence for partial agonism of synthetic peptides. *Br.J.Pharmacol.* **132**: 760-766.

301. Trigatti, B., Rigotti, A. and Krieger, M. (2000). The role of the high-density lipoprotein receptor SR-BI in cholesterol metabolism. *Curr.Opin.Lipidol.* **11**: 123-131.

302. St Clair, R. W. (1998). Estrogens and atherosclerosis: phytoestrogens and selective estrogen receptor modulators. *Curr.Opin.Lipidol.* **9**: 457-463.

303. Neufeld, E. B., Remaley, A. T., Demosky, S. J., Stonik, J. A., Cooney, A. M., Comly, M., Dwyer, N. K., Zhang, M., Blanchette-Mackie, J., Santamarina-Fojo, S. and Brewer, H. B., Jr. (2001). Cellular localization and trafficking of the human ABCA1 transporter. *J.Biol.Chem.* **276**: 27584-27590.

304. Mauch, D. H., Nagler, K., Schumacher, S., Goritz, C., Muller, E. C., Otto, A. and Pfrieger, F. W. (2001). CNS synaptogenesis promoted by glia-derived cholesterol. *Science* **294**: 1354-1357.

PUBLICATIONS

Original Articles

1. **Mulcahy, J. V.**, Riddell, D. R. and Owen, J. S. (2002). Human scavenger receptor class B, type II (SR-BII) and cellular cholesterol efflux. *J. Lipid Res.* submitted.

2. Tagalakis A. D., Diakonov, I. A., Graham, I. R., Heald, K. A., Harris, J. D., **Mulcahy, J. V.**, Dickson, J. G. and Owen, J. S. Apolipoprotein E (apoE) delivery by microencapsulation of recombinant cells improves the hyperlipidaemic profile in apoE knockout mice. *Manuscript in preparation.*

3. Manzano, A., Mohri, Z., **Mulcahy, J.V.**, Dickson, J.G. and Owen, J.S. ApoAI natural mutations (Milano and Paris): understanding their characteristics. *Manuscript in preparation.*

Review Articles

1. **Mulcahy, J. V.** and Owen, J. S. (2002). HDL-C transport and atheroprotection. *Science & Medicine* **8**:76-85.

2. Owen, J. S. and **Mulcahy, J. V.** (2002). ATP-binding cassette A1 protein and HDL homeostasis. *Atherosclerosis* in press.

Poster Presentations

1. **Mulcahy, J. V.**, Reed, C. A. B., Riddell, D. R. and Owen, J. S. The cytoplasmic tail of scavenger receptor class B, type II (SR-BII) interacts with the SH3 domain of phospholipase C-γ. **18th International Congress of Biochemistry and Molecular Biology**, Birmingham, UK – July 2000.

2. **Mulcahy, J. V.**, Riddell, D. R. and Owen J. S. Scavenger receptor class B, type II (SR-BII) and mobilisation of stored intracellular cholesteryl esters. **7th Annual Scandinavian Atherosclerosis Conference**, Copenhagen, Denmark – May 2001

3. Manzano, A., Mohri, Z., **Mulcahy, J. V.**, Graham, I. R., Dickson, J. G. and Owen, J. S. Taking advantage of apoA-I natural mutations: cell models and gain-of-function chimeraplasty. **9th Meeting of the European Society of Gene Therapy**, Antalya, Turkey – November 2001.